THIS NUMBER COMPLETES VOLUME 8

EXPERIMENTAL CELL RESEARCH

UNIVERSITY OF HAWAII
LIBRARY
JUL 30 '55

Published under the auspices of

THE INTERNATIONAL SOCIETY FOR CELL BIOLOGY

EDITORS:

H. BAUER · T. CASPERSSON · E. FAURÉ-FREMIET

H. B. FELL · G. MONTALENTI · J. T. RANDALL · J. RUNNSTRÖM

F. O. SCHMITT · P. WEISS · R. W. G. WYCKOFF

VOLUME 8 · JUNE 1955 · NUMBER 3

ACADEMIC PRESS INC., PUBLISHERS, NEW YORK, N.Y.

EXPERIMENTAL CELL RESEARCH

EDITORS:

H. BAUER, Max Planck Institut f. Meeresbiologie, Wilhelmshaven 23, Germany
T. CASPERSSON, Department of Cell Research, Karolinska Inst., Stockholm 60, Sweden
E. FAURÉ-FREMIET, Collège de France, Paris V:e, France
HONOR B. FELL, Strangeways Laboratory, Cambridge, England
G. MONTALENTI, Istituto di Genetica dell' Università di Napoli, Naples, Italy
J. T. RANDALL, Wheatstone Physics Laboratory, King's College, London W. C. 2, England
J. RUNNSTRÖM, Wenner-Gren Institute for Experimental Biology, Stockholm Va., Sweden
F. O. SCHMITT, Massachusetts Institute of Technology, Cambridge 39, Mass., U.S.A.
P. WEISS, Rockefeller Institute for Medical Research, New York 21, N.Y., U.S.A.
R. W. G. WYCKOFF, Laboratory of Physical Biology, National Institute of Health, Bethesda, Md., U.S.A.

Editorial Secretary: A. ENGSTRÖM, Department for Physical Cell Research, Karolinska Institutet, Stockholm 60, Sweden.
Papers should be submitted to one of the editors or to the Editorial Office, Norrtullsgatan 16, Stockholm Va., Sweden.

ADVISORY BOARD:

W. BLOOM (Chicago), J. BRACHET (Bruxelles), F. BUCHTHAL (Copenhagen), A. BUZZATI-TRAVERSO (Pavia), R. CHAMBERS (New York), E. CHARGAFF (New York), J. F. DANIELLI (London), C. D. DARLINGTON (London), J. N. DAVIDSON (Glasgow), M. DEMEREC (Cold Spring Harbor, N.Y.), J. ENGELBRETH-HOLM (Copenhagen), A. FISCHER (Copenhagen), A. FREY-WYSSLING (Zürich), N. FRIES (Uppsala), R. J. GAUTHERET (Paris), L. GEITLER (Wien), G. GOMORI (Chicago), A. HADDOW (London), E. HAMMARSTEN (Stockholm), B. HANSTRÖM (Lund), E. NEWTON HARVEY (Princeton, N.J.), L. V. HEILBRUNN (Philadelphia, Pa.), G. C. HERINGA (Amsterdam), A. HOLLAENDER (Oak Ridge, Tenn.), H. HOLTER (Copenhagen), J. HOLTFRETER (Rochester, N.Y.), P. KOLLER (London), F. LEHMANN (Bern), P. L'HÉRITIER (Paris), G. LEVI (Torino), P. E. LINDAHL (Uppsala), G. LINDEBERG (Uppsala), C. C. LINDEGREN (Carbondale, Ill.), R. J. LUDFORD (London), S. E. LURIA (Urbana, Ill.), A. LWOFF (Paris), A. MIRSKY (New York), H. OKKELS (Copenhagen), O. OLIVO (Bologna), A. W. POLLISTER (New York), W. J. SCHMIDT (Giessen), F. SCHRADER (New York), W. SEIFRIZ (Philadelphia, Pa.), T. M. SONNEBORN (Bloomington, Ind.), J. M. SOSA (Montevideo), J. SPEK (Rostock), W. M. STANLEY (Berkeley, Calif.), E. SUOMALAINEN (Helsingfors), E. L. TATUM (Stanford University, Calif.), T. TEORELL (Uppsala), A. TYLER (Pasadena, Calif.), W. WILBRANDT (Bern).

Subscriptions

EXPERIMENTAL CELL RESEARCH

will be published in two volumes annually at $12:— per volume. Please send your subscription orders to Academic Press Inc., 125 East 23 St., New York 10, N.Y.

Experimental Cell Research, 8, *411–435 (1955)*

STUDIES ON MITOCHONDRIA

VI. THE RELATIONSHIP BETWEEN THE STRUCTURE, OSMOTIC REACTIVITY AND ATPase ACTIVITY OF MITOCHONDRIA FROM PIGEON SKELETAL MUSCLE[1]

J. W. HARMAN and A. KITIYAKARA

Department of Pathology, University of Wisconsin Medical School, Madison, Wisc., U.S.A.

Received July 7, 1954

Recent investigations upon isolated mitochondria have emphasized a close correlation between the morphology and the enzymatic activity of these organelles (11, 13). The mutual interdependence of structural integrity and oxidative phosphorylation is salient (12) and indicates that the physical state of the mitochondria is a critical factor governing its metabolic activity. Collateral evidence which substantiates this association of structure and enzymatic function has since been accumulated in other laboratories (20, 29, 32, 35). Current studies have, therefore, been much preoccupied with the stabilization of this relationship and have forced the realization that technical requirements which preserve integrated enzymatic activity are designed to ensure structural integrity also. Although some variations in interpretation have occurred in the precise evaluation of the phenomenon, it is proposed that conditions proper for the optimal biochemical activity of integrated enzyme systems are such as preserve them intact within the mitochondrion (8).

In a previous study in this laboratory (18) the distribution in skeletal muscle of enzymes acting upon phosphorylated nucleotides was investigated. This was part of an inquiry into the localization and activity in muscle of enzymes with autolytic propensities, which under abnormal circumstances might affect the structure and hence the function of the cellular constituents. The mitochondria were found to contain a magnesium activated ATPase, which with myokinase contributed considerably to the autolytic dephosphorylations in muscle dispersions. Other observers have identified similar enzymes in liver mitochondria (16) and in the mitochondria of mammalian and insect muscle (2, 31). The considerable concentration of such an enzyme in the mitochondrion appears hazardous to the conservation of the ~ P fabricated into ATP by the mitochondria. It is a potential intrinsic weakness which by a diversion of ~ P could disperse structure and impair function.

[1] Aided by grants from the Muscular Dystrophy Associations of America, Inc., the Life Insurance Medical Research Fund and the Wisconsin Alumni Research Foundation.

Control of such an enzyme appears essential to survival of the organelle and may also be profitable to the cell, although direct evidence of its function is lacking. The present study is concerned with the elucidation of morphological changes that influence the activity of this enzyme and especially of the environmental alterations which affect structure and consequently moderate activity.

EXPERIMENTAL PROCEDURES

Isolation of the mitochondria. The mitochondria from the *pectoralis major* muscle of the pigeon were isolated by differential centrifugation, as previously described (18). The temperature was maintained at 0°–4°C during the whole procedure of isolation. When hypertonic sucrose was used as a homogenizing medium, the centrifugation times were sufficiently prolonged to compensate for the resistance of the more viscous medium. Each preparation was examined by phase microscopy in order to determine the purity of the suspension and the shapes of the mitochondria. In most cases the experiments were done immediately after the mitochondria had been isolated.

Cytological technique. In most experiments in which the relationship between the morphology of the mitochondria and the concentration of sucrose was studied, the mitochondria were isolated and suspended in 0.88 M sucrose kept at pH 7.0 by addition of a minute quantity of 1 per cent potassium hydroxyde. Aliquots of the suspension were transferred to tubes containing various molar concentrations of sucrose or electrolyte and kept at a temperature of 10°C for 30 minutes before the mitochondria were fixed and examined.

Mitochondria were fixed with 11.5 per cent formalin at pH 7.4 or with 4 per cent osmium tetroxide buffered at pH 7.4 by sodium diethyl barbiturate (26). An equal volume of fixative was added to the mitochondrial suspension, which was allowed to fix for 3 hours or longer. The mitochondria fixed in osmium tetroxide were washed 3 times with distilled water before examination, whereas the suspensions fixed with formalin were examined directly without washing. A differential count of mitochondrial types in the suspensions was done as previously described (11). The efficacy of fixation was assured by performance of parallel counts on both fresh and fixed suspensions, as further reported under "results".

The relationship between the morphology of the mitochondria and the pH of the medium was investigated at 21°C in the presence of 0.02 M acetate barbiturate buffer. The mitochondria were isolated and suspended in 0.25 M sucrose before transference of aliquots of 0.5 ml to tubes containing the same volume of 0.25 M sucrose buffered at various pH's. The pH suspensions were checked with a Beckman glass electrode pH meter 30 minutes after addition of the mitochondria. Differential counts of the various forms of the mitochondria at different pH's were done on similar preparations fixed in 2 per cent osmium tetroxide.

Analytical procedures. The relationship between the ATPase activity of the mitochondria and the concentration of sucrose in the medium was studied in a system containing 10 μM of ATP and a varying sucrose concentration in the absence usually of activating cations or buffer in a total volume of 2.0 ml. The ATP served as both

substrate and buffer at pH 7.0. The temperature of the medium was raised to 10° C before 0.2 ml of the cold mitochondrial suspension was added. The reaction was stopped after 60 minutes incubation at 10° C by addition of trichloracetic acid to the final concentration of 5 per cent. The protein precipitate was removed by centrifugation and inorganic phosphate determined by the method of Lowry and Lopez (21) with readings at 660 mμ using a Coleman Universal Spectrophotometer No. 14. Some variations from the above description will be mentioned below. Parallel similar sets of mitochondrial suspensions were also prepared for cytological study in order to correlate the mitochondrial morphology with the enzymatic activity. At the end of the incubation period these mitochondria were fixed with buffered osmium tetroxide and examined by phase contrast microscopy.

In experiments in which attempts were made to dissociate ATPase from the mitochondria by various treatments, the distribution of the enzyme activity in the suspending fluid and the mitochondrial residue was determined after centrifugation. The mitochondria were thickly suspended in the 0.25 M sucrose and an aliquot subjected to comminution in the Waring blendor for 3 minutes to break the mitochondria into small fragments[1]; crushed frozen medium was added during the procedure to maintain the temperature at 0° C and to facilitate fragmentation. Another untreated aliquot of the suspension was used as a control. Both aliquots were diluted with 15 volumes of the suspending medium, and after a 30-minute storage at 0° C to allow equilibration between the comminuted mitochondria and the suspending fluid, the suspensions were centrifuged at 18,000 × g for 45 minutes.[2] Each fraction was made up with medium to a volume equal to that of the original dilute suspension. Small aliquots of each fraction were tested for the ATPase activity in a system containing 10 μM of ATP in the presence of 0.0125 M sodium diethyl barbiturate buffer, 5×10^{-3} M $MgCl_2$ and 0.01 M KCl in final concentrations with a total volume of 2.0 ml for an incubation period of 15 minutes at 26° C. In order to obtain a maximal activity the amount of the enzyme preparation used was adjusted so that not more than 25 per cent of the terminal labile phosphate of ATP was liberated. The content of the enzyme in each aliquot was calculated on the basis of units of activity. One unit of enzyme is expressed as the amount which liberates 1 μM of inorganic phosphate from ATP in a system saturated with the latter under standard conditions just described. The total amount of ATPase in each fraction was estimated on the basis of the content of the enzyme in the aliquot tested. Protein nitrogen of the preparations was determined by the method of Johnson (14).

Other procedures used in the chemical analyses included estimates of free sulfhydryl groups by titration with potassium ferricyanide by the method of Mirsky (23). Readings were taken at 690 mμ in a Coleman Universal Spectrophotometer No. 14. The free α-amino groups of the enzyme preparations were also investigated by the reaction with ninhydrin (22) and the free ammonia released determined by the microdiffusion method of Conway (4). The procedure in detail was as follows. Samples

[1] A regular 150 ml monel Waring blendor cup was used throughout and the volume of the suspension limited so that it remained within the stem of the cup. Larger volumes were less effective for fragmentation of mitochondria. Comminution with a microblendor (35) for 8 minutes left a major proportion of mitochondria unfragmented.

[2] For high speed centrifugations the multispeed attachment of the International Refrigerated PR-1 Centrifuge was used.

of mitochondrial suspensions or standard amino acid solutions were mixed with an equal volume of a ninhydrin citrate buffer suspension (22). The tubes were capped and placed in a boiling water bath for 23 minutes. They were then cooled rapidly, 2 ml of 5 per cent citrate buffer added and the suspension filtered through No. 2 Whatman paper. Aliquots of the filtrate were placed in the outer chamber of No. 1 Conway units, 1 ml of saturated KOH added and the lid sealed. Ammonia was allowed to diffuse over into the 1 per cent boric acid in the center chamber for 4 hours at 38° C. The boric acid solution was then titrated with standard 0.02 N HCl using a Conway microburette and the ammonia calculated after suitable blank estimations had been subtracted, e.g., the preformed ammonia in both the reagents and samples. By this technique recoveries from a variety of purified amino acids averaged between 95 and 101 per cent with the exceptions listed previously (22).

Materials. Disodium adenosine triphosphate (Pabst Brewing Co., Milwaukee, Wisconsin) containing 0.04 μM of inorganic phosphate per mg as an impurity was used in these studies. The acid labile phosphate was determined by hydrolysis in 1 N HCl at 100° C for 7 minutes. The sequestrene NA_4 (tetrasodium ethylenediaminetetra-acetate dihydrate) used in this study was obtained from the Alrose Chemical Company, Providence, Rhode Island. The solutions of these reagents were adjusted to pH 7.0 by the addition of potassium hydroxide and checked with a glass electrode.

Crystallized trypsin of bovine origin in 50 per cent $MgSO_4$ (Armour Laboratories, Chicago, Ill.) was prepared as an 0.4 per cent solution in 0.25 M sucrose buffered at pH 7.4 with 0.01 M sodium diethyl barbiturate. A twice crystallized salt free trypsin (Worthington Biochemical Sales Co., Freehold, New Jersey) was similarly prepared. The amino acids, glutathione and glycylglycine used for the amino nitrogen procedure were products of Nutritional Biochemical Corp., Cleveland, Ohio.

RESULTS

Morphology of the mitochondria. The shapes assumed by mitochondria of muscle have been previously documented (11, 13, 3, 37). Rodlets represent the form seen in the intact myofibers (Figs. 1, 2, 3 and 4) and observed in

Fig. 1. Portion of a myofiber from muscle homogenized in 0.25 M sucrose is shown. The dense rodlet mitochondria are horizontally aligned. Many minute spherical sarcosomes are situated at the ends and between mitochondria. This and all subsequent photomicrographs are taken at a magnification of 2,900 × with dark low phase contrast.

Fig. 2. The elongated mitochondria are aligned parallel with the myofibrils. There are a few sarcosomes. Preparation is the same as in Fig. 1.

Fig. 3. Both elongated and short dense rodlets are observed in a suspension of mitochondria suspended in 0.25 M sucrose held at 0° C until the slide is prepared. Most elongated mitochondria manifest areas of constriction.

Fig. 4. There is a bent dense rodlet as well as a few smaller mitochondria. Mitochondria were isolated in 0.25 M sucrose.

Fig. 5. The mitochondria isolated in 0.25 M sucrose are allowed to stand at 25° C for 30 minutes. The rodlets are undergoing swelling. In one elongated beaded mitochondrion (arrow) half is swollen and half remains condensed. The other units are loose and irregular.

Fig. 6. Further exposure of mitochondria to 25° C thermal transformation allows appearance of loose fluffy rodlets as illustrated (arrow).

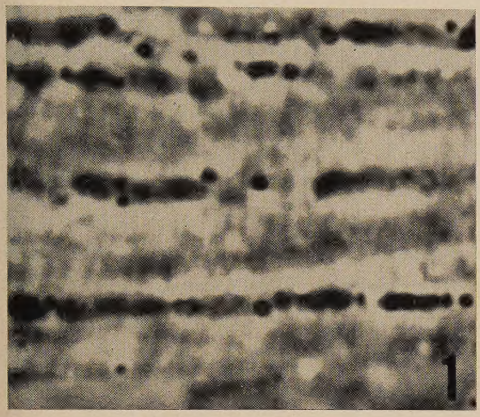
1

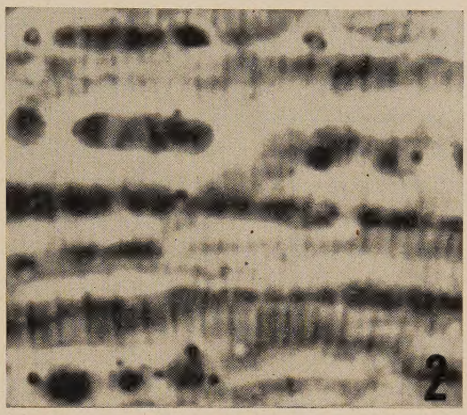
2

3

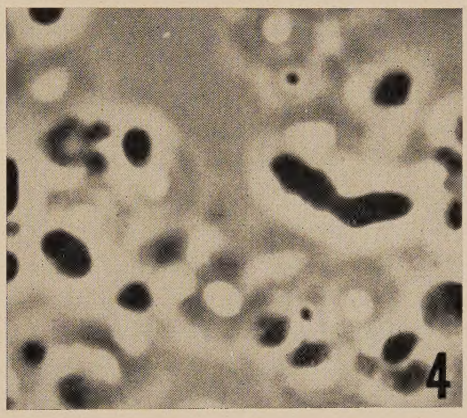
4

5

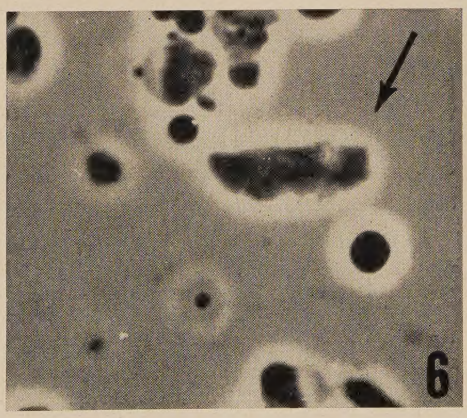
6

TABLE I

Comparison of differential crescent counts on both fresh suspensions and suspensions fixed with formalin and osmium tetroxide.

Experiment	Fixative	Total	Crescents	% Crescents
1	OsO_4	300	67	22
	Formalin	253	53	20
	,,	410	80	19
2	OsO_4	336	122	38
	,,	505	204	40
	Formalin	408	177	43
	,,	303	126	41
3	OsO_4	420	120	31
	,,	501	127	25
	Formalin	322	88	27
	,,	273	76	28
4	OsO_4	540	240	44
	,,	399	177	44
	Formalin	611	300	49
	,,	529	241	46
5	None	467	87	18
	,,	441	65	14
	Formalin	508	66	13
	,,	616	72	12
6	None	484	40	8.2
	,,	470	62	13
	Formalin	532	48	9
	,,	749	81	11
7	None	403	130	30
	Formalin	658	169	25
8	None	318	87	27
	Formalin	718	179	25

In all experiments except 5 and 6 a preliminary period of preincubation of the suspensions at 30°C preceded the fixation and count. Formalin fixed suspensions were not washed before the counts were made. Those in OsO_4 were thrice washed and resuspended in distilled water.

either teased preparations or homogenates. Other forms are derived from the rodlet and consist of the loose rod (Figs. 5 and 6), the spherical dense and the crescent (Figs. 7 and 8), which are degenerative types in which volume and density are altered. Targets are seen only in actively phos-

phorylating unfixed suspensions. The various types of mitochondria are well preserved for protracted examination and statistical differential analysis by fixation with either formalin or osmium tetroxide. Direct observation of the mitochondria under cover slip conditions as the fixative is rapidly drawn across the slide establishes that mitochondrial distortion is not incurred during the process of fixation and ensures that the forms seen prior to fixation are accurately perpetuated. This stabilization is emphasized in results recorded in Table I in which the proportion of crescents in the fresh suspension is faithfully reflected by the fixed specimens. The permanency of the preservation is indicated by persistence in the established forms of both form and density after repeated washing and prolonged storage. Consideration of the fixatives used indicates that proteins and possibly lipids participate in the stable mitochondrial structure, since both fixatives exert their action through protein linkages and the osmium may affect the lipids (27). Although previous studies have related various forms with metabolic activity, they were concerned mainly with the production of different forms by variation of osmolarity of the medium. Here the interest is directed to other factors as well, including thermal activation, conducive to the conversion of the native rodlet into the other types. Many individual rods have been observed undergoing alterations, and although the relationships discussed in later sections are statistical, the phenomena described in this section comprise data obtained from examinations of individual units.

The factors which are capable of altering the mitochondrial morphology with the appearance of the degenerative forms illustrated above are of several types. They are grouped together and designated as transforming agents. Such transformers are defined as a series of chemical agents and physical conditions which transform the conjugated pyridino-protein enzymes of the integrated system into dissociated classical forms and simultaneously modify the structural integrity of the mitochondria (8). The connotation, as originally expressed, intended to indicate both a significant biochemical and a morphological alteration or transformation of the mitochondria. These agents are conveniently subdivided into 5 categories, depending on their mode of action: 1) osmotic, such as hypo-osmotic solutions and solutions of compounds which freely penetrate the mitochondria; 2) thermal, which by the elevation of temperature initiates structural alterations which permit swelling, even in a hyperosmotic environment of nonelectrolytes; 3) the solvent, which disperses the lipid-protein structure and causes dissolution of structure, of which such agents as desoxycholate and caprylic alcohol are examples; 4) specific ionic agents, which in anosmotic minute quantities

(e.g., 10^{-3} M) elicit swelling and crescent formation, such as calcium, magnesium and hydroxyl ions; 5) mechanical, such as prolonged shearing and repeated slow freezing and thawing which disrupt the mitochondrial structure by expansive and distorting stresses.

The form changes induced by thermal transformation, which is a facsimile of other types, are most simply studied under cover slip conditions by bringing the slide to ambient room temperature, usually 25° C irrespective of the molarity of the sucrose medium. After a brief latent period the mitochondria expand slightly, lose some density and assume the fuzzy outline of the loose rodlet with manifestation of a fine internal reticular structure (Fig. 6). Subsequently from the side of such rodlets a bubble-like excrescence emerges and increases gradually at the expense of the rodlet until it becomes mainly a vesicle with a small remnant of the original rod confined to a portion of the margin, i.e., the crescent. On the other hand, many rods initially bend and enspherulate, become dense spheres and subsequently expand into crescents. Sometimes a bleb appears on a dense rodlet and without formation of either a loose rodlet or dense sphere is converted directly into a crescent which retains the residuum of the original rod as a dense condensation rind along part of the border (Figs. 9, 10 and 11). The development of the rods into such forms is handicapped by keeping the suspension at 0–5° C. It may also be considerably delayed by the incorporation of 0.001 M sequestrene or calgon in the medium (Fig. 12). The other transforming agents, except the solvent and mechanical transformers, provoke a sequence of metamorphoses indistinguishable from those produced thermally. However, with the specific ionic transformers the changes are exceptionally rapid.

It is of special interest, as will be seen later, that hyperosmotic potassium chloride induces the appearance of bizarre forms and a more voluminous swelling than occurs with distilled water. It is also peculiar that although

---

Fig. 7. The suspension of mitochondria in 0.25 M sucrose exposed for 15 minutes to 25° C thermal activation consists of rodlets, crescents and spherical dense (arrow) mitochondria.
Fig. 8. A suspension of mitochondria in 0.25 M sucrose was resuspended in distilled water for 60 minutes and then fixed with 1 per cent osmium tetroxide buffered at pH 7.4. The mitochondria are all crescent shaped. Osmium impregnation enhances the density of the vesicular interface.
Fig. 9. A suspension of mitochondria in 0.25 M sucrose is depicted showing an elongated and a blunt rodlet immediately on making the slide.
Fig. 10. The same mitochondria after 15 minutes at 25° C have swollen and manifest initial vesiculation, a prelude to crescent formation. The bleb (arrow) at the end of the elongated rodlet is conspicuous.
Fig. 11. The mitochondria have swollen further after 30 minutes at 25° C with loose structure and extension of the vesiculation along the under belly of the elongated rodlet.
Fig. 12. The mitochondria are predominantly rodlet and spherical dense after 30 minutes at 25° C when suspended in 0.25 M sucrose to which 0.001 M sequestrene is added.

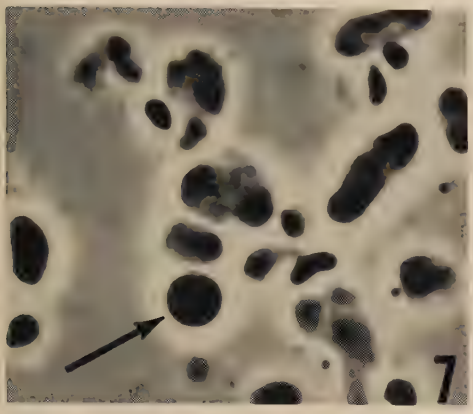
7

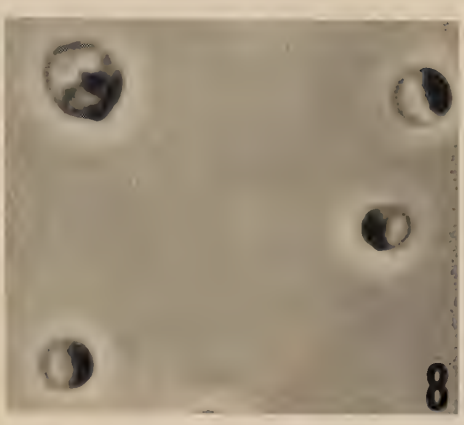
8

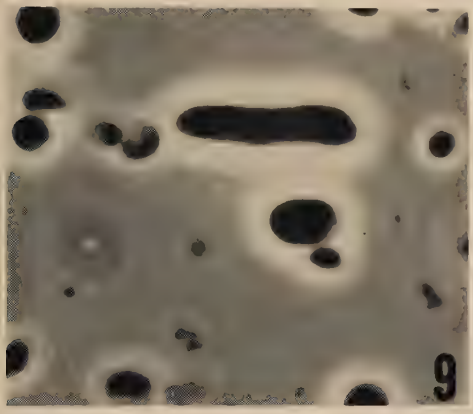
9

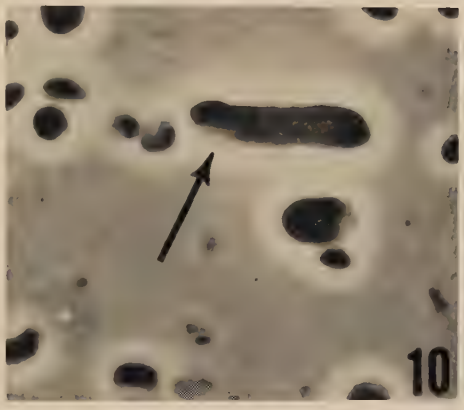
10

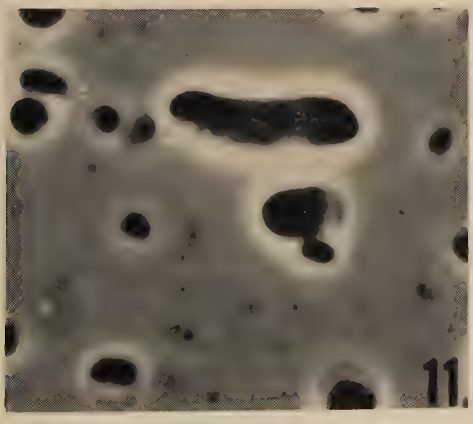
11

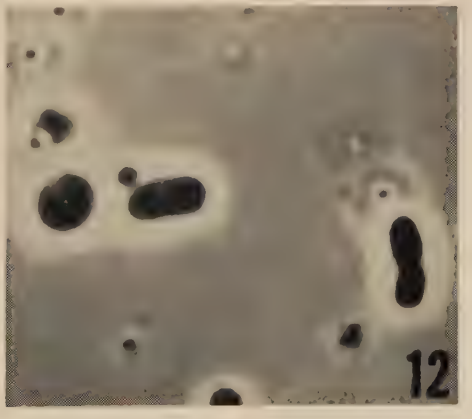
12

swelling may be considerable with these osmotic transformers, rupture or lysis with dispersions into smaller particles is not seen if mechanical agitation of the swollen forms is avoided. The salient morphological effect of 0.5 M potassium chloride is the conversion of the rods into either gigantic crescents or loose reticular spheres which are much larger and more translucent than in the mitochondria swollen by thermal transformation or treatment with water. These forms, which possess a ragged surface and a lattice interior structure, occur only in the suspensions in 0.5 M potassium chloride.

It is of some importance to determine reversibility of the transformation phenomenon. The swellings caused by mechanical and solvent transformers have been irreversible and unaffected by the application of refrigeration, chelating agents and hyperosmotic conditions. On the other hand, the transformation produced osmotically is largely reversible and that induced thermally only slightly less so. An assessment of the reversibility of the voluminous swelling observed, e.g., in hyperosmotic KCl, is obtained by exposure of such swollen mitochondria to 1.25 M sucrose. As the sucrose flows across the slide and replaces the electrolyte, shrinkage rapidly occurs (Figs. 13–16). Condensation of structure is apparent by diminution in size, increased density and optical homogeneity. However, scattered over the surface of many mitochondria there are several large holes or hiati, as depicted in Figs. 17 and 18, which do not preclude osmotic shrinkage. Most of the mitochondria finally assume a spherical dense shape; some remain as bulky loose rodlets; a few resume the configuration of dense refractile rods similar to the original native shape. Concomitant slight thermal transformation due to heating on the slide has not been excluded in such experiments, so the participation of the two types of transformation has not been separated completely. The limited reversibility may be due in part to the intervention

---

Fig. 13. Mitochondria suspended in 0.25 M sucrose are resuspended in 1 M potassium chloride. The crescent form is seen with numerous minute hiati in the surface.

Fig. 14. The same mitochondrion is seen as in Fig. 13 after a solution of 1.25 M sucrose has replaced the electrolyte solution. Condensation is apparent with conversion of the crescent to a dense sphere.

Fig. 15. The filtered homogenate of muscle in 0.25 M sucrose when the particles are resuspended in 1 M potassium chloride. There are a crescent, a loose fluffy rodlet (arrow) and an egg-shaped rodlet adjacent to a myofibril.

Fig. 16. Subsequent to replacement of the 1 M potassium chloride by 1.25 M sucrose all the mitochondria have shrunk to minute dimensions and transformed into spherical dense units. Compared with the mitochondria in Fig. 15 they are one-fourth to one-third as large.

Fig. 17 Mitochondria prepared in 0.25 M sucrose and resuspended in 1 M potassium chloride have enspherulated. Many have hiati in the surface (arrow) with complete interruption of the interface.

Fig. 18. The mitochondria depicted in Fig. 17 have shrunk under the influence of 1.25 M sucrose, although there are surface defects. One has reassumed rodlet form, part of which is very dense.

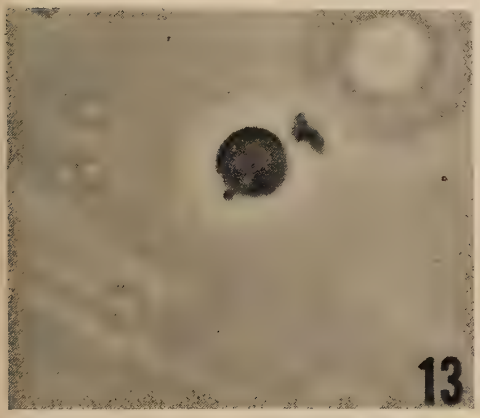
13

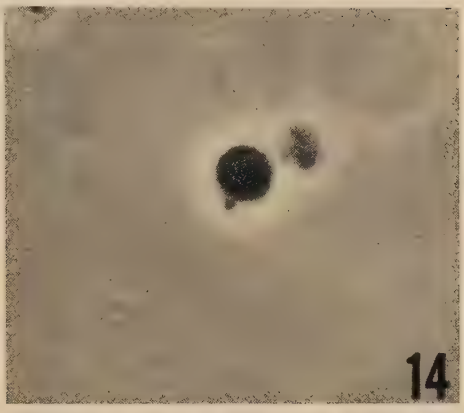
14

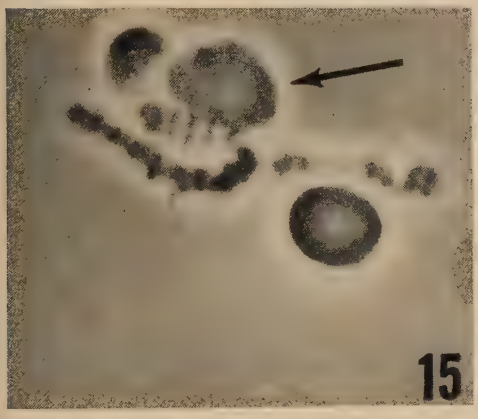
15

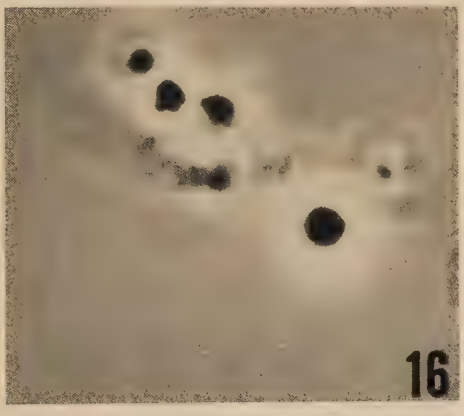
16

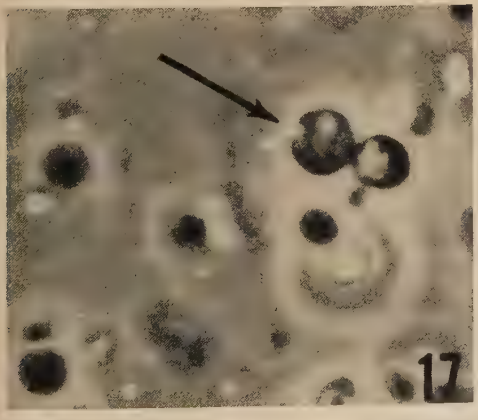
17

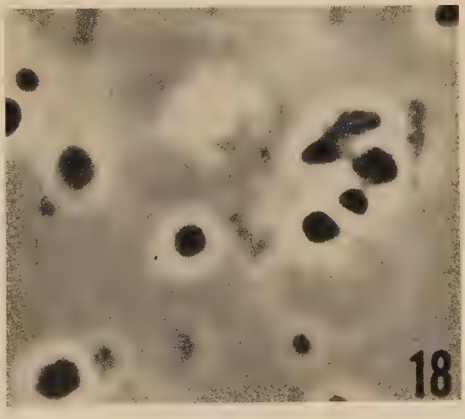
18

of thermal transformation during examination, but since the extent of the osmotic transformation and its duration also influence the reversibility, it is likely that some structural changes of a permanent nature are also brought about by the hypo-osmotic swelling. As will be seen under the section on enzyme studies, there is other evidence for this view, although it is possible to reconvert some crescents into dense rods.

Relationship between the morphology of the mitochondria and the molarity of sucrose and electrolytes. When the mitochondria are suspended in a solution of sucrose, the proportion of the crescent forms increases with decreasing molar concentration of sucrose, as shown in Textfig. 1. Although the sudden increase of crescents when the concentration of sucrose falls below 0.22 M suggests a breakdown of the mitochondria in a hypotonic solution, consideration of the osmotic pressure of the medium invalidates this hypothesis. The number of crescents parallels the reciprocals[1] of the osmotic pressure of the sucrose solution closely even when the concentration of sucrose is far below the "isotonic" level. This indicates that on a statistical basis the mitochondria behave as perfect osmometers for the sucrose solutions. Although the form which an individual mitochondrion will assume at a certain concentration of sucrose cannot be predicted with certainty, the percentage of the crescent forms in the total population of mitochondria can be accurately estimated whether unfixed or fixed suspensions are used.

Addition of a trace of bivalent cations causes a considerable increase in crescents, especially at the hyperosmolar level of sucrose (Textfig. 1). In the presence of magnesium the number of crescents deviates from parallelism with the osmotic pressure of the sucrose solution to a considerable degree, although the general trend of the curve still roughly follows that of the reciprocals of the osmotic pressure. At sucrose concentration below 0.22 molar the differential count of crescents approximates the general trend of the reciprocals of the osmotic pressure more closely. Calcium has a singular effect in that it not only increases the number of crescents to a higher degree than magnesium, but also obliterates completely the parallelism between the differential count of the crescents and the reciprocals of the osmotic pressure.

The remarkable effect of bivalent cations indicates that the control of these metals as free ions is important for the study of osmotic and morphological behavior of the mitochondria in a sucrose solution. In order to remove traces of the metals that might be present in the suspension, a chelating agent, sequestrene, was added to the system. Sequestrene has no effect

[1]The reciprocals of the osmotic pressure at 10° C were derived from the data compiled by Morse and Morse (24) of the pressures of standard sucrose solutions.

whatever in the absence of bivalent cations on the process of swelling of the mitochondria in relation to the decreasing concentrations of sucrose alone, whereas it precludes the deviations caused by the addition of calcium, as would be anticipated from its specific chelating action.

When the mitochondria are suspended in potassium chloride, a large number of crescents are present, even at a concentration far above the

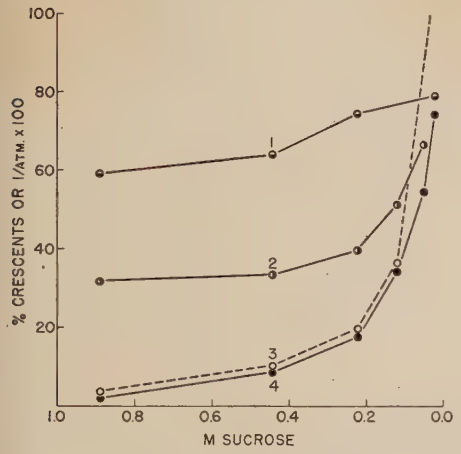

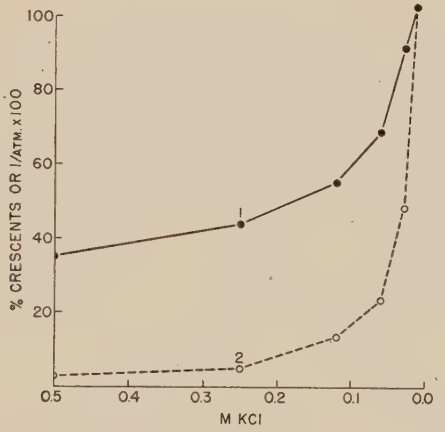

Textfig. 1 (left). Relationship between the morphology of the mitochondria and the molarity of sucrose. The ordinate represents the percentage of the crescent forms in the population of mitochondria in the presence of 0.012 M Ca^{++} (1) and 0.012 M Mg^{++} (2) and without additional ion (4) in various concentrations of sucrose. Reciprocals of the osmotic pressure of the sucrose solution (1/atm × 100) are shown in (3).

Textfig. 2 (right). Relationship between the morphology of the mitochondria and the molarity of KCl. The mitochondria were isolated in 0.88 M sucrose, resuspended in 0.5 M KCl and transferred into various concentrations of KCl: 1) the percentage of crescents in various concentrations of KCl and 2) the calculated osmotic pressure of the KCl solution.

"isotonic" level (Textfig. 2), demonstrating that the osmotic behavior of the mitochondria is far from perfect in a solution of this eletrolyte. The general pattern of the curve is remotely similar to that of the reciprocals of osmotic pressure as calculated theoretically, but at a higher concentration of KCl the number of crescents widely deviates from the trend of the osmotic pressure established with sucrose.

To ascertain whether the formation of the swollen forms of the mitochondria is related to a denaturation of their protein component, free sulfhydryl groups of the suspensions were determined in preparations at varying sucrose concentrations. No SH-groups are detected in the fresh mitochondria suspended in sucrose or water when all the mitochondria are extremely

swollen, although 1.0 ml of an original suspension of the mitochondria contains 0.504–0.669 μM of SH-groups after it has been denatured by a saturated urea solution. This observation establishes that swelling of the mitochondria due to the decreasing sucrose concentration is not related immediately to denaturation of their protein component as measured by the liberation of the bound sulfhydryl groups.

Effects of pH of the medium on the morphology of the mitochondria. The mitochondria are suspended in 0.25 M sucrose or 0.5 M KCl containing acetate barbiturate buffer at various pH's in order to study the effects of varying pH's on the morphology of the mitochondria. Table II shows the pH's of the medium before and after addition of the mitochondrial suspension. In either medium the mitochondria tend to shift the pH of the medium towards neutrality, indicating that the mitochondria act as effective buffers. Textfig. 3 shows the percentage of crescent forms at various pH levels of the medium. The number of crescents does not vary greatly until the pH reaches 9.0 when all the mitochondria become crescents. A differential count of the mitochondria below pH 4.0 is impossible because of agglutination by the granules.

Although the contours of the mitochondria vary only slightly at various pH levels below pH 9.0, their sizes are remarkably different. An accurate measurement of the size of the mitochondria is difficult by the present technique, but the differences can be seen clearly under the phase microscope. At pH 5.0 all the mitochondria are many times smaller than those suspended in a medium at the neutral pH; tiny spheres and bent rodlets are numerous

Table II

The buffering action of mitochondria at different pH's.

Suspending media	0.25 M sucrose		0.5 M KCl	
Mitochondria added*	0	+	0	+
pH observed	3.94	4.40	4.98	5.28
	5.08	5.30	6.02	6.13
	5.98	6.12	6.93	7.20
	7.02	6.90	7.92	8.03
	8.00	7.50	9.50	8.50
	9.02	8.35	11.00	10.10

* The suspensions were held for 30 minutes in the buffer at 21°C before readings were taken with a Beckman glass electrode pH meter.

even in saline, whereas the few crescents are much smaller than usual. As the pH rises, the size of the mitochondria also gradually enlarges. When the pH increases above 9.0, all the mitochondria become giant crescents many times larger than those at the slightly lower pH's. Some mitochondria assume bizarre forms, especially in the 0.5 M KCl medium. On drawing a drop of 1.0 M sucrose onto the slide from the edge of the cover slip, the

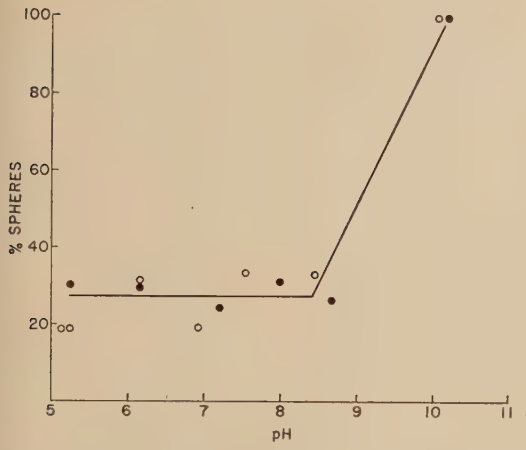

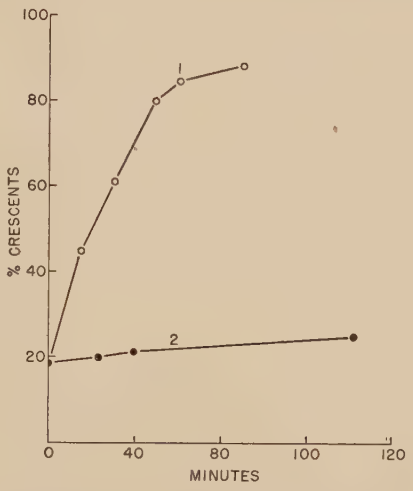

Textfig. 3 (left). Effects of pH of the medium on the morphology of the mitochondria. The percentage of the spherical forms in the population of mitochondria suspended in 0.25 M sucrose (solid circles) and 0.5 M KCl (open circles) at various pH's is shown on the ordinate.
Textfig. 4 (right). Thermal swelling of the mitochondria. Formation of crescents when the mitochondria in 0.25 M sucrose medium in the absence (1) and presence (2) of 0.001 M sequestrene is shown with regard to time of incubation at 30°.

grossly enlarged crescents in an unfixed 0.5 M KCl preparation at pH 10.1 become one-fourth to one-eighth the size they were before addition, although the shape of the crescents remains the same. Neither rupture nor fragmentation of the mitochondria is observed under these conditions. This indicates that the size of the mitochondria is partly reversible, although the forms are permanently changed from rods to spheres by change in pH. The remarkable changes in size and shape of the mitochondria at pH's above 9.0 are not accompanied by denaturation of their protein component as measured by the liberation of the bound SH-groups or release of free amino groups. The increase of hydrions condenses, and the decrease disperses the structure.

Effects of temperature on the forms of the mitochondria. When mitochondria are incubated at 30° C, the crescent forms gradually increase in number, as

TABLE III

The influence of temperature and trypsin on the free α-amino groups of the mitochondria.

Mitochondria	Trypsin	Amino acid	Free α-amino nitrogen*		
			Minutes incubated		
			0	60	120
+	–	–	0.0	0.0	0.0
–	+	–	5.92	–	5.92
+	+	–	5.92	24.76	27.00
None	None	Lysine**	–	10.0	–
,,	,,	Glycine	–	9.8	–
,,	,,	Glutamic	–	9.6	–
,,	,,	Tyrosine	–	9.5	–
,,	,,	Alanine	–	9.7	–
,,	,,	Threonine	–	9.9	–
,,	,,	Glycylglycine		9.4	–
,,	,,	Gluthathione	–	9.0	–

Aliquots of 0.5 ml of mitochondrial suspensions in 0.25 M sucrose were incubated at 37°C for varying periods in the presence of 0.005 M $CaCl_2$ and of 0.0125 M barbiturate buffer at pH 7.6 with the addition of 0.4 per cent crystalline trypsin in some instances. Final volumes were 2.0 ml. As controls, free amino nitrogens of the mitochondria and the trypsin were determined and the recoveries from samples of purified amino acids assayed.

* Free amino nitrogen estimated in micrograms.

** Amino acids were employed in 10.0 micromole quantity and the α-amino nitrogens assayed as micromoles of ammonia derived from such quantity.

shown in Textfig. 4. The presence of sequestrene in the medium prevents thermal swelling of the mitochondria almost completely. Although the exact mechanism of the thermal swelling is not known, this experiment indicates that it differs in some respects from the swelling which occurs with osmotic transformation because sequestrene is without effect on the formation of crescents during the latter process.

The relation of thermal activation to the time of incubation is suggestive of an autolytic process associated with the activation of proteolytic enzymes. However, no increase of free α-amino groups (Table III) is detected after 60 minutes incubation at 37° C and in the presence of calcium, although the divalent ion initiates the expansion of the mitochondria and appearance of crescents. Trypsin under similar conditions causes both a release of detectable α-amino groups and the formation of giant crescents and vesicles.

Relationship between the ATPase activity and the morphology of the mitochondria. To determine the relationship between the morphology of the mitochondria under various osmotic conditions and their functional activity, ATPase activity of the suspension under these conditions is studied. When the mitochondria, isolated and suspended in 0.88 M sucrose, are transferred to assay systems containing lower concentrations of sucrose, a gradual rise

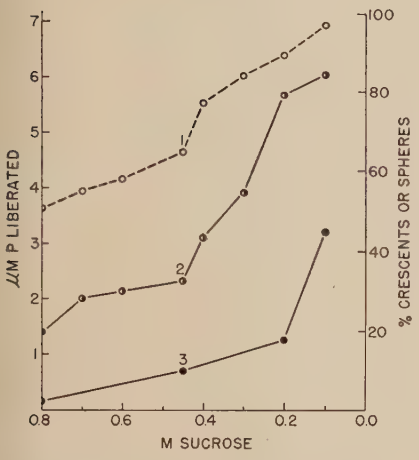

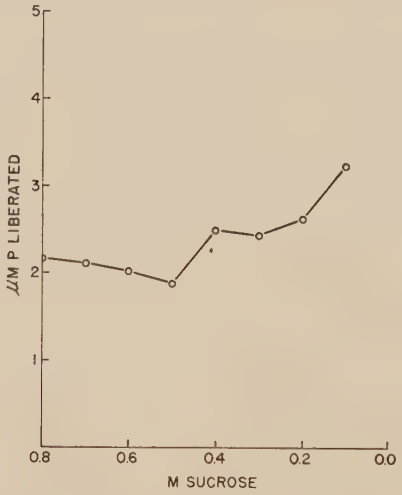

Textfig. 5 (left). Relationship between the adenosinetriphosphatase activity and the morphology of the mitochondria. The mitochondria were isolated in 0.8 M sucrose. Other conditions are as described in the text: 1) the ATPase activity of the mitochondria, 2) differential count of the spherical forms and 3) differential count of the crescents.

Textfig. 6 (right). Relationship between the adenosinetriphosphatase activity of the mitochondria and molarity of sucrose in the medium. The mitochondria were isolated in 0.25 M sucrose before being transferred to assay systems containing various concentrations of sucrose as described in the text.

of the ATPase activity is observed as the molarity of sucrose decreases (Textfig. 5). Two stages of activation of the ATPase are present. The activity is considerable at 0.88 M sucrose (cf. 2) and increases slightly as the concentration of sucrose falls from 0.8 to 0.45 M. At sucrose concentrations lower than 0.45 M there is a sharp rise of ATPase activity. The increases in ATPase activity and in the number of crescents are not parallel. But, when the dense spherical forms and crescents are enumerated together as total spherical forms, the curves representing the morphological changes and ATPase activity are almost exact replicas and indicate that the spherical units are more active. The ATPase activity is very different in mitochondria first

isolated and suspended in 0.25 M sucrose before transference to assay sytems as above. The stage of slow activation disappears, whereas the sharp rise of activity when the concentration decreases below 0.45 M persists (Textfig. 6), and no point of minimum activity at 0.2 M is detected.

Mitochondrial structure and activation of ATPase. The mitochondria have been subjected to transformers which cause drastic changes in morphology, such as suspension in large volumes of glass distilled water and in 0.5 M KCl at various pH's and prolonged shearing in the Waring blendor to determine whether such procedures release significant quantities of the enzyme and nitrogen into the suspending fluids. The results are shown in Tables IV–V in which the total units of active enzyme in each fraction are presented. The percentage distribution of the enzyme is so calculated that the sum of the activity of the corresponding mitochondrial residue and the supernatant is considered as 100 per cent. This diverges from the customary procedure of accepting the total activity of the original suspension as the basis for such calculations (33). The sum of the enzyme contents of the two fractions is then compared with the original suspension under "recovery".

Approximately 90 per cent of the ATPase activity remains attached to the mitochondrial residues after washing with large volumes of various media which cause drastic swelling of the mitochondria (Table IV). The amounts of the active enzyme in various suspending fluids do not differ from that of the control suspension in 0.25 M sucrose by more than 4 per cent. Considerable amounts of nitrogen are recovered from the supernatants of 0.5 M KCl suspension at alkaline pH, and by the solubility indices of nitrogen, the amount of protein extracted increases as the pH rises from 7.0 to 10.3. These observations conform with the difference in morphological appearances of the mitochondria in water and 0.5 M KCl and, since rupture of the units is not seen in either case, exclude the occurrence of lysis as an agency of protein release. The net-like form of mitochondria in KCl indicates a direct effect of the ions on the structure of the mitochondria. In the case of 0.5 M KCl, in which the amount of the extracted proteins increases as pH rises, there is a corresponding fall of the specific activity of the supernatants, whereas that of the residues increases disproportionately so that activation of the enzyme in the residue is not only a function of purification.

Mechanical fragmentation of the mitochondria considerably increases the ATPase activity of the suspension. The distribution of the ATPase between the fragmented mitochondrial residue and the supernatant in 0.25 M sucrose is practically the same as that of the unfragmented preparation. In 0.5 M KCl at pH's 7.0 and 9.0 the proportions of the enzyme in the supernatants are

TABLE IV

The distribution of ATPase activity and nitrogen in mitochondria and supernatant in various media.

Expt. No.	Medium	ATPase					Nitrogen				
		Original Suspension	Residue	Super-natant	Recovery	Solubility index	Original Suspension	Residue	Super-natant	Recovery	Solubility index
1	0.25 M sucrose										
	Total	721.4	791.3	61.4	858.7		9.81	9.02	1.36	10.38	0.151
	Per cent		92.9	7.1	119.0	0.077		86.8	13.20	105.80	
	Sp. act.	74.0	88.4	45.0							
2	H_2O										
	Total	530.0	678.2	37.8	656.0		8.40	8.36	0.683	9.047	0.082
	Per cent		94.2	5.8	123.6	0.062		92.40	7.60	107.70	
	Sp. act.	61.6	73.95	55.0							
3	0.5 M KCl (pH 7.0)										
	Total	562.5	590.0	73.6	663.6		7.58	7.27	0.90	8.17	0.124
	Per cent		89.1	10.9	118.0	0.125		89.00	11.00	107.6	
	Sp. act.	74.2	81.1	72.0							
4	0.5 M KCl (pH 9.0)										
	Total	405.0	438.0	52.1	490.3		7.56	6.75	1.845	8.59	0.273
	Per cent		89.3	10.7	121.1	0.119		78.50	21.50	113.00	
	Sp. act.	53.6	65.7	28.8							
5	0.5 M KCl (pH 10.3)										
	Total	440.0	483.0	52.6	535.6		6.35	4.46	1.987	6.447	0.447
	Per cent		90.17	9.83	121.9	0.109		69.30	30.70	101.30	
	Sp. act.	69.2	106.2	26.2							

TABLE V

Distribution of ATPase activity in mitochondria after communition in sucrose and potassium chloride.

Expt. No.	Medium	ATPase					Nitrogen				
		Original Suspension	Residue	Super-natant	Recovery	Solubility index	Original Suspension	Residue	Super-natant	Recovery	Solubility index
1	0.25 M sucrose										
	Total	1043.5	1093.4	85.1	1178.5		9.15	6.60	2.24	8.84	0.348
	Per cent		92.8	7.2	112.9	0.078		74.8	25.20	96.60	
	Sp. act.	114.0	165.7	37.9							
3	0.5 M KCl (pH 7.0)										
	Total	949.5	1020.0	181.0	1201.0		7.20	5.15	2.46	7.61	0.478
	Per cent		85.0	15.0	126.8	0.177		67.7	32.3	105.8	
	Sp. act.	103.2	198.2	73.1							
4	0.5 M KCl (pH 9.0)										
	Total	519.8	387.1	58.5	445.5		6.795	4.265	2.340	6.605	0.549
	Per cent		86.6	13.4	85.7	0.151		60.0	40.0	97.2	
	Sp. act.	76.5	83.5	25.0							

only 4.1 and 2.7 per cent higher than those from the intact suspensions. It is evident that although the structure of the mitochondria is destroyed, the bulk of the enzyme is still attached to the residue. Large quantities of nitrogen are now recovered from the supernatants after the mitochondria have been fragmented, especially in 0.5 M KCl at alkaline pH. The specific activity of the supernatants is even lower than that recovered from the corresponding unfragmented suspensions because the nitrogenous compounds extracted from the fragmented mitochondria are inert with regard to the ATP-ase activity. It is noteworthy that the fragmented residue is no longer osmotically reactive.

DISCUSSION

The present studies serve to establish the close correlation between the mitochondrial structure and the manifestation of ATPase activity. This complements the earlier study in which the essential relation of morphology and oxidative phosphorylation was demonstrated (12). Viewed from either aspect it becomes apparent that both the elaboration and the destruction of ATP are intimately associated with maintenance of structural integrity of the mitochondria. The findings of Raabflaub (29) and of Sacktor (32) are in agreement with the concept that ATP is critical for the preservation of the native compact structure of the mitochondria at raised temperatures. It is still obscure, however, whether the ATP acts directly on the structure as Raabflaub holds or whether it provides a depot for endergonic energy transfers essential for structure, as we preferred to believe previously (12). On the other hand, the present studies show that deviation from the rodlet configuration is attended by an enhanced ATPase activity even at very low temperatures when autolytic interference is minimized. Like the insect muscle mitochondria (31), those from pigeon muscle are not completely latent but manifest activity in 0.88 M sucrose. Chappell and Perry found only partial latency also (2).

Since the delay of mitochondrial degeneration is imperative for the perpetuation of function, it is pertinent to define clearly what constitutes the usual native intracellular configuration. The cytologists who have recorded the intracellular shape in fixed muscle and many other tissues depict typical rodlets (13, 15, 28, 30, 36). Recent cinematographic analyses by phase microscopy of isolated contracting myofibers (10) have confirmed the rod shape of the interstitial mitochondria of skeletal muscle. This has also been substantiated by electron microscopy (1, 17). The observations of Cleland and Slater (3) and of Watanabé and Williams (37), who employed mitochondria

isolated from cardiac and insect muscle respectively, are at variance with this. They suggest that the mitochondria are normally spherical. Although the approach of the latter workers affords evidence that proteins are beneficial and provide stability, it is probable that the discrepancy arises from the assumption by both groups that the intracellular osmolarity is similar to that of serum and consequently that mitochondria isolated in media isotonic with serum are close to normal; however, analyses of intracellular osmotic activity by Opie (25) indicate that the cytoplasm is strongly hyperosmotic compared with blood. The use of nonproteinaceous media isotonic with serum for the isolation of morphologically intact mitochondria therefore may stultify the objective, since such media expose the structures to hyposmotic stresses which have been shown to alter the shape considerably and lead to impaired enzyme activity.

Another problem is met with in the interpretation of the mechanism of mitochondrial swelling. It is becoming apparent that there are several varieties of swelling. One is associated with autolytic or thermal distention of the units, which is inhibited by citrate (11), chelating agents (3) and addition of ATP (29). The second is a distention induced by exposure of the mitochondria to hyposmotic conditions and has been regarded as independent of the former. Some difference between these is apparent in that certain agents which impede the thermal expansion of the mitochondria are ineffective against the osmotic swelling. It is probable, however, that the difference is not real and that the nature of the swelling in each instance depends upon a similar mechanism which is obscured by preconceived interpretations of mitochondrial structure.

One of the difficulties encountered in the analysis of swelling concerns the fine structure of mitochondria and resolves around the problem of a surface membrane and its permeability. It can scarcely be denied that a surface interface exists, for this was observed by Koelliker (19), but doubt has been expressed that such a surface manifests a semipermeability comparable to cellular membranes (5, 9, 29). In the present studies the dissimilar behavior of the mitochondria in the presence of electrolytes and sucrose might be interpreted as due to difference in rate of penetration of the two classes of compound through a membrane. This may be in part true but is probably an oversimplification. The influence of pH and electrolytes on the solubility of mitochondrial protein and enzymes indicates the participation of other forces in the reactivity and stability of mitochondrial structure. Whether such forces are concentrated approximate to the surface or distributed within a deeper framework is moot. The powerful dispersive

action of KCl on mitochondrial form and its ability to remove a considerable amount of protein substantiate the view that electrolytes labilize restrictive linkages and so induce the volume and morphological changes which exceed even those observed after immersion in distilled water. Contrary to the claims of Schneider (33), neither we nor Dianzani (5) have released significant quantities of protein or caused lysis by prolonged treatment with water. Sucrose and similar nonelectrolytes derive their osmotic potency not only by a slow penetration into the mitochondrial framework but also by their inert behavior toward mitochondrial constituents. The appearance of hiati in the structure still susceptible to osmotic shrinkage also prompts hesitancy in accepting the current hypothesis of the semipermeable membrane but would not conflict with the hypothesis of a mitochondrial gel. The latter type of structure could be affected by osmotic forces irrespective of such rents as we observed in the fabric (6), whereas gaps of microscopically visible dimension in a semipermeable membrane would be incompatible with its efficiency. The gel structure is in part supported by the dimensional responses of the mitochondria to changes in pH insofar as these imply that hydrogen bonds (7) may be important forces affecting the morphology, whereas participation of SH and peptide links are not demonstrable in the present studies. The increase of hydrions condenses the structure, as Watanabe and Williams also observed, whereas an increase of hydroxyl ions causes dispersion. Since excess potassium salt has a similar dispersive action, it merits consideration that both the potassium and hydroxyl ions displace hydrogen bonds essential to structural integrity. A similar displacement of bonds by hydration may play a role in the process of thermal dissolution of structure.

SUMMARY AND CONCLUSIONS

The mitochondria of pigeon skeletal muscle behave as almost perfect osmometers and reflect the osmolarity of sucrose solutions in a statistical manner which follows a pattern established by the reciprocals of the osmolarity. Deviation from the regular osmometric pattern is induced by transforming agents, e.g., the divalent ions Ca^{++} and Mg^{++}, by immersion in 0.5 M KCl, by exposure to thermal activation and by mechanical dispersion. The reaction of the suspending medium also independently alters the size and shape of the mitochondria.

Comminution of the mitochondria obliterates osmotic reactivity. This property is peculiar to the whole organelle, although it persists even under conditions in which the mitochondria assume an imperfect and defective

surface structure. Maintenance of osmometric responsiveness in mitochondria with perforated surfaces conflicts with the current theory that they possess semipermeable mitochondrial membranes. Other factors indicate that the structure and behavior of the mitochondria are primarily associated with a gel-like internal matrix.

The ATPase activity of the mitochondria is partly regulated by morphology. In the native rodlets it is cryptic and is activated by enspherulation and crescent formation. Fragmentation produces maximal activation of the dephosphorylation mechanism. A minimal release of the enzyme occurs with mechanical dispersion, whereas the activity is persistently associated with the insoluble residue of the comminuted organelles. Aging causes a considerable deterioration of the enzyme in the residue and slight alteration of the solubilized fraction.

The authors wish to thank Prof. D. Murray Angevine for his helpful interest. They also gratefully acknowledge the assistance of Mrs. Muriel Feigelson with the development of the technique of α-amino acid estimation and of Dr. Stanley Weinreb with the photography.

REFERENCES

1. Bennett, H. S., and Porter, K. R., *Am. J. Anat.*, **93**, 61 (1953).
2. Chappell, J. B., and Perry, S. V., *Biochem. J.*, **55**, 586 (1953).
3. Cleland, K. W., and Slater, E. C., *Quart. J. Microscop. Sci.*, **94**, 329 (1953).
4. Conway, E. J., Microdiffusion Analysis and Volumetric Error. Lockwood Crosby and Son, Ltd., London, 1947.
5. Dianzani, M. U., *Biochim. et Biophys. Acta*, **11**, 353 (1953).
6. Ferry, J. D., *Advances in Protein Chem.*, **4**, 15 (1948).
7. Frey-Wyssling, A., Submicroscopic Morphology of Protoplasm and Its Derivitives. Elsevier Pub. Co., N.Y., p. 129, 1948.
8. Harman, J. W., *Exptl. Cell Research*, **1**, 382 (1950).
9. —— *ibid.*, **1**, 394 (1950).
10. —— *Federation Proc.*, **13**, 430 (1954).
11. Harman, J. W., and Feigelson, M., *Exptl. Cell Research*, **3**, 47 (1952).
12. —— *ibid.*, **3**, 509 (1952).
13. Harman, J. W., and Osborne, U. H., *J. Exptl. Med.*, **98**, 81 (1953).
14. Johnson, M. J., *J. Biol. Chem.*, **137**, 575 (1941).
15. Jordon, H. E., *Anat. Rec.*, **16**, 217 (1919).
16. Keilley, W. W., and Keilley, R. K., *J. Biol. Chem.*, **200**, 213 (1953).
17. Kisch, B., and Bardet, J. M., Electron Microscope Histology of the Heart. Brooklyn Medical Press, N.Y., p. 70, 1951.
18. Kitiyakara, A., and Harman, J. W., *J. Exptl. Med.*, **97**, 553 (1953).
19. Koelliker, A., *Z. wiss. Zoöl.*, **47**, 689 (1888).
20. Laties, G. G., *Plant Physiol.*, **28**, 557 (1953).
21. Lowry, O. H., and Lopez, J. A., *J. Biol. Chem.*, **162**, 421 (1946).
22. Macfadyen, D. A., *ibid.*, **153**, 507 (1944).
23. Mirsky, A. E., *J. Gen. Physiol.*, **66**, 709 (1941).
24. Morse, H. N., and Morse, H. V., *Am. Chem. J.*, **39**, 667 (1908).
25. Opie, E. L., *J. Exptl. Med.*, **99**, 29 (1954).

26. Palade, G., *ibid.*, **95**, 285 (1952).
27. Porter, K. R., and Kallman, F., *Exptl. Cell Research*, **4**, 127 (1953).
28. Prenant, A., *J. Anat. Physiol.*, **47**, 647 (1911).
29. Raabflaub, J., *Helv. Physiol. Pharmacol. Acta*, **11**, 157 (1953).
30. Retzius, G., *Biol. Untersuch.*, N. F., **1**, 51 (1890).
31. Sacktor, B., *J. Gen. Physiol.*, **36**, 371 (1953).
32. —— *ibid.*, **37**, 343 (1954).
33. Schneider, W. C., *J. Histochem. Cytochem.*, **1**, 212 (1953).
34. Sorof, S., and Cohen, P. P., *Exptl. Cell Research*, **2**, 299 (1951).
35. Slater, E. C., and Cleland, K. W., *Biochem. J.*, **53**, 557 (1953).
36. Villmitjana, L., *Bol. Real. Soc. Espan. Hist. Nat.*, **47**, 283 (1949).
37. Watanabe, M. J., and Williams, C. M., *J. Gen. Physiol.*, **37**, 71 (1953).

VII. THE RELATIONSHIP BETWEEN THE CONTROL OF STRUCTURE AND THE DINITROPHENOL STIMULATION OF ADENOSINETRIPHOSPHATASE IN LIVER MITOCHONDRIA[1]

JANE C. KALTENBACH and J. W. HARMAN

Received July 26, 1954

A reciprocal influence of structural integrity and oxidative phosphorylation has been established for mitochondria of cardiac and skeletal muscle. Conditions favorable to the perpetuation of efficient oxidative phosphorylation are also responsible for the stabilization of mitochondrial structure (6). Conversely, the agents most competent in uncoupling the phosphorylation have considerable effect on the structure and rapidly induce degenerative transformations. Insofar as these transformations are also associated with an enhanced ATPase[2] activity in muscle mitochondria (7), the precise site at which the deleterious agents initiate their action is obscure. Any of the enumerated points, i.e., the ATPase, the failure of oxidative phosphorylation and the direct dissolution of structure, may represent the principal primary operative location of the transforming agents. On the other hand, the agents may simultaneously affect all locations. Although studies of muscle mitochondria provide evidence for a close correlation between enzymatic activity and

[1] Studies supported by the Life Insurance Medical Research Fund and the Muscular Dystrophy Associations of America.

[2] The following abbreviations are used: ATP, adenosine triphosphate; ADP, adenosine diphosphate; AMP, adenosine monophosphate; DNP, 2,4 dinitrophenol; ATPase, adenosine triphosphatase, which represents in this study the sum of the reactions involved in the splitting of inorganic phosphate from ATP and not a solitary specific enzyme.

structure, the earliest changes are partly complicated by a high rate of ATPase activity, even in the "resting" state (3, 7, 18). This may be attributable to the loose structure and the absence of any well defined surface membranes in muscle mitochondria, as indicated by both phase and electron microscopy (5), since the ATPase is firmly bound to the hull of the mitochondrion.

In other tissues, however, the ATPase is less apparent in "resting" mitochondria and in carefully prepared suspensions may be completely inert. Imposition of conditions which are designed to damage the mitochondria concomitantly evokes appearance of the ATPase. The application of the stressing agent may be graded in intensity and duration so as to vary the degree of ATPase response. In view of this "latency" of the contained ATPase, the liver mitochondria are more suitable for a study of the site at which transforming agents impose their effects on the integrated system. The present communication is directed to the elucidation of the mechanism by which the latent ATPase of liver mitochondria is activated under the influence of various transforming agents. Especial interest is given to the mode of action of 2,4 dinitrophenol because of its established effect on both oxidative phosphorylation and ATPase.

METHODS

Preparation of mitochondria. The mitochondria were prepared from the livers of Sprague-Dawley rats weighing about 200 grams and fed *ad libitum*. They were killed by cervical dislocation. The excised livers were rapidly weighed and immersed in 0.5 M sucrose ice slush and small fragments successively homogenized with a teflon homogenizer in 0.5 M sucrose at pH 7.2. Tissue fragments were of such size that 10 complete strokes of the pestle provided dispersion. The completed homogenate was made up as a 10 per cent suspension and submitted to differential centrifugation (19). Coarse cell clumps, nuclei and connective tissue were removed by centrifugation at 1,700 × g for 10 minutes in the angle head of a PR1 International Refrigerated Centrifuge. This residue may be reprocessed to augment the yield as needed. Combined supernatants from the first centrifugation process are evenly divided between the cups and then spun at 3,500 × g in the multi-speed attachment for 10 minutes. Before the residue is harvested the supernate is decanted, and the loose fluffy layer (16) is swirled up in a small volume of 0.5 M sucrose and discarded. The residue is then rewashed, and at this stage the 0.5 M sucrose in some cups may be replaced by either 0.25 M sucrose or distilled water. After recentrifugation at 3,500 × g for 10 minutes in the multispeed attachment, the residues were resuspended in a small volume of either 0.5 M sucrose or the alternative suspending media so that 1 ml contained approximately 1.5 mg of mitochondrial nitrogen.[1] During the preparative

[1] In view of the variable mitochondrial density from one preparation to another the expedient of mitochondrial equivalents (16) was deemed less quantitative than an exact estimate of the nitrogen contents and assessments of specific activities.

procedures, cytological control examinations by phase microscopy routinely checked the various steps to ensure the clean separation of the requisite mitochondrial fractions.

Assay of enzyme activity. The ability of mitochondria to dephosphorylate ATP[1] was studied under standard conditions in a medium containing either 5 or 15 μM ATP and a final sucrose concentration varying between 0.01–1.0 osmolarity. A pH of 7.2 was maintained with 0.001 M sodium veronal buffer, and magnesium was usually added to a final concentration of 3.3×10^{-4} M as magnesium chloride. A volume of 1.4 ml of such media was preincubated in a Dubnoff apparatus in open 20 ml beakers at 30° C for 5 minutes before addition of 0.1 ml of ice cold mitochondrial suspension. The reaction proceeded for the required interval and was stopped by the addition of trichloracetic acid to a final concentration of 5 per cent. The protein precipitate was removed by centrifugation and the inorganic phosphate determined by the procedure of Lowry and Lopez (14) with a Coleman Universal Spectrophotometer No. 14. The protein nitrogen was determined with direct nesslerization by the method of Johnson (9).

Cytologic technique. In order to correlate the enzymatic activity with mitochondrial morphology, parallel sets of beakers were similarly prepared as above. At time of removal of beakers for enzyme analysis, parallel suspensions were fixed with an equal volume of 11.2 per cent formalin pH 7.3 and set aside for differential counts. In a previous report the efficacy of formalin in the preservation of mitochondrial form was established (7). In the current studies the fixative power of the formalin was routinely checked by a differential count on the unfixed and preserved suspensions. The relationship between the enzymatic activity and the mitochondrial morphology was investigated by phase microscopy and electron microscopy. The differential counts of the formalin fixed suspensions were performed as described in preceding studies (6, 7). The forms most especially distinguished were rodlets, dense spheres and crescents. For phase microscopy a Spencer turret condenser was used, and the clearest distinction between forms was possible with the 1 mm dark contrast L lens with a 100 watt Mikrack zirconium arc lamp as light source. For electron microscopy the suspensions were fixed in 2 per cent buffered osmium tetroxide (15). They were washed 3 times and suspended in distilled water. A drop was placed on the Formvar coated screen, allowed to dry and subsequently shadowed with uranium. Representative pictures were made with an R.C.A. Universal type electron microscope.

RESULTS

The influence of magnesium on ATPase activity. In view of the considerable specific stimulatory action of Mg^{++} ions on the ATPase of muscle mitochondria (12) and that of liver (11), it is necessary to determine the optimal concentration of the ion for the current standard assay system. It is observed that without the ion there is after 15 minutes incubation at 30° C with 15 μM ATP a slight liberation of inorganic phosphate (Textfig. 1). As

[1] ATP was a commercial product procured from Pabst Brewing Co., Milwaukee, Wisconsin, as the disodium salt and contained 0.04 μM inorganic phosphate per mgm as impurity.

the level of magnesium is elevated, the rate of dephosphorylation is slightly augmented to a maximum occurring in the region of 10^{-4} to 10^{-3} M concentration, above which there is a decline to the initial activity of the ion free system at 6.6×10^{-2} M concentration. The curve of activity applies to the mitochondria suspended both in 0.5 M and 0.25 M sucrose with occasional slight variation in the optimal peak from one preparation to another. These prep-

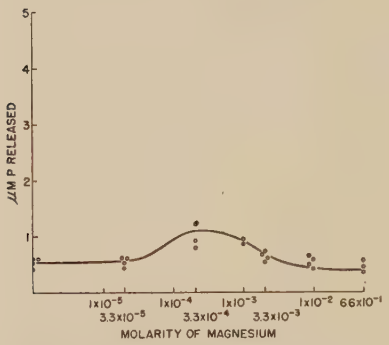

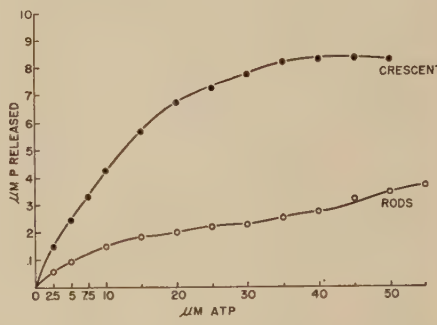

Textfig. 1 (left). The velocity of ATPase as a function of magnesium concentration. Mitochondria suspended in 0.25 M sucrose are added to cups with a 1.5 ml final volume, a pH maintained at 7.2 by veronal buffer and the osmolarity held at 0.25 M by addition of appropriate amount of sucrose. There is 0.7 mgm mitochondrial nitrogen per cup. ATP content of cups is 15 μM. Incubation for 15 minutes at 30° C. Curve represents average of 4 experiments.
Textfig. 2 (right). Comparison of the effect of concentration of ATP on the activity of ATPase in crescent and rod mitochondria. Complete system contains 3×10^{-4} M magnesium, 0.01 M veronal buffer, pH 7.2 and sufficient sucrose to maintain osmolarity at 0.5 M in cups containing rodlets in a final volume of 3.0 ml. Incubation for 5 minutes at 30° C.

arations are not entirely inert, as found by other observers. The level of magnesium chosen for subsequent experiments was 3×10^{-4} M because it represented the maxima for mitochondria in both molarities, although the activity in the 0.5 M sucrose consistently exceeds slightly that at 0.25 M level.

Relationship of mitochondrial structure and activity. It is observed that in 0.5 M sucrose at 0° C the mitochondria maintain a rodlet shape. If a portion of such a suspension is exposed to an environment of distilled water and held at 37° C for 30 minutes prior to examination, all the mitochondria are swollen and converted into crescents. Under these conditions of hypotonicity or thermal exposure or a combination of both, the mitochondria are transformed to crescents, approaching but not attaining dissolution. In view of the different states of dispersion, it might be anticipated that the 2 types of mitochondria require different concentrations of ATP to achieve saturation of the dephosphorylation mechanism. In Textfig. 2 there is demonstrated a behavioral disparity between rods and crescents, which indicates how rapidly the cres-

cents are saturated by substrate and reach an asymptote at a level of 35 μM ATP. On the other hand, the rodlets are affected in a more linear manner by crowding them with substrate molecules, split off orthophosphate more slowly and do not approach an asymptote even at a very high substrate concentration. This ability to saturate the crescents or disperse units but not the rods or dense units supports the view that an accessibility barrier or a concentration gradient operates in the latter and is obliterated in the crescent by the process of enspherulation and swelling.

As a further probe into this relationship, an alternative mitochondrial-substrate relationship was investigated. A constant substrate level was maintained and ascending concentrations of crescents and rodlets employed. It is seen (Textfig. 3) that the 2 forms again diverge in pattern. That the rods, in this instance at a low concentration, attain an even plateau of dephosphorylation supports the previous observation and emphasizes the importance of a concentration gradient in the regulation of their dephosphorylation mechanism. In the crescents, on the other hand, the process of dephosphorylation is not so impaired by a great excess of mitochondria, even when the saturation ratio established previously is not maintained. Since the extent of dephosphorylation manifest in Textfig. 2 is nearly approximate to the complete removal of 1 equivalent PO_4 from the substrate at very low levels of substrate only and inhibition is considerable at the higher ATP concentrations, it is apparent that the superabundant ATP suppresses the dephosphorylation process. When the relationship is reversed and the substrate made the limiting factor, a second phase in the dephosphorylation sequence is revealed with the splitting of the second equivalent (Textfig. 3) when the inhibition arising from excess substrate is not participating.

The relative velocities of the mechanism in the crescents and rodlets is exemplified in Textfig. 4. Within 15 minutes of incubation the thermally induced crescents, which are very swollen mitochondria, have reached a dephosphorylation of one-half an equivalent. This extent of activity necessitates a period of 30 minutes by crescents formed in cold distilled water, but the rodlets require an interval of over two hours to approximate a comparable release of orthophosphate. From the initial velocity and the sudden cessation of activity in the crescents, it is clear that enzyme substrate reaction is immediate and adequate and is rapidly suppressed by events during the splitting of the first equivalent phosphate, as already noted previously. Other workers have encountered a similar retardation and attribute it to accumulation of ADP (11). In the rodlets a slower velocity precludes the appearance of the suppressive phenomenon.

The connection between the ratio of substrate to mitochondrial nitrogen (S/N) and the manifestation of the suppression of dephosphorylation indicated that study of the velocity at a lower ratio might supply further information. At a level of 5 μM ATP and a suitable S/N ratio the suppression vanished as the mechanism accelerated. The complete dephosphorylation of the first equivalent is accomplished by the crescents in 15 minutes and by the rodlets

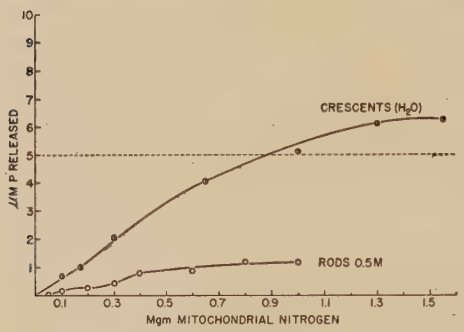

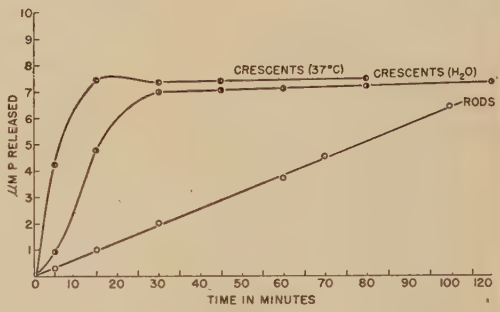

Textfig. 3 (left). Influence of mitochondrial morphology on ATPase activity as a function of mitochondrial concentration. System contains 5 μM ATP, 3×10^{-4} Mg^{++}, veronal buffer, pH 7.2, 0.001 M and sucrose in rod containing cups to maintain a 0.5 M concentration in a final volume of 3 ml. Incubation for 5 minutes at 30°C.

Textfig. 4 (right). Relative velocities of ATPase activities in crescents and rod mitochondria. System contains 15 μM ATP, 3×10^{-4} Mg^{++}, veronal buffer, 0.001 M, pH 7.2 and adequate sucrose to maintain the osmolarity of 0.5 M in cups containing rods. Final volume is 3.0 ml. Incubation for times indicated on abscissa at 30°C. Mitochondrial nitrogen per cup is 0.7 mgm.

in 90 minutes (Text-fig. 5). After a lag period of 35 minutes the second equivalent is split off slowly and is completely removed by 120 minutes. An addition of 5 μM AMP during the lag phase suppresses the second period of dephosphorylation. The occurrence of a lag phase and the parallel behavior observed in muscle systems suggest the possibility of a myokinase reaction.

During the foregoing enzymatic analysis the cytological examinations of the incubated suspensions confirm the maintenance of the typical forms throughout the duration of the experiments. It is of significance that over a period of 120 minutes in the various experiments on rodlets the percentage of degenerative forms, i.e., crescents, never exceeded 9 per cent. In view of earlier studies (6) it is probable that the extramitochondrial ATP contributed much to this stability.

It, at first hand, seems as if the structure of the mitochondria defines the activity of the dephosphorylation mechanism. Studies such as those by Berthet *et al.* (2) and others (4), however, introduce the possibility that dispersion of mitochondrial structure may facilitate solubilization of mitochon-

drial constituents and the enzymes which dephosphorylate ATP. This hypothesis is tested by a centrifugal separation (at a force of 20,000 × g applied for 60 minutes) of the supernates and residues from both water suspended and sucrose suspended mitochondria. Ample time is provided for equilibration of the systems and for discharge from the mitochondria of such components as may be released by exposure to distilled water. The considerable

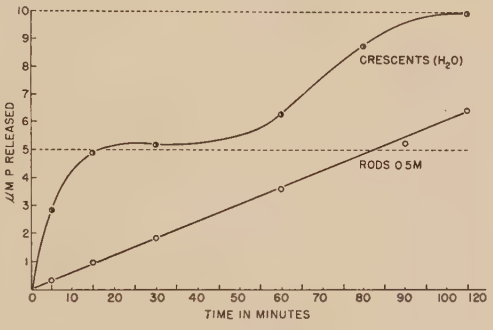

Textfig. 5. Relative velocities of mitochondrial ATPase of rods and crescents at a low substrate concentration. System as in Textfig. 4 except that 5 μM ATP is used. Lines horizontal to abscissa at 5 and 10 μM levels indicate first and second equivalent PO_4 molecules of ATP. Incubation as indicated on abscissa at 30° C.

activation of dephosphorylation ensuing upon crescent formation is demonstrated in Textfig. 6. This activation is not associated with a release of significant quantities of either enzyme or nitrogenous substances into the supernate, which precludes lysis as a process by which the rate of dephosphorylation is enhanced and points to unfolding of mitochondrial structure as the agency responsible.[1] Further evidence of the critical implication of morphology in the activation process is provided by the effect of repeated washing on the mitochondrial activity and structure, since the additional manipulation during the period of preparation causes both an increase in crescent formation and a considerable enzyme activation without liberation of soluble enzyme. Since relatively low gravitational forces are used for separation, it is unlikely that fragmentation contributes to the effect.

If the dephosphorylation system is thus firmly attached to the mitochondrial structure and is apparently influenced by the state of dispersion of the latter, the degree of enzyme activity may be modified by alteration of the structural state. The application of this association is investigated, as exemplified in Textfig. 7. Prolonged storage and manipulation of the mitochondria in distilled water over a period of 140 minutes produces an increase of over 200 per cent in specific activity compared with units isolated in 0.5 M sucrose.

[1] The process of hyposmotic lysis in mitochondria has been reported by several observers (2, 4) with the use of indirect techniques. By direct microscopy and mitochondrial enumeration this process cannot be substantiated. Application of fragmentation procedures are required for release of "soluble" mitochondrial proteins (7).

Resuspension of the mitochondria in 1 M sucrose subsequent to hyposmotic activation converts the bloated units to irregular and denser rodlets which have an activity appreciably less than the parent suspension in 0.5 M sucrose. Since, as shown above, no enzyme and little nitrogen are lost by hyposmosis, the comparison between different suspensions on the basis of specific activity is valid and necessary. The series of structural alterations associated with

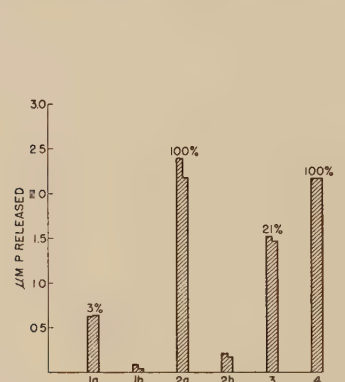

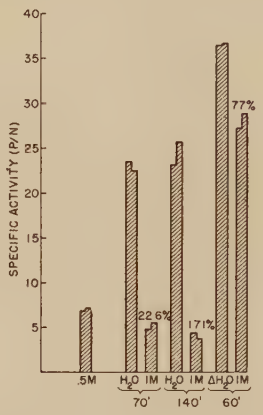

Textfig. 6 (left). Effect of hyposmotic transformation on the distribution of ATPase between supernatant and mitochondria. System and incubation as in Textfig. 5. 1a and b represent residues and supernatants respectively of mitochondria in 0.5 M sucrose and 2a and b for the mitochondria suspended in water. 3 is a thrice recentrifuged mitochondria suspension in 0.5 M sucrose, and 4 is a suspension of thrice washed crescents. Figures above the columns signify the percentage of crescents in the suspension. Double columns represent the duplicate analysis.

Textfig. 7 (right). Effect of osmolarity on the velocity of mitochondrial ATPase. Mitochondria isolated in 0.5 M sucrose are resuspended in water at 2°C for the period specified and then returned to an osmolar environment of 1.0 M sucrose. Similar exposure is made to water at 37°C (ΔH_2O) for 60 minutes. Figures above 1.0 M columns indicate the percentage of crescents in such suspensions. System as in Textfig. 6 with incubation for 5 minutes at 30°C. Double barred columns indicate duplicate runs. P/N on ordinate signified specific activity, i.e., μM P released per mgm nitrogen. The broken peak at the top of each column represents the difference in check runs.

these procedures are depicted in Figs. 1–4, which show the electon micrographs of the initial dense rodlets (Fig. 1) and crescents, which forms are considerably enlarged owing to dispersion in water (Figs. 2 and 3). The disperse forms are not reconverted by the 1 M sucrose into the original shape but assume the appearance of fuzzy elongated rods which have variable areas of condensation. The tremendous swelling caused by aqueous transformation has induced irreversible alterations in form which prevent perfect resumption of the initial shape (Fig. 4). A combination of thermal and osmotic transformation accomplished considerably more dispersion of the mitochondrial hull with shredding and fragmentation of the gel. This is also attended by

both a greater augmentation of dephosphorylation and a more limited reversibility. In the latter instance (Textfig. 7) the crescent population is reduced to 77 per cent and the specific activity to 76 per cent, whereas in the mitochondria distended in cold water the reductions in crescents and activity are 23 per cent and 22 per cent respectively. The rate of dephosphorylation is governed by the structural state of the mitochondria and can be reversibly altered so long as the mitochondria remain responsive to the manipulative procedures.

The enzymatic control exerted by the structural state of the mitochondria, as demonstrated above, prevails over a wide range of osmolarity. The previous analyses suggest that a decline in environmental osmolarity is uniformly attended by an increase in rate of dephosphorylation. The application of extremes of osmolarity favors this simple relationship; however, the establishment of intermediate molarities detects departure from a smooth ascent in dephosphorylation and reveals a plateau of high activity between 0.374 M to 0.65 M sucrose, a sharp minimum at 0.125 M sucrose and a steep rise of activity between 0.125 M and the point of minimal molarity. The constancy of these points in all our osmolar curves (Textfig. 8) and the observations of others (16) prompt analysis of the concomitant cytological condition of the mitochondria over the range of molarities studied. In Textfig. 9 the structural variations are observed as the reciprocal distribution between rodlets, spherical dense and crescent mitochondria. Until the molarity drops to 0.375 M sucrose, the mitochondria are almost exclusively rodlets (90 per cent) with a small accompaniment of dense spheres. No special qualitative or statistical alteration in the mitochondria is observed over the higher range of 0.35 M to 1.0 M sucrose to account for the enzymic plateau and drop of enzymatic activity seen at 0.80 M. The rodlets are slightly blunter at 0.5 M sucrose than elsewhere, and longer rodlets prevail at 1.0 M sucrose. Below the 0.375 M sucrose the rodlets are progressively converted to small dense spheres until they constitute about 75 per cent of the mitochondrial population at 0.125 M sucrose, where the decline in enzyme activity reaches its lowest value except for that at 0.88 M. Further decrease of molarity is associated with a proportional replacement of the dense spheres and rodlets by crescents, which rapidly increase in number until they represent all the units at the lowest attainable molarity. The progressive increment of crescents is paralleled by a similar upswing of enzymatic activity. The decline of activity between 0.375 M and 0.125 M sucrose represents a transformation of rodlets to dense spheres, which are much less active than either the preceding rodlets or ensuing crescents. The ability of enspherulation to depress

1

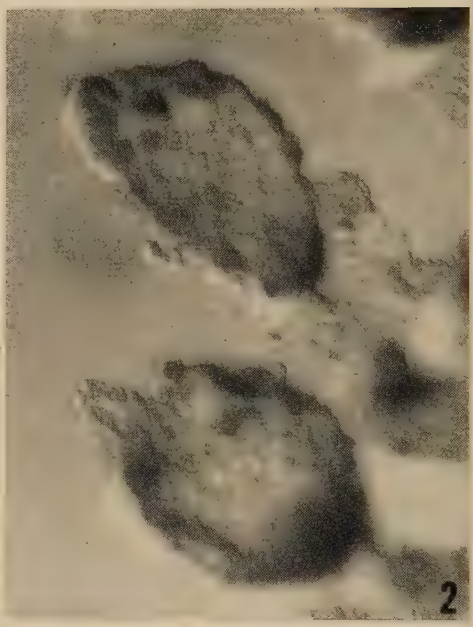
2

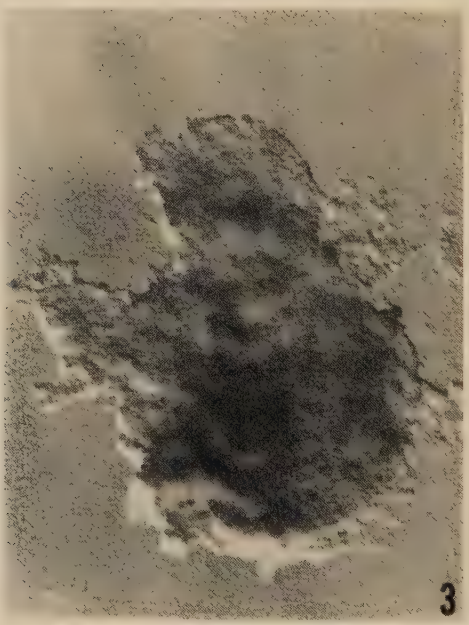
3

4

TABLE I

Influence of sucrose molarity and magnesium concentration on DNP stimulation of ATPase activity.

Molarity magnesium	Specific activity**			
	0.25 M sucrose		0.5 M sucrose	
	− DNP	+ DNP*	− DNP	+ DNP*
0	3.24	15.5	2.71	3.24
3.3×10^{-5}	3.32	16.5	3.08	3.32
3.3×10^{-4}	6.45	20.1	5.15	6.45
9.9×10^{-4}	6.16	18.3	6.65	6.16
3.3×10^{-3}	6.30	15.5	3.85	6.30
9.9×10^{-3}	4.17	15.2	4.06	4.71
6.6×10^{-2}	3.32	4.17	2.54	3.32

* DNP = 2.75×10^{-5} M.

** Specific activity is the amount of phosphorus, expressed as μM, released in 5 minutes by 1 mg nitrogen equivalent of mitochondria. Incubation for 5 minutes at 30°C. Final volume is 3.0 ml and ATP concentration 15 μM.

the dephosphorylation suggests that the enzymatic mechanism lies not at or close to the surface but is situated in the depth of the mitochondrion. Location of the enzymes at the surface would only slightly affect the enzyme substrate interaction whatever the shape of the mitochondrion, whereas a deeply situated enzyme is more inaccessible as the container is converted from a flat rodlet to a sphere. Whatever the precise relationship is on a molecular level, it is apparent that the structural state and enzymatic activities are replicas.

Effect of dinitrophenol on structure and dephosphorylation. During the preceding studies on the interrelation between structure and enzymatic de-

Fig. 1. The mitochondria are dense short rodlets which cast shadows indicating the height. They are suspended in 0.5 M sucrose and fixed in 1 per cent buffered osmium tetroxide. Magnification 22,500 ×.

Fig. 2. Mitochondria prepared in 0.5 M sucrose and finally suspended in distilled water are depicted after osmium fixation, Great enlargement and loss of height are conspicuous, as only minimal shadows are cast. Surface is granular and has no abrupt interface. There is a rolled edge. Magnification 22,500 ×.

Fig. 3. Mitochondria prepared in 0.5 M sucrose and allowed to stand for 30 minutes in water at 37°C before fixation with osmium. Flattening is extreme with only a faintly suggested shadow. The edges are ragged, fragmented and the surface still granular. Magnification 22,500 ×.

Fig. 4. Mitochondria prepared in 0.5 M sucrose were passed through distilled water for 30 minutes at 37°C and resuspended in 1.25 M sucrose. Fixation was with 1 per cent buffered osmium tetroxide. The elongated condensed rodlets with crenated surface relief comprise the mitochondrial population. Assumption of height is indicated by the shadow cast. Compare this mitochondrion with that depicted in Fig. 1, from which it is derived. Although osmotic shrinkage allows resumption of the rodlet configuration, the return to the initial small size is not realized. Magnification 22,500 ×.

phosphorylation, a salient difference was seen between the mitochondria suspended in various media. It is also apparent (Table I) that the osmolarity of the medium conditions the response of mitochondria to stimulation by DNP. The various levels of Mg^{++} ions alter the extent of stimulation produced by DNP on mitochondria in 0.25 sucrose, but in 0.5 M sucrose the mitochondrion is inert to the presence of 2.75×10^{-5} DNP regardless of the Mg con-

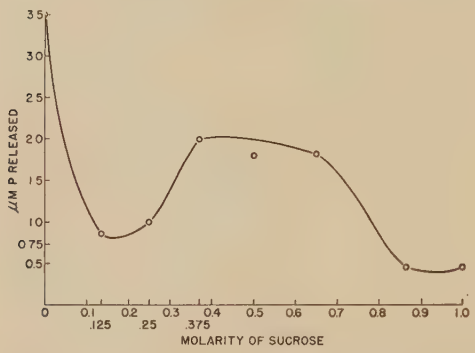

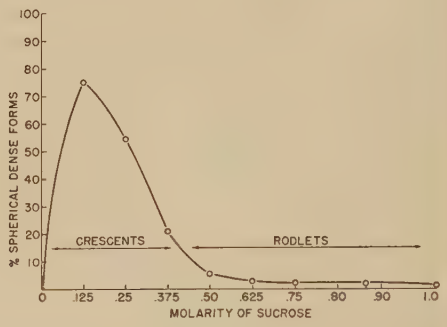

Textfig. 8 (left). Effect of osmolarity on the velocity of mitochondrial ATPase. System as in Textfig. 5.
Textfig. 9 (right). Effect of osmolarity on mitochondrial morphology. Curve represents percentage of spherical dense forms. Horizontal arrowed bars indicate zones where rods and crescents constitute significant component of population.

centration. A more extensive survey of the relation between osmolarity and response to DNP is represented in Textfig 10. In the range of osmolarity above 0.375 M sucrose, the mitochondria are inert toward the DNP. Below this molarity the DNP produces a stimulation which reaches a maximum at 0.125 M and then decreases proportionately as the control activity rises with the expected appearance of crescents at the lower molarities. The interval of osmolarity where DNP augments the dephosphorylation is the span in which the mitochondria are converted from rodlets into spherical dense and finally crescents (Textfig. 9). As is seen in Textfig. 10, the initiation of crescent formation appears at a higher osmolarity with 2.57×10^{-5} M DNP and runs parallel with the extent of dephosphorylation. At the 0.5 M level of sucrose the DNP depresses the enzyme reactions but is not associated with any peculiar alteration of form.

The variation of response to DNP in relation to the molarity and morphology indicates a critical influence of pretreatment. With this in mind the reactivity of the mitochondria, both structurally and enzymatically, was examined in the sensitive range of osmolarity. In order to clarify the precise relation of form and activity, two varieties of mitochondria are

exposed to a wide range of DNP concentrations. One suspension had been preincubated at 37° C for 30 minutes; the other held at 0° C until used. It is significant that the maximal effective stimulation of the dephosphorylation by DNP is realized at different concentrations of the compound for the 2 preparations of mitochondria and that curves of enzyme activity are exact replicas of the fluctuations in crescent population (Textfig. 11). Sensitivity

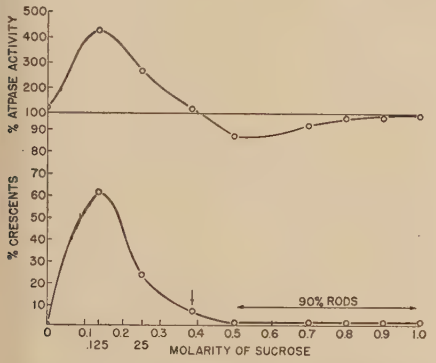

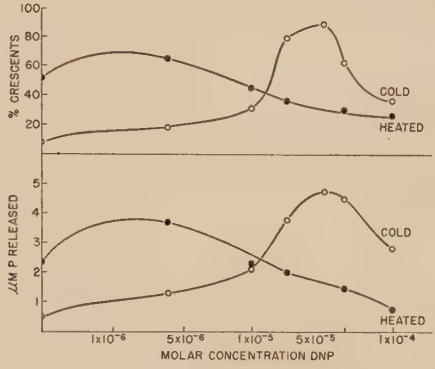

Textfig. 10 (left). Effect of 2,4 dinitrophenol on ATPase activity and mitochondrial morphology as a function of osmolarity. One hundred per cent ATPase represents full activity of control suspension as a horizontal line with the curve demonstrating the DNP activated mitochondria. The percentage of crescents signifies the difference between per cent found in the stimulated and control suspensions, i.e., per cent DNP suspension minus per cent control suspension. System as in Textfig. 5 and contains 2.57×10^{-5} DNP. Vertical arrow indicates point of osmolarity where conversion between rods and spheres occurs.

Textfig. 11 (right). Influence of preincubation on response of ATPase and morphological transformation to various DNP concentrations. System as in Textfig. 5 except that final volume is 1.5 ml and molarity of 0.25 M maintained. Incubation for 15 minutes at 30°C.

to DNP stimulus is not only conditioned by osmotic pretreatment therefore but is modified by thermal transformation. From earlier studies of thermal effects it is compatible that heat induced crescents require a low operative DNP concentration, but the remission of both crescent population and enzyme activity below the control levels is at present inexplicable and can only be regarded as an effect by DNP of undetermined cause.

The evidence provided by the reactivity of the 2 mitochondrial suspensions implies that the period of preincubation so alters the mitochondrial configuration that subsequent DNP treatment may be stimulatory, inert, or depressive. To test this contingency the mitochondria in 0.25M sucrose were challenged with DNP after staggered intervals of preincubation. The probative concentration 2.5×10^{-5}M of DNP selected was such as had produced a near maximal stimulus with the chilled mitochondria and an insignificant depression with the preincubated suspension. In these experi-

ments (Textfigs. 12 and 13) the native mitochondria are greatly stimulated and many converted into crescents. As the preincubation period is prolonged, there is a decrease in dephosphorylation and concomitantly a decline in crescent production, which then stabilize at constant values after from 30 minutes to an hour of preincubation. The decreased responsiveness with longer periods of incubation as compared with the mitochondria held at 0° C is

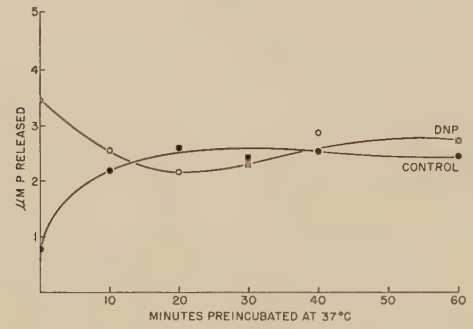

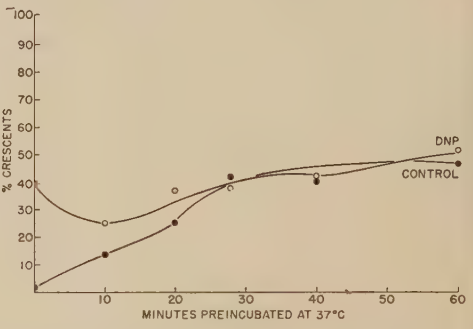

Textfig. 12 (left). Effect of preincubation on the responsiveness of ATPase to DNP stimulation. Mitochondria are isolated in 0.25 M sucrose. System as in Textfig. 5 and includes 2.57×10^{-5} M DNP. Incubation for 15 minutes at 30° C.

Textfig. 13 (right). Effect of preincubation on mitochondrial morphology and transformation by DNP. Conditions identical to those in Textfig. 12.

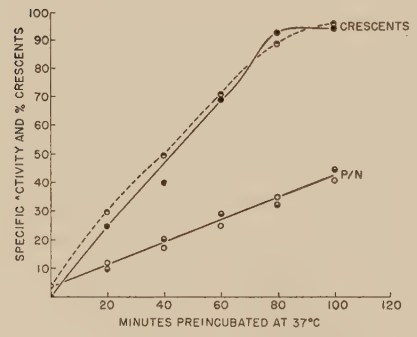

Textfig. 14. Effect of preincubation on ATPase and morphological response of mitochondria to DNP as a function of hyperosmolarity. Mitochondria isolated in 0.5 M sucrose. Conditions as in Textfig. 12 except that osmolar concentration is 0.5 M.

genuine and reproducible. In similar experiments with the mitochondria suspended in 0.5 M sucrose (Textfig. 14), the DNP effect was obliterated, and the trend of the dephosphorylation followed that of the upsurge in thermally induced crescent populations. In the light of the experience that mitochondria suspended in 0.5 M sucrose (Textfig. 10) are unaltered by the DNP in form and activity, the fact emerges that dephosphorylation activity is parallel to and controlled by the transformation rate of the mitochondria from rodlets and dense spheres into crescents. Only insofar as DNP can change the rate

of metamorphosis in zones of molarity is it capable of affecting the dephosphorylation mechanism. Since such mitochondrial sensitivity to DNP is delimited to molarities below 0.375 M where the population is partly composed of dense spheres, the significant relationship is established that DNP must be applied to the enspherulated units to elicit a response.

DISCUSSION

The present studies substantiate the observations on the mitochondria of skeletal muscle, which revealed a relation between ATPase activity and structure. It is logical that in deference to these correlations between structural integrity of the cell particles and the behavior of the enzyme peculiar to the organelles, investigations on the enzymes establish careful standardization of the structure in order to ensure strictly comparable experimental conditions. Variations in thermal, osmotic and ionic environment can induce metamorphoses, which are reflected in the behavior of many enzymes, both oxidative (3) and phosphorylative (6). Because of this, the comparative analyses of mitochondrial bound enzymes require an accurate appraisal of the mitochondrial structure with each critical variation in experimental conditions concerned with enzyme assay. An evaluation of the mitochondrial structure in the different preparations may often inform the investigator as to the cause of unanticipated biochemical discrepancy between seemingly identical suspensions of mitochondria (2). The gradations of mitochondrial activity encountered by Potter (17) and classified as degrees of transition to aging are undoubtedly reflections of the structural alterations associated with the application of the various manipulative procedures. It would be of advantage that the quantitative analyses of mitochondrial density as performed by Allard *et al.* (1) be fortified with differential estimates of the mitochondrial population. It is possible that there occur not only fluctuations in total enzyme per mitochondrion but also variable reactivities of the mitochondria at several periods of regeneration predetermined by alterations in size and shape during growth of liver cells (1). It is clear that the small spherical mitochondria are not only most "latent" but also most reactive. Our experience with the bound "ATPase" has convinced us that a principal source of error and confusion in assay of mitochondrial attached enzymes is the indiscriminate comparison between intact and transformed mitochondria. There is a current tendency to treat the mitochondria as enzymes because they contain a specific enzyme reaction, whereas they are preferably handled as the vehicle of enzymes with a cautious regard for the limitations

imposed upon the enzymatic activity and integrity by the organization of mitochondrial structure.

The association of a minimal enzyme activity with the sphere is a proof that the "latency" depends upon the cryptic position of the enzyme within the mitochondrion. Most current fractionation techniques (19) have uniformly employed 0.25 M sucrose as the medium of choice on the arbitrary contention that this molarity approximates to isosmolarity with serum. At this osmolarity the dephosphorylating enzymes are concealed in the depth of the spherical mitochondria and are more inaccessible to the substrate than in the rodlets at higher osmolarity. Several observers have established the osmolar range of 0.125 to 0.25 M sucrose as the zone of minimal activity (17, 21, 18). The proposition that mitochondria so isolated are "resting" is consequently deceptive. The sluggishness of the dephosphorylating mechanism imposed by the intermediate molarities is not maintenance of a natural enzymic inertia but is a product of structural deformation, which masks the enzyme activity by imposing a diffusion gradient that operates as an accessibility barrier.

The catalytic influence of DNP is effective in restricted ranges of osmolarity and proportional to the ability of the compound to transform the enspherulated mitochondria into crescents. The compound is without action on native rodlets. Several workers have demonstrated the variety of agents (8, 16, 13) which can activate the mitochondrial ATP dephosphorylating mechanism. All indicate that after a maximal effect by such agents a further activation by DNP is precluded or minimal. The structural finding demonstrates that these activations result in a common final mitochondrial deformity, the crescent formation, which uncovers the full operation of dephosphorylation mechanisms. If DNP exerts a special action on the enzyme independent of preliminary structural modifications, it might be expected that the DNP would augment the activation induced by other agents; however, the relation between DNP and other activators is reciprocal and not supplementary. Complete activation by one agent is not enhanced by another unless additional structural dispersion is concomitantly induced. The evidence offered (13) that the DNP activates the soluble "ATPase" found in extracts from dried acetone treated mitochondria needs to be reconciled with the fact that structure plays a critical role during activation in whole mitochondria. The techniques of desiccation and assay may allow preservation of sufficient structure to enable the DNP to exert an appreciable effect on the constituents of the very considerable quantities of mitochondrial protein employed in the final test system. It is suggested that DNP produces its effect by structural

alteration in the acetone treated mitochondria insofar as the acetone preparations from fresh mitochondria retain more reactivity than those from preincubated suspension. In view of some other evidence that DNP has failed to stimulate the acetone dried mitochondria, the considerations here must remain subjudice for the present.

It is well established that DNP effectively uncouples oxidation and phosphorylation (8). Participation of an activated ATPase may be invoked to explain the Loomis-Lippman effect when the DNP can eliminate the requirement for inorganic phosphate. Tepley (20) postulates the discharge of "gel P" to account for this phenomenon. It is not inconsistent to believe that the action of DNP exerts these multiple effects simultaneously by the direct dispersion of the mitochondrial structure. The degenerative structural transformation induced by DNP so alters the integrated enzyme systems that the endergonic processes are impaired, the bound "gel P" released and "ATPase" rendered manifest. The difficulty encountered in the establishment of a connection between these events is obviated by the recognition that they are all initiated by a common process of mitochondrial degeneration, although they may be otherwise enzymatically independent. Failure of oxidative phosphorylation and the destruction of the ~ P in the adenine nucleotide reservoir by enhanced "ATPase" activity are in part independent; evidence for this is provided in the observations that not all the phosphorylations involved in the oxidation of α-ketogluterate are equally sensitive (10) and that the phosphorylation associated with anaerobic dismutation of α-ketoglutarate is resistant to DNP, as is the phosphorylation accompanying glycolysis.

SUMMARY

The ATPase activity of isolated mitochondria is conditioned by the osmolarity of the suspending medium. Effectiveness of stress and transforming agents in eliciting adequate ATPase stimulation depends upon their ability to induce structural alterations. This interdependence of enzymatic reactivity and mitochondrial metamorphosis is a fundamental mitochondrial phenomenon. It is established that the structural transformation precedes the enzymatic changes and that dinitrophenol evokes its effect by a primary action on mitochondrial structure.

The authors wish to thank Dr. Stanley Weinreb for his help with the electron microscopy and photographic procedures.

REFERENCES

1. Allard, C., and Cantero, A., *Can. J. Med. Sci.*, **30**, 295 (1952).
2. Berthet, J., Berthet, L., Appelmans, F., and de Duve, C., *Biochem. J.*, **50**, 182 (1951).
3. Chappell, J. B., and Perry, S. V., *ibid.*, **55**, 586 (1953).
4. Claude, A., *J. Exptl. Med.*, **84**, 51 (1946).
5. Harman, J. W., *Proc. Amer. Assoc. Pathol. Bacteriol., Am. J. Pathol.* (in press).
6. Harman, J. W., and Feigelson, M., *Exptl. Cell Research*, **3**, 509 (1952).
7. Harman, J. W., and Kitiyakara, A., *ibid.*, **8**, 411 (1955).
8. Hunter, F. E., Phosphorus Metabolism, Vol. I, edited by McElroy, W. D., and Glass, B., John Hopkins Press, Baltimore, p. 297, 1951.
9. Johnson, M. J., *J. Biol. Chem.*, **137**, 575 (1941).
10. Judah, J. D., *Biochem. J.*, **49**, 271 (1951).
11. Keilley, W. W., and Keilley, R. K., *J. Biol. Chem.*, **191**, 485 (1951).
12. Kitiyakara, A., and Harman, J. W., *J. Exptl., Med.*, **97**, 553 (1953).
13. Lardy, H. A., and Wellman, H., *J. Biol. Chem.*, **201**, 357 (1953).
14. Lowry, O. H., and Lopez, J. A., *ibid.*, **162**, 421 (1946).
15. Palade, G., *J. Exptl. Med.*, **95**, 285 (1952).
16. Potter, V. R., and Recknagel, R. Z., Phosphorus Metabolism. Vol. I, ed. by McElroy, W. D., and Glass, B., Johns Hopkins Press, Baltimore, p. 377, 1951.
17. Potter, V. R., Siekevitz, P., and Simonson, H. C., *J. Biol. Chem.*, **205**, 893 (1953).
18. Sacktor, B., *J. Gen. Physiol.*, **36**, 371 (1953).
19. Schneider, W. C., and Hogeboom, G. M., *J. Biol. Chem.*, **183**, 123 (1950).
20. Tepley, L. J., *Arch. Biochem.*, **24**, 383 (1949).
21. Witter, R. F., and Cottone, M. A., *Federation Proc.*, **13**, 323 (1954).

Experimental Cell Research, **8**, *453–458 (1955)*

PRESENCE OF CARBOHYDRATES IN THE ACROSOME OF THE GUINEA PIG SPERMATOZOON

Y. CLERMONT, R. E. GLEGG and C. P. LEBLOND

Department of Anatomy, McGill University, Montreal, Canada

Received July 30, 1954

Until recently the acrosome of spermatozoa was a controversial, ill-defined structure, often confused with the head cap (11, 14) and the perforatorium (3). The situation was clarified by the utilization of the periodic acid-Schiff (PA-Schiff) technique, which stains the acrosome selectively (10). With this technique the development of the acrosome was traced from the Golgi zone of the spermatid where the so-called acrosomic granule arose and produced acrosome and head cap (both of which form the acrosomic system of the spermatozoon). The acrosome has been demonstrated in deer (16), rat (9), mouse, hamster and guinea pig (10), ram (1), bull (1, 15) and even lower vertebrates and invertebrates (15). Comparison of PA-Schiff and iron-hematoxylin preparations as well as examination of electron micrographs of osmic acid fixed material showed that the PA-Schiff reactive acrosomic granule consisted of a core—or *inner* acrosomic granule (stainable with iron-hematoxylin and opaque under the electron microscope)—and a shell—or *outer* acrosomic granule (unstainable with iron-hematoxylin and transparent to the electron beam). The inner acrosomic granule plays a major role in the eventual production of the mature acrosome, while the outer acrosomic granule produces the head cap (2).

Owing to the uncertainties of the definition of the acrosome, it is little wonder that the problem of its chemical nature was not investigated until very recently, and at that, only by histochemical techniques. By such methods it was found that the acrosomic system may contain a basic protein (4, 12, 15) and the enzyme, acid phosphatase (4, 13, 17). In addition, the stainability of this system by the PA-Schiff technique which is believed to be specific for carbohydrates containing 1,2-glycol and α-amino alcohol groups (5, 8), suggested the presence of one or more such carbohydrates. Therefore, the present investigation was undertaken to extract the acrosomic system and identify its carbohydrate components.

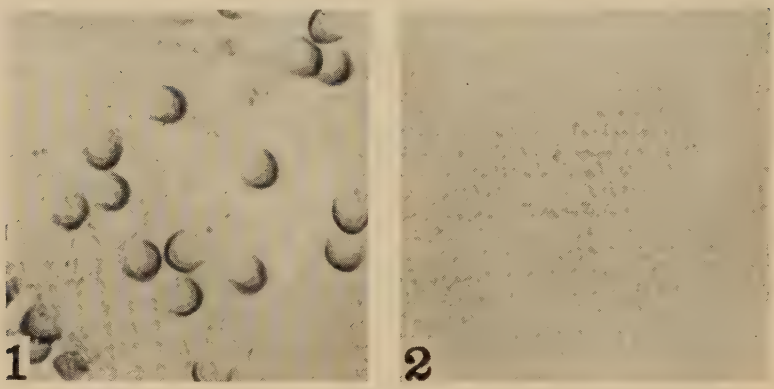

Fig. 1. Guinea pig spermatozoa washed three times in saline, smeared, fixed with formalin fumes and stained with the periodic acid-Schiff technique. The large, well stained crescent-like acrosomes are clearly visible. The unstained nuclei and tails are seen as refringent structures. × 800.
Fig. 2. Guinea pig spermatozoa washed three times in saline, treated with 0.1 N NaOH, smeared and fixed with formalin fumes. The smear was then stained with the periodic acid-Schiff technique. No acrosomes can be seen, the clumped nuclei and tails can be outlined by their refringence. × 800.

EXPERIMENTAL

The guinea pig was chosen as the experimental animal since the large acrosome exhibited by its spermatozoa in the epididymis can be stained intensely with the PA-Schiff technique (Fig. 1). The overall procedure involving the isolation of spermatozoa and alkaline extraction of the acrosomic material was followed histologically. For this purpose, smears of material were made at various steps of the procedure and examined after staining with the PA-Schiff and Feulgen techniques.

After clamping off the vas deferens—to prevent loss of spermatozoa—the epididymis was excised by way of the abdominal cavity from 60 adult guinea pigs under ether anesthesia, placed immediately in 0.9 per cent sodium chloride, cut into small pieces, and gently stirred to release the contents of the ducts including the spermatozoa. The suspension was filtered through cheese cloth, and microscopic examination of the filtrate showed it to be free from tissue. The spermatozoa were separated from the saline supernatant by centrifugation and then washed three times with saline. The washings and the original supernatant were pooled. Under the microscope, the washed spermatozoa (Fraction A) were seen to be intact, with only a few showing dissolution of the acrosome. Presumably, the saline washings, in addition to the material released from the dissolved acrosomes, contained the epididymal secretions. This material was precipitated by addition of two volumes of alcohol to yield Fraction B.

The spermatozoa (Fraction A) were placed in 0.1 N sodium hydroxide for 90 minutes and then centrifuged. The insoluble material (Fraction C) was found to consist of tails and nuclei devoid of acrosomes, while the sodium

Fig. 3. Paper chromatogram of the hydrolysates of various fractions obtained from the epididymis. Galactose, mannose and fucose are present in fractions B, D, and E, but absent from Fraction C. (The spot seen at the origin of Fraction C was present before spraying with the developing reagent: aniline hydrogen oxalate.)

hydroxide supernatant was presumed to contain the dissolved acrosomic material.

The sodium hydroxide solution was adjusted to pH 5.8 with acetic acid and two volumes of alcohol were added. After standing in the cold overnight, the alcohol insoluble precipitate (Fraction D) was centrifuged down. When the supernatant alcoholic solution was evaporated to dryness, another Fraction (E) was obtained.

All the fractions were washed three times with absolute alcohol, once with ether and then dried *in vacuo* at 40° C.

In order to identify any monosaccharides present as components of these materials, they were hydrolysed in the presence of a cation exchange resin (6) and the hydrolysates analysed by ascending paper chromatography (6, 7).

Two types of experiments were carried out. In the first, relatively large amounts of material were hydrolysed and increasing concentrations were placed on the paper to assure the identification of all monosaccharides. In the second, the amounts of the hydrolysates placed on the paper were adjusted so that they corresponded to equivalent fractions of the various materials isolated from the intact spermatozoa. For this purpose, 50 mg each of preparations B, C and D, and 30 mg of E were hydrolysed for 48 hours, the hydrolysates evaporated to dryness, and the residues dissolved in 83, 183, 60 and 155 μl respectively. 6 μl aliquots of each of the solutions were used for chromatography (Fig. 3).

RESULTS

When hydrolysates of whole spermatozoa (Fraction A) were chromatographed, they were found to contain galactose, mannose, fucose and ribose. When the spermatozoa had been extracted with 0.1 N sodium hydroxide, the heads and tails were still intact but the acrosome and head cap could no longer be seen by phase contrast microscopy or after PA-Schiff staining (Fig. 2). These spermatozoa devoid of acrosomes (Fraction C) were hydrolysed prior to chromatographic analysis. Ribose was the only sugar present and was attributed to nucleic acids of the nucleus. (The spot for this sugar does not appear in Fig. 3, because the amounts of material hydrolysed in this experiment were too small.)

The material extracted from the spermatozoa with 0.1 N sodium hydroxide, that is, essentially the acrosome and head cap, was separated into an alcohol insoluble fraction (D) and an alcohol soluble fraction (E), both of which

contained galactose, mannose and fucose, with the mannose predominating in Fraction D. In addition to these aldoses, Fraction D contained 2.6 per cent hexosamine[1] and its high nitrogen content (15.8 per cent) suggested that large amounts of protein are associated with the carbohydrate moiety.

The saline soluble portion of the contents of the epididymis (Fraction B), that is, mainly epididymal secretions, contained galactose, mannose and fucose with the galactose predominating. The differences seen in the chromatographic patterns of Fractions D and B confirm that the material isolated from the sperm by sodium hydroxide treatment is different from that found in the epididymal secretions.

CONCLUSION

Spermatozoa were isolated from the epididymis of the guinea pig and extracted with 0.1 N sodium hydroxide to remove the periodic acid-Schiff staining material of the acrosomic system. The extract was treated with alcohol to yield alcohol insoluble and soluble fractions. These materials, as well as the extraction residue (consisting of nuclei and tails) were hydrolysed and analysed by paper chromatography for the identification of monosaccharides.

While whole spermatozoa contain among other substances, galactose, mannose, fucose and ribose, the residual portion of the spermatozoa after sodium hydroxide extraction contains ribose only. The alkaline extract which includes the acrosomic material is separated by alcohol treatment into two fractions, both of which show the presence of galactose, mannose and fucose.

It is concluded that the acrosomic system of the guinea pig spermatozoa contains a substance or substances made up at least partly by units of galactose, mannose, fucose (and hexosamine), and that some of these units are responsible for the periodic acid-Schiff staining.

This work was done with the help of research funds granted by Eli Lilly and Company. The assistance of D. Eidinger in the preparation of the chromatograms is acknowledged.

REFERENCES

1. Clermont, Y., *Anat. Rec.*, **112** (Suppl.), 319 (1952).
2. Clermont, Y., and Leblond, C. P., *Am. J. Anat.* (in press).
3. Duesberg, J., *Arch. Zellforsch.*, **2**, 137 (1908).

[1] The hexosamine determination was kindly carried out by Dr. R. H. Pearce, University of Western Ontario, London, Ontario, Canada, according to the method of Elson and Morgan as modified by G. Blix, *Acta Chem. Scand.*, **2**, 467 (1948).

4. Friedlaender, M. H. G., and Fraser, M. J., *Exptl. Cell Research*, **3**, 462 (1952).
5. Glegg, R. E., Clermont, Y., and Leblond, C. P., *Stain Technol.*, **27**, 277 (1952).
6. Glegg, R. E., and Eidinger, D., *Anal. Chem.*, **26**, 1365 (1954).
7. Glegg, R. E., Eidinger, D., and Leblond, C. P., *Science*, **118**, 614 (1953).
8. Hotchkiss, R. D., *Arch. Biochem.*, **16**, 131 (1948).
9. Leblond, C. P., *Am. J. Anat.*, **86**, 1 (1950).
10. Leblond, C. P., and Clermont, Y., *ibid.*, **90**, 167 (1952).
11. Lenhossek, M. von, *Arch. mikroskop. Anat.*, **51**, 215 (1898).
12. Marza, V. D., *Bull. Histol. appl.*, **8**, 85 (1931).
13. Melampy, R. M., Cavazos, L. F., and Porter, J. C., *J. Dairy Sci.*, **35**, 140 (1952).
14. Randall, J. T., and Friedlaender, M. H. G., *Exptl. Cell Research*, **1**, 1 (1950).
15. Schrader, F., and Leuchtenberger, C., *Chromosoma*, **4**, 404 (1951).
16. Wislocki, G. B., *Endocrinology*, **44**, 167 (1949).
17. — *Anat. Rec.*, **108**, 645 (1950).

Experimental Cell Research, **8**, *459–465 (1955)*

SOME CHEMICAL AND PHYSICAL PROPERTIES OF MICROSOMES[1]

L. G. ABOOD and LORRAINE ROMANCHEK

Department of Psychiatry and Department of Biochemistry, University of Illinois, College of Medicine, Chicago, Ill., U.S.A.

Received August 12, 1954

The ground substance of most cells is believed to consist of an elaborate framework of fibrils comprised of submicroscopic particles arranged in beaded chains (13, 4). This reticulate structure is extremely plastic, usually assuming the orientation and configuration intrinsic in the pattern and physical forces within the cell (13, 4). In addition to providing a structural framework for the cell, the cytoplasmic fibrils may comprise units of functional activity such as motility, contractility, and conduction. Muscle contraction is due to the folding of the polypeptide chains of myofibrils (19), while the neurofibrils have long been suspected of being involved in nerve conduction (14). Monné is of the opinion that energy-yielding processes within the submicroscopic particles are essential for maintaining the dynamic state of the fibrils. The presence of adenosinetriphosphatase (ATPase) in the microsomes of liver (15), nerve (1), and muscle (8) has been established; and Monné concluded that ATPase was present in the cytoplasmic fibrils in general since they are contractile and exhibit birefringence of flow (12).

The present communication deals with an attempt to compare and characterize the isolated microsomes from different tissues and to reconstitute them into fibrillar structures resembling the cytoplasmic fibrils *in vivo*. When microsomes from rat liver, kidney, muscle, brain, and nerve were prepared in 0.25 M sucrose by differential centrifugation, they were found to be spheres 20–150 mμ in diameter (1) and to exhibit birefringence of flow. The sedimented microsomes formed a sol which behaved like a thixotropic gel when extruded into water, in much the same manner as actomyosin.

METHODS

Isolation of the microsome fraction of rat tissues was done after the method of Hogeboom *et al.* (7). Homogenates of the various tissues in 0.25 M sucrose were first sedimented at 15,000 × g to remove mitochondria, nuclei, and stroma and then at 100,000 × g to isolate the microsomes. Centrifugation was done in the Spinco Model

[1] This work was supported by a contract between the Office of Naval Research and the University of Illinois.

L ultracentrifuge at −5 degrees. The hydrophilic microsomal sol was drawn into a 0.5 ml hypodermic syringe whose tip was drawn out to a 0.1 mm bore, and when the sol was carefully extruded into 10^{-3} M magnesium chloride (pH 6.0–7.0), fine gelatinous threads resembling actomyosin were formed.

The histochemical technique for ATPase was that of Gomori (6). Rat sciatic nerves were placed in Maximow depression slides and then dissected into single fibers or bundles of usually less then 5 fibers. A medium containing 0.02 M ATP, 0.001 M magnesium chloride, 0.02 M calcium chloride, and histidine buffer, pH 7.5 was then added to the slide and the system incubated for 20 minutes at 37 degrees. Preliminary fixation of the nerves in ice-cold acetone or 70 per cent alcohol did not in any way improve the histochemical technique.

ATPase activity was determined on the microsome fraction according to the method of DuBois and Potter (3), except that histidine buffer replaced veronal and 0.001 M magnesium chloride was substituted for calcium chloride. Adenylic kinase was determined by the method of Kornberg (9), and adenylic deaminase was measured by following the disappearance of adenylic acid at 260 mμ in the Beckman DU Spectrophotometer.

Separation of the "acid-insoluble" fractions was done following the method of Schneider (18). Sodium and potassium were removed from the microsomes by boiling in water for 10 minutes and then determined on the filtrate, using the Beckman flame photometer. Silica glassware, which was low in sodium and potassium, was used whenever analysis for the alkali metals was made.

RESULTS AND DISCUSSION

When particles exhibiting double refraction of flow are forced through a narrow tube they align themselves parallel to the direction of flow (5). With

TABLE I

Acid insoluble components and electrolytes in microsomes of various tissues.

	Total N	Lipid	Lipid P	Nucleic acid (as nucleotide)	"Phospho-protein" P	K	Na	K/Na
	μM/mg dry wgt.	% dry wgt.	Micromoles/micromoles of total Nitrogen					
Brain	5.7	57	60.0	1.08	16.0	47	14	3.4
Peripheral nerve . . .	5.5	59	50.1	1.00	3.5	40	12	3.4
Muscle . . .	6.5	61	40.1	1.20	4.0	44	11	4.0
Liver	7.0	60	33.3	1.25	4.7	28	9	3.1
Kidney . . .	7.5	63	41.5	1.30	5.1	21	7	3.0

Average of 4 values agreeing within 6 per cent.

Fig. 1. Unfixed, unstained fiber prepared artificially from nerve fiber microsomes. Magnification 200 ×.

the correct salt concentration they would tend to coalesce and form a stable gel if properly oriented. The microsomes of all tissues studied possessed this property of flow birefringence, and as long as the microsomal salt concentration was at least 3 mM/ml, a stable gel formed. The microsomes aligned themselves into numerous parallel fibrils longitudinal to the fiber axis (Figs. 1 and 2). In a thread 0.5 mm in diameter as many as 50 of these filaments could be observed at magnifications of 200 ×. In the absence of magnesium, in 0.25 M sucrose, or in a slightly alkaline solution the threads lacked the filar structure and would more readily disintegrate. Unlike actomyosin, the threads would not contract upon the addition of ATP.

About 60 per cent of the total dry weight of the microsomes from all tissues was comprised of lipid. The phospholipid content of microsomes from nervous tissues was somewhat greater than in the case of the other tissues where the values were quite similar. In general, the nucleic acid

Fig. 2. Fibers prepared by extrusion of nerve fiber microsomes into 5 per cent formalin and stained with 0.01 per cent methylene blue. Magnification 200 ×.

content of the various tissues was also similar, although slightly lower in neural tissue. With the exception of an extremely high content in brain, the "phosphoprotein" content of the microsomes of various tissues was in close agreement. The potassium and sodium concentration of the microsomes of neural and muscular tissue were similar, being considerably greater than in liver and kidney.

A considerable amount of ATPase was found to be present in the microsomes of all tissues (Table II). The activity of brain and kidney was less than half that of muscle and over twice as great as the ATPase activity of liver and peripheral nerve. Adenylic kinase and adenylic deaminase activity of the microsomes seemed to vary from tissue to tissue in the same proportion as ATPase with the exception of kidney.

Cytoplasmic fibrils have long been suspected of being comprised of submicroscopic particles, although considerable controversy exists as to the

exact nature of the particles involved. Monné (13) and Runnström (16) are of the opinion that they are equivalent to the microsomes, while Frey-Wyssling (4) considers it unlikely that morphogenesis and metabolism are performed by the same elements. The cytoplasmic fibrils, however, are not mere structural elements but appear to be in a state of continual reorganization and reconstitution as determined by the variable morphogenetic and

TABLE II

Enzymes of adenylate system in microsomes of various tissues.

Tissue	ATP-ase	Adenylate kinase	Adenylic deaminase
	μM ATP split/15′/μM N	μM ATP formed/10′/μM N	μM AA/10′/μM N
Muscle	1.07	0.30	0.0350
Brain	0.43	0.10	0.0090
Kidney	0.45	0.053	0.0046
Liver	0.21	0.035	0.0020
Peripheral nerve	0.22	0.028	0.0015

Average of 4 values agreeing within 8 per cent.

functional requirements of the cell. Among the numerous types of fibrils, known to respond during functional activity are the myofibrils, neurofibrils, epithelial fibrils, and cilia. This activity usually consists of a visible contraction or motility involving rearrangements in polypeptide chains. Polymerization of actomyosin occurs upon the addition of ATP (11), and dissociation of the protein complex follows the dephosphorylation of ATP. It is believed that the polypeptide rearrangements associated with most cytoplasmic fibrillar activity involve an energy-releasing mechanism comparable to the ATPase system of myofibrils. The present findings that the ATPase of nerve fibers appears to be located in fibrillar structures, possibly including the neurofibrils, lend support to the hypothesis that ATPase activity is associated with nerve conduction (13, 1).

On the basis of present evidence it cannot be determined to what extent the microsomal fraction of neural tissue originated from the neurofibrils. Beadlike fibrils observed by DeRobertis and Schmitt (2) in the electron

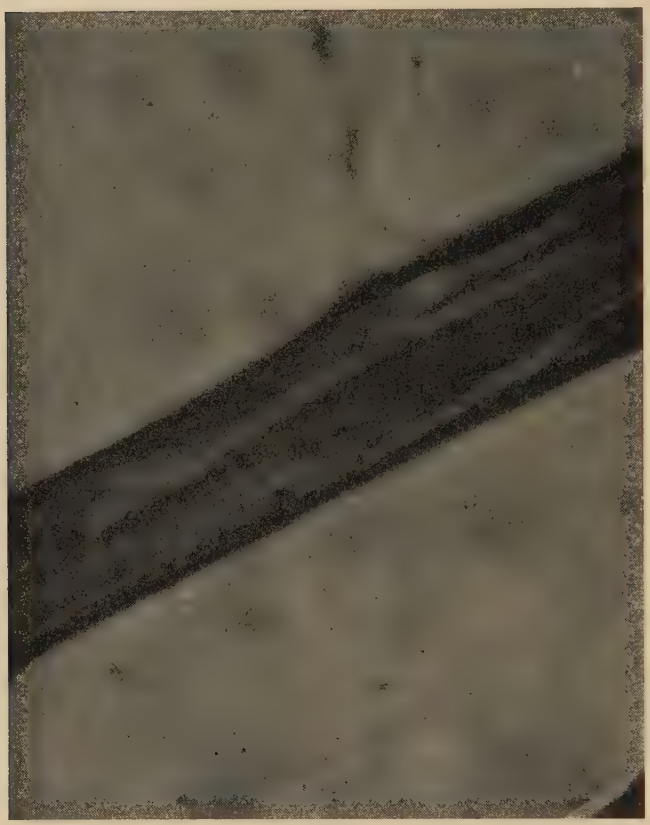

Fig. 3. Single nerve fiber stained for ATPase. Magnification 1000 ×.

microscope were described as axonal constituents, but later believed to be from connective tissue sheath (17). In nerve fibers fixed in osmic acid it has been possible to observe within the axoplasm contorted beadlike filaments 100–200 Å wide, which are believed to be neurofibrils (17). The finding of Libet (10) that the ATPase of the squid nerve is largely in the sheath would tend to vitiate the hypothesis that the ATPase containing microsomes are of axoplasmic origin. Undoubtedly the microsomes isolated from rat nerve originated from the sheath as well as axoplasm, although their enzymatic and chemical homogeneity remains a question.

The presence of high K/Na ratios within the microsomes, particularly those of neural or muscular origin suggested that the artificial fibers might manifest a surface potential. With the ultramicroelectrode potentials were measured exceeding 30 millivolts in freshly prepared threads immersed in 0.25 M sucrose containing 0.001 M magnesium chloride. Potentials of threads

prepared from liver microsomes measured less than 10 millivolts. This difference in potential is to be expected because of the greater electrolyte content of conductive tissue.

SUMMARY

Microsomes from a number of rat tissues have been examined with respect to certain chemical and physical properties. In addition to a Mg-activated ATP-ase, the microsomes contain adenylic kinase and adenylic deaminase. By extrusion of the microsomal gel into 10^{-3} magnesium chloride, artificial fibers are obtained with internal structures resembling cytoplasmic fibrils.

REFERENCES

1. Abood, L. G., and Gerard, R. W., *J. Cellular Comp. Physiol.*, **43**, 379 (1954).
2. De Robertis, E., and Schmitt, F. O., *ibid.*, **31**, 1 (1948).
3. Dubois, K. P., and Potter, V. R., *J. Biol. Chem.*, **150**, 185 (1943).
4. Frey-Wyssling, A., Submicroscopic Morphology. Elsevier Publ. Co., New York, 1953.
5. Glasstone, S., Textbook of Physical Chemistry. 2nd ed. Van Nostrand, New York, 1946.
6. Gomori, G., *Proc. Soc. Exptl. Biol. Med.*, **42**, 23 (1939).
7. Hogeboom, G. H., Schneider, W. C., and Palade, G. E., *J. Biol. Chem.*, **172**, 619 (1948).
8. Kielley, W. W., and Meyerhof, O., *ibid.*, **183**, 391 (1950).
9. Kornberg, A., *ibid.*, **182**, 779 (1950).
10. Libet, B., *Federation Proc.*, **7**, 72 (1948).
11. Mommaerts, W. F. H. M., Muscular Contraction. Interscience Publ., New York, 1950.
12. Monné, L., *Experientia*, **2**, 153 (1946).
13. —— *Advances in Enzymol.*, **8**, 1 (1948).
14. —— *Arch. exptl. Zellforsch. Gewebezücht*, **23**, 157 (1949).
15. Potter, V., *Advances in Enzymol.*, **4**, 201 (1944).
16. Runnström, J., *ibid.*, **9**, 241 (1949).
17. Schmitt, F. O., in Genetic Neurology. Ed. P. Weiss, U. of Chicago, 1950.
18. Schneider, W. C., *J. Biol. Chem.*, **161**, 293 (1945).
19. Szent-Györgyi, A., Chemistry of Muscular Contraction. Acad. Press, New York, 1947.

CHANGES IN THE PROTEINS OF THE SEA URCHIN EGG AT FERTILIZATION

G. GIARDINA and A. MONROY

Laboratory of Comparative Anatomy, University of Palermo, Italy

Received August 16, 1954

In previous papers solubility changes of some protein fractions of the sea urchin egg as a result of fertilization have been described (10, 11). These observations, while extending Mirsky's discovery (8) on the coagulation of a protein fraction at fertilization, suggested that egg activation is accompanied by a reorganization of the egg proteins. As on the other hand, experiments using isotopes (4, 5) and serological studies (12, 13) have shown that synthesis of new proteins begins much later in development (see also (14, 15)), the observed early changes must be assumed to be restricted to a structural rearrangement of the protein molecules. To learn more about the nature of such changes would be of the utmost importance as they may be one of the key phenomena of the activation of the egg. The results presented in this paper are a further attempt to throw some light on this question.

On a first approximation, such structural changes at the molecular level may be considered under three aspects: a) the change in the configuration of the protein molecule proper (e.g. folding or unfolding); b) the aggregation of simpler units into more complex ones (including the binding of prosthetic groups); c) opposite to these, the breaking-down of large complexes. All of them may be expected to lead to a changed sensitivity of the proteins to proteolytic enzymes and to denaturing agents (see (6, 9)).

Therefore the supernatant obtained by high-speed centrifugation of homogenates of unfertilized and newly fertilized eggs of *Arbacia lixula* and protein fractions thereof have been investigated for their sensitivity to trypsin and for their ability to be denatured by heat. In this latter study advantage has been taken of the possibility of distinguishing between non-denatured and denatured proteins using as a criterion the solubility in a salt buffer mixture worked out at the Carlsberg Laboratory (3, 6) in which only native proteins have been found to be soluble, while denatured proteins are precipitated out. A similar method had already been used by Anson and Mirsky (1). It must be emphasized, however, that in our case the use of this mixture is rather arbitrary, as there is no indication that the proteins extracted from sea

urchin eggs do behave in the same way as *e.g.* egg albumin and lactoglobulin. There is in fact the possibility that some of them may be precipitated out even in the native condition. This question will be discussed later.

RESULTS

Sensitivity to trypsin of the proteins of unfertilized and fertilized eggs. Supernates of unfertilized and newly fertilized eggs of *Arbacia lixula* were tested for their ability to be digested by trypsin. Tables I and II show that

TABLE I

Mg of Protein-N in the supernate of unfertilized and fertilized eggs at zero time and after 30 minutes incubation with trypsin.

Unfertilized			Fertilized		
0	30 min.	Per cent decrease	0	30 min.	Per cent decrease
0.180	0.159	−11.6	0.485	0.389	−20
0.614	0.538	−12.4	2.110	1.790	−15
0.644	0.564	−12.4	0.884	0.758	−14.2
1.108	1.044	− 5.4	0.958	0.690	−28
0.576	0.480	−16.7	0.432	0.332	−23.2
2.004	1.896	− 5.7	0.788	0.684	−13.2
1.136	1.087	− 4.2	1.086	0.947	−12.8

TABLE II

Mg of protein-N in the fractions obtained from the supernate of unfertilized and fertilized eggs at zero time and after 30 minutes incubation with trypsin.

Fraction I						Fraction II					
Unfertilized			Fertilized			Unfertilized			Fertilized		
0	30 min.	Per cent decrease	0	30 min.	Per cent decrease	0	30 min.	Per cent decrease	0	30 min.	Per cent decrease
0.340	0.248	−27	0.532	0.404	−24	0.840	0.695	−17	0.512	0.320	−38
						0.352	0.236	−33	0.384	0.248	−35.4
0.788	0.676	−14.4	0.791	0.716	− 9.5	0.524	0.364	−30.5	0.404	0.236	−44
0.420	0.336	−20	0.392	0.324	−17.5	0.468	0.420	−10	0.440	0.352	−20
0.553	0.461	−16.6	0.391	0.322	−17.6	0.480	0.380	−20.8	0.328	0.216	−34.1

supernates of newly fertilized eggs are considerably more sensitive to trypsin than those of unfertilized eggs.

The possibility must, however, be considered that this may be due to the removal of an inhibitor present in the unfertilized eggs rather than to a change in the protein themselves. Indeed it has been observed by Lundblad (7) that extracts of lyophilized unfertilized eggs are able to inactivate the proteolytic sperm enzyme upon prolonged contact.

The results of experiments in which the fibrin plate method of Astrup and Müllertz (2) was used, disprove this hypothesis (Table III).

Table III

Inhibition of fibrinolytic activity of trypsin by supernate of unfertilized and fertilized eggs. Inhibition as per-cent/1 mg N in the supernate.

Unfertilized	Fertilized
15.6	15.0
32.0	27.0
28.4	31.4

It appeared then of interest to investigate whether the increased susceptibility to trypsin after fertilization is a change that involves all the proteins of the egg or if it is rather restricted to one or to a group of protein fractions.

As a preliminary approach, the supernate was separated into two fractions by precipitation with ammonium sulphate. It was first precipitated at 50 per cent saturation and after removal of the precipitated fraction, the supernatant was re-precipitated by raising the ammonium sulphate concentration to 75 per cent. These fractions will be referred to as fraction I and II respectively and it is clearly understood that each of them is likely to be made up by a mixture of possibly several protein fractions.

The data collected in Table II show that fraction I of fertilized eggs is slightly less sensitive to trypsin than the same fraction prepared from unfertilized eggs, whereas the reverse is true for fraction II.

Hence the effect that appears in the total supernate is the result of the interplay between the change in sensitivity to trypsin in these two groups of protein fractions.

Heat denaturation of the proteins of unfertilized and fertilized eggs. Just as in the experiments with trypsin, this series has been carried out on supernates and fractions thereof. The results are summarized in Tables IV and V.

TABLE IV

Precipitation of the supernate of unfertilized and fertilized eggs by the salt buffer at room temperature and after 10 minutes heating (°).

Total N mg	Unfertilized precipitate					Total N mg	Fertilized precipitate				
	Before heating		After heating				Before heating		After heating		
	mg N	Per cent of total N	mg N	Per cent gain	Per cent of total N		mg N	Per cent of total N	mg N	Per cent gain	Per cent of total N
0.720	0.280	39.0	0.356	27.0	49.5	0.668	0.188	28.2	0.316	41.0	47.3
0.940	0.330	35.0	0.472	43.0	49.8	0.864	0.288	33.4	0.410	43.0	47.5
0.832	0.336	40.4	0.480	43.0	57.7	0.872	0.268	31.0	0.424	58.0	48.7
1.215	0.480	39.6	0.584	21.7	48.0	0.959	0.296	31.0	0.400	35.0	41.7
0.616	0.260	42.2	0.312	20.0	50.5	0.632	0.204	33.0	0.316	55.0	50.0
0.732	0.320	43.7				0.684	0.292	42.7			
0.672	0.308	46.0				0.720	0.264	36.6			

(°) Heating temperature was 65°C in the first two experiments, 55°C in the third and 60°C in the fourth and fifth.

TABLE V

Precipitation of fraction I from the supernate of unfertilized and fertilized eggs by the salt buffer at room temperature and after heating at 60°C for 10 minutes.

Total N mg	Unfertilized precipitate					Total N mg	Fertilized precipitate				
	Before heating		After heating				Before heating		After heating		
	mg N	Per cent of total N	mg N	Per cent gain	Per cent of total N		mg N	Per cent of total N	mg N	Per cent gain	Per cent of total N
0.952	0.524	55.0	0.696	32.8	73.0	0.496	0.220	44.4	0.292	32.7	58.9
0.612	0.356	58.0	0.440	23.6	72.0	0.472	0.252	53.0	0.320	27.0	68.0
0.868	0.564	65.0	0.648	15.0	74.7	0.616	0.364	59.0	0.440	21.0	71.3
0.952	0.568	59.6				0.496	0.224	45.0			
0.612	0.352	57.5				0.472	0.236	50.0			

First of all it has been observed that treatment with the salt buffer of supernates of unfertilized and newly fertilized eggs at room temperature: a) causes more proteins to precipitate from the former than from the latter; b) in the supernates of unfertilized eggs a flocculent precipitate appears almost imme-

diately upon addition of the salt buffer and rapidly settles while in the supernates of fertilized eggs the precipitate is much finer, takes some time to appear and begins to settle only after long standing.

Heating between 55° C and 65° C, however, causes more proteins to precipitate from supernates of fertilized than of unfertilized eggs upon addition of the salt buffer. But taking as reference the total N of the supernate, it appears that the total amount of precipitable proteins (i.e. those precipitated at the zero time + those precipitated after heating) is slightly lower in the supernates of fertilized eggs.

The same experiment carried out with the fractions obtained as previously described, shows that fraction I duplicates the results obtained with the supernates, whereas fraction II is not precipitated by the salt buffer even after heating in boiling water. Thus it appears that it is only fraction I that is responsible for the changes observed in the supernates.

DISCUSSION

The present experiments indicate that the most complex changes appear to occur upon fertilization in fraction I. These changes involve:

1. decreased sensitivity to trypsin; 2. decreased precipitability by the salt buffer at room temperature; 3. upon heating it looks as if more proteins were precipitated: in reality, however, the total amount of precipitable proteins (i.e. of those precipitated at room temperature + those precipitated upon heating) is lower.

As stated before, it is not possible at present to say anything about the conditions of the proteins precipitated by the salt buffer at room temperature. This may be due either to the configuration of the protein molecules or to the presence of large complexes susceptible to the salt buffer. These results may lead to the following alternative interpretations:

1. a large complex present in the unfertilized egg is split at fertilization with release of one part that is precipitated by the salt buffer only after heat denaturation (lower proportion of proteins precipitated at room temperature and higher proportion of them precipitated after heating) and of another part that on the contrary does not seem to be affected by heating (lower amount of total precipitable proteins). In connection with this also the finer appearance of the precipitate in fertilized eggs has to be considered.

2. there may upon fertilization be a change in the configuration of a group of protein molecules (e.g. a re-folding of unfolded molecules). It is difficult at present to decide between these two interpretations, although

both types of changes may be acting concurrently. Both of them may account for the decreased sensitivity of this fraction to trypsin upon fertilization.

It seems here also appropriate to recall that by electrophoretic studies it was just in the fraction collected at 50 per cent saturation of ammonium sulphate from *Paracentrotus* eggs that the most impressive changes were observed to occur at fertilization (10). On the other hand the fraction that as shown by Mirsky (8), undergoes coagulation at fertilization is again a part of this fraction.

An opposite type of changes seems to occur in fraction II as it appears to become more sensitive to trypsin upon fertilization. Its resistence to heat suggests, however, a rather low molecular weight.

It might be tempting to classify the observed changes under the headline of "reversible denaturation" and it is quite possible that such an interpretation may ultimately prove to be correct. At present, however, although being an indication of the extensive reorganization of the egg proteins taking place upon fertilization, our experiments do not permit to draw any definite conclusion as to the nature of the changes involved. Nor can any suggestion be presented as to the factor(s) bringing them about.

EXPERIMENTAL

Preparation of the material. The eggs of *Arbacia lixula* were collected in sea water by the spontaneous shedding that follows cutting of the shells. After washing with sea water, each batch was divided into two parts, one of which was fertilized. Fertilization was checked by microscopic inspection and about 10 minutes after the onset of the visible changes of fertilization, the water was acidified by the addition of an appropriate amount of 0.1 N HCl in sea water to bring the pH to about 3.5 in order to dissolve the jelly coat. The same was done at the same time with the suspension of unfertilized eggs. The two suspensions were rapidly centrifuged at low speed: in this way practically no sperm were carried down with the fertilized eggs. After careful removal of the supernatant, the packed eggs were taken up and homogenized in ice-cold borate buffer 0.05 M, pH 8.2. Pyrex homogenizers with teflon pestles were used. Both unfertilized and fertilized eggs are rapidly disrupted by this procedure. The homogenate was then used for the experiments after removal of the insoluble part by centrifugation (i.e. the supernate) usually for 20 minutes at 20,000 × g in the International Refrigerated Centrifuge.

Fractionation of the homogenate. The supernate was dialyzed in the cold against 2–3 changes of 50 per cent ammonium sulphate neutralized with a few drops of 1N ammonia. The precipitate was collected by centrifugation, washed with 50 per cent ammonium sulphate and dialyzed until free of sulphate first against 0.9 per cent NaCl and then against the borate buffer to be used in the experiments. After removal of the fraction precipitated at 50 per cent saturation, the supernatant was dialyzed

against 75 per cent saturation ammonium sulphate and the precipitate submitted to the same treatments of the previous fraction.

Trypsin digestion. 0.1 cc of a 0.05 per cent solution of crystalline trypsin (Armour) in 0.002 N HCl was added to two series of tubes each containing 1.0 cc of the supernate or solution of a fraction in borate buffer of respectively unfertilized and fertilized eggs. They were incubated in a thermostatic water-bath at 33°C and at certain time intervals one tube of each series was withdrawn and 0.2 cc of a chilled 50 per cent solution of trichloroacetic acid was added. In the zero time tubes the trichloroacetic acid was added immediately after the addition of trypsin. After standing at room temperature for about 1 hour the tubes were centrifuged, the clear supernatant carefully removed and the precipitate used for N determination.

In each experiment homogenates or fractions of unfertilized and fertilized eggs from the same batch were handled simultaneously.

Heat denaturation. Two series of tubes, one for the unfertilized and one for the fertilized eggs, each containing 0.5 cc of supernate or solution of a fraction in borate buffer, were heated in a thermostatically controlled water-bath. Temperatures between 55°C and 65°C were used. At certain time intervals one tube of each series was withdrawn, 5.0 cc of the salt buffer added from a burette and the mixture rapidly stirred. In the zero time tubes the buffer was added without any previous heating. After about 1 hour standing at room temperature, the tubes were centrifuged and the precipitate used for N determination.

The salt buffer is made up as follows (3):

Acetic acid, 0.8 moles; sodium acetate, 0.4 moles; and magnesium sulphate, 0.5 moles per liter.

N was determined by direct Nesslerization and the colour was read in a Klett-Summerson photoelectric colorimeter.

Test for the inhibition of the fibrinolytic activity of trypsin. This was done according to Astrup and Müllertz (2). 10 cc of a 1 per cent Armour Bovine fibrinogen were clotted in Petri dishes by the addition of a few drops of a thrombin solution, kindly prepared for us by the Istituto Sieroterapico Italiano, Naples. On the surface of the clot drops of 0.03 cc were placed from a 0.1 cc pipette, all containing the same concentration of trypsin and varying concentrations of the homogenate. After about 20 hours at 37°C, the area of fibrinolysis was measured and compared with that of control drops in which trypsin was diluted with the buffer.

SUMMARY

The sensitivity to trypsin and to heat denaturation of extracts of unfertilized and newly fertilized eggs of *Arbacia lixula* has been studied. The extracts have been also fractionated by precipitation at 50 per cent (fraction I) and 75 per cent (fraction II) saturation of ammonium sulphate and the fractions submitted to the same tests.

Extracts of fertilized eggs are more sensitive to trypsin than those of unfertilized eggs and the same is true for fraction II, whereas fraction I becomes slightly less sensitive after fertilization.

By the combined methods of the solubility in a salt buffer mixture and heat denaturation, it has been shown that upon fertilization the group of proteins of fraction I undergoes a decreased precipitability by the salt buffer at room temperature. The total amount of proteins precipitated by the salt-buffer after heating is also lower after fertilization. The significance of these results is discussed.

We wish to express our indebtedness to Professor J. Runnström and Dr. A. E. Mirsky for their suggestions and for reading the manuscript and to Dr. K. Bailey for an interesting and stimulating correspondence. The technical assistance of Mr. A. O. Oliva is acknowledged. The present investigations were supported by Grants of the Rockefeller Foundation and Consiglio Nazionale delle Ricerche.

REFERENCES

1. Anson, M. L., and Mirsky, A. E., *Physiol. Rev.*, **10**, 506 (1930).
2. Astrup, T., and Müllertz, S., *Arch. Biochem. Biophys.*, **40**, 346 (1952).
3. Christensen, L. K., *Compt. Rend. Trav. Lab. Carlsberg, Sér. Chim.*, **28**, 37 (1952).
4. Hoberman, H. D., Metz, Ch. B., and Graff, J., *J. Gen. Physiol.*, **35**, 639 (1952).
5. Hultin, T., Proceedings from the Symposium on the Biochemical and Structural Basis of Morphogenesis in *Arch. Néerl. de Zool.*, **10**, 76 (1953).
6. Linderström-Lang, U. K., Proteins and Enzymes. Stanford Univ. Press, 1952.
7. Lundblad, G., *Arkiv Kemi*, **4**, 537 (1952).
8. Mirsky, A. E., *Science*, **84**, 333 (1936).
9. —— *Cold Spring Harbor Symposia on Quant. Biol.*, **9**, 78 (1941).
10. Monroy, A., *Exptl. Cell Research*, **1**, 92 (1950).
11. Monroy, A., and Monroy-Oddo, A., *J. Gen. Physiol.*, **35**, 245 (1951).
12. Perlmann, P., and Gustafson, T., *Experientia*, **4**, 481 (1948).
13. Perlmann, P., *Exptl. Cell Research*, **5**, 394 (1953).
14. Runnström, J., *The Harvey Lectures, Ser.* **46**, 116 (1950/51).
15. —— *Symposia Soc. Exptl. Biol.*, **6**, 39 (1952).

MORPHOLOGY OF *BACTERIUM TULARENSE* DURING ITS GROWTH CYCLE IN LIQUID MEDIUM AS REVEALED BY THE ELECTRON MICROSCOPE

E. RIBI and C. SHEPARD

U. S. Department of Health, Education, and Welfare, Public Health Service, National Institutes of Health, National Microbiological Institute, Rocky Mountain Laboratory, Hamilton, Montana, U.S.A.

Received August 20, 1954

Bacterium tularense was first described by McCoy and Chapin (6) as a small, nonmotile, questionably encapsulated pleomorphic organism. Ohara, Kobayashi, and Kudo (9), Ota (10), and Ohara (8) observed coccoid and bacillary forms, motile by means of a single polar "special flagellum", and also described capsules. Hesselbrock and Foshay (3) reported coccoid, cylindrical and flattened bacillary forms, globules and globi, filaments and "minimal reproductive units" as the morphological units of *B. tularense*. These authors claimed to have observed multiple modes of reproduction which led them to compare *B. tularense* with organisms of the pleuropneumonia group. They could not demonstrate reproduction by binary fission. The structures that were earlier believed to be flagella, were described by Hesselbrock and Foshay as delicate non-motile filaments of flagellar size, the formation of which was correlated with the mode of reproduction. The same authors also stated that the capsular structures which had been described were not of extracellular nature but actually were cell walls.

The foregoing studies of the morphology of *B. tularense* were carried out by means of staining techniques and examination under the light microscope. With the help of the electron microscope, Eigelsbach, Chambers, and Coriell (1), confirmed the existence of the multiple morphological units described by Hesselbrock and Foshay (3) and revealed, in particular, the extremely delicate structure of the cell wall. Most of the specimens examined by Eigelsbach, Chambers, and Coriell were obtained by using water and saline suspensions of growth from solid media or suspensions from liquid media which had been diluted with water. We have found, however, that the cell wall of *B. tularense* is extremely susceptible to changes in osmotic pressure of the environment (12). Thus, for example, rod-shaped cells from cultures in solid and liquid media immediately changed into spherical cells when suspended in water. Furthermore, many of the cells suspended in water

ruptured during the process of desiccation on the specimen membrane. If very thin films of saline suspensions of organisms were used, the cells, after drying in air, appeared to be plasmolyzed, presumably because of the increasing salt concentration.

In an effort to preserve the original morphology of *B. tularense* for electron microscopic studies, various methods of specimen preparation were investigated. It was found that a modification of a technique previously described (11) yielded the most satisfactory results. Employing this method, it was possible to follow the morphology of *B. tularense* during the growth cycle by examination of samples obtained from liquid cultures at appropriate intervals.

MATERIALS AND METHODS

Cultures. A culture of *B. tularense* strain 46, maintained in the collection of the Rocky Mountain Laboratory, was selected for study. Organisms from a 24-hour slant culture grown on glucose-cystine-blood agar were inoculated into glucose-cystine broth and incubated with continuous shaking at 37° C. Aliquots of samples of the broth culture were taken at the desired intervals to determine the number of cells and, at the same time, to prepare specimens for electron microscopy. The total number of cells was estimated by use of the Beckman spectrophotometer and the number of viable cells was determined by means of pour plates.

Preparation of specimens for electron microscopy. The usual specimen membrane of formvar was covered with a metal layer, a few Ångstrom units in thickness, by evaporation of a copper alloy in high vacuum. The copper component, oxidized by air, constituted a positively charged colloid which enabled the specimen membrane to adsorb the negatively charged bacterial cell from aqueous suspensions. A drop of broth culture was placed on the specimen membrane and then immediately removed with a fine capillary. It was thus possible to obtain specimens of dispersed cells adsorbed directly from the liquid culture which could be examined under the electron microscope without fixation by chemical agents or purification procedures. Greater clarity was achieved by removing the small residues of culture medium from the specimen membrane. For this purpose, the air-dried specimen was exposed to vapor of one per cent osmic acid solution for about 20 minutes. The residual materials could then be washed off with water without causing changes in the electron microscopic morphology of the cells. With one exception (Fig. 8), all reproductions in the present paper are of specimens fixed with osmic acid vapor, washed with water as described, and subsequently shadowed with a platinum-palladium alloy.

RESULTS

The growth curves of *B. tularense* strain 46, cultured on liquid medium at 37° C, are shown in Fig. 1. At each point shown on these curves, cells were removed and prepared for electron microscopic examination. The upper

curve represents the relation between the total number of cells and the time after inoculation, and the lower curve shows the relation between the number of viable cells and time. It is evident that a phase of logarithmic growth began a few hours after inoculation and persisted at least through the twelfth hour of incubation.

Cells during the phase of active growth, i.e., cells obtained from 8- and 12-hour broth cultures, are shown in Figs. 2, 3, 4, and 5. These cells are seen to be more or less homogeneous and highly opaque rods; such homogeneous cells are characteristic of other bacteria when they are observed during the logarithmic phase of growth. However, a transparent area was frequently observed at one end of the cell. A comparison with micrographs of purified preparations of cell walls indicated that the transparent sites consisted of cell wall covering little or no protoplasmic material. The organisms were often curved (Figs. 2 and 4) or boomeranglike (Fig. 3). Many organisms, especially the curved or boomeranglike forms, showed a distinct constriction (Fig. 4) and thus appeared as paired or presumably dividing cells.

In the stationary phase, two main types of cells were found; in different cultures either one or the other of these two forms predominated. One form (Fig. 6) was a slender rod which had an opaque central body and semitransparent terminal areas where the protoplasm was distinguishable as more or less uniform granules. The second form (Figs. 7 and 8) was an oval-ellipsoidal cell containing two opaque bodies, one near each pole. The cells shown in Fig. 6 may represent resting forms, whereas the cells in Figs. 7 and 8 may represent slow-growing forms.

Unusual morphological changes occurred during the death phase when the cell walls became filamentously elongated and thus appeared as tubes, if filled with protoplasm, or flat ribbons, if emptied of protoplasm. The tubes reached a final diameter of about 30 to 40 mμ. The ribbons were transparent to electrons and showed a width of approximately 40 to 60 mμ. Both the tubes and ribbons were up to several microns in length. Figs. 9 and 10 show cells of the 48-hour culture in which the number of viable organisms was decreasing. The cells shown in Fig. 9 represent an intermediate stage in elongation of the cell wall, while Fig. 10 demonstrates cells with various degrees of elongation of the walls. Organisms from a 96-hour culture with tubes 30 to 40 mμ in diameter are seen in Fig. 11.

Most of the protoplasm of the extremely elongated cells was located at one or both ends of the filaments (tubes and ribbons), but sometimes in their middle. In addition to these, many intermediate forms, characterized by irregular distribution of protoplasmic constituents within the filaments, were

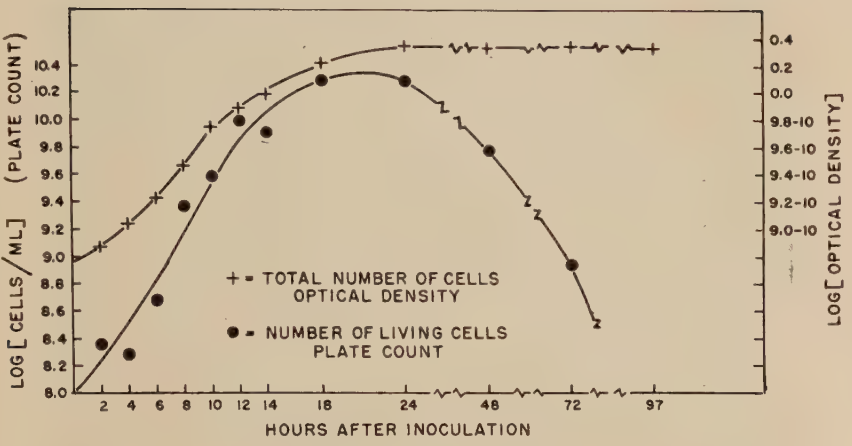

Fig. 1. Growth curves of *Bacterium tularense* cultured in glucose-cystine broth.

Fig. 2. *Bacterium tularense* from the 8-hour-old broth culture. Logarithmic phase of growth. 20,000 ×.

Fig. 3. *Bacterium tularense* from the 8-hour-old broth culture. Logarithmic phase of growth. 40,000 ×.

Fig. 4. *Bacterium tularense* from the 8-hour-old broth culture. Logarithmic phase of growth. 46,000 ×.

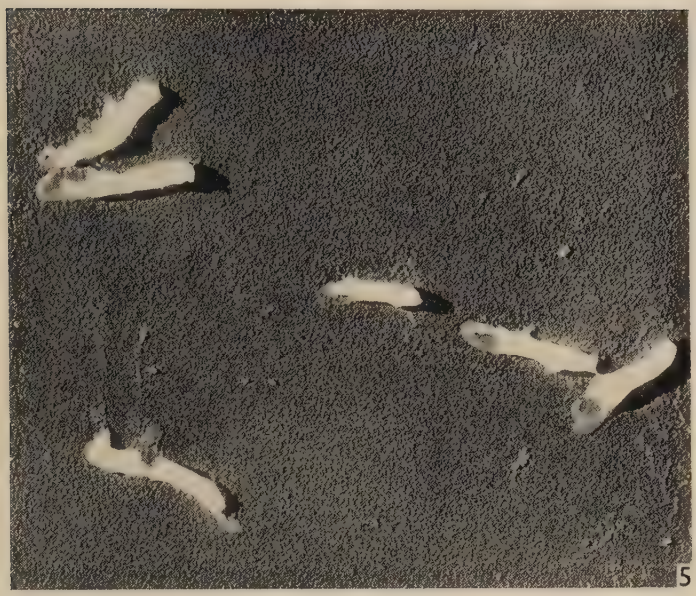

Fig. 5. *Bacterium tularense* from the 12-hour-old broth culture. Logarithmic phase of growth. 19,000 ×.

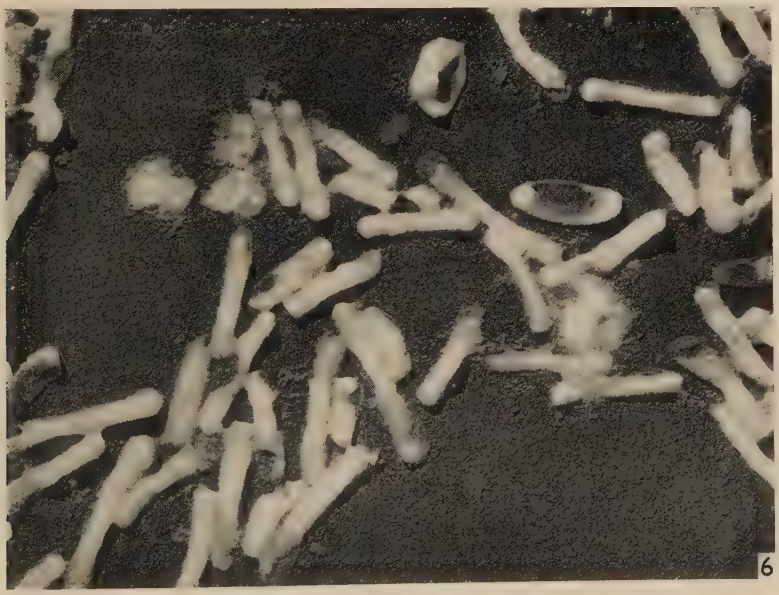

Fig. 6. *Bacterium tularense* from the 18-hour-old broth culture. Stationary phase of growth. 21,000 ×.

Fig. 7. *Bacterium tularense* from the 24-hour-old broth culture. Stationary phase of growth 24,000 ×.

Fig. 8. *Bacterium tularense* from the 24-hour-old broth culture. Stationary phase of growth. Unfixed, unwashed and unshadowed. 18,000 ×.

Fig. 9. *Bacterium tularense* from the 48-hour-old broth culture. Phase of decline. 21,000 ×.

Fig. 10. *Bacterium tularense* from the 48-hour-old broth culture. Phase of decline. 29,000 ×.

Fig. 11. *Bacterium tularense* from the 96-hour-old culture. Phase of decline. 19,000 ×.

Fig. 12. *Bacterium tularense* from the 72-hour-old culture. Phase of decline. 16,000 ×.

Fig. 13. *Bacterium tularense* from the 96-hour-old culture. Phase of decline. 39,000 ×.

observed. Observation of a series of pictures showed that the form of the filamented cell present in the death phase was determined by the previous morphology of the cell from which it was formed. For example, if cells from the stationary phase of a given culture had the protoplasm distributed predominantly at the poles, the resulting filamented cells found in the death phase would also have the protoplasm distributed at the poles, while cells with the protoplasm located terminally or subterminally at one end only, gave rise to filaments with the protoplasm likewise at one end.

Frequently, the filamented cells were fragmented, especially in later stages of the death phase. The disintegration products were dense protoplasmic bodies of various sizes which were either free or attached to shorter or longer tubes and ribbons. Also, unattached single tubes and ribbons of various lengths were observed (Fig. 12). A demonstration of the brittle nature of the filamented cells is given by Fig. 13, where the fragmentation obviously was due to the desiccation of the specimen upon the supporting membrane.

DISCUSSION

The technique of preparing specimens for electron microscopy includes adsorption of cells suspended in culture medium onto the specimen membrane, fixation in osmic acid vapor, and removal of residues by washing with water. Distortion which can be caused by other fixation and purification procedures is then minimized. Apparently, the only uncontrolable distortion of the cells that can cause artefacts is the desiccation upon the specimen membrane. In another communication (12) we described the changes in morphology of the *B. tularense* organism occurring if mild fixatives were added to withdrawn samples of the liquid culture, which then was washed and dried on the specimen grids. The latter method can be used successfully for other bacteria with cell walls less delicate than those of *B. tularense*, for example *Escherichia coli*. Successful techniques of specimen preparation which permit the cytological processing of bacterial cells with a minimum of physical or chemical disturbance have been developed by Hiller, Knaysi, and Baker (4), Mudd and Smith (7), and Kellenberger (5). However, the method used in the present study has the advantages of simplicity and rapidity. Furthermore, it permitted us to follow the electron microscopic morphology during the growth cycle of a broth culture of *B. tularense* by examination of samples removed at appropriate intervals. At the same time, growth could be followed by measurements of optical density and by plate counts.

Hesselbrock and Foshay (3) described *B. tularense* as "polygenthodic", possessing multiple modes of reproduction. They stated that division by binary fission was not observed. However, micrographs which show a few cells suggesting division by fission were presented by these authors. The results of the present investigation suggest binary fission as the mode of reproduction, since electron microscopic observations of actively growing cultures proved what appeared to be division into daughter cells by constriction. "Morphologic units" described by Hesselbrock and Foshay as belonging to a complex life cycle like the pleuropneumonia group were observed exclusively during the phase of decline.

The elongation of the cell wall, and thus the formation of filamented cells, was observed as characteristic of the phase of decline. In broth cultures studied, this phase was found to be comparatively short, and there is little doubt that the filamented cells represented dead or dying organisms. These cells were observed to be fragile. They easily broke into dense protoplasmic

bodies of various sizes and into filaments of various length. The protoplasmic bodies appeared as discrete particles attached to, or within, shorter and longer filaments. These disintegration products which we observed by means of the electron microscope, corresponded to forms noted by Hesselbrock and Foshay (3) in cultures examined by means of dark field microscopy. However, the latter authors believed the "particles" to be "minimal reproductive units" (MRU), and they correlated the appearance of the filaments with various modes of reproduction. The statement of Hesselbrock and Foshay that these "true morphologic units" were never seen earlier than four days after inoculation of a gelatin hydrolyzate medium, suggests that their observations were made on cultures during the phase of decline.

Foshay and Hesselbrock (2) found that cultures of *B. tularense* yielded filtrates infective for mice when screened through membranes with 600 mμ average pore diameter (APD), but not when screened through 500 mμ APD or smaller membranes. They also observed that the bacteria recovered from mice by culture produced all the morphologic variants which they had found to be characteristic for this organism. Such filter-passing "particles" would be expected to have a diameter in the range of 300 to 350 mμ, and it was assumed that the typical *B. tularense* cell would exceed such limits. Foshay and Hesselbrock presented this demonstration of filterability as evidence that the minute forms which they had observed microscopically were indeed "minimal reproductive units" somewhat analogous to the filtrable MRU described for the pleuropneumonia group (13).

In commenting on this interpretation, we should like to refer in particular to those MRU which were described by Hesselbrock and Foshay (3) as minute bodies located within or at the tips of shorter or longer filaments. Our studies with the electron microscope on various strains of *B. tularense* showed that the filaments were about 30 to 60 mμ in width. Therefore, these forms should pass a 500 mμ APD membrane even if the diameters of the filamentously attached protoplasmic bodies were several times larger than the diameter of the filaments.

The nature of the infective forms in the 600 mμ APD membrane filtrate is not mysterious. It is doubtless a matter of definition of the term "filtrable", since we observed that the viable cells of *B. tularense* vary greatly in size and shape under different environmental conditions and at different stages of growth. Attention is directed to the very slender cells which appeared during the phase of decline, as shown in Fig. 9. Since the width of three of the slender rods seen in the upper right portion of the figure is not larger than about 300 mμ, these cells would be able to pass through a 600 mμ APD

membrane. The slender cells which were observed to gradually decrease in number during the death phase must be distinguished from the unbroken bizarre cells, the walls of which were filamentously elongated. Most of the filamented cells showed the protoplasm accumulated in one large body which would not pass a 600 mμ membrane (Fig. 11). Counts on the electron micographs indicated an increasing ratio of the filamented forms to the slender rods during the death phase. This ratio agrees reasonably well with the ratio of dead to live bacteria as obtained from turbidity measurements and plate counts, and it thus appears likely that the bizarre forms are not living and the slender rods are viable.

It is noteworthy that Foshay and Hesselbrock (2) found that 0.2 to 1.0 ml of their filtrate from a 600 mμ APD membrane produced sterile cultures and that only four of ten mice injected with 0.5 ml amounts of the same filtrate developed tularemia. Since mice are extremely susceptible to this infection it would seem that the concentration of infective particles was very low in this filtrate, probably of the order of 1 organism per ml, and that the "discrete particles" observed in the filtrate therefore, could hardly correspond to viable units.

We tend to regard the formation of filaments as a manifestation of change in the internal structure of the cell wall which would alter such physical properties as rigidity, ductility, and elasticity. Thus, it has been observed by us in unreported experiments that, in contrast to the walls of the slender viable organisms, the tubelike walls of the bizarre cells were not elastic enough to swell on treatment with water and were consequently very brittle. Moreover, the filamentous fragments of broken, death phase cells were very similar to the filamentous morphologic elements that resulted when water suspensions of purified cell walls from young cells of *B. tularense* were shaken with ether (12, 14). The formation of these filaments is apparently due to a process of denaturation of the protein skeleton substance of the cell wall (12). In this case the denaturation is caused by the action of an organic solvent, ether, and by mechanical action. The natural formation of filaments from the cell wall in aged cultures of *B. tularense* could also be due to a process of denaturation. Thus, denaturation inducing substances could be present in the accumulated end products in the culture; the unfavorable environmental effects of such end products are well known. Too, mechanical forces contributing to denaturation could be provided by the continuous shaking during growth of such cultures.

SUMMARY

Electron microscopic studies of the morphology of *Bacterium tularense* during the various stages of its life cycle were carried out. A technique of preparation is described, based on direct adsorption of cells from liquid cultures onto copper containing metal layers. A growth curve was plotted for the moderately virulent strain 46 and specimens were prepared for electron microscopic study at each point of the curve. Cells with constrictions, suggesting reproduction by binary fission, were observed during active growth. During the death phase the cell walls became filamentously elongated, forming tubes about 30 to 40 mμ in diameter and up to several microns in length. The filamented cells, which appeared to be dead, showed little mechanical solidity and fractured easily into pieces corresponding to the forms visualized by Hesselbrock and Foshay with the aid of light microscopy. The results presented here do not support their contention that these minute forms are "true morphologic units" belonging to a developmental cycle and capable of reproduction, but indicate that these forms are disintegrated dead cells. It is therefore concluded that *B. tularense* does not have a complex life cycle like the pleuropneumonia group, but most likely has a mode of reproduction common to many other gram negative rods.

REFERENCES

1. Eigelsbach, H. T., Chambers, L. A., and Coriell, L. L., *J. Bacteriol.*, **52**, 179 (1946).
2. Foshay, L., and Hesselbrock, W., *ibid.*, **49**, 233 (1945).
3. Hesselbrock, W., and Foshay, L., *ibid.*, **49**, 209 (1945).
4. Hillier, J., Knaysi, G., and Baker, R. F., *ibid.*, **56**, 569 (1948).
5. Kellenberger, E., *Experientia*, **8**, 263 (1952).
6. McCoy, G. W., and Chapin, C. W., *J. Infectious Diseases*, **10**, 61 (1912).
7. Mudd, S., and Smith, A. G., *J. Bacteriol.*, **59**, 561 (1950).
8. Ohara, H., *Proc. Third Internatl. Cong. Microbiol.*, p. 678 (1940).
9. Ohara, H., Kobayashi, T., and Kudo, J., *Tohoku J. Exptl. Med.*, **25**, 650 (1935).
10. Ota, I., *Kokumin Eisei*, **13**, 43 (1936).
11. Ribi, E., and Rånby, B., *Experientia*, **6**, 27 (1950).
12. Ribi, E., and Shepard, C., In preparation.
13. Sabin, A. B., *Bact. Revs.*, **5**, 1 (1941).
14. Shepard, C., Ribi, E., and Larson, C., *J. Immunol.* (In press.)

THE EFFECT OF COLCHICINE ON STRIATED MUSCLE IN TISSUE CULTURE[1]

G. C. GODMAN[2]

Histochemistry Research Laboratory, Columbia University, College of Physicians and Surgeons, New York, N.Y., U.S.A.

Received August 23, 1954

Mature differentiated striated muscle in tissue culture is capable of extensive regenerative growth, forming long plasmodial fibers or ribbons, designated sarcoblasts (24). These may attain continuous lengths up to 3 mm, and commonly vary from 5 to 15 μ in width. The sarcoblast cytoplasm is refractile, viscous and gelated (6), and often faintly birefringent (16). Under favorable conditions structural differentiation, with the development of longitudinal and cross-striations may occur. However, even structurally undifferentiated sarcoblasts often exhibit strong fibrillatory and pulsatile contractions. In the course of studies on striated muscle in tissue culture it was observed that colchicine, a well-known mitotic poison, induced a remarkable series of changes in the structure of the sarcoblast-ribbons (11), which will be described in detail and further discussed in this report.

METHODS

Explants from the gluteal and femoral muscle of suckling rats were cultured, using the double cover slip method of Maximow (20), in a mixture composed of 1 part chicken plasma, 2 parts human placental serum, and 1 part 50 per cent chick embryo extract. Thrice weekly (at 48 or 72 hour intervals) the cultures were washed in Simms X-7 balanced salt solution (27) and fed a solution in which the plasma of the planting mixture was replaced by ox-serum ultrafiltrate. The proportion of embryo-extract was subsequently gradually reduced somewhat, to promote differentiation. 215 successful preparations were maintained for periods from 15 to 75 days, two being kept for 185 days. At various ages groups of 2 to 10 cultures were treated with colchicine and the following substances, made up in the feeding mixture to the final concentrations indicated:

Colchicine, from 10^{-5}M in 5-fold dilutions to 10^{-8}M; chloral hydrate, 10^{-3} and 10^{-6}M; benzoquinone, 10^{-3} and 10^{-6}M; sodium barbital, 10^{-5}M; heparin, 0.25 mgm/ml, quinine dihydrochloride, 2.5×10^{-5}M; procaine base 4×10^{-5}M; "vera-

[1] Aided by grants from the Damon Runyon Memorial Fund for Cancer Research, and the Jane Coffin Childs Fund for Medical Research.

[2] Fellow of the Damon Runyon Memorial Fund.

trine", 10^{-5} gm/ml; tubocurarine hydrochloride, 10^{-5}M; "mapharsen" (3 amino 4 hydroxyphenylarsenoxide hydrochloride) 5×10^{-5}M; plasmocid, 0.1 mgm/ml.

In other experiments with possible antagonists or synergists cultures were exposed simultaneously to colchicine (in concentration from 10^{-5} to 10^{-7}M) and one of the following compounds: m-inositol, 10^{-3}M; ATP disodium, 5×10^{-3}M; l-cysteine, 10^{-5}M; glutathione, 10^{-5}M. Controls were provided by administration of each drug alone, and by untreated cultures of comparable age.

The standard test period during which each agent was first permitted to act on a group of cultures was 48 hours. Periods of 12, 18, 24 and 36 hours and from 4 to 20 days of continuous exposure to colchicine with subsequent refeeding, were also tested. Treatment was terminated by thorough washing in 2 changes of balanced saline, and the cultures either fixed or refed and allowed to recover. Measurements of living sarcoblasts were made by means of an ocular micrometer. Birefringence was sought in formalinized material, using a first order red plate and selenite wedge. Preparations were stained with haematoxylin, iron haematoxylin, or Pollak's method for mitochondria, after various fixation.

RESULTS

Form of intact muscle cultures. After a relatively long latent period, outgrowth of muscle slips proceeded rapidly, and was well-established in about 15 days. Subsequently the rate of proliferation declined, and structural differentiation of individual sarcoblasts became more prominent. Measurements of the lengths of all the muscle ribbons in representative fields of the outgrowth zone, when plotted as a histogram, had a characteristic bimodal distribution, reflecting the presence of long, continuous centrally attached fibers, from 1.0 to 3 mm, and smaller numbers of short strap forms, of from 0.2 to 0.7 mm. (Table I.)

Structural effects caused by colchicine. The addition of effective concentrations of colchicine to such cultures was invariably followed by characteristic changes leading to disruption of the sarcoblasts. At various intervals along the fibers there first developed slight, gradual expansions which then drew apart, remaining connected for some time by an attenuating bridge of sarcoplasm. Most commonly the filaments bridging the retreating segments seemed to be pulled taut and then snap, resulting in separate wide segments with straight terminal filaments at each end. In other regions of the fiber, adjacent continuous segments underwent marked focal expansion, leaving between them a constricting waist, at which they finally sundered. Sharp fracture lines appeared at the same time in the detached segments and in the remaining lengths of the ribbons. Transverse, longitudinal, tangential and eccentric clefts split the sarcoblasts into short elements, which then separated as though by an oblique lateral shearing or slipping movement. (Fig. 3.)

The picture as it appeared at 36 to 48 hours was one of generalized fragmentation of the original muscle slips into distinctly widened somewhat angulated segments averaging 0.1 to 0.4 mm in length, and of rhomboidal, fusiform or clubbed shape. These elements usually lay linearly disposed

TABLE I

Influence of colchicine on length of sarcoblastic elements and recovery therefrom.

Typical micrometer measurements of lengths of living fibers in representative fields of muscle cultures before and at intervals after standard 48 hour treatment with colchicine, 10^{-5} M, showing the shortening of the muscle elements due to segmentation and contraction. Recovery through regrowth occurs within a week.

Culture	Age at treatment (days)	Days after treatment	Fiber lengths, mm		
			Mode	Median	Mean
D16	19	Control	0.4, 1.2	1.2	0.96
		2	0.1	0.15	0.22
		6	0.5, 1.5	0.8	0.87
D6	21	Control	1.0	0.85	0.61
		0	0.1	0.15	0.16
		2	0.05	0.1	0.14
		14	0.4	0.5	0.84
D7	14	Control	0.4, 1.5	0.5	0.48
		1	0.1	0.1	0.16
		4	0.05	0.1	0.11
		11	0.3	0.3	0.40
H18	27	Control	0.4, 1.5	0.5	0.84
		0	0.15	0.2	0.21
		3	0.05	0.1	0.09
		7	0.2	0.25	0.23
H14	19	Control	0.9, 2.0	1.5	1.2
		2	0.1	0.15	0.24
		6	0.25	0.55	0.55
		8	0.4	0.55	0.55

Fig. 1. Control culture of striated muscle at 15 days. Long, slender plasmodial ribbons (sarcoblasts). Living, × 150.

Fig. 2. 15 day old culture after 48 hours of treatment with 5×10^{-7} M colchicine. Shortened, widened segments resulting from disruption of fiber. Living, × 150.

Fig. 3. 32 day old culture 60 hours after beginning of treatment with 10^{-5} M colchicine, showing focal expansion (e), filamentous bridges between separating segments (b), and fractures (f). Living, × 150.

Fig. 4. Same culture as in Fig. 3, 120 hours after beginning treatment with 10^{-5} M colchicine. The segments have been reduced to blunted masses and globules. Living, × 150.

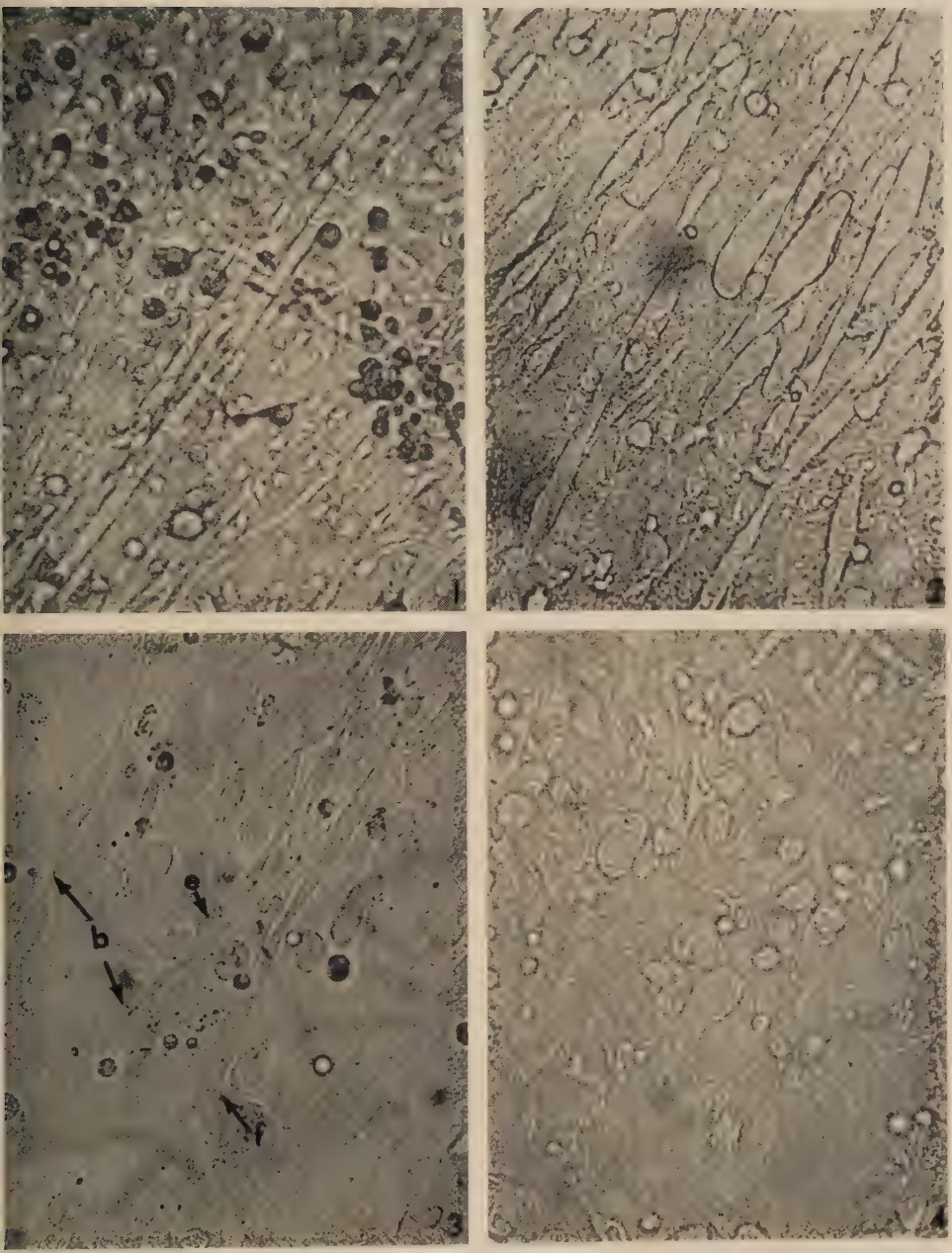
b

along the former path of their parent fiber. As the effect of the colchicine continued, the pieces shortened and spread, most of them now measuring between 0.03 and 0.1 mm long and 20–30 microns (3 × the width of comparable intact fibers) across. They presented themselves as rather widely spaced, discrete sessile globules with rounded contours, of definitely enhanced transparency, diminished refractility and apparently decreased consistency, without remnant of striation (Figs. 4 and 8). Further exposure to colchicine often resulted in an appearance of blebs and protuberances at the surface and even detachment of fragments of protoplasm.

Examination of fixed and stained preparations confirmed that each of the surviving segments, particularly at intermediate stages in the breaking of the fibers, possessed many more nuclei than comparable lengths of intact sarcoblasts. (Fig. 7.) This nucleosis probably results not from proliferation but from simple condensation of nuclei normally present in long stretches of the fiber consequent on the marked shortening and widening of the pieces, and the passage of nuclei from the filamentous bridges into the surviving segments.

Other effects. Anucleate sections (sequestra), as well as occasional nucleated segments, degenerated and disappeared. Most of the nucleated segments, however, remained quite viable, with relatively clear transparent cytoplasm, even after prolonged continuous exposure to colchicine.

The cytoplasm of fibroblasts and "histiocytoid" cells was sometimes irregularly expanded into droplike protrusions on the surface, apparently due to decreased viscosity.

Dosage and differentiation. In quantitatively evaluating the effects of colchicine, the drug concentration, the duration of its action, and the age of the culture (as an index of the size and degree of differentiation of its sarcoblasts), were assessed as related variants (Table III). Colchicine, in dilution to a minimum of 10^{-8} M, acting during the usual 48 hour test period, elicited the characteristic changes in sarcoblast fibers. The earliest times of appearance of these changes in relation to concentration and culture age are indi-

---

Fig. 5. Control culture of striated muscle at 15 days. Iron-haematoxylin, × 125.
Fig. 6. 22 day old culture after 48 hours of treatment with 10^{-6} M colchicine, illustrating filaments, pointed segments, and longitudinal fissure (f). Iron-haematoxylin, × 125.
Fig. 7. 24 day old culture after 48 hours of treatment with 10^{-7} M colchicine. Long segment showing marked nucleosis, general widening and focal expansion. Haematoxylin, × 180.
Fig. 8. 22 day old culture, 120 hours after beginning treatment with 10^{-6} M colchicine, showing details of the segments, which are similar to those of Fig. 4. Some nuclei are deformed (n). Iron haematoxylin, × 610.
Fig. 9. Control culture at 15 days. Sarcoblast ribbon showing the strict adlineation and longitudinal array of the mitochondria. Polak method, × 610.
Fig. 10. 15 day old culture after 36 hours of treatment with 5×10^{-6} M colchicine. Segment, showing random orientation of mitochondria. Polak method, × 610.

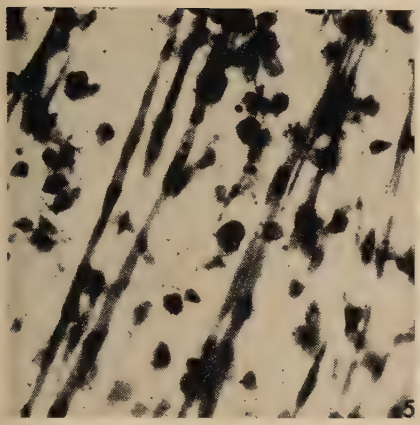
5

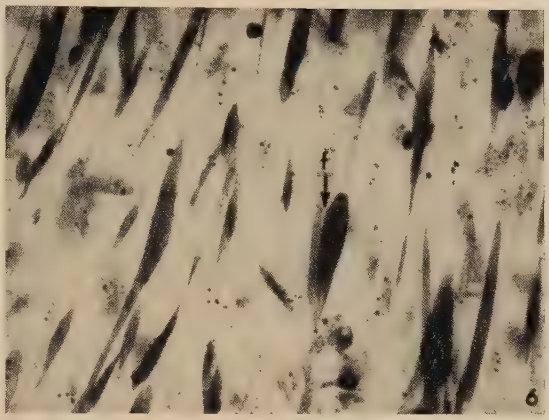
6

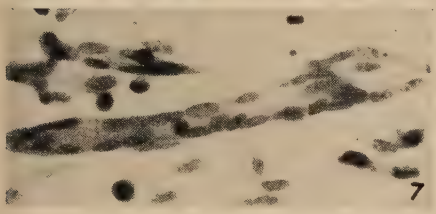
7

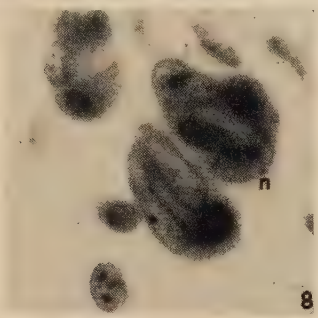
n
8

9

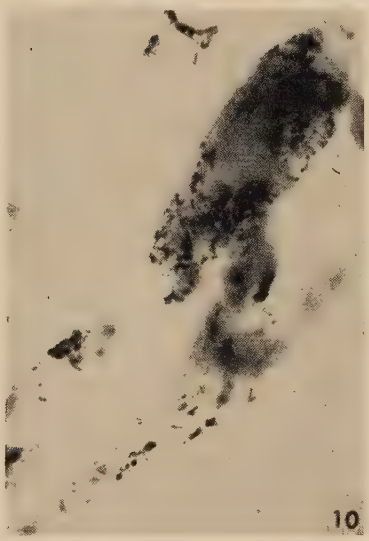
10

cated in Table III, which reveals a dependence upon both of these variables. During 18 to 36 hours of exposure to effective concentrations of colchicine, most of the slender undifferentiated ribbons were segmented, while the

TABLE II

Influence of colchicine on width of sarcoblastic elements, and recovery therefrom.

Maximal diameters of sarcoblasts in representative fields of muscle cultures before, during and at intervals after exposure to colchicine, indicating the marked expansion of fiber segments, and recovery.

Culture	Age at treatment (days)	Duration of exposure (hours)	Days after treatment	Fiber widths, Maxima, Microns		
				Mode	Median	Mean
Series G. (Combined)	Control	—	—	9, 12	10	9.5
Colch. 5×10^{-7} M; total	15	2	0	15	15	13
exposure 96 hr.		8	0	20	19	16
		20	0	18	19	18
		28	0	16, 24	21	19
		48	0	21	23	23
Series I. Colch. 10^{-6} M;	Control	—	—	8, 15	10	9.3
total exposure 18 hr.	22	18	0	18	18	20.2
		18	$^1/_2$	20	25	24
		18	3	15	14	13.5
		18	8	5	7	6.5
		18	18	7	6	6.5

TABLE III

Relation of colchicine concentrations and ages of cultures to effect on sarcoblast fibers.

	Onset of changes, hours after addition of colchicine					Estimated extent and severity of effect at 24 hours after addition of colchicine				
	10^{-5}	10^{-6}	5.10^{-7}	10^{-7}	10^{-8}	10^{-5}	10^{-6}	5.10^{-7}	10^{-7}	10^{-8}
Group A										
15–30 days old . .	3	4–5	5–7	7	20	+ + +	+ + +	+ + +	+ + +	± − +
Group B										
30–50 days old . .	?	8	?	10–12	?	+ +	+ − #	?	+	±
Group C										
Older than 50 days	5–8	?	8–10	10–12	?	+	+	?	+	?

broadest or more differentiated (striated) fibers, apparently more resistant, usually exhibited only early changes. Older cultures with higher populations of differentiated or larger sarcoblasts were generally somewhat slower to respond, although ultimately even cross-striated ribbons were broken in the manner described. Cleavage or expansion of the adult muscle fibers in the original explant was not observed, however. Differentiating sarcoblasts often retained distinct longitudinal fibrillar striations throughout early and intermediate stages of their segmentation. The advanced stages were usually uniformly homogeneous.

Contracting fibers continued to fibrillate actively during their colchicine induced segmentation, the partially or wholly separated pieces contracting independently. In the late stages of the colchicine effect, as the segments widened, contractility was lost.

In both degree and extent (i.e. numbers of fibers involved), the magnitude of the effects elicited by colchicine on fibers of comparable girth and degree of differentiation was proportional to dosage, i.e., concentration $\times$ time of exposure. It is of interest that after addition of effective concentrations of colchicine, the changes were maximal 4 to 5 days later, regardless of whether the culture was continually exposed to the drug through this time, or whether it had been washed and fed with colchicine-free medium after the standard 48 hour treatment. It would seem that colchicine, having penetrated, continues to act within the sarcoblast for some time.

Recovery. Even after prolonged continuous exposure to colchicine, the nucleated segments were capable of regeneration when the drug is withdrawn.

In this process, the regenerating piece put forth a delicate filiform process which rapidly elongated, sometimes exhibiting a ruffled advancing tip. These processes merged with the bodies of adjacent segments encountered in their line of growth, in this way joining them in a single new fibre. Since each segment could regenerate independently, sheaves of slender new fibers were formed in this way along a track previously occupied by the single ribbon from which the segments had been derived. Subsequent union and growth, however, reduced the numbers of elements. In recovered cultures, only a disorientation in the fibres with respect to the explant center remained to testify to the severe antecedent effects of colchicine. The rapidity and completeness of this recovery were inversely proportional to the dosage of the drug. After a standard treatment with effective concentrations, recovery was complete usually in a fortnight. Restitution did not occur in the continued presence of colchicine.

Mitochondrial orientation and birefringence. The assumption that mitochondrial orientation reflects the pattern of molecular organization of the

cytoplasm (25) would seem to have been particularly well borne out by studies made on developing muscle fibers (8, 31). With this in view, studies were made on the mitochondrial orientation of the sarcoblastic ribbons. The filamentatous mitochondria of the untreated differentiating fiber were always regimented in parallel with the long axis of the fiber, in strict array. (Fig. 9.) After limited colchicine treatment, this mitochondrial orientation in the resulting segments was lost, the arrangement becoming entirely random. (Fig. 10.) In late stages, after extreme shortening and spreading of the segments, the mitochondria appeared as granules or globules rather than as rodlets. Birefringence could not be detected in the segments resulting from advanced colchicine treatment, also indicating a disorientation of submicroscopic elements.

To verify qualitatively that colchicine is capable of acting on the contractile protein of muscle, threads of actomyosin gel were exposed to relatively strong solutions of colchicine. There was no apparent change in the dimensions or appearance of the treated threads as compared with the controls; however, the colchicine-treated threads failed to respond perceptibly by syneresis to the addition of ATP, indicating that colchicine had rendered the actomyosin less reactive.

Other agents and controls: Changes of the nature described were never seen either in untreated muscle cultures, or in those given any of the 10 active agents listed above, in concentration similar to that of the colchicine. These disruptive effects on sarcoblastic ribbons were infallibly and sensitively elicited only by colchicine among the agents tested.

Neither cysteine, glutathione, m-inositol, nor ATP had any verifiable effect on the action of colchicine. Cysteine and glutathione were somewhat toxic at a concentration of 10^{-5} M.

DISCUSSION

Concentrations of colchicine acting for effective mitotic poisoning *in vitro*, are usually in excess of 10^{-6}M; in the case of rat fibroblasts it is about 2×10^{-6}M (21). Such concentrations of colchicine act not only to destroy or to inhibit the formation of the mitotic spindle (5, 9, 13, 17) but also to decrease general cytoplasmic viscosity (3, 5, 9, 10, 19, 21, 22, 32). Mitotic arrest reaches its height in about 20 hours (21), and the apparent depression of cytoplasmic viscosity even more rapidly (19); both effects are relatively quickly reversible, even in the continued presence of colchicine (19, 21).

As we have seen, colchicine also profoundly influences the structural integrity of the immature muscle fiber, in lower minimal concentration (10^{-8}M) than that affecting mitosis in cells of the same species. However, a longer

treatment is necessary, and more time must elapse after colchicine administration before the fullest effect becomes observable; moreover, once established, the changes in the sarcoblasts are not reversible while colchicine remains in the medium. The more differentiated elements respond more slowly, and with minimally efficient concentrations, incompletely.

The findings concerning the relation of dosage and differentiation of the sarcoblasts to the observed changes, parallel those of Gaulden and Carlson (9) on the mitotic spindle, in which the effectiveness of colchicine was found to be directly proportional to its concentration, and inversely related to the degree of spindle development.

Colchicine causes the spindle to shorten, lose its birefringence (13, *inter al.*) and disappear, often leaving a residual "hyaline globule" (9). It appears to reduce cytoplasmic viscosity in several cell types, as deduced from visually observable changes (5, 9, 10, 19, 21) or centrifugation experiments (3, 22, 32). These phenomena have some apparent counterparts both microscopic and molecular, in many of the changes occurring in the sarcoblast after colchicine treatment.

The achromatic figure is a gelated and birefringent structure (13, 26, 28), believed to be formed, at least in major part, of extended oriented chains of asymmetric molecules (fibrous protein) (7, 13, 26), for which a contractile function has sometimes been postulated (4, 13, 15, 30 *inter al.*). It has therefore been suggested that asters are gels of a "myosin-type" protein. Indeed, "myosin-like" or fibrous proteins (e.g. renosin, structure protein) have been extracted from a variety of different cells (1, 18, 29). They have been regarded as the 'structural', 'framework' or 'contractile' proteins of the cytoplasm (1, 7, 12).

It is therefore significant that colchicine, in concentration to about 2.5×10^{-8}M can bring about a 25–30 per cent decrease in the rate of fall of the viscosity of actomyosin gels induced by ATP, as Barány and Palis (2) have shown. This is of the same order of concentration as that found to be minimally effective in causing changes in the sarcoblasts; such doses are perhaps more nearly comparable to those inhibiting mitosis, causing chromosome contraction, or inducing changes in cytoplasmic viscosity (19), than to the higher concentrations which have so far been found to be capable of affecting known enzyme systems *in vitro* (14, 15).

It is reasonable to assume that the ribbon like continuity of the sarcoblast plasmodium, its gelated state, and birefringence are all explainable in terms of a parallel arrangement of such extended long-chain protein micelles, longitudinally oriented and associated. Colchicine probably specifically

interferes with the maintenance of this organised submicroscopic pattern, as is further evidenced by the disorientation of the normally strict mitochondrial arrangement, and the ultimate loss of birefringence, resulting from exposure of the sarcoblast fiber to colchicine.

In molecular terms, colchicine might effect a folding of elongated protein chains from fibrous to globular (23), or a dissociation of micellar aggregates, either directly by disrupting their linkages (27), or indirectly by influencing a constituent which keeps them extended, polymerized and associated with each other (13).

Lettré has proposed that colchicine inhibits a reaction between ATP and a contractile system of the actomyosin type inside the cell during mitosis (15). The failure of added ATP to influence the disruption of sarcoblast fibers by colchicine, may mean that ATP was insufficiently stable in the medium, that it failed to penetrate into the sarcoplasm, or that it did not antagonize the action of colchicine within the cell. These experiments, and the fact that rhythmical contraction of a fiber may continue for some time after the colchicine effect has begun, are not quite consonant with the theory advocated by Lettré (15) that the action of colchicine is antagonized by ATP, at least in the case of muscle. For the transfer of energy which ATP mediates to be translated into cell movement or gross morphologic change, must require an intact structural substratum. It is probable that colchicine reacts directly with such structural systems of linked fibrous protein molecules to disturb their relationships or internal configurations, or both.

The inability of meso-inositol to affect the colchicine-induced change in the sarcoblasts, in contrast to the proven ability of the former to reverse the effect of colchicine in mitosis (21) might mean that a different mechanism is involved in each case. But whatever the mechanism of the action of colchicine on anisotropic systems, it appears to result finally in a more random arrangement of particles. This evidently, may be elicited in cell components of fibrillar arrangement concerned with structure and movement, whether in the hyaloplasm or ectoplasm, the atractoplasm (achromatic figure) or the muscle proto-fibrils. In the case of the sarcoblast fiber this action of colchicine is visibly expressed in destruction of continuity, shortening and expansion. In the spindle it is manifested by contraction and dissolution, and in the cytoplasm by a general reduction of viscosity. Colchicine appears to affect a basic arrangement of submicroscopic fibrillar elements common to all cells, and in the case of the sarcoblast, one in which the alignments, length and number of these contractile chains are most highly developed.

SUMMARY

Colchicine, in concentrations of 10^{-8}M or greater, causes a disruption of sarcoblast ribbons grown in tissue culture. The resulting segments are markedly shortened and widened, and of diminished consistency. They remain viable and capable of regeneration. Evidence is offered that these changes are due to the action of colchicine on an oriented system of extended protein micelles, presumably actomyosin protofibrils. The effect of colchicine on sarcoblasts is discussed in relation to its known action on the spindle and cytoplasm.

The author's thanks are due to Miss Priscilla Goettler for expert assistance, to Dr. A. W. Pollister for helpful criticisms, and to Dr. M. R. Murray.

REFERENCES

1. Banga, I., and Szent-Györgyi, A., *Enzymologia*, **9**, 111 (1940–1941).
2. Barány, E. H., and Palis, A., *Acta Physiol. Scand.*, **25**, 174 (1952).
3. Beams, H. W., and Evans, J. C., *Biol. Bull.*, **79**, 188 (1940).
4. Brachet, J., Chemical Embryology. New York, Interscience Publ., 1950.
5. Brues, A. M., and Jackson, E. D., *Am. J. Cancer*, **30**, 504 (1937).
6. de Renyi, G. S., and Hogue, M. J., *Arch. Exptl. Zellforsch.*, **11**, 304 (1931).
7. Frey-Wyssling, A., Submicroscopic Morphology of Protoplasm. Amsterdam, Elsevier, 1953.
8. Friedheim, A. H., *Arch. exptl. Zellforsch.*, **11**, 303 (1931).
9. Gaulden, M., and Carlson, J. C., *Exptl. Cell Research*, **2**, 416 (1951).
10. Gavrilov, W., and von Bistram, D., *Bull. Ass. franç. étude cancer*, **28**, 319 (1939).
11. Godman, G. C., and Murray, M. R., *Proc. Soc. Exptl. Biol. Med.*, **84**, 668 (1953).
12. Goldacre, R., *Internatl. Rev. Cytology*, **1**, 135 (1952).
13. Inoué, S., *Exptl. Cell Research, Suppl.* **2**, 305 (1952).
14. Lecomte, J., *Arch. Intl. Pharmacodynamie*, **78**, 440 (1949).
15. Lettré, H., *Naturwissenschaften*, **38**, 547 (1951).
16. Levi, G., and Chèvremont, M., *Arch. Biol.*, **52**, 523 (1941).
17. Ludford, R. J., *Arch. exptl. Zellforsch.*, **18**, 411 (1936).
18. Mirsky, A., *Science*, **84**, 333 (1936).
19. Miszurski, B., *Exptl. Cell Research, Suppl.* **1**, 450 (1949).
20. Murray, M. R., in Methods of Medical Research, Visscher, N. B. (ed.) 4, 211, Chicago, Year Book Publishers, 1951.
21. Murray, M. R., deLam, H., and Chargaff, E., *Exptl. Cell Research*, **2**, 165 (1951).
22. Northen, H. T., *Am. J. Botany*, **37**, 705 (1950).
23. Östergren, G., *Hereditas*, **30**, 429 (1944).
24. Pogogeff, I., and Murray, M. R., *Anat. Rec.*, **95**, 321 (1946).
25. Pollister, A. W., *Physiol. Zool.*, **14**, 268 (1941).
26. Schmidt, N. J., *Naturwissenschaften*, **24**, 463 (1936).
27. Simms, H. S., and Sanders, M., *Arch. Pathol.*, **33**, 619 (1942).
28. Swann, M. M., *Internatl. Rev. Cytology*, **1**, 195 (1952).
29. Szent-Györgyi, A., Chemistry of Muscular Contraction. New York, Academic Press, 1951.
30. Weber, H. H., *Biochim. et Biophys. Acta.*, **12**, 150 (1950).
31. Weed, I. G., *Z. Zellforsch. u. mikoskop. Anat.*, **25**, 516 (1936).
32. Wilbur, K. M., *Proc. Soc. Exptl. Biol. Med.*, **45**, 696 (1940).

NOTE SUR LA RÉDUCTION INTRACELLULAIRE DU TRIPHÉNYL-TÉTRAZOLIUM DANS LES ŒUFS D'OURSIN

P. H. GONSE et Y. YOTSUYANAGI

Station Biologique de Roscoff et Laboratoire d'Embryogénie comparée du Collège de France, Paris, France

Reçu le 26 Août, 1954

Les sels de tétrazolium ont pour propriété de donner par réduction des cristaux rouges de formazan peu solubles dans l'eau. Cette propriété a été utilisée en histologie pour déceler les tissus riches en deshydrogénases et au cours de ces dernières années elle a été appliquée à la mise en évidence des mitochondries dans les micro-organismes (4, 5). Les travaux de Harman (2) ont en effet montré que les deshydrogénases les plus importantes dans la respiration sont localisées au niveau des mitochondries. Nordmann et Gauchery (6) ont observé que les suspensions de mitochondries isolées par centrifugation fractionnée réduisent les sels de tétrazolium. Il existe donc actuellement une tendance à considérer ces derniers comme des colorants des mitochondries.

Cependant d'après les travaux récents de Fauré-Fremiet et Gauchery (1) sur les Ciliés et de l'un des auteurs (8) sur des cellules végétales il semble que le formazan, dans les matériaux étudiés, ne colore pas les mitochondries mais les inclusions lipidiques.

Il nous a donc paru nécessaire de préciser le mécanisme de la réduction sur un matériel approprié. Nous nous sommes limités à l'aspect cytologique du phénomène en portant notre attention sur deux points:

La réduction du tri-phényl-tétrazolium (TPT dans la suite du texte) a-t-elle lieu au niveau des mitochondries, celles-ci sont-elles alors colorées?

Quelle est la signification de la coloration des lipides, s'agit-il d'un phénomène secondaire?

Nous avons utilisé pour cette étude les œufs de *Psammechinus miliaris* en raison de leur faible teneur en pigment rouge. La marche de la coloration a été étudiée sur des œufs stratifiés ou fragmentés par centrifugation.

TECHNIQUE

Les œufs ont été centrifugés selon la méthode de E. B. Harvey (3). On utilise des tubes de 60 mm de haut et de 13 mm de diamètre intérieur. Les $^2/_3$ inférieurs du

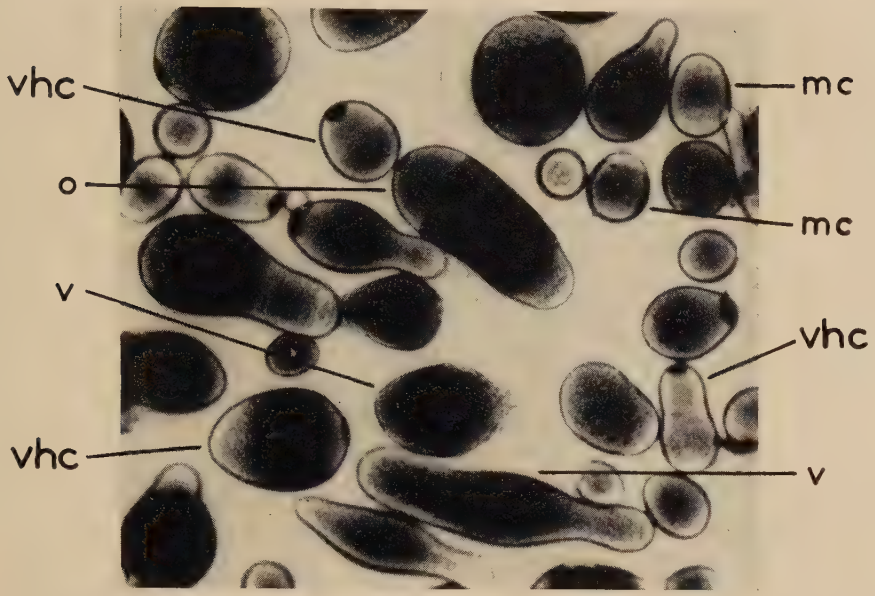

Fig. 1. Œufs centrifugés fixés par l'acide osmique (conc. finale 0,02 %). — O : œuf complet stratifié. m c: fragment lourd; mitochondries et cytoplasme. v h c : fragment leger ; vitellus, cytoplasme, huile et noyau. v : fragment intermédiaire ne contenant que du vitellus.

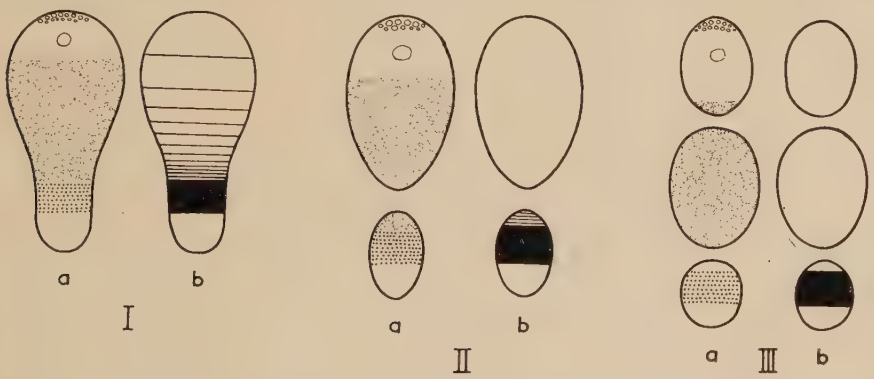

Fig. 2. Ia, IIa, IIIa : stratification et fragmentation des œufs. — Les mitochondries sont indiquées par des points noirs, le vitellus est en pointillé fin, l'huile, au pole centripète est indiquée par des cercles. Ib, IIb, IIIb : en noir ou hachuré zones colorées en rouge par réduction du TPT. Ib : à la lumière après 30 min. IIb, IIIb : à l'obscurité dans des fragments isolés les uns des autres après 1 h. 30.

tube sont remplis d'une solution isotonique de saccharose (1,02 M à Roscoff), dans le $^1/_3$ supérieur on place une suspension d'œufs dans l'eau de mer. Avant la centrifugation le tube est agité doucement afin de réaliser un gradient de densité de 1 cm

environ en mêlant les deux couches autour de leur zone de contact. Dans ces conditions nos résultats sont un peu différents de ceux de Runnström et Kriszat (7), car nous obtenons une zone de cytoplasme léger centripète.

La centrifugation est effectuée à température constante : 15° C. Pendant un premier temps (15 min. à 10.000 g) on provoque la stratification intracellulaire, on accroit ensuite la force jusqu'à 16.000 g maintenus pendant 20 min. pour obtenir la fragmentation des œufs. Les œufs sont fragmentés en 2 ou 3 parties, certains œufs restent complets mais sont très allongés et stratifiés. Les différents types de fragments se trouvent étagés à différents niveaux du tube correspondant à leur densité propre.

Les œufs étirés et les fragments sont triés avec une pipette freinante (Braking pipette) sous le microscope et classés par catégories (Fig. 1 et 2) :

œufs complets étirés et stratifiés; fragments lourds contenant les mitochondries et du cytoplasme (mc) ; fragments legers contenant du vitellus, de l'huile, du cytoplasme et le noyau (vhc).

Ces tris sont effectués dans l'eau de mer. Les œufs ou les fragments sont ensuite montés entre lame et lamelle dans une solution de TPT au 1/1.000ème dans l'eau de mer fraîchement préparée. La lamelle est maintenue écartée de la lame par des baguettes de verre de 300 μ d'épaisseur environ. La préparation est lutée à la vaseline, la réduction ne s'effectuant convenablement qu'en anaérobiose. Pour chaque expérience on prépare en général dans les mêmes conditions : 1 lame avec des œufs complets stratifiés, 1 lame avec des fragments lourds, 1 lame avec des fragments légers, 1 lame avec des fragments lourds et légers (toutes ces lames contenant à peu près la même quantité de matériel biologique), enfin 1 lame témoin sans cellules.

Par coloration au vert janus on a mis en évidence les mitochondries et constaté qu'après la centrifugation elles se rassemblent au pôle centrifuge au dessus d'une calotte de cytoplasme.

RESULTATS

Au cours d'expériences préliminaires on a constaté que, dans les conditions de montage précédentes, des cristaux de formazan peuvent se former dans une solution de TPT au 1/1.000ème sans addition d'aucun matériel biologique.

Dans les lames exposées à la lumière du jour la coloration du milieu est bien développée en 2 heures. Par contre dans les lames laissées à l'obscurité ou à la lumière artificielle il n'y a pas de coloration sensible après 24 heures. La lumière du jour a également un effet accélérateur sur la réduction intracellulaire dans les œufs d'oursin.

L'addition de citrate de Na (trisodique, conc. finale 0.02 M) ou de glycérophosphate de Na (même concentration) n'accélère pas de façon nette le phénomène dans les œufs.

Expérience I; œufs complets stratifiés (Fig. 2, I) lumière du jour. Après la centrifugation le vitellus et les mitochondries ne restent distinctement strati-

fiés que pendant 3 à 4 heures. On a donc effectué ces expériences à la lumière du jour pour obtenir une réduction rapide du TPT.

On observe 30 min. après avoir luté la préparation une coloration rouge vif dans la région centrifuge de la cellule et plus précisement au niveau des mitochondries. La coloration gagne ensuite le vitellus qui devient rose. Les régions à cytoplasme sans inclusions restent incolores.

Expérience II; fragments (*Fig. 2, II et III*) *lumière du jour.* Une réduction extracellulaire a lieu.

1) fragments lourds (mc); en 30 min. la région des mitochondries devient rouge. Après 1 h. 30 des cristaux intracellulaires de formazan se forment tandis que la coloration au niveau des mitochondries disparaît;

2) les fragments légers se colorent lentement (vhc). Leur coloration évolue parallèlement à celle du milieu. Lorsque cette dernière est bien développée, après 2 heures, le vitellus et l'huile sont roses. Des cristaux se forment également dans ces fragments; très rapidement dans ceux qui ne contiennent que peu de vitellus (Fig. 2, III), plus lentement dans les autres (20 h.).

Expérience III; fragments (*Fig. 2, II et III*) *obscurité.* La réduction extracellulaire n'a pas lieu.

1) Dans la lame ne contenant que des fragments lourds (mc) on observe après 1 h. 30 une coloration rose au niveau des mitochondries, cette coloration se développe lentement au cours des 12 heures suivantes mais il n'y a pas de cristallisation du formazan;

2) dans la lame contenant des fragments légers (vhc) il n'y a aucune coloration pendant la durée de l'expérience (12 h.). Si, après 12 heures, cette lame est placée à la lumière du jour la réduction extracellulaire a lieu rapidement. Quand elle s'est un peu développée (après 1 h.) le vitellus et l'huile deviennent roses puis rouges. Les cellules étant groupées au centre de la préparation on observe autour de celles-ci un halo clair correspondant à une concentration moindre de formazan extracellulaire.

CONCLUSION

D'après l'ensemble de ces résultats il semble possible de conclure que dans les œufs de *Psammechinus miliaris* la réduction du TPT est effectuée de façon prépondérante par les mitochondries.

Une observation à fort grossissement ne permet pas d'affirmer que les mitochondries sont réellement colorées. La coloration se développe au voisinage de celle-ci et est très intense à leur niveau. Si le fragment cellulaire ne contient que du cytoplasme et des mitochondries à l'exclusion de tout

matériel lipidique le cytoplasme reste clair et la masse de mitochondries tassée par la centrifugation est fortement colorée mais seulement pendant un temps limité (2 à 3 heures dans nos conditions expérimentales). Après quoi très rapidement des cristaux de formazan se forment et la coloration des mitochondries disparaît complètement. Si le fragment cellulaire contient également du vitellus qui est riche en lipides la coloration, tout en étant plus intense au niveau des mitochondries, apparaît diffuse et gagne rapidement les inclusions de vitellus.

Le vitellus comme l'huile ont la propriété d'absorber fortement le formazan formé extracellulairement. On pourrait donc supposer que dans les cellules complètes contenant à la fois des lipides et des mitochondries le formazan formé au niveau de ces dernières est rapidement absorbé par les lipides au fur et à mesure de sa formation. Dans ce cas il n'y aurait pas, à aucun moment, de coloration réelle du chondriome.

Il semble par conséquent que le TPT ne doit être utilisé qu'avec la plus grande prudence pour la mise en évidence des mitochondries surtout lorsque les cellules renferment également des inclusions lipidiques.

RÉSUMÉ

On a étudié le mécanisme de la réduction du TPT dans les œufs de *Psammechinus* stratifiés ou fragmentés par centrifugation.

Les mitochondries sont responsables de la réduction intracellulaire du TPT.

Si la cellule ne contient pas d'inclusions lipidiques les mitochondries peuvent être colorées pendant un temps court avant que les cristaux de formazan n'apparaissent.

Si des lipides sont présents (vitellus, huile) les mitochondries ne seront pas mises en évidence, seules les inclusions lipidiques seront colorées.

SUMMARY

The mechanism of TPT intracellular reduction has been studied on centrifuged, stratified or broken into fragments *Psammechinus* eggs.

Mitochondria are responsable for TPT reduction.

If there are no lipidic inclusions in the cell, the mitochondria can be stained for a short time before the crystallization of formazan takes place.

If lipids are present (vitellus, oil) the mitochondria will not be demonstrated and the staining will be limited to the lipidic inclusions.

Nous exprimons nos remerciements à M. le Professeur E. Fauré-Fremiet qui a bien voulu s'intéresser à ces recherches. Nous sommes reconnaissants au Dr. T. Gustafson de ses conseils. L'un des auteurs (Y.Y.) remercie MM. les Professeurs Teissier et Drach pour leur aimable acceuil à la Station Biologique de Roscoff.

REFERENCES

1. Fauré-Fremiet, E., et Gauchery, M., *Compt. Rend. Soc. Biol.*, **148**, 640 (1954).
2. Harman, J. W., *Exptl. Cell Research*, **1**, 382 (1950).
3. Harvey, E. B., *Biol. Bull.*, **64**, 125 (1933).
4. Mudd, S., Symposium on the Bacterial Cytology, Rome, p. 67, 1953.
5. —— *Internatl. Rev. Cytol.*, **2**, 133 (1953).
6. Nordmann, J., Nordmann, R., et Gauchery, O., *Bull. Soc. Chim. Biol. France*, **33**, 1826 (1951).
7. Runnström, J., and Kriszat, G., *Exptl. Cell Research*, **1**, 284 (1950).
8. Yotsuyanagi, Y., non publié.

A MORPHOLOGICAL AND BIOCHEMICAL ANALYSIS OF THE EARLY PHASES OF CELLULAR GROWTH IN THE ROOT TIP OF *VICIA FABA*

W. A. JENSEN

Kerckhoff Biological Laboratories, California Institute of Technology, Pasadena, Calif., U.S.A.

Received August 26, 1954

The development of the cell can be studied in many organisms, in many stages, using many techniques. The aim of the present investigation is to study the early phases of cell growth as they occur in the root tip of the broad bean, *Vicia faba*. For the purposes of this study early phases are defined as those through which a cell passes between the time it divides and the period of maximum elongation.

In the broadest possible terms, the problem has been divided into two parts: first, a morphological characterization of the cells in the first three millimeters of the tip; second, a biochemical characterization of the same cells in terms of composition and enzymatic activity. This report gives the results of these investigations, neither of which are complete for all analyzable entities, but which offer a basis for an understanding of some of the basic correlates of growth.

The present work differs from several other recent reports (1, 2, 3) on cell growth in roots by attempting at all times to recognize the complex structure and pattern of development of the root. Thus the cell number was determined by measurements from histological preparations after a complete morphological analysis of the root tip had been made. The cell number per section arrived at by this approach is different than that obtained when the section is treated as homogeneous and cell counts made by use of a hemocytometer. This difference, while not great, is sufficient to give an entirely different interpretation of the results on a cellular level. Further an attempt has been made to work with as small a number of roots in a given determination as possible and to keep adequate control on the position of the sections either by subsequently preparing them histologically or where the section was destroyed during the determination, preparing an alternate section.

GROWTH CONDITIONS

The seeds of *Vicia faba* var. broad Windsor were placed in a shallow dish and covered with water. After 12–24 hours the seed coats were removed and the embryos were placed in moist vermiculite in partially covered square battery jars at room temperature.

The growth rate of the primary root is dependent on a large number of factors. Therefore, selection of root tips for experimental work was not based on the age in terms of days after planting but rather on physiological age based on the growth pattern of the root. During the first stages of growth the growing tip of the primary root is relatively thick and somewhat stubby. After the root has attained a length of 2–3 cm the growing tip becomes smaller in diameter and then retains this thickness more or less constantly until the period of secondary root formation occurs. Under the growth conditions provided, secondary roots appeared when the primary root was from 8–10 cm long. The tips used, then, were from primary roots 3–8 cm in length or after the initial decrease in diameter and before secondary root formation took place.

Tips of roots grown under these conditions were excised and fixed in Conant's modification of Navashin's solution and imbedded according to the standard tertiary butyl alcohol-paraffin method. Cross and longitudinal sections cut at 15 microns were stained according to Foster's tannic acid-ferric chloride and safranin method. From these preparations the general histological observations, diagrams and photomicrographs were made. Some root tips were also prepared by the freeze-dry method (5) and stained with Heidenhain's hematoxylin.

MORPHOLOGICAL ANALYSIS

The general anatomy of the root is indicated in Fig. 1. The six cross-sectional photographs represent the areas from which the 200-micron sections were taken for further morphological analysis and for use in the Cartesian diver experiments. These sections were selected on the basis of morphological distinctness and may be designated as follows:

1. root cap (R.C.), 2. general meristem (G.M.), 3. provascular (P.V.), 4. protophloem (P.P.I), 5. protophloem (P.P.II), and 6. protoxylem (P.X.). The cellular compositon of the sections and their distance from the tip of the root may be seen in Fig. 1.

Each 200-micron section was analyzed for number of cell types or tissues present; volume of each cell type or tissue; cross-sectional area, height, and volume of average cell in each cell type or tissue; number of cells of each cell type or tissue; and total number of cells in each 200-micron section. The analysis was based on the median 15-micron section of the 200-micron section from roots fixed and stained as described above. Camera lucida drawings were made of the tissue areas in the sections and of the cross-

sectional cell area. The area of the tissues and cells was then measured from the drawings by means of a planimeter. For each cell type or tissue in each section 25 to 50 cells were measured by this method; five roots were thus analyzed.

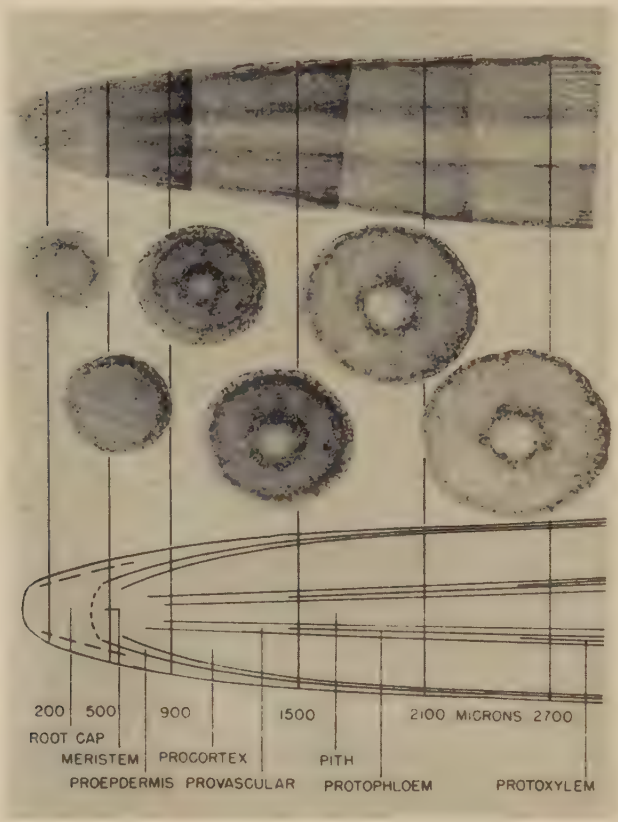

Fig. 1. Longitudinal photomicrograph and diagram of the first three millimeters of the root of *Vicia faba* together with cross-sectional photomicrographs of the sections used in the cell analysis and oxygen uptake study.

Cell heights were obtained from photomicrographs of the median 15-micron longitudinal section; these were projected for additional magnification. The same numbers of cells and roots were analyzed as for the area measurements.

Cell volumes were calculated by multiplying mean cell area by mean cell height of the different cells in each section. Tissue volumes were calculated by multiplying the area occupied by the tissue by the height of the total section (in all cases 200 microns). Cell numbers were obtained by dividing tissue volume by mean cell volume of that tissue.

In making the above calculations the following assumptions have been

made: a) that the area occupied by a tissue or cell type in the 200-micron section is uniform throughout the section, or that it increases or decreases uniformly from one surface to the other so that by measuring the median

TABLE I

The volume occupied by the various tissues, cell area, height, and cell volume per tissue, cell number per tissue, and total cell number of six selected 200 micron sections from the first 3 mm of the root tip of *Vicia faba*.

Tissue and cell		Cell area $mm^2 \times 10^{-4}$	Cell height $mm \times 10^{-2}$	Cell vol. $mm^3 \times 10^{-6}$	Tissue vol. mm^3	Cell number	Total cell number
Root cap	A*	7.71	4.0	30.81	0.025	810	
	A_1	3.90	6.5	42.25	0.013	340	
							1,150
General meristem	A	5.19	3.9	20.20	0.012	545	
	A_1	3.26	7.6	24.80	0.030	1,220	
	M	3.37	1.3	4.38	0.034	7,770	
							9,535
Provascular	A	3.04	7.8	23.70	0.031	1,318	
	B	2.83	2.0	5.67	0.016	2,820	
	C	5.32	1.4	7.45	0.037	4,960	
	D	1.90	1.7	3.23	0.011	3,410	
	E	3.25	2.5	8.13	0.002	246	
							12,754
Protophloem I	A	2.96	12.7	37.60	0.029	772	
	B	4.34	1.4	6.07	0.017	2,800	
	C	7.63	1.4	10.70	0.077	7,195	
	D	2.46	1.6	3.62	0.012	3,318	
	E	3.42	3.7	12.67	0.005	395	
							14,480
Protophloem II	A	2.52	12.4	31.22	0.018	576	
	B	4.83	1.4	6.77	0.016	2,362	
	C	7.64	1.5	11.70	0.105	8,980	
	D	2.94	1.9	5.58	0.016	2,862	
	E	3.34	5.9	19.70	0.009	457	
							15,237
Protoxylem	A	2.46	22.0	54.10	0.008	148	
	B	4.30	1.5	6.45	0.019	2,942	
	C	8.91	1.7	15.15	0.128	8,440	
	D	3.19	2.2	7.03	0.018	2,560	
	E	3.96	7.0	27.74	0.012	437	
							14,527

* A — root cap cell (marginal), A_1 — root cap cell (central), M — meristematic cell, B — epidermis, C — cortex, D provascular, E — pith.

section a representative value is obtained for the area, and b) that the individual cells measured have a uniform cross-sectional area throughout their entire length. This second assumption holds for the majority of the cells analyzed, with the greatest discrepancy occurring in the outer root-cap cells, and, to a lesser extent, in the meristematic cells.

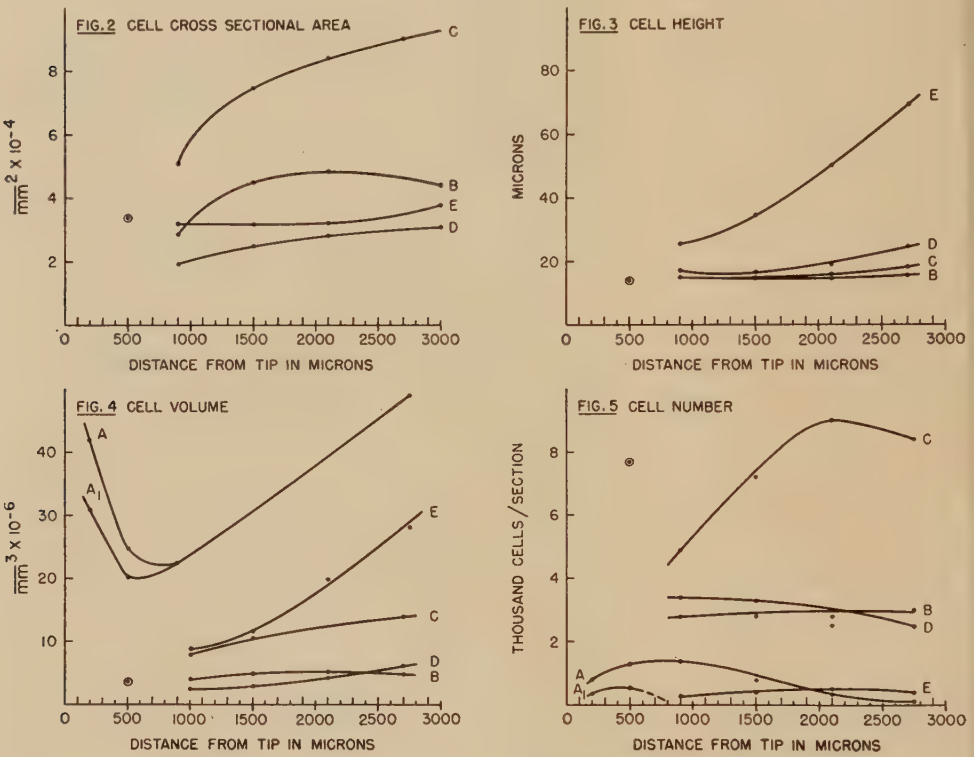
FIG. 2 CELL CROSS SECTIONAL AREA
mm² X 10⁻⁴
DISTANCE FROM TIP IN MICRONS
FIG. 3 CELL HEIGHT
MICRONS
DISTANCE FROM TIP IN MICRONS
FIG. 4 CELL VOLUME
mm³ X 10⁻⁶
DISTANCE FROM TIP IN MICRONS
FIG. 5 CELL NUMBER
THOUSAND CELLS / SECTION
DISTANCE FROM TIP IN MICRONS

Fig. 2. Cell cross sectional area. ⊙ = general meristematic cell, B = proepidermis, C = cortex, D = provascular, and E = pith. Root cap not included.
Fig. 3. Cell height. Same notation as in Fig. 2.
Fig. 4. Cell volume. A = marginal root cap cells, A_1 = central root cap cells. Remainder of notation as in Fig. 2.
Fig. 5. Cell number. Notation as in Fig. 4.

The results of these measurements are presented in Table I. This includes cell cross-sectional area, cell height, cell volume and tissue volume data together with cell number per tissue and per section. The cell cross-sectional area data, except for the root cap cells, are presented graphically in Fig. 2 and the cell height data, without root cap cells, in Fig. 3. Cell volume results are presented in Fig. 4 and cell numbers in Fig. 5. The number of cells per

section has not been presented graphically. It must be emphasized with regard to these data that total cell number per section is a composite of two factors: 1) cell division which increases cell number and 2) cell elongation which decreases cell number. These factors are operative in all sections analyzed here. For example: between the general meristem and approximately 1500 microns from the tip, average cell height in three tissues is constant but because radial divisions are occurring which tend to decrease cell height, elongation must be occurring to restore the height of the daughter cells. These considerations make it impossible to determine the per cent of cell division occurring at various levels on the basis of the present data.

Further it must be emphasized with regard to these data that a tissue may increase its cell number by cell division within the tissue or by gaining derivatives from other tissues through cell differentiation. The latter occurs when the cells on the fringe area of two tissues grow more distinct, as, for example, between the cortex and provascular regions or provascular and pith regions. There are two ways for a tissue to show loss in cell number. First, by loss of derivatives through differentiation or, second, by cell enlargement so that fewer cells occupy a given volume. The continual decrease in cell number of the provascular tissue (curve D) (Fig. 5) is a good example of both. The early decrease is probably from a loss of cells to the cortex and the pith, while the later decrease reflects the increased length of the cells.

BIOCHEMICAL ANALYSIS

Material and methods. — For the reduced weight, total carbohydrate, total glucose and nitrogen determinations consecutive 200-micron sections of the root tip, obtained by the following procedure, were used: a block of paraffin melting at 52°C was attached to the holder of a rotary microtome, and a hole was made in the top of the block with a needle. The tip of the root cap was marked with India ink and a 5 to 10-mm segment of the tip was cut off. This tip segment was then placed in the hole in the paraffin, marked end up, and the paraffin surrounding it was melted with a warm needle. By this method the tissue was imbedded in the paraffin without being infiltrated and with a minimum of heating. The block and holder were then placed in a rotary microtome, and the block was sectioned at 25 micron thickness until the ink mark at the root tip was reached. Then 200-micron sections were cut and placed in half-strength three salt Shive's solution (1.2 ml 0.5 M $Ca(NO_3)_2$, 0.9 ml 0.5 M $MgSO_4$, 0.9 ml 0.5 M KH_2PO_4 per 200 ml H_2O). These were inspected under low magnification, and the diameters measured with an ocular micrometer. Sections from each root tip were periodically treated by the normal histological techniques to assure the correct morphological localization of the other sections used. The first 15 consecutive 200-micron sections were used for all determinations except oxygen studies. For the oxygen consumption determinations six selected

200-micron sections were used. These were from the same positions in the root as those used in the morphological analysis.

The reduced-weight determinations were made by using the Cartesian diver balance (9, 13). The diver balance employs essentially the same principles as the Cartesian diver in that a change in buoyancy of the diver balance when loaded can be related to the weight of the object on the balance. Since the weighings are made in a liquid medium, there is no problem of water loss and, since the balance weighs reduced weights with an accuracy of $\pm$ 0.01 microgram, single sections can easily be used. Reduced weight (R.W.) of an object was defined by Linderstrøm-Lang and Holter (8) as the weight, W, of the objects minus the weight of the volume of the medium (water) it displaces, $v \cdot d_m$, where v is the volume of the object and d_m the density of the medium. Thus:

$$RW = W - v \cdot d_m = v\,(d_0 - d_m) = W\left(\frac{1 - d_m}{d_0}\right)$$

where d_0 is the density of the object. The reduced weight is thus independent of changes in the amount of water in the tissue.

The medium used for the reduced weight determinations was a half strength three salt Shive's solution. Various solutions were tested by making repeated weighings of a series of sections over a period of 4 hours. The greatest change occurred in distilled water and the least in Shive's solution. In Shive's solution the greatest change was less than ten per cent in four hours with most sections changing less than five per cent.

Nitrogen determinations were made by a method similar to that of Levy (7). A 200-micron section was placed in a 10 mm $\times$ 72 mm tube and 0.4 ml digestion mixture added (11). The tubes were placed in an aluminum block 2 $\times$ 3 $^1/_4$ $\times$ 3 $^1/_4$ in. containing twenty-five holes of slightly larger diameter than the tubes and $^3/_8$ inch deep. The block was heated on a hot plate slowly to 245 $\pm$ 5°C and held at that temperature for two hours. The block and tubes were then cooled and 0.05 ml. 30 per cent H_2O_2 was added to each tube. The tubes were then slowly reheated to 245 + 5°C and held there for one hour. The block was cooled and more H_2O_2 was added followed by reheating. Finally the tubes were cooled and 3 ml H_2O was added followed by 0.5 ml Nessler's color reagent (1 part Eimer and Amend reagent in 4 parts 10 per cent NaOH). During the addition of the color reagent the solution was agitated by a stream of air from drawn glass tubing. The color was then determined in a Beckman spectrophotometer model DU at 420 mμ. The range of the method is 0.5–10.0 μg $\pm$ 0.02 μg.

For protein nitrogen the tissue was extracted three times, each for two hours with 0.4 ml of 1 M trichloracetic acid. The TCA supernatants were combined and analyzed for soluble N. The precipitated (protein N) nitrogen was also measured. For the soluble nitrogen determinations after the digestion fluid was added the mixture was placed in an oven at 110°C for twelve hours to reduce water volume before heating.

The procedure for total carbohydrates was based on that of Sørensen and Haugaard (12) in which the color of the oricinol derivative is measured. The 200-micron section was added to 0.3 ml of 2 per cent orcinol in 20 per cent H_2SO_4 and 2.5 ml

of 60 per cent H_2SO_4. The mixture was heated for thirty minutes in a water bath at 80°C. The extinction was read directly after cooling in the Beckman spectrophotometer at 425 mμ. The total carbohydrate was measured in terms of glucose equivalents, i.e. glucose was used for the standard curve. The procedure has a range of 0.5 to 50 μg ± 0.1 μg.

Total glucose including glucose from polysaccharides were measured using the method of Mandl (10) which is based on a furfural derivative formed with hot sulfuric acid and which yields a cherry red color. The 200-micron section was placed in 0.3 ml of concentrated H_2SO_4 in a small test tube and placed in boiling water for 6 1/2 minutes. After cooling the color was determined at 520 mμ in a Beckman spectrophotometer using a microcuvette attachment. The range of the method is 0.5 to 20 μg ± 0.1 μg.

Fructose was measured by the method of Koch and Hanke (6) for ketoses after being scaled to a micro level. Two 200-micron sections were placed in 0.5 ml 0.2 per cent resorcinal in 12 per cent HCl and heated at 100°C for 15 minutes. After cooling the color was read at 420 mμ. The range of the test is 0.5 to 15 μg ± 0.02 μg.

The Cartesian diver microrespirometer was used to measure oxygen uptake. The standard Cartesian diver (4) was used in these measurements—one having an inner neck diameter of 0.9–1.0 mm, a neck length of 10 mm, and a total volume of 10–12 microliters. The inside of the diver was siliconed with dimethyldichlorosilane (General Electric Co.).

The divers were filled as follows: a) 0.6-microliters of 0.1 M NaOH was introduced into the bottom of the diver; b) if a substance were to be mixed with the tissue later in the experiment, it was placed as a 0.5-microliter side drop directly below the tissue seal; c) the neck of the diver was filled with half strength three salt Shive's solution, and the tissue was placed in the top of the neck; d) after the tissue had sunk, or in some cases was pushed down with a needle, to the bottom meniscus of the Shive's solution, the excess solution was removed so that a total of 0.6-microliter of tissue and Shive's solution remained as a seal in the neck; e) a 0.6 microliter paraffin oil seal was then placed across the neck; f) finally the neck seal was set according to the specifications of the diver.

In a normal experiment seven divers were used, six containing the tissue and the seventh a control. The oxygen uptake was measured for two to five hours, although occasionally longer periods were employed.

RESULTS

Reduced weight, total carbohydrates, total glucose, total fructose. The results of these determinations are presented in Table II, both as total amount per section in μgm per section and as amount per cell in mμgm per cell. Fig. 6 gives the data on the amount per cell as a function of cell location in the root.

The first striking feature of the data of Fig. 6 is the high reduced weight of the first two sections composed of the root-cap cells. From the carbohydrate analysis it appears that this is the result of the presence of large amounts of glucose-containing carbohydrates, probably starch and cellulose.

Starch granules are abundant in the root cap cells in the young primary root of *V. faba*. They tend to disappear or to become greatly reduced in number after secondary root formation is well under way.

TABLE II

Reduced weight (R.W.), total carbohydrate (T.C.), total glucose (T.G.) and total fructose (T.F.) of consecutive 200-micron sections of the first 3 mm of the root tip of *Vicia faba*.

Distance of middle point of section from tip in microns	Reduced weight		Total carbohydrate		Total glucose		Total fructose	
	Section μg	Cell mμg	Section μg	Cell mμg	Section μg	Cell mμg	Section μg	Cell mμg
100	2.0	4.08	14.0	28.60	6.2	12.70	2.70	5.72
300	2.6	0.95	14.1	5.12	9.2	3.34	0.90	0.33
500	4.0	0.42	12.2	1.28	3.7	0.39	0.95	0.01
700	4.6	0.39	19.6	1.67	9.8	0.83	0.70	0.06
900	5.8	0.45	15.4	1.21	6.0	0.47	0.95	0.07
1100	6.8	0.50	20.2	1.48	7.0	0.51	0.70	0.05
1300	8.2	0.59	21.6	1.54	9.7	0.69	1.05	0.80
1500	7.7	0.53	21.3	1.47	12.1	0.83	1.40	0.10
1700	9.8	0.60	28.5	1.93	14.2	0.94	1.60	0.11
1900	8.8	0.65	24.0	1.58	11.7	0.79	3.05	0.20
2100	6.7	0.44	22.2	1.46	10.4	0.68	2.80	0.18
2300	6.9	0.45	28.4	1.86	13.8	0.90	2.10	0.14
2500	6.4	0.43	28.8	1.92	13.3	0.89	2.25	0.15
2700	6.9	0.48	30.3	2.09	10.6	0.73	1.95	0.14
2900	7.2	0.51	30.7	2.24	15.5	1.03	2.05	0.16

The next section (500 microns from the root tip) contains the general meristem which although fairly high in total carbohydrates is low in glucose-containing carbohydrates. Since this section is composed of only two cell types (the root cap cells and the meristematic cell), and the carbohydrate and glucose content of the root cap cell is known from the preceding section, the amount of total carbohydrate and total glucose per meristematic cell can be calculated. The meristematic cell can be shown by these means to contain only 0.075 mμgm glucose, 1.075 mμgm total carbohydrate, and, by difference, 1.00 mμgm non-glucose carbohydrate. Similar calculations can be performed with the data from higher sections so that the carbohydrate and glucose content per non-root cap cell can be found. The results of these calculations are shown in Fig. 7.

The broken line in the total glucose curve in Fig. 7 represents the probable cellulose content of the cell. The peak in the 700-micron region is probably

due to soluble glucose or soluble glucose containing compounds. These are probably soluble because they do not appear in the R.W. curve (Fig. 6), but are probably not sucrose as there is no corresponding peak due to the fructose (Fig. 7). The small peak at 1700 microns may be due to sucrose as there is a corresponding peak in the fructose curve (Fig. 6) and the peak in the total carbohydrate curve (Fig. 7) is just twice that due to glucose alone. Further, it is in this region that the first formed protophloem can be identified.

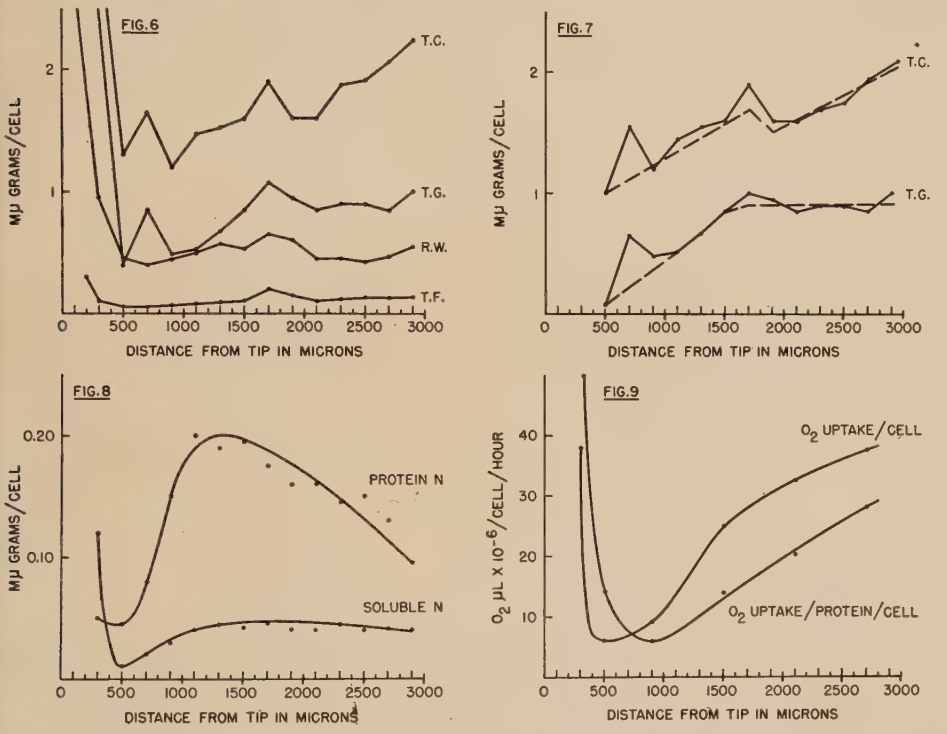

Fig. 6. Total carbohydrate (T.C.), total glucose (T.G.), total fructose (T.F.), and reduced weight (R.W.) per cell.
Fig. 7. Total carbohydrate (T.C.) and total glucose (T.G.) per non-root cap cell. See text for explanation.
Fig. 8. Protein nitrogen and soluble nitrogen per cell.
Fig. 9. Oxygen uptake per cell and oxygen uptake per protein nitrogen per cell.

The cellulose content of the cell would appear to remain constant from 1700 to 3000 microns while a non-glucose carbohydrate increases steadily in the same area (compare the dotted lines in the carbohydrate and glucose curves in Fig. 7). This is interesting as it is at 1700 microns that cell elongation begins. It must be made clear that even at 3000 microns from the tip in

Vicia faba the cells have not completed elongation, so that as the cell begins elongation cellulose formation ceases, at least temporarily, and some other saccharide is formed.

TABLE III

Protein and soluble nitrogen per section and per cell, and change in protein nitrogen per cell related to change in cell volume.

Distance of section from tip in microns	Protein N		Soluble N		Section name	Mean cell volume	Cell inc. per cent	Protein N cell	Inc. per cent	Per cent inc. N / inc. V
	Section μg	Cell mμg	Section μg	Cell mμg						
100	—	—	—	—						
300	0.14	0.05	0.33	0.12						
500	0.43	0.04	0.14	0.01	G.M.	4.4*		0.04		
700	0.93	0.08	0.24	0.02			−50		+220	4.40
900	1.93	0.15	0.50	0.03	P.V.	7.1		0.15		
1100	2.53	0.20	0.53	0.04						
1300	2.40	0.17	0.50	0.03			−38		+ 27	0.71
1500	2.73	0.19	0.83	0.06	P.P. I	9.7		0.19		
1700	2.43	0.16	0.43	0.03						
1900	2.43	0.16	0.73	0.05			−22		− 16	−0.73
2100	2.43	0.16	0.70	0.04	P.P. II	11.8		0.16		
2300	1.87	0.12	0.63	0.04						
2500	2.23	0.15	0.66	0.04			−12		− 16	−1.33
2700	1.87	0.13	0.70	0.05	P.X.	13.3		0.13		
2900	1.23	0.09	0.71	0.05						

* Value of meristematic cell.

Nitrogen. The results of the nitrogen determinations are presented in Table III. Total, protein and soluble nitrogen are given both in μgm per section and mμgm per cell. The values per cell are presented graphically in Fig. 7.

The most striking feature of the data is the low value obtained for the 500-micron section which contains the general meristem. The region of protein synthesis appears to lie between the general meristem (500-micron section) and the beginning of cell elongation (1900 to 2100 micron). Furthermore as the cells begin elongation protein synthesis apparently ceases and protein content per cell actually decreases. This can clearly be seen in the second part of Table III.

Oxygen uptake. The data obtained from the oxygen uptake determinations are presented in Table IV on a per section, per cell, per protein N per section and per protein N per cell basis together with per cent change in oxygen

uptake with added glucose. The per cell and per protein N per cell amounts are shown graphically in Fig. 8.

Several remarkable facts can be seen in these data. First is the low oxygen uptake of the meristematic cells and that oxygen uptake per cell increases in both directions from the meristem. When increase in cell volume is considered in this connection it can be shown that the low oxygen consumption in the meristematic cells is not merely a result of their small volume, and that

TABLE IV

The oxygen uptake per section, per cell, and per protein nitrogen per cell and percentage change in oxygen uptake with added glucose of six selected 200-micron sections.

Section	Oxygen uptake			Per cent change in O_2 uptake with 0.05 M glucose per section
	Section 10^{-3} µl	Cell 10^{-6} µl	Protein N	
R.C.	3.39	29.4	589	+210
G.M.	6.00	6.3	140	+100
P.V.	11.75	9.2	61	+ 10
P.P. I	38.19	25.7	135	− 10
P.P. II	49.20	32.4	202	− 40
P.X.	54.10	37.0	282	− 60

in the last three sections (P.P. I, P.P. II, and P.X.) the oxygen uptake is proportional to cell volume increase, i.e. if the oxygen uptake per cell is divided by the mean cell volume of that section the figure obtained is constant for the last three sections. It is in these sections that elongation is occurring.

Second, when the oxygen uptake is put on a protein nitrogen basis the low point in oxygen consumption is in the region where the rate of protein formation is maximal (P.V.-section). In the basal sections oxygen consumption increases in inverse ratio to protein loss so that the less protein present per cell the greater the oxygen consumption. This later relation is again clearly confined to elongating cells.

Third, when glucose is given to the sections there are several rather dramatic changes. First the root cap and general meristem sections increase their oxygen consumption markedly. When the increase is calculated on a per cell basis and the larger number of root-cap cells present in the G.M.-section recalled, it seems probable that the increase in the G.M.-section is actually the result of the root cap cells present. It may also be possible that the ten per cent increase in the P.V.-section is a result of the root cap cells which

surround it. Basal to the P.V.-section the proportion of root cap cells to the total number of cells becomes so small as to probably rule out any effect on respiration. It is in these basal sections that the second change occurs, namely the depression of oxygen uptake with added glucose. Although the per cent depression on a per cell basis is small, it is none the less real and shows a definite pattern of increased inhibition the more basal the section. It is in these sections that the cells of the cortex are becoming more numerous, better defined, and elongated and, as the root cap cells seem to account for the change in oxygen consumption in the lower sections, so perhaps the elongating cortical cells, more than other cell types, account for the decrease in oxygen uptake in this region. This leaves the intervening dividing and actively differentiating cells with a low oxygen consumption under any condition.

DISCUSSION

The root does not grow in a simple pattern of cell division at one place, cell elongation at another and cell maturation at a third. Thus, while the cells of the provascular region are dividing, the adjacent pith cells are elongating on one side and procortex cells enlarging radially on the other. The provascular cells are not only dividing but some are also differentiating into cortical cells, so that although some continue dividing, they number no more cells per section than before.

From this mass of information, however, several patterns do stand out. First, cell differentiation, enlargement, and maturation occur both apically and basally to the general meristem. This is a fact which can profoundly effect certain measurements in apical sections. Second, the cells immediately after division differentiate so that only 100 or 200 microns above the general meristem the potential mature tissue systems can be distinguished. The development of the vascular tissue and other specialized tissues differentiate from these general areas later. The point is, however, that the cell divides and begins differentiation, part of the differentiation pattern being a stage in which the cell elongates. The differentiation pattern terminates when the cell is mature and further changes can only be induced by strong stimulus. *Further the differentiation pattern includes, in all cells except the pith and root cap, a stage where the cells enlarge radially before they begin elongation.* This can be clearly seen by comparing cell cross-sectional area (Fig. 2) and cell height (Fig. 3). Whereas cell area markedly increases, particularly in the cortex cells, from the general meristem to 1500 microns from the tip, cell

elongation does not begin, except in the pith, until approximately 1500 microns from the tip. This stage of radial enlargements assumes a position of importance when the biochemical determinations are considered. Third, cell division occurs in all the tissues studied here and is the most unique stage of development present. Actually it does not represent a stage at all for it can occur at any time during the early course of cell development and not affect it. However, as a starting point in development, the cells of the general meristem may be considered as representative of the stage of division and will be so considered in this discussion.

Four major stages of cellular development may be recognized from the morphological data: 1) division, 2) radial enlargement, 3) transition to elongation and 4) elongation. The cells in each of the cell types, with the exception of the pith, pass through these stages during development. It must be remembered that the root tip is in a highly dynamic state and that these various stages flow into one another so that there are no precise dividing lines. Obviously there are more stages between the elongating cell and the mature cell, but they are beyond the scope of this work. The root cap cell represents a mature cell type.

1) In the cell division stage of growth the function of the cell appears to be the production of nuclear components. The cell is low in protein content, has almost no cellulose, and a very low oxygen uptake. The low oxygen consumption could indicate that the energy required for the synthetic activities is derived either from glycolysis or the utilization of high energy compounds produced by other cells.

2) In the radial enlargement stage the large increase in the protein and cellulose is particularly dramatic. Oxygen consumption is still no greater than in the first phase. It is interesting that where the cell is synthesizing large amount of compounds oxygen consumption is low.

3) In the transition stage at the beginning of elongation net protein synthesis falls off, cellulose formation ceases (at least temporarily), and oxygen uptake increases. The cessation of synthetic activity could indicate that elongation, in its initial stages, requires a large amount of energy and that other synthetic activities must temporarily cease, or that compounds other than those measured here are being synthesized, or possibly that this stage is the source of high energy compounds that may be utilized by cells in the earlier stages.

4) In the elongation stage net protein formation has not only ceased but total protein content is decreasing. Oxygen consumption is increasing in direct proportion to cell volume and inversely proportional to protein con-

tent. The non-glucose carbohydrate fraction of the cell is increasing while the cellulose content remains constant.

The root cap cell is the only mature cell studied here and probably represents a point in the life of the cell several stages removed from the final stage discussed above. It is the cell with the highest oxygen uptake and has, except for the meristematic cell, the lowest protein content of any cell studied. The high carbohydrate content is indicative of a high general carbohydrate environment for the meristem. That the root cap cells will increase their oxygen uptake and their reduced weight when given more glucose may indicate that the high oxygen consumption is the result of the oxidative assimilation of glucose.

An exceedingly interesting picture of early cell growth can thus be drawn from the data. The dividing cell is portrayed as producing nuclei and the bare minimum of material necessary for the new cells. In the new cells protein and cellulose formation then begin on a large scale. As the mass synthesis stage is completed the cell begins to elongate and take up water. With this shift in activity aerobic respiration becomes more predominate and oxygen uptake increases in proportion to cell volume. The cell continues to make various compounds and, while cellulose formation has ceased, a non-glucose carbohydrate (probably a pentose) is being formed. It is also clearly conceivable that, even while total protein content is decreasing, specific proteins are being made.

This picture of early cell growth is one possible interpretation of the data presented. These conclusions, however, particularly with regard to time of protein formation, are in disagreement with the conclusions of other workers using root tips. Brown and co-workers (1, 2) report data on a per cell basis that indicate an increase in protein content during cell elongation. When the data is compared on a per section basis the agreement with the data presented here is quite good. The difference then ultimately rests on the cell number determinations. Brown macerated sections of the root and made estimates of cell number using a hemocytometer. Brown derived cell volume by dividing the total volume to the section by the number of cells in the section. This method assumes that the root is homogeneous at any given level which is decidedly not the case. Further, the hemocytometer is designed to estimate numbers of cells that are uniform in size while the cells at any given level in the root may vary in size by several magnitudes.

The present method works from the opposite approach by determining the mean cell volume in each cell type present at that level in the root and hence working to the cell number. This method, while not as rapid, not only allows

a more detailed analysis of the root to be made morphologically but also allows the biochemical data to be correlated not only with gross changes in cell size but also to the types of cells present.

Finally, the description of cell development presented above is a mere outline. It is an outline that still lacks many details which may lend support or disprove parts. A long list of desirable measurements could be made. Such a list would include measurement of the nucleic acids, a detailed analysis of cell wall components, and measurement of enzyme systems. The main point of this research is, however, that such measurements can be made and that this approach allows a more accurate correlation of morphological, chemical and biochemical evidence on a cellular level.

SUMMARY

The early stages in the growth of cells of the root tip of *Vicia faba* were studied from a combined morphological and biochemical approach.

The first three millimeters of the root were analyzed first for general histology; then six selected 200-micron section were analyzed on the basis of a) volume occupied by the various tissues, b) mean cell cross-sectional area per tissue, c) mean cell height per tissue, d) mean cell volume per tissue, e) cell number per tissue and f) total number of cells per section. Cell number was found to increase most in the region of the general meristem, although cell divisions occurred throughout the entire area. Cell volume increased in two directions from the general meristem, below in the root cap cell and above in all the cells. Cell enlargement was demonstrated to be unequal in rate between different tissues and not uniform at any given level in the root tip. Further, cell enlargement is a combination of increase in cell cross-sectional area and cell height. The greatest increase in cell cross-sectional area occurred before 1500 microns from the tip where the rate of area or radial enlargement had decreased.

Reduced weight, total carbohydrate, total glucose, total fructose, and protein and soluble nitrogen determinations were made on consecutive 200-microns sections. Using Cartesian divers, the oxygen uptake of the six selected 200-micron sections was measured both with and without added glucose. The results of these determinations have been calculated on a per cell basis.

The results indicate that there are four stages of cell development present in the first three millimeters of the root, excluding the root cap cells that represent mature cells. They are: 1) the meristematic stage, 2) the stage of radial enlargement, 3) the stage of beginning elongation and 4) the stage of

active elongation. There are several more stages between the stage 4 and the mature cell but they are not treated here.

The meristematic stage is characterized by a low carbohydrate, low glucose content, low reduced weight, and low oxygen uptake. The stage of radial enlargement, distinguished morphologically by increase in cell cross-sectional area without elongation, appears to be the stage of mass protein synthesis and cellulose formation although oxygen uptake is still low. The beginning of elongation (stage 3) is characterized by a cessation of cellulose formation and protein synthesis and an increase in oxygen and water uptake. The stage of active elongation is marked by continued increase in oxygen and water uptake, a decrease in protein content, and an increase of non-glucose carbohydrates. The root cap cell has a high carbohydrate content, a low protein content and a high oxygen consumption.

The writer gratefully acknowledges the encouragement given by Dr. J. M. Beal of the University of Chicago and the instruction and encouragement given by Dr. and Mrs. H. Holter, Drs. Andresen, and others of the Carlsberg Laboratory, Copenhagen and Dr. A. Galston and Dr. S. Siegel of the California Institute of Technology, Pasadena. This work was made possible by fellowships from the Atomic Energy Commission and the National Institutes of Health, National Cancer Institute.

REFERENCES

1. Brown, R., and Broadbent, D., *J. Exptl. Biol.*, **1**, 249 (1950).
2. Brown, R., Reith, W. S., and Robinson, E., *Soc. Exptl. Biol. Symposia*, **6**, 290 (1952).
3. Erickson, R. O., and Goddard, D., *Growth*, **15**, Suppl., 86 (1951).
4. Holter, H., and Linderstrøm-Lang, K., *Compt. rend. Lab. Carlsberg, Ser. Chim.*, **24**, 333 (1943).
5. Jensen, W. A., *Stain Technol.*, **29**, 143 (1954).
6. Koch, F. C., and Hanke, M. E., Practical Methods in Biochemistry. Williams and Wilkins Co., Baltimore, 1948.
7. Levy, M., *Compt. rend. Lab. Carlsberg, Ser. Chim.*, **21**, 101 (1936).
8. Linderstrøm-Lang, K., and Holter, H., Die Methoden der Fermentforschung. Leipzig, 1940.
9. Løvtrup, S., *Compt. rend. Lab. Carlsberg, Ser. Chim.*, **27**, 125 (1950).
10. Mandl, A., Personal communication through S. Løvtrup, Carlsberg Lab., Copenhagen.
11. Miller, G. L., and Miller, E., *Anal. Chem.*, **20**, 481 (1948).
12. Sørenson, M., and Haugaard, G., *Biochem. Z.*, **260**, 247 (1933).
13. Zeuthen, E., *Compt. rend. Lab. Carlsberg, Ser. Chim.*, **26**, 244 (1948).

Experimental Cell Research, 8, *523–532 (1955)*

ÜBER DIE KERNE DER GANGLIEN- UND GLIAZELLEN UND IHRE VERÄNDERUNGEN IN ROHRZUCKERLÖSUNGEN[1, 2]

E. ALBERT und K. FELIX

Institut für vegetative Physiologie der Universität und Frankfurter Forschungsstelle für Gehirnpathologie und Psychopathologie, Frankfurt a. M., Deutschland

Eingegangen am 27. August, 1954

Nach unserer heutigen Ansicht haben die Zellkerne zweierlei Aufgaben zu erfüllen, 1) bei der Teilung die Erbeigenschaften auf die Tochterzellen zu übertragen und 2) in den Zeiten dazwischen die Funktionen des Zytoplasmas zu unterstützen, manchmal auch erst zu ermöglichen, indem sie ihm Proteine und Fermente liefern. Die beiden Möglichkeiten schliessen sich bis zu einem gewissen Grade aus. Wenn die Zelle sich zur Teilung anschickt, dann stellt der Kern seine Mitwirkung an den Aktivitäten des Zytoplasmas vorübergehend ein und umgekehrt ruht sein genetischer Apparat, wenn er Proteine und Fermente für das Zytoplasma synthetisieren muss. Der sichtbare Ausdruck für seine Mitwirkung an den Aufgaben des Zytoplasmas ist das Kernkörperchen, das während der Teilung in der Regel verschwindet.

Man darf wohl vorwegnehmen, dass die Kerne der einzelnen Gewebe sich unterscheiden, je nachdem, welche der beiden Tätigkeiten vorwiegt. Die beiden denkbaren Extreme werden durch den Kern der Spermatozoen und den der Ganglienzellen repräsentiert. Jener hat nur die väterlichen Erbqualitäten zu übertragen und beteiligt sich nicht an den Aufgaben des Zytoplasmas. Das Spermatozoon lebt nur kurze Zeit, sezerniert nicht, legt keine Reserven an und tut auch sonst nichts, woran sich der Kern durch Lieferung von Proteinen und Fermenten beteiligen könnte. Seine einzige Aufgabe ist, sich weiter zu bewegen und auf ein Ei zu treffen.

Die Nervenzelle teilt sich nicht mehr. Der Genapparat ihres Kerns scheint stillgelegt, der synthetische hingegen versorgt das Zytoplasma laufend mit Material und das Kernkörperchen ist entsprechend gross. Aus der Analyse des Ganglienzellkerns kann man vielleicht etwas Grundsätzliches über diesen synthetischen Apparat des Zellkerns erfahren.

Die graue Substanz enthält mehrere Zellarten, Ganglien-, Glia- und Mesenchymzellen und ausserdem marklose, aber auch markhaltige Nerven-

[1] Herrn Professor Karl Kleist zum 75. Geburtstag gewidmet.

[2] Mit Mitteln der Deutschen Forschungsgemeinschaft ausgeführt.

fasern. Das Homogenat ist somit ein Gemisch aus den Partikeln der verschiedenen Zellarten und den Bruchstücken der Fasern und es gilt, die Ganglienzellkerne hieraus zu isolieren.

Von den verschiedenen Verfahren, die zur Isolierung von Zellkernen aus solchen Gemischen empfohlen werden, erschien uns die Homogenisierung in Rohrzuckerlösung und das fraktionierte Zentrifugieren am geeignetsten (9). Es führt rasch zum Ziel; die damit gewonnenen Kerne sollen homogen sein und sich von denen in der intakten Zelle nicht unterscheiden. Einige Autoren haben allerdings auch morphologische Veränderungen (1) und den Austritt von Inhalt beobachtet (5, 7, 13, 2, 6, 11).

Unseres Wissens haben bis jetzt nur D. Richter und R. P. Hullin (15) versucht, Nervenzellkerne zu isolieren. Sie homogenisierten menschliches Leichengehirn und Tiergehirne in verdünnter Zitronensäure von pH 6,0–6,2. Ihr Präparat enthielt zu 40 % Ganglienzellkerne, zahlreiche Gliakerne, ganze Zellen und Kapillarendothelien. Über etwaige morphologische Veränderungen der Kerne wird nichts berichtet.

Unser Endsediment in Zuckerlösung (vergleiche experimentellen Teil) besteht zu etwa 70 % aus Ganglienzellkernen und zu etwa 30 % aus Gliazellkernen. Daneben sieht man krümelige Anhäufungen von ausgetretenem Kerninhalt.

Bei diesem Verfahren der Darstellung bewahrt ein Teil der Nervenzellkerne sein ursprüngliches Aussehen.

Sie sind gross (⌀ 12 μ), rund und haben ein zentral gelegenes, grosses, scharf begrenztes Kernkörperchen. Unter dem Phasenkontrastmikroskop erscheint der Kernleib homogen oder höchstens ganz zart gekörnelt. Lässt man die Kerne sich im Flüssigkeitsstrom drehen, so bieten sie sich von allen Seiten als glatte Kugeln dar, die manchmal etwas abgeplattet sind.

Die Gliakerne sind deutlich kleiner (⌀ 5–6 μ) und kompakter als die Nervenzellkerne; ein Nucleolus ist nicht zu erkennen. Weder im ungefärbten noch im gefärbten Präparat zeigen sie Strukturen. Ihre Gestalt ist ebenfalls die einer glatten Kugel.

Je häufiger man das Präparat mit Zuckerlösungen wäscht, desto stärker werden die Kerne durch das fremde Milieu, die osmotischen und mechanischen Einwirkungen verändert. Früher oder später wird ihr Inhalt körnig. Die Konzentration des Rohrzuckers hat darauf nur insofern einen Einfluss, als dies bei niedriger Konzentration (8–12 %) langsamer und bei höherer (30–40 %) rascher geschieht. Dafür sind sie in dünneren Zuckerlösungen empfindlicher gegen mechanische Einflüsse.

Schliesslich gehen sie zugrunde unter anderen Erscheinungen als die

Gliakerne. Im wesentlichen tritt bei beiden der Inhalt aus und löst sich der Kern auf.

Bei den Nervenzellkernen erscheint im ungefärbten Präparat die vorher glatte Oberfläche mit einem Mal gewellt, der Kern wird grösser (bis 20 μ) und der Inhalt erst fein- und dann grobkörnig. Die Kerne werden immer durchsichtiger und heben sich kaum noch von der Umgebung ab. Gleichzeitig tritt der Inhalt aus, fast flüssig in isotonischer und körnig und fädig in konzentrierteren Lösungen. Entsprechend lassen sie sich immer weniger mit Toluidinblau anfärben und die Färbbarkeit mit Methylgrün-Pyronin ändert sich zunehmend von grün zu rot.

Die Existenz einer Membran oder Hülle gibt sich am ungefärbten, intakten Kern nur indirekt in der glatten Begrenzung zu erkennen. Auch am frischen, gefärbten Kern hebt sich keine Membran ab. Geht dagegen der Kern zugrunde, dann wird mit einem Male die äussere Begrenzung als dunkler, mit Toluidinblau färbbarer Reif sichtbar, der sich bald in einzelne Perlen auflöst, die zunächst ganz dicht stehen und dann auseinander rükken. Durch die Zwischenräume tritt färbbare Substanz aus.

Wir konnten nicht entscheiden, ob das, was sich färbt, wirklich die Membran selbst ist oder Kernmaterial, das sich hinter ihr angesammelt hat. Vielleicht besteht die Membran aus einem dehnbaren Netzwerk, dessen Maschen bei der Denaturierung weiter werden. Dehnbar deswegen, weil bei den angeschwollenen Kernen die Hülle gefaltet ist und zu weit aussieht.

Die Kerne der Gliazellen gehen rascher zugrunde als die der Nervenzellen. Schon im ersten Sediment sind sie häufig verändert, vergrössert (⌀ 7 μ) und gekörnt und nach dem dritten Waschen sieht man nur noch wenige unveränderte Gliakerne. Die Kernsubstanz tritt aber hier nicht diffus aus, sondern quillt nur an einzelnen, umschriebenen Stellen in cumulusartigen steifen Massen hervor.

Der Inhalt des Gliakerns hat offenbar eine festere Konsistenz als der des Ganglienzellkerns. Im ungefärbten Präparat blitzen jene Ausstülpungen hell auf, sind also stark lichtbrechend. An ihnen hängt wie ein Schatten die blasse, leere Kernhülle. Mit Toluidinblau färbt sich nur der Kernrest blau an, die Ausstülpungen bleiben ungefärbt. Mit Methylgrün-Pyronin dagegen färbt sich der Kernrest grün und die Ausstülpungen rot. Letztere legen sich manchmal um die Aussenfläche des Kerns herum und können dann mit Pyronin färbbare Plasmasäume vortäuschen (18). Mit weiterem Auswaschen tritt die grüne Komponente immer mehr zurück und das Kernfragment färbt sich in schillerndem Rot bis Gelb, manchmal glänzend wie

ein Metallblättchen. Doch kann es schliesslich auch jede Färbbarkeit verlieren.

Wenn es zutrifft, dass Desoxyribonucleinsäure von Methylgrün und Ribonucleinsäure von Pyronin selektiv angefärbt werden (4), spricht der eben beschriebene Wechsel in der Färbbarkeit dafür, dass bei der Kernauflösung zunächst die Desoxyribonucleinsäure verschwindet, oder vielleicht auch nur in nicht färbbare Produkte aufgespalten wird. Die Ribonucleinsäure dagegen bleibt viel länger erhalten und nimmt nur ganz allmählich ab. Die aus dem Innern der Gliakerne vorquellenden Massen scheinen vorwiegend aus Ribonucleinsäure zu bestehen.

Somit ergibt sich aus unseren Versuchen, dass Rohrzuckerlösungen, gleichgültig welcher Konzentration, nicht imstande sind, die Struktur der Kerne der Nerven- und Gliazellen längere Zeit unverändert zu bewahren, im Gegensatz zu dem, was in der Literatur über das Verhalten anderer Kerne aus pflanzlichen und tierischen Geweben berichtet wird (10 u. a.). Im wesentlichen entmischen die Rohrzuckerlösungen den Inhalt des Kerns und erhöhen die Durchlässigkeit der Hülle. Diese entmischende Wirkung konnten wir auch an Forelleneiern und den Dottern des Hühnereis beobachten.

Von verschiedenen Autoren wird der Zusatz anorganischer Salze zu der Rohrzuckerlösung empfohlen. In einer Reihe von Versuchen haben wir Rohrzucker zu 12–30 % in Phosphat-Bicarbonatpuffer von N. G. Anderson und K. M. Wilbur (1) (0,0094 m. KH_2PO_4, 0,0125 m. K_2HPO_4, 0,0015 m. $NaHCO_3$) gelöst. Er wirkte aber stark hypertonisch, die Kerne schrumpften und verloren den Inhalt schneller als in reiner Rohrzuckerlösung. Noch ungünstiger wirkte der Zusatz von 0,0018 m. (18) bis 0,009 m. Calciumchlorid. Die Kerne schwollen an und wieder trat der Inhalt aus.

Da nach Versuchen verschiedener Biologen korpuskuläre Elemente aus Pflanzen- und Tierzellen ihren Inhalt in Lösungen hochmolekularer Stoffe besser behalten als in Rohrzuckerlösungen (8, 12, 18), verwandten wir in einer weiteren Versuchsreihe als Medium Lösungen von Gummi arabicum, Amylose, Dextrin und Glykogen. Lediglich in der Glykogenlösung blieben die Kerne einigermassen unverändert. Weiter versuchten wir noch ein synthetisches Kolloid, das Polyvinylpyrrolidon, das uns die Badische Anilin- und Sodafabrik in den Molekülgrössen 10000, 28000, 260000 und 500000 freundlicherweise überliess. Es ist der Hauptbestandteil des Blutersatzmittels Periston. Wir verwandten 10%ige Lösungen in Wasser und in isotonischer Rohrzuckerlösung. In beiden Medien hielten sich die Kerne jedoch nicht so lang als in reinen Rohrzuckerlösungen.

Solange der Kern noch unverändert ist, lassen sich weder im gewöhnlichen noch im Phasenkontrastmikroskop ausser dem Kernkörperchen Strukturelemente erkennen. Vielleicht wären solche mit der Röntgen-Interferrenz-Analyse doch nachzuweisen. Wenn man unveränderte Kerne zerquetscht, tritt aus ihnen eine scheinbar homogene Flüssigkeit aus, in der gelegentlich einzelne Fäden vorkommen. Erst wenn sie mehrmals mit der Rohrzuckerlösung behandelt und mechanischen Einwirkungen (Zentrifugieren, Homogenisieren) ausgesetzt worden sind, verwandelt sich ihr Inhalt in krümelige und fädige Strukturen. Wir glauben nicht, dass diese Strukturen etwas mit den Chromosomen (17) zu tun haben, sondern halten sie nur für den Ausdruck kolloidchemischer Veränderungen.

In den bisher beschriebenen Versuchen wurde die graue Substanz sofort verarbeitet. Lässt man sie dagegen vor dem Homogenisieren etwa vier Stunden im Kühlraum (unter +4°C) liegen, so erweisen sich die Kerne als bedeutend widerstandsfähiger gegen mechanische Einflüsse und Änderungen des Milieus. Schliesslich gehen sie aber, wenn auch langsamer, auf die gleiche Weise zugrunde.

Wenn es darauf ankommt, die Zusammensetzung der Kerne zu analysieren, wird man abgelagertes Gewebe vorziehen. Zur Untersuchung des Fermentgehaltes dürfte frisches Gewebe geeigneter sein. Allerdings muss man dann Verluste in Kauf nehmen.

EXPERIMENTELLER TEIL

Entblutung des Gehirns

Es wurde das Gehirn von geschächteten oder durch Genickschuss getöteten Rindern genommen, weil Rinde und Grosshirngefässe unverletzt sind. Der Kopf wird rasch abgetrennt, sofort Kanülen in die Carotiden eingebunden und unter Druck (1,80 m Wassersäule) mit je 10 l eiskalter physiologischer Kochsalzlösung durchströmt, die zur besseren Gefässerweiterung mit Kohlensäure angereichert wird. Der Druck in der Durchströmungsleitung wird dadurch erzeugt, dass wir die Wassersäcke, in die die Kochsalzlösung eingefüllt wurde, in die Höhe ziehen. Das ausgewaschene Gehirn wird aus dem Schädel entnommen, auf Eis transportiert und im Kühlraum (unter +4°C) weiterverarbeitet.

Homogenisieren

Die Grosshirnrinde wird nach Entfernung der Hirnhäute mit einem Skalpell sanft abgelöst und gewogen. Von einem ganzen Gehirn erhält man im Durchschnitt etwa 120 g Rinde. Es lässt sich nicht völlig vermeiden, dass an der Basis der abgetra-

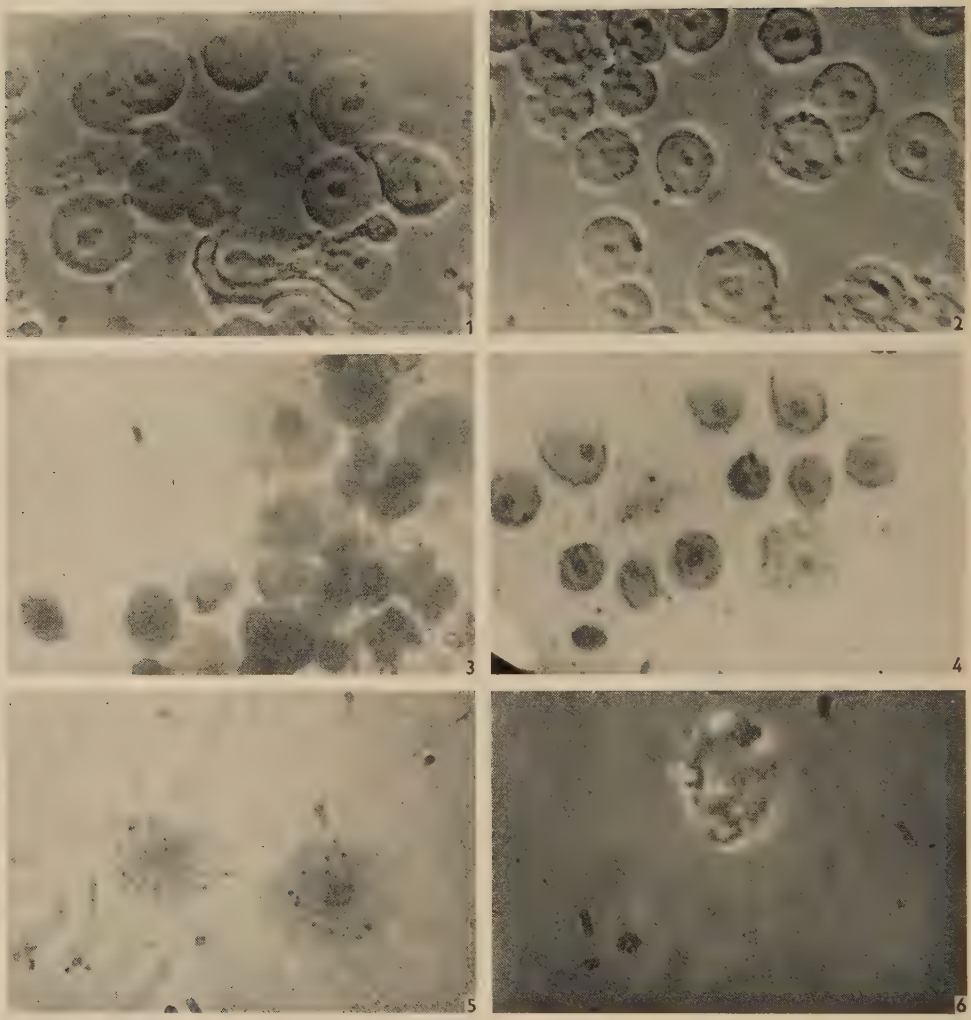

Abb. 1. Gut erhaltene Nervenzellkerne, dazwischen einige Gliazellkerne und Myelin. Phasenkontrast, 8,6%ige Saccharoselösung.
Abb. 2. Krümelige Substanz tritt in Form kleiner Kügelchen ringsum aus den Kernen aus. Phasenkontrast 15/23/30%ige Saccharose.
Abb. 3. Dick aufgeblähte Kerne neben solchen von normaler Grösse. Toluidinblau 10/20%ige Saccharose.
Abb. 4. Geblähte Kerne in Auflösung. Die Lage der Kernhülle wird durch dunkle Säume angezeigt, durch die Substanz nach aussen hindurchgetreten ist. Toluidinblau 15/24/32%ige Saccharose.
Abb. 5. Riesige ausgelaugte Kernschatten ohne Membran mit Resten des dunklen Saums in Gestalt einiger schwarzer Perlen im Innern. Toluidinblau 15/23%ige Saccharose.
Abb. 6. Gliakern mit mehreren aus dem Kerninnern hervorbrechenden, glänzenden Prolapsen. Phasenkontrast 15/23/30%ige Saccharose.

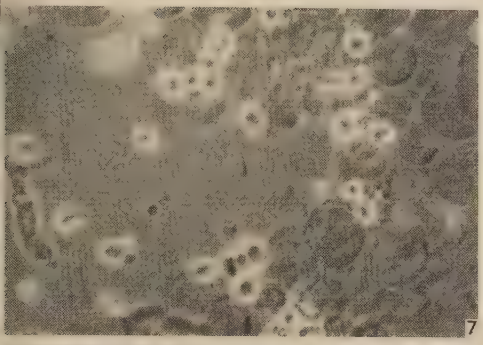

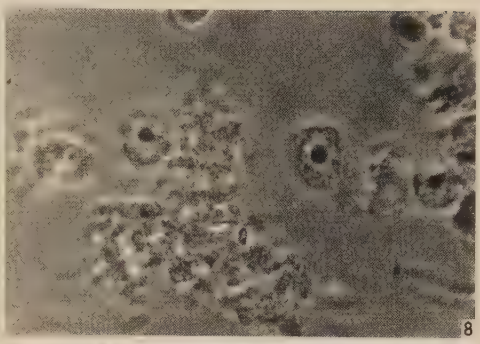

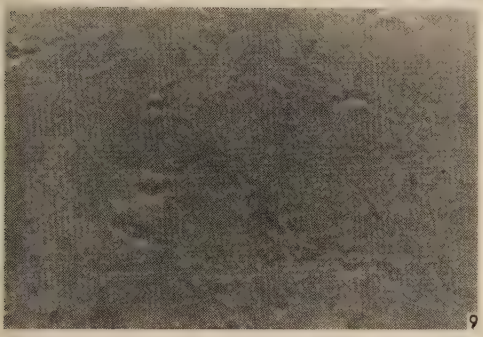

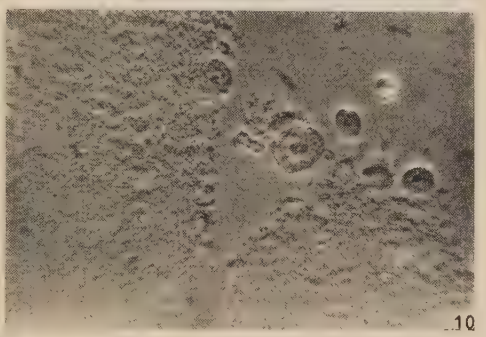

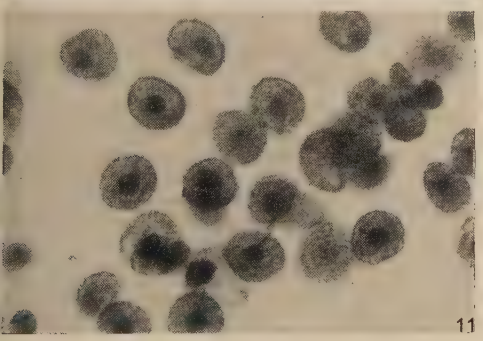

Abb. 7. Hell aufblitzende, nach aussen gestülpte Gliakerne zwischen unveränderten Nervenzellkernen. Phasenkontrast 10/20%ige Saccharose.
Abb. 8. Deutliche Schrumpfung der Nervenzellkerne im Phosphat-Bicarbonatpuffer. Phasenkontrast 18/25%ige Saccharoselösg.
Abb. 9. Kerne in 8,6%iger Saccharose gequetscht durch Druck auf das Deckglas. Zerfliessende Figuren ohne erkennbare Strukturen im Innern. Die krümeligen Beimengungen lagen schon vorher zwischen den Kernen, Phasenkontrast.
Abb. 10. Grosse Krisselfelder aus im Homogenisator zerriebenen Nervenzellkernen. Phasenkontrast 20/30/40%ige Saccharose.
Abb. 11. Erhaltene doch abgeplattete Nervenzellkerne aus abgelagertem Hirngewebe. Toluidinblau 10/19/28%ige Saccharoselösg.

genen Kuppe noch etwas weisse Substanz mit abgehoben wird. Die Rindenbröckchen werden mit der 10fachen Menge 15%iger eiskalter Rohrzuckerlösung durch ein Haarsieb gestrichen. Dann wird das so vorzerkleinerte Gewebe homogenisiert. Wir verwenden den Homogenisator nach Potter-Elvehjem (14), und zwar ein Modell, dessen Stempel viel Spielraum hat. Um das Schlagen zu vermeiden, wurden

am Stiel zwei durchlöcherte Führungsringe aus Metall angebracht. Der Stempel wird im allgemeinen bis zu 10mal langsam auf und abbewegt (Drehzahl des Motors bis zu 1500/Min).

Das Homogenat wird dreimal coliert, erst durch doppelten Mull, dann durch sechsfachen Mull und schliesslich durch zwei Lagen Watte.

Isolierung der Kerne aus dem Homogenat

Das rohe Homogenat wird zunächst 5 Min bei 1800 UpM (500 × mittlere Endbeschleunigung) zentrifugiert und der Überstand verworfen. Bei höherer Geschwindigkeit setzen sich noch andere Partikel ab (bes. Myelinschollen, Bruchstücke von Nervenfasern und Nisslschollen), die später nur mehr unvollkommen aus dem Sediment zu entfernen sind. Das erste Sediment resuspendieren wir in reichlicher Menge 15%iger Rohrzuckerlösung und schichten es vorsichtig über eine Schicht 22%iger Rohrzuckerlösung, in Analogie zu den Angaben von G. H. Hogeboom, W. C. Schneider und M. J. Striebich (10), und zentrifugieren dann von neuem. Diese konzentriertere Rohrzuckerlösung hat die Funktion einer Behrensschen Sperrschicht (3) und lässt nur die spezifisch schwereren Teile durchtreten. An der Grenzfläche bildet sich ein dichter Trübungsring von kleineren Zellbestandteilen, die nicht übertreten können. Das 2. Sediment wird in der 22%igen Saccharose resuspendiert und über eine Schicht von 30%iger Zuckerlösung übergeschichtet. Die Kerne, die sich nach der zweiten Unterschichtung abgesetzt haben, werden noch einmal mit 30%iger Rohrzuckerlösung gewaschen, wobei etwas kürzer, nur 4 Min, zentrifugert wird, während vorher die Laufzeit immer 5 Min war. Die Gliakerne werden dadurch, dass sie sich ausstülpen und Inhalt verlieren, leichter und können auch aus diesem Grunde von den Nervenzellkernen besser abzentrifugiert werden.

Im allgemeinen arbeiteten wir in den angegebenen Stärken der Rohrzuckerlösung, doch verwandten wir auch manchmal andere Konzentrationen zwischen 8–70 %.

Wenn während der Verarbeitung viele Kerne zugrunde gehen, kann man das schon makroskopisch daran erkennen, dass feine, bräunliche Flöckchen in der Suspension herumschwimmen, die nur z. T. an der Sperrzone zurückbleiben, zum Teil auch hindurchtreten und sich oft am ganzen Glas entlang wie fettige Schuppen absetzen. Mikroskopisch sind es ausgedehnte Felder krisseliger Kernreste.

Mikroskopische Präparate

Zur morphologischen Beobachtung. Ausstriche eignen sich für die morphologische Untersuchung der Kerne nicht, da beim Ausstreichen die empfindlichen Kerne noch zusätzlich geschädigt werden. Wir geben vielmehr eine Suspension der Kerne in Rohrzuckerlösung auf den Objektträger, legen das Deckglas darüber und beobachten im gewöhnlichen Lichtmikroskop und im Phasenkontrastmikroskop. Zur Färbung mischen wir eine Öse des Sedi-

mentes auf dem Objektträger mit einem Tropfen der Farblösung (1%ige wässrige Toluidinblaulösung oder eine 5%ige wässrige Methylgrün-Pyroninlösung von Grübler / Leipzig und Bad Cannstadt) und betrachten unter dem Deckglas mit Ölimmersion bei 600-bis 1000facher Vergrösserung.

Diese Methode erlaubt es, die Kerne von allen Seiten zu betrachten. Man braucht nur mit einem Stäbchen auf das Deckglas aufzutippen oder leicht daran zu schieben, so bilden sich in der Flüssigkeitsschicht Strömungen, in der die Kerne mitgerissen werden und sich dabei von allen Seiten darbieten. So kann man am besten die Formverbiegungen beurteilen.

Das ungefärbte Bild ist wichtiger als das gefärbte, weil hier die Kerne noch ganz unverändert sind. Durch Zutropfen der Farblösung werden die Ganglienzellkerne kleiner, stark gekörnelt und wie von einem groben Maschenwerk durchzogen. In isotonischer Lösung platzen die Kerne sogar bei Zutropfen der Farbe. Schuld daran ist entweder die Erniedrigung des osmotischen Druckes durch die wässrige Farblösung oder die stark saure Reaktion der Farblösung: Toluidinblau pH 2,7; Methylgrün-Pyronin pH 3,7.

Zum Auszählen der Kerne. Das Endsediment wird in wenig Rohrzuckerlösung suspendiert und nach der Leukocytenmethode ausgezählt. Wir beschicken dazu die Kammer mit der unverdünnten Kernsuspension. Die umgewandelten Gliakerne sieht man als glänzende Körperchen aufleuchten. Mischt man in der Mischpipette die Kernsuspension vorher mit Farblösung, so geht dieser Unterschied verloren.

ZUSAMMENFASSUNG

Die Grosshirnrinde des Rindes wurde in Rohrzuckerlösung homogenisiert und die Kerne abgetrennt. Das Endsediment besteht etwa zu 70 % aus Ganglienzellkernen und der Rest aus Gliazellkernen. Beide Kernarten verändern sich in Rohrzuckerlösung und gehen schliesslich zugrunde. Die Erscheinungen, die dabei zu beobachten sind, können kaum osmotisch erklärt werden, sondern beruhen eher auf der heterogenen Zusammensetzung des Kerninhaltes.

Der Inhalt der Gliakerne besitzt eine höhere Konsistenz als der der Nervenzellkerne.

Erst bei der Auflösung der Kerne tritt ein Gebilde hervor, das als Membran angesehen werden könnte.

Kerne aus abgelagertem Gewebe sind widerstandsfähiger.

LITERATURVERZEICHNIS

1. Anderson, N. G., and Wilbur, K. M., *J. Gen. Physiol.*, **35**, 781 (1952).
2. —— *Federation Proc.*, **9**, 254 (1950).
2a. —— *J. Gen. Physiol.*, **34**, 647 (1951).
3. Behrens, M., *Z. Physiol. Chem.*, **209**, 59 (1932).
4. Brachet, J., Embryologie Chimique. Paris, Masson et C^{ie}, 1944.
5. Callan, H. G., *Hereditas*, **35**, Suppl. 547 (1949).
6. Caspersson, T., *Symposia Soc. Exptl. Biol.*, **1**, 127 (1947).
7. Chambers, R., and Black, M., *Am. J. Botany*, **23**, 364 (1941).
8. Harris, D. L., *Biol. Bull.*, **85**, 179 (1943).
9. Hogeboom, G. H., Schneider, W. C., and Palade, G. E., *J. Biol. Chem.*, **172**, 619 (1948).
10. Hogeboom, G. H., Schneider, W. C., and Striebich, M. J., *ibid.*, **196**, 111 (1952).
11. Hyden, H., *Acta Physiol. Scand.*, Suppl. **XVII** (1943).
12. McClendon, J. H., and Blinks, L. R., *Nature*, **170**, 577 (1952).
13. Pollister, A. W., and Leuchtenberger, C., *Proc. Natl. Acad. Sci. U.S.*, **35**, 66 (1949).
14. Potter, V. R., and Elvehjem, C. A., *J. Biol. Chem.*, **114**, 495 (1936).
15. Richter, D., and Hullin, R. P., *Biochem. J.*, **48**, 406 (1951).
16. Ris, H., and Mirsky, A. E., *J. Gen. Physiol.*, **31**, 1 (1947); **32**, 489 (1949).
18. Schneider, R. M., and Petermann, M. L., *Cancer Research*, **10**, 751 (1950).
19. Stafford, H. A., Thesis, University of Pennsylvania (1951).

Experimental Cell Research, **8**, *533–542 (1955)*

A STUDY OF RIBONUCLEASE AND DESOXYRIBONUCLEASE DURING THE EARLY DEVELOPMENTAL STAGES OF *RANA PIPIENS*[1]

F. J. FINAMORE[1, 2]

Department of Physiology, Florida State University, Tallahassee, Florida, U.S.A.

Received August 30, 1954

Protein-nucleic acid relationships. Numerous observations have suggested that ribose nucleic acid[3] is associated with protein synthesis. Caspersson (9) and Brachet (5) demonstrated that cells which were actively engaged in protein synthesis contained a high content of RNA. It was then shown by Brachet and Jeener (8), as well as others, that the major portion of the RNA was bound to the microsomes. Studies by Hultin (13), Keller (15), Siekevitz and Zamecnik (22) and others, using isotopically labeled amino acids, showed that the amino acids were readily incorporated into the microsomes. The above demonstration gave support to the idea of the intimate association of RNA with protein synthesis. This concept is quite widely accepted in spite of the fact that the exact role of the nucleic acids in protein sythesis has not been elucidated.

The importance of the nucleic acids in embryonic differentiation has been strongly emphasized by Brachet (6). In 1947, he indicated that the evocating power of a tissue was directly proportional to its RNA content. Later (7), he pointed out that there existed a striking prallelism between the "morphogenetic potential" of a given area of the egg and its content of RNA. He has postulated that specific proteins are responsible for histological differentiation and that these proteins are synthesized under the influence of ribonucleoprotein particles (microsomes). Thus, according to this concept, there is a link between the nucleic acids and differentiation.

The role of the nucleus in protein synthesis. Evidence supplied from the studies on enucleated cells (11) pointed toward an indirect role of the nucleus

[1] Taken from a dissertation submitted to the Graduate Council of Florida State University in partial fulfillment of the requirements for the degree of Doctor of Philosophy.

[2] Present address: Institution for Tuberculosis Research, University of Illinois Medical School, Chicago, Illinois.

[3] Throughout the remainder of this paper the abbreviations RNA and RNase will be used for ribonucleic acid and ribonuclease, respectively and DNA and DNase will be used to designate desoxyribonucleic acid and desoxyribonuclease, respectively.

in protein synthesis. In support of this, Brachet (7) showed that multiplication of the microsomes was controlled by the nucleus, the absence of which eventually led to the disappearance of the microsomes accompanied by loss of power for the synthesis of cytoplasmic proteins. Caspersson (10), however, stated that the nucleus is the chief center of protein synthesis in the cell. According to his concept, the euchromatin supposedly regulates the synthesis of complex proteins for use by the chromosomes. The heterochromatin, on the other hand, controls the synthesis of histones which accumulate in the nucleolus of the interphasic nucleus and then diffuse into the cytoplasm. In the perinuclear zone, these histones induce the synthesis of ribonucleoproteins and these, in turn, are active in the synthesis of proteins of the cytoplasm. The isotopically labeled amino acid studies, however, show that the cytoplasm rather than the nucleus incorporates the amino acids more readily (13). This suggests that the nucleus does not itself synthesize the bulk of the proteins but it may have a controlling effect on this synthesis by the cytoplasm.

The nucleic acids during amphibian embryonic development. Brachet (6) found a decrease in RNA comparable to an increase in DNA during the development of *R. fusca*. Furfural measurements were used in this study. In 1941, however, he re-studied this phenomenon and found that both RNA and DNA increased during development. It appeared that the jelly membranes interfered with the furfural determinations used in the previous work.

Barth and Graff (2) found no change in the total purine content of *R. pipiens* eggs during cleavage. Beginning with gastrulation, however, the total amount of purines increased. This information was used to show that no significant synthesis of nucleic acid took place until gastrulation.

In *Amblystoma*, Bodenstein and Kondietzer (3) found that both RNA and DNA increased steadily. These measurements, however, were made at the later stages of development.

Kutsky (18), studying *R. pipiens*, found that the DNA P increased steadily whereas the RNA P remained essentially constant during development. She also found, using P^{32}, that the relative specific activity of RNA P was low compared to that of DNA P and concluded that it was highly improbable that RNA was a precursor of DNA. In this connection it should be mentioned that Jeener and Szafarz (14) have reported that nuclear RNA of embryonic mouse liver has a much higher turnover rate than cytoplasmic RNA and that this might satisfy the requirements of a DNA precursor. They suggest that RNA is synthesized in the nucleus and then passes through the nuclear membrane. In the perinuclear zone it occurs in the form of molecules small

enough to be non-sedimentable when subjected to high centrifugal force. The RNA is then integrated into larger cytoplasmic particles and finally disappears. Marshak (19) investigated the heterogeneity of the nuclear and cytoplasmic RNA's in liver cells and suggested that the nucleus contains a special nucleoprotein which differs from RNA and DNA. He stated that this compound acts as a precursor to cytoplasmic RNA when the cells are in a non-mitotic state, but when the cells are undergoing mitosis, this compound acts as a precursor to DNA.

From all the contradictory information which has appeared in the literature, two conclusions are apparent:

1. Although there is no direct evidence for interconversion of the nucleic acids, the possibility of such a conversion can not be excluded on the basis of available information.

2. If differentiation is the result of the production of specific proteins (7), and if the nucleic acids are involved in protein synthesis, then it may be expected that the nucleic acids are active in differentiation. Since recent studies have not yielded evidence for a spectacular role of these compounds in development, it is probable that the nucleic acids act in a subtle manner which has been undetectable thus far.

In view of the generally accepted theory concerning the intimate association of protein synthesis with RNA content, and in view of the evidence which suggests that the nucleus controls the synthesis of microsomes which are concerned primarily in protein synthesis (7), the present investigation was undertaken to study the following relationships: 1) differences in activity of RNase as an indication of the metabolism of RNA during morphological differentiation in the embryo and 2) differences in the activity of DNase as an indication of the metabolism of DNA in an attempt to demonstrate a possible type of control over differentiation and/or protein synthesis.[1]

METHODS OF ENZYME ASSAY

Ribonuclease. Eggs of *R. pipiens* were obtained by the pituitary injection technic and were maintained at about 25° C in an air-conditioned room. At the desired stages of development, 45 eggs were manually stripped of jelly and homogenized in a glass tissue grinder in 25 ml of tris (hydroxy) methyl-aminomethane buffer at pH 7.4.

[1] DNA is one of the most important components of the nucleus and, as such, it may exert a definite influence on differentiation and protein synthesis. However, recent evidence supplied by Sze (24), among others, suggests that the cytoplasm as well as the nucleus of the frog's egg contains DNA. This observation limits the interpretations that could be made concerning the physiological role of this important compound because it is conceivable that the DNA of the nucleus differs both structurally and functionally from the DNA of the cytoplasm.

Two ml of the homogenate were placed in two small erlenmeyer flasks and equilibrated to 25°C in a water bath. This temperature had to be maintained as accurately as possible because of the high Q_{10} of this particular enzymatic reaction. To one of these flasks (the control), 5 ml of purified RNA containing 1.0 mg/ml prepared in 0.03 M tris (hydroxy) methylaminomethane buffer at pH 7.4 were added to the homogenate from a pipette simultaneously with 25 ml of acid alcohol[1] added from a burette. To the other flask (test flask), 5 ml of purified RNA were added to

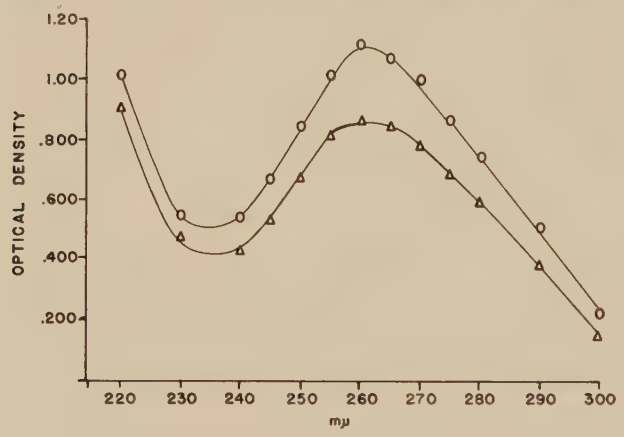

Fig. 1. Ultraviolet absorption spectra on filtrates from "control" and "test" flasks. 2.0 ml of embryo homogenate taken at stage 12 A were used. 5.0 ml of 1.0 mg/ml RNA substrate solution in tris (hydroxy) methylaminomethane buffer at pH 7.4 added to both flasks. The reaction in the test flask proceeded for 3 minutes at 25°C before addition of acid alcohol. The difference in optical density at 260 mμ was taken as an expression of RNase activity. △ Optical density of filtrate from "control" flask. ○ Optical density of filtrate from "test" flask.

the homogenate and at the beginning of the addition, a stop-watch was started. At exactly 3 minutes, 25 ml of acid alcohol were added. The acid alcohol stops the enzyme reaction and precipitates the unhydrolyzed RNA and most of the proteins but the products of the hydrolysis of RNA by RNase remain soluble in the acid alcohol. After standing one hour to obtain complete precipitation, the contents of both control and test flasks were filtered through Whatman No. 4 filter paper and the ultraviolet absorption of the filtrate was read at 260 mμ on a model DU Beckman spectrophotometer. All values were calculated in terms of the dry weight of the sample taken or of the number of eggs used and the difference in the absorption between the filtrates from the test and control flasks was taken as a measure of RNase activity. Fig. 1 illustrates the difference in the U.V. absorption spectra of the filtrates from the control and test flasks using embryo homogenates. The distinct difference in absorption at 260 mμ is readily apparent.

Desoxyribonuclease. From the same homogenate which was used for the RNase determinations, 2 ml aliquots were removed, placed in control and test flasks and equilibrated to 25°C. To the control flask, 10 ml of DNA substrate solution[2] were added simultaneously with 25 ml of acid alcohol as previously described. To the

[1] The acid alcohol solution was prepared by adding 80 ml of concentrated HCl to 120 ml of distilled water and making the solution up to one liter with 95 per cent ethyl alcohol (21).

[2] The DNA substrate solution was prepared by adding 10.0 ml of DNA stock solution (2.0 mg/ml in tris (hydroxy) methylaminomethane buffer) to 50.0 ml of 0.05 M $MnSO_4$ and making the solution up to 100.0 ml with buffer (17).

test flask, 10 ml of DNA substrate solution were added, and precisely at the beginning of the addition, a stop-watch was started. At exactly ten minutes, the reaction was stopped by the addition of 25 ml of the acid alcohol. In this case also, the products of the DNase hydrolysis of DNA are soluble in the acid alcohol whereas the unhydrolyzed DNA is not. After standing one hour, the contents of the flasks were filtered as described and the absorption of the filtrates at 260 mμ was read. The difference between the absorption in the test and control filtrates, calculated in

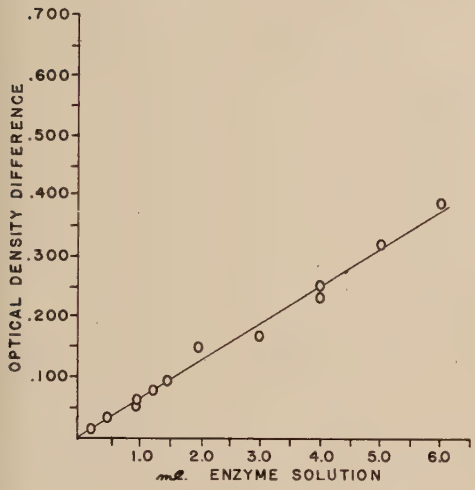

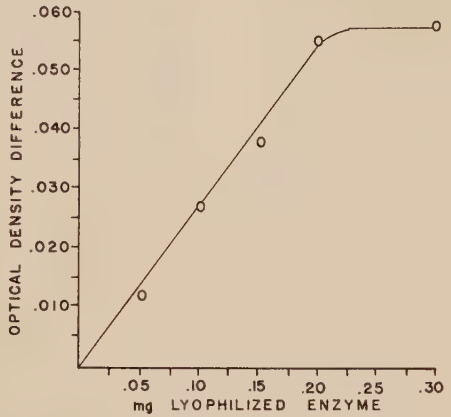

Fig. 2 (left). Relation between RNase concentration and production of acid-soluble products. 2.1 micrograms/ml of crystalline RNase (Worthington) was prepared in tris (hydroxy) methyl-aminomethane buffer at pH 7.4. 5.0 ml of 1.0 mg/ml solution of RNA in buffer at pH 7.4 was used as substrate and reactions allowed to proceed for 3 minutes at 25°C before addition of acid alcohol. The ordinate represents the optical density difference between the filtrates from the "test" and "control" flasks.

Fig. 3 (right). Relation between DNase concentration and production of acid-soluble products. Variable amounts of lyophilized DNase (Worthington) were used with 10.0 ml of DNA substrate solution at pH 7.4 and 25°C. Reaction proceeded for 10 minutes before addition of acid alcohol.

terms of dry weight or number of eggs used, was taken as an expression of the DNase activity.

Test of the spectrophotometric method. Pure system. Pure or relatively pure enzymes were used to test this method. Several experiments were performed using crystalline RNase and lyophilized DNase (Worthington Biochemical Co.) in place of the embryo homogenates. Fig. 2 shows the effect of increasing the RNase concentration on the appearance of acid-soluble products. It can be seen from this graph that the reaction is linear under the prevailing conditions at least up to 2.6 micrograms of enzyme.

In addition, a study of the liberation of acid-soluble products by RNase indicated that the reaction is linear for at least the first three minutes.

Similar results were obtained with lyophilized DNase. Fig. 3 shows the effect of increasing the DNase concentration on the production of acid-soluble compounds.

This figure shows that under existing conditions of substrate concentration and purity of enzyme, the reaction is linear until 0.2 mg of lyophilized enzyme is exceeded.

Also, a study of the appearance of acid soluble products with time indicated that the reaction is linear for at least the first ten minutes.

Tissue homogenates. Experiments were next performed to determine if the linear relationships could be obtained using embryo homogenates. It was found that up to about 33 mg dry weight of tissue homogenate, the enzymatic reactions are linear. In all experiments reported in this paper, the dry weights of the samples taken were in the range of 9.0–15.0 mg where the enzyme activity is linearly related to the amount of homogenate.

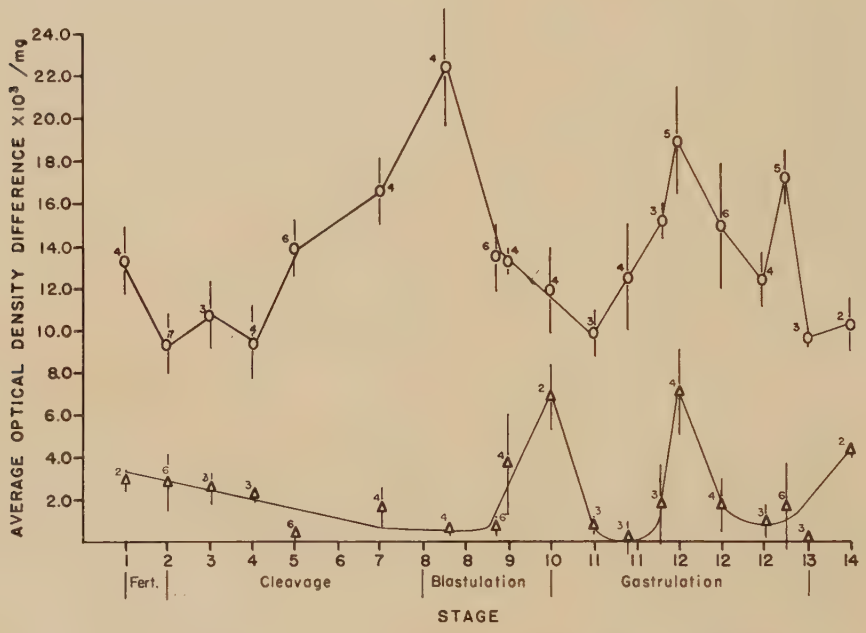

Fig. 4. Average enzyme activity per mg dry weight at various stages of development. The small numbers at each point represent the number of determinations used to calculate the average value. The vertical lines represent the extent of the standard deviation from the mean. — ○ Ribonuclease activity. △ Desoxyribonuclease activity.

RESULTS

The results of the RNase and DNase activity assays are shown in Fig. 4 and 5. In Fig. 4, the RNase and DNase activities are reported in terms of dry weight of the embryo homogenate and in Fig. 5, the activities are reported on a "per embryo" basis. It can be seen by comparing the two graphs that the trends in the enzyme activities are the same in both. Fig. 4 depicts

only average values and the standard deviations of the enzyme activities, whereas Fig. 5 shows the individual enzyme determinations plotted against time after fertilization at 25° C.

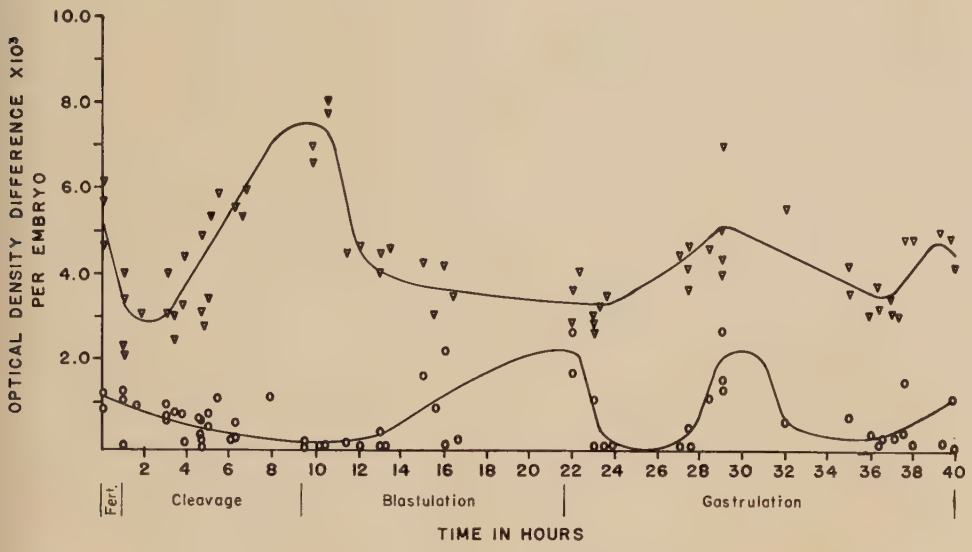

Fig. 5. Individual determinations of enzyme activity reported "per embryo" at various times after fertilization. Embryos were maintained at about 25°C. — ▽ Ribonuclease activity. ○ Desoxyribonuclease activity.

On fertilization, the RNase activity decreases but then increases progressively throughout cleavage and reaches a maximum during early blastulation. From mid-blastulation through the beginning of gastrulation, there is a rapid decrease in RNase activity. At mid-gastrulation the activity abruptly increases to a maximum value and then declines until just prior to neural plate formation. At this time, the activity again increases rapidly but soon declines when the neural plate becomes evident.

There is only a slight decrease in DNase activity on fertilization. The activity declines slowly during cleavage and early blastulation but during mid-blastulation, there is an abrupt increase which reaches a maximum at beginning of gastrulation. It then declines sharply to a minimum value during the early gastrulation stages. At mid-gastrulation there is another rapid increase in DNase activity which reaches a maximum and then declines until just prior to neural plate formation, at which time a slight increase in activity is seen.

DISCUSSION

The cyclic nature of the enzyme activities reported here may not be peculiar to these two enzymes alone. Unfortunately, almost all of the enzyme and/or substrate assays which have been made previously on amphibian embryos have been directed at specific stages of development like those chosen by Kutsky (18) or have been made only at long time intervals such as the alkaline phosphatase measurements made by Krugelis *et al.* (16). The fact that enzyme activity may vary under different physiological conditions due to such factors as the presence of activator or inhibitor molecules, or the accumulation of products, necessitates making measurements at very short time intervals particularly when complicated morphological, physiological, and biochemical processes are underway as during embryonic development. Important biochemical changes may be overlooked if this fact is not taken into consideration.

The data obtained from the study of the activity of the enzymes hydrolyzing RNA and DNA are difficult to correlate with the quantitative determinations of the substrates as reported by Hoff-Jørgensen and Zeuthen (12), Kutsky (18), Sze (24), Krugelis *et al.* (16), and Steinert (23). There are two obvious reasons why previous substrate data cannot be used for comparative purposes: 1) the quantitative measurements which have been reported were made at long time intervals during embryonic development and 2) the measurements have not been made at frequent intervals during any one stage of development. For example, previous substrate information for gastrulation cannot be used because at this stage the enzyme activity twice changes from a minimum to a maximum. Careful successive analyses for substrates during these periods have not been reported for amphibian development.

Since the nucleic acids are important components of the chromosomes, it might be expected that the activity of the enzymes associated with the nucleic acids would show variations in activity which could be correlated with stages of mitosis. This type of variation was not found for RNase and DNase in the present study. During the cleavage stages there appears to be a general increase in RNase activity and a general decline in DNase activity but no other variations were observed.

Mazia (20), Allfrey and Mirsky (1), among others, reported that by far the greater portion of DNase activity is found in the cytoplasm and not in the nucleus of cells. Indeed, Allfrey and Mirsky feel that it is unlikely that

DNase activity is limited to some simple role in the mechanics of cell division. They feel that a broader interpretation should be given which would correlate over-all desoxypentose nucleotide metabolism with DNase activity. Evidence supplied by Sze (24) and Hoff-Jørgensen and Zeuthen (12) indicate that DNA is present in the cytoplasm of the frog's egg and it is conceivable that the variations in the DNase activity which occur in the frog embryo during early developmental stages is an expression of the metabolism of cytoplasmic DNA.

As can be noted from Figs. 4 and 5, the RNase and DNase activities vary in opposite directions during cleavage and blastulation. At about mid-gastrulation, however, the activities of these enzymes vary in the same direction. The importance of this shift is unknown but perhaps it is linked to the phenomenon of determination which occurs during gastrulation.

It would be unwise to speculate further concerning the embryological significance of the variations in enzyme activity as reported here until the determinations of the substrates at short time intervals, which are now being made in this laboratory, are completed.

SUMMARY

1. A spectrophotometric method for the determination of RNase and DNase activities in frog embryo homogenates has been described.

2. Cyclical variations in RNase and DNase activities have been found during the early development of the frog.

3. RNase activity decreases on fertilization but progressively increases throughout cleavage and reaches a maximum during early blastulation. From mid-blastulation through the beginning of gastrulation, there is a rapid decrease in RNase activity. At mid-gastrulation the activity abruptly increases to a maximum value and then declines until just prior to neural plate formation. At this time the activity again increases rapidly but soon declines when the neural plate becomes evident.

4. DNase activity declines only slightly on fertilization. It declines slowly during cleavage and early blastulation but during mid-blastulation, there is an abrupt increase in activity which reaches a maximum at the beginning of gastrulation. It then declines sharply to a minimum value during the early gastrulation stages. At mid-gastrulation, there is another rapid increase in DNase activity which reaches a maximum and then declines until just prior to neural plate formation at which time a slight increase in activity is seen.

The author takes pleasure in acknowledging the generous advice and encouragement of Drs. F. R. Hunter and A. S. Baker whose suggestions aided immeasureably the preparation of this paper. The author is also indebted to many others, particularly Drs. Lloyd M. Beidler and Earl Frieden who constructively criticized this work.

LITERATURE CITED

1. Allfrey, V., and Mirsky, A. E., *J. Gen. Physiol.*, **36**, 227 (1952).
2. Barth, L. G., and Graff, S., *Cold Spring Harbor Symposia Quant. Biol.*, **6**, 103 (1938).
3. Bodenstein, D., and Kondietzer, A. A., *J. Exptl. Zool.*, **107**, 109 (1948).
4. Brachet, J., *Arch. Biol.*, Paris, **44**, 519 (1933).
5. —— *ibid.*, **53**, 207 (1942).
6. —— *Cold Spring Harbor Symposia Quant. Biol.*, **12**, 18 (1947).
7. —— *Symposia Soc. Exptl. Biol.*, **6**, 173 (1952).
8. Brachet, J., and Jeener, R., *Enzymologia*, **11**, 196 (1944).
9. Caspersson, T., *Naturwissenschaften*, **29**, 33 (1941).
10. —— *Symposia Soc. Exptl. Biol.*, **1**, 127 (1947).
11. Hammerling, J., Cited in Brachet, J., *Symposia Exptl. Soc. Biol.*, **6**, 187 (1952).
12. Hoff-Jørgensen, E., and Zeuthen, E., *Nature*, **169**, 245 (1952).
13. Hultin, T., *Exptl. Cell Research*, **1**, 276 (1950).
14. Jeener, R., and Szafarz, D., *Arch. Biochem.*, **26**, 54 (1950).
15. Keller, E. B., *Federation Proc.*, **10**, 206 (1951).
16. Krugelis, E. J., Nicholas, J. S., and Vosgian, M. E., *J. Exptl. Zool.*, **121**, 289 (1952).
17. Kunitz, M., *J. Gen. Physiol.*, **33**, 349 (1950).
18. Kutsky, P. B., *J. Exptl. Zool.*, **115**, 429 (1950).
19. Marshak, A., *J. Cellular Comp. Physiol.*, **32**, 381 (1948).
20. Mazia, D., *ibid.*, **34**, 17 (1949).
21. Roth, J. S., and Milstein, S. W., *J. Biol. Chem.*, **196**, 489 (1952).
22. Siekevitz, P., and Zamecnik, P. C., *Federation Proc.*, **10**, 246 (1951).
23. Steinert, M., Cited in Brachet, J., *Symposia Soc. Exptl. Biol.*, **6**, 177 (1952).
24. Sze, L. C., *J. Exptl. Zool.*, **122**, 577 (1953).

Experimental Cell Research, **8**, *543–549 (1955)*

METABOLISM OF THE EMBRYONIC CHICK HEART FIBROBLAST GROWN IN TISSUE CULTURE[1]

B. SHANNON DANES[2]

Cytochemistry Department, Carlsberg Laboratory, Copenhagen, Denmark

Received August 28, 1954

The metobolism of cells grown in tissue culture has been studied by several investigators (4, 5, 6, 8, 10, 11, 13, 14, 15, 16, 19, 20, 21, 22, 24). However, technical difficulties such as lack of precise methods for measurement of metabolic activity and for determination of cell number have hindered a quantitative study of the metabolism of tissue culture cells. Therefore, in none of these studies were the results obtained claimed to be anything more than approximate indications of the metabolic level of tissue culture cells.

In the present study the metabolism of cells grown in tissue culture has been measured by methods elsewhere described in detail (3). Respiration and anaerobic glycolysis of a small number of cultured cells were measured at 37.5° C by an adaptation of the Cartesian diver technique (12, 9, 1). The number of cells in the culture was determined by a modification of the nuclear enumeration method of Sanford, Earle, Evans, Waltz and Shannon (18). By this combined technique the metabolism of the embryonic chick heart fibroblast has been studied.

MATERIALS AND METHODS

Culturing procedure. Methods and tests for the culturing of a small number of cells, measurement of respiration and determination of cell number have been described elsewhere in detail (3).

The tissue was obtained from the apical region of 7-day embryonic chick hearts by routine culture methods (7). This tissue was cut into pieces approximately 0.5 mm in diameter.

The cultures were grown directly on the inner surface of weighed[3] glass capillary cylinders (outside diameter 0.7–0.8 mm, inside diameter 0.5–0.6 mm, length 1.0 mm, weight approximately 1.0 mg).

[1] This work was done under an American Cancer Society Fellowship recommended by the Committee on Growth of the National Research Council.

[2] Present address: Department of Physiology, State University of Iowa, Iowa City, U.S.A.

[3] The weight of the culture cylinder was determined in order to avoid an error in the calculation of the diver constant, V.

A piece of heart tissue was inserted close to one end of the cylinder. The culture cylinder was placed in a Carrel flask containing 2 ml of nutrient medium which consisted of four parts cockerel serum, two parts embryonic chick extract and four parts either Tyrode's solution or glucosol[1] depending upon the metabolic activity to be measured. The flask was incubated at 37.5°C for the following 48 hours.

In preparing for measurements the culture cylinder was removed from the Carrel flask and placed on a sterile glass plate on the stage of a binocular microscope. The

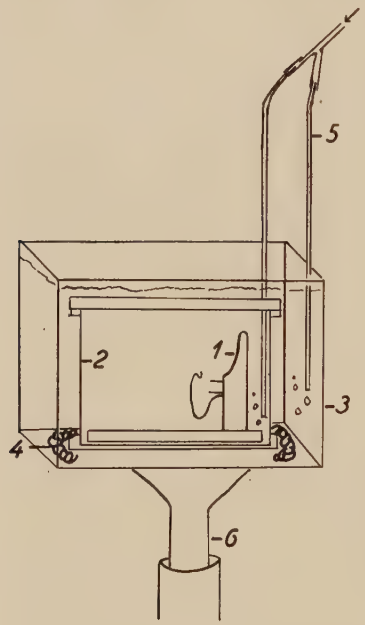

Fig. 1. Apparatus for filling and gassing Cartesian diver at 37.5°C. — The Cartesian diver held in a metal holder, 1, was placed in the plastic gassing chamber, 2, filled with water (23). This vessel was then placed in a larger plastic tank, 3, in which the water was heated by a heating coil, 4. Gas was bubbled through the water in the outer tank for circulation. The entire apparatus was mounted on a rack and pinion, 6.

explant was removed (plucked out) by means of a hooked glass needle. The culture was immediately put back into the Carrel flask and incubated for an additional 24 hours to permit recovery from any damage that might have been done during removal of the explant.

Measurements. The cylindrical divers used had the following dimensions: Inside diameter 1.0–1.2 mm, thickness of wall 0.10–0.14 mm, length 13 mm, volume 10–12 μl, weight 15–20 mg. The divers were coated on the inside with water repellent silicone[2] (17, 23).

Respiration: The filling of the diver was done at room temperature (22°C). The diver was completely filled with nutrient medium from the Carrel flask and the culture cylinder was introduced by forceps. When the culture cylinder had sunk to the bottom, excess nutrient medium was removed until the culture cylinder was

[1] The composition of glucosol was: 8.00 g NaCl, 0.20 g KCl, 0.20 g anhydrous $CaCl_2$, 0.10 g $MgCl_2 \cdot 6\ H_2O$, 0.05 g $NaH_2PO_4 \cdot H_2O$ and 1.00 g glucose in 1 liter of glass distilled water. In the case of Tyrode's solution, 1.00 g $NaHCO_3$ was added (2).

[2] 5 per cent phenyl silicone in toluene.

just covered by fluid. The height of the bottom drop of fluid (approximately 1.5 mm) was measured accurately by means of a horizontal microscope. The wall of the diver was dried with filter paper. After this, the seals of NaOH (0.5 μl), paraffin oil (0.5 μl) and the neck seal were placed in the usual manner (9).

The measurements were made at 37.5°C for periods of one to eight hours. The measurements and calculations were done according to the method described by Holter (9).

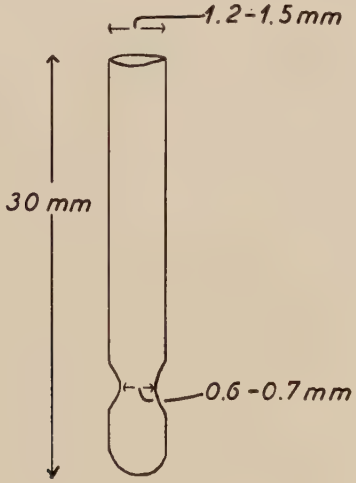

Fig. 2. Constriction tube for nuclear enumeration method.

Anaerobic glycolysis: The nutrient medium was gassed with 95 per cent nitrogen and 5 per cent carbon dioxide for five minutes. The diver was filled with gassed medium and the culture placed in the diver as described. After the excess medium had been removed, the diver was placed in a gassing chamber (23). Since it was detrimental to the cells to be kept at room temperature too long, the gassing chamber was placed in a small bath maintained at 37.5°C (Fig. 1). The gassing of the diver was done by the method described by Waterlow and Borrow (23). After the diver had been placed in the flotation vessel, a glass stopper was inserted in the neck seal (9).

Anaerobic glycolysis was calculated according to the equations given by Boell, Needham and Rogers (1).

It was necessary to do preliminary experiments in order to determine the behavior of gas-filled divers at 37.5°C. If no stopper was put in the neck seal, the diver gained weight constantly throughout the three hour measurement period. A diver containing a stopper that fitted poorly gained just about as much as a diver without a stopper. Whereas, if the neck stopper fitted (a diameter of about 0.5 mm less than the diameter of the diver neck), the behavior of the gassed diver was comparable to that of an air-filled diver.

Nuclear enumeration method. The nuclear enumeration method used is a modification of the procedure described by Sanford, Earle, Evans, Waltz and Shannon

(18) for use in determining the number of cells in a tissue culture. The method is described in detail elsewhere (3). The essential steps are as follows:

After measurements the neck seals were removed from the diver. Then the diver was filled with 0.1 M citric acid warmed to 37.5°C. By placing the diver upside down with its neck in a dish filled with citric acid, the culture cylinder fell into the dish. The culture cylinder was then placed in a constriction tube (Fig. 2) filled with citric acid and incubated at 37.5°C for one hour.

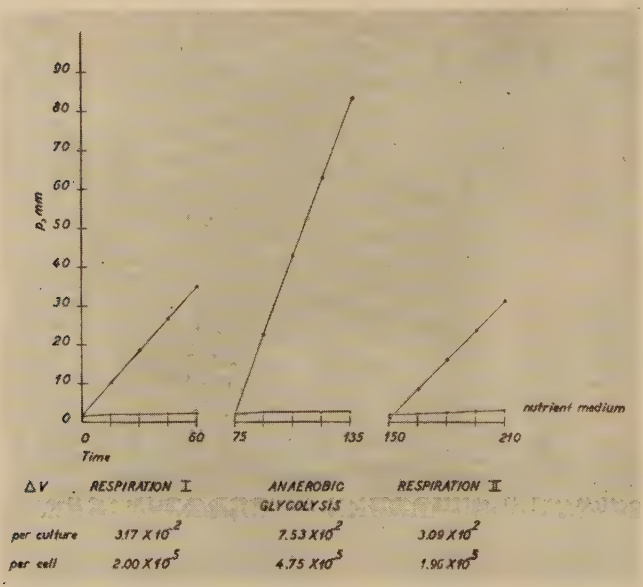

Fig. 3. A typical experiment — the measurement of respiration and anaerobic glycosis of a culture containing 1584 cells.

After removal of approximately half the fluid, the constriction tube was filled with 0.1 per cent crystal violet dissolved in 0.1 M citric acid, fused at its open end and incubated at 37.5°C for twelve hours.

In order to remove the nuclei from the wall of the culture cylinder, the tube was cautiously shaken and then centrifuged at 2,720 times gravity.

The nuclei, now in the bulb of the constriction tube, were then washed with crystal violet solution. The third and last time 0.5 per cent methocel dissolved in 0.1 M citric acid was added instead of crystal violet solution. Then the fluid was withdrawn to the constriction. The remainder, containing the nuclei (approximately 5 μl), was taken up in a braking pipette (9) whose tip had been carefully fire polished. The suspension was discharged onto a counting cover slip and the total number of nuclei determined.

The accuracy of the nuclear enumeration method was determined by studying each step individually. The order of magnitude of cells per sample was 1000. The total error in the nuclear enumeration method was found to be approximately 3.5 per cent. This loss occurred equally during shaking and pipetting; whereas, washing caused only a slight but constant loss of nuclei.

RESULTS

To work out technique, respiration and anaerobic glycolysis (total acid production) were measured on different cultures in preliminary experiments. These results are not reported here as they agree with those obtained from measuring respiration and glycolysis on the same culture.

A typical experiment is shown in Fig. 3. The second measurement of respiration was done as a check of the overall procedure. Any error due to experimental procedure was excluded by varying the order of measurements. Regardless of the order of measurements, respiration II averaged 4 per cent lower than respiration I.

The experimental results are listed in Table I. The respiration of the embryonic chick heart fibroblast was found to be $1.91 \times 10^{-5} \pm .04$ μl/hr. cell (3). Whereas, anaerobic glycolysis was $4.99 \times 10^{-5} \pm .12$ μl/hr. cell.

DISCUSSION

It is difficult to compare the above results with those reported by other workers (8, 10, 11, 13, 14, 15, 16, 19, 20, 21, 22) who calculated metabolic activity on a weight basis. As discussed previously (3) the oxygen consumption per cell (5×10^{-7} μl/hr at 22° C) reported by Zamecnik (24) varied by a factor of 10 from those reported previously (3) and in this paper even if the temperature difference was taken into account. In repeating Zamecnik's work it was found that the respiration fell off gradually at 20.2° C (3). As these cultures had been grown at 37.5° C, they were probably not under optimal conditions during measurement period. This would probably also apply to Zamecnik's work as the cultures were grown at 38.0° C and measurements done at 22° C.

Danes, Christiansen and Leinfelder (5) reported that the respiration of the embryonic chick heart fibroblast was of the order of 1.76×10^{-3} μl/hr.cell. Respiration per cell was calculated on the basis of the oxygen consumption of a culture containing a tissue explant as well as migrated cells. By necrosis such an explant might have made adequate measurement of cellular respiration impossible.

The standard deviations for respiration and anaerobic glycolysis measurements are shown in Table I. The standard deviations for respiration I and II were the same, 0.04. Whereas, the standard deviation for anaerobic glycolysis was 0.12. The relative variation of respiratory activity and glycolysis therefore appeared to be the same.

TABLE I

Date Expt.	Culture Number	Number of Nuclei/ culture	Respiration I ΔV (ΔV per cell) μl	Anaerobic Glycolysis ΔV (ΔV per cell) μl	Resp./ Gly. %	Respiration II ΔV (ΔV per cell) μl
3/7	1	3026	5.92×10^{-2} (1.95×10^{-5})	1.58×10^{-1} (5.22×10^{-5})	37.1	5.86×10^{-2} (1.94×10^{-5})
	2	3552	6.87×10^{-2} (1.95×10^{-5})	1.75×10^{-1} (4.97×10^{-5})	39.3	5.70×10^{-2} (1.89×10^{-5})
3/11	3	1584	3.17×10^{-2} (2.00×10^{-5})	7.53×10^{-2} (4.75×10^{-5})	42.1	3.09×10^{-2} (1.96×10^{-5})
	4	1527	2.37×10^{-2} (1.55×10^{-5})	6.48×10^{-2} (4.25×10^{-5})	36.6	2.30×10^{-2} (1.51×10^{-5})
3/20	5	1037	2.02×10^{-2} (1.95×10^{-5})	5.39×10^{-2} (5.19×10^{-5})	37.5	1.96×10^{-2} (1.89×10^{-5})
	6	656	1.42×10^{-2} (2.16×10^{-5})	3.65×10^{-2} (5.56×10^{-5})	38.9	1.35×10^{-2} (2.06×10^{-5})
3/22	7	1975	3.92×10^{-2} (1.98×10^{-5})	1.05×10^{-1} (5.32×10^{-5}	37.3	3.90×10^{-2} (1.98×10^{-5})
	8	1227	2.50×10^{-2} (1.97×10^{-5})	6.67×10^{-2} (5.43×10^{-5})	37.4	2.20×10^{-2} (1.79×10^{-5})
3/24	9	1306	2.23×10^{-2} (1.71×10^{-5})	6.09×10^{-2} (4.67×10^{-5})	36.6	2.23×10^{-2} (1.71×10^{-5})
	10	1563	2.71×10^{-2} (1.73×10^{-5})	7.21×10^{-2} (4.61×10^{-5})	37.6	2.39×10^{-2} (1.53×10^{-5})
3/25	11	1607	3.06×10^{-2} (1.90×10^{-5})	7.26×10^{-2} (4.25×10^{-5})	42.1	3.01×10^{-2} (1.87×10^{-5})
	12	921	1.94×10^{-2} (2.10×10^{-5})	5.34×10^{-2} (5.79×10^{-5})	36.3	1.77×10^{-2} (1.92×10^{-5})
3/26	13	1420	2.77×10^{-2} (1.96×10^{-5})	7.13×10^{-2} (5.01×10^{-5})	38.8	2.71×10^{-2} (1.91×10^{-5})
	14	1361	2.49×10^{-2} (1.83×10^{-5})	6.50×10^{-2} (4.77×10^{-5})	38.3	2.40×10^{-2} (1.76×10^{-5})
		Average	($1.91 \times 10^{-5} \pm .04$)	($4.99 \times 10^{-5} \pm .12$		($1.84 \times 10^{-5} + .04$)

. It was amazing that there was not a greater loss than 4 per cent of respiratory activity from the first to the second measurement. Whether this small difference was due to loss and damage of cells or to a reduction in respiration rate per cell cannot be said.

CONCLUSIONS

The metabolism of the 7-day embryonic chick heart fibroblast has been studied. Respiration was found to be of the order of 1.91×10^{-5} µl/hr. cell. Anaerobic glycolysis was 4.99×10^{-5} µl/hr. cell.

I wish to thank Dr. and Mrs. Heinz Holter for their guidance, encouragement and interest in this research. I am grateful to Dr. E. J. Boell for his advice on measurement of anaerobic glycolysis and preparation of the text. K. Max Møller designed the apparatus for filling the Cartesian diver at 37.5°C. The tissue cultures for this study were prepared at the Carlsbergfondets biologiske Institut.

REFERENCES

1. Boell, E. J., Needham, J., and Rogers, V., *Proc. Roy. Soc., B*, **127**, 322 (1939).
2. Cameron, G., Tissue Culture Technique. 2d ed. Academic Press, Inc., New York, 1950.
3. Danes, B. S., *Compt. rend. trav. lab. Carlsberg, Sér. chim.* (In press.)
4. Danes, B., Christiansen, G. S., and Leinfelder, P. J., *Exptl. Cell Research*, **5**, 234 (1953).
5. —— *J. Cellular Comp. Physiol.* (In press.)
6. Danes, B., and Leinfelder, P. J., *ibid.*, **37**, 427 (1951).
7. Fischer, A., Gewebezüchtung. 3. Aufl., 1930.
8. Gemmill, C. L., Gey, G. O., and Austrian, R., *Bull. Johns Hopkins Hosp.*, **66**, 167 (1940).
9. Holter, H., *Compt. rend. trav. lab. Carlsberg, Sér. chim.*, **24**, 399 (1943).
10. Laser, H., *Biochem. Z.*, **215**, 2 (1932).
11. —— *ibid.*, **264**, 72 (1933).
12. Linderstrøm-Lang, K., *Nature*, **140**, 108 (1937).
13. Lipmann, F., *Biochem. Z.*, **244**, 177 (1932).
14. —— *ibid.*, **261**, 157 (1933).
15. Meier, R., *ibid.*, **231**, 247 (1931).
16. —— *ibid.*, **231**, 253 (1931).
17. Schwartz, S., *Compt. rend. trav. lab. Carlsberg, Sér. chim.*, **27**, 79 (1949).
18. Sanford, K. K., Earle, W. R., Evans, V. J., Waltz, H. K., and Shannon, J. E., *J. Natl. Cancer Inst.*, **11**, 773 (1951).
19. Tiedemann, E., and Fischer, A., *Biochem. Z.*, **247**, 68 (1932).
20. Victor, J., *Am. J. Physiol.*, **11**, 477 (1935).
21. Victor, J., and Lewis, W. H., *Am. J. Cancer*, **29**, 503 (1937).
22. Warburg, O., and Kubowitz, P., *Biochem. Z.*, **189**, 242 (1927).
23. Waterlow, J. C., and Borrow, A., *Compt. rend. trav. lab. Carlsberg, Sér. chim.*, **27**, 93 (1949).
24. Zamecnik, P., *ibid.*, **24**, 59 (1941).

RECHERCHES SUR LA PHYSIOLOGIE DE L'OVOGENÈSE CHEZ *PHASCOLOSOMA VULGARE*

P. H. GONSE

Station Biologique de Roscoff, Roscoff, Finistère, France

Reçu le 16 septembre, 1954

Il existe beaucoup de travaux cytologiques et histochimiques sur les ovocytes de nombreuses espèces animales. La croissance de ces cellules, cependant, n'a presque pas été étudiée sous l'angle physiologique. Sur un matériel approprié, les ovocytes du Sipunculide *Phascolosoma vulgare*, nous cherchons par des méthodes convergentes à mettre en évidence les diverses étapes de la croissance et les modalités de la différenciation. Les variations de la vitesse de croissance ont été enregistrées par des mesures de fréquence des tailles (1); l'organisation intracellulaire a été étudiée par des techniques cytologiques et histochimiques classiques; on a mesuré la respiration des ovocytes (2). Afin de mettre en rapport les variations du taux respiratoire avec le taux de croissance des divers élements intracellulaires on a effectué des expériences de stratification par centrifugation.

Les ovocytes sont centrifugés à 16.000 g pendant 25 minutes et à 15° C dans une solution isotonique à 4 volumes de saccharose pour 6 volumes d'eau de mer : solution de même densité que les cellules. Aussitôt après la centrifugation les ovocytes sont fixés par l'acide osmique (conc. finale 0,02 %) pendant 5 min. jusqu'à noircissement modéré des graisses. Les cellules sont alors lavées et montées entre lame et lamelle dans une lame légèrement creuse. On a contrôlé par des experiences effectuées sur des ovocytes d'une taille determinée que cette technique n'altère pas sensiblement le volume des cellules. Les différentes couches séparées sont depuis le pôle centrifuge dans un ovocyte de taille moyenne (Fig. 1, d) :

1) une calotte de petits granules incolores ; il s'agit d'un *polysaccharide* et probablement de galactogène (G),

2) une couche de *cytoplasme lourd* incolore (Cy I) contenant les *mitochondries* (m),

3) une couche d'*inclusions lipidiques* noircies par OsO_4 (L),

4) une calotte de *cytoplasme léger* (Cy II) dépourvue d'inclusions et brunie par OsO_4. Dans les gros ovocytes (Fig. 1, g) cette région est occupée par des *plaquettes vitellines* incolores (PV).

D'autres centrifugations ont été suivies de fixation au formol (conc. finale 1,5 %). Après coupes à congélation les cellules ont été colorées par la technique de Mac Manus ou au noir soudan. Quelques centrifugations ont été effectuées dans le vert janus au 1/1.000ème pour mettre en évidence les mitochondries. Celles-ci sont granu-

laires comme le polysaccharide mais ces granules mitochondriaux ne sont pas isolés et forment des amas d'importance variable. Dans les conditions de centrifugation précédentes les mitochondries ne sont pas stratifiées ou refluent très rapidement dans le cytoplasme tandis que le polysaccharide reste tassé pendant plusieurs heures (Fig. 1, b).

Après le montage des cellules des dessins sont faits à la chambre claire (Gross. 680). D'après ces dessins on calcule le volume en valeur absolue des différentes couches en assimilant celles-ci à des segments de sphère, on soustrait le volume de la fraction du noyau présente dans la couche considérée. A titre de contrôle le volume du noyau a été également mesuré sur des cellules non centrifugées. Les dessins ont été groupés en 9 catégories selon la taille des ovocytes. Dans chaque catégorie 7 à 15 cellules ont été étudiées pour obtenir la moyenne des volumes occupés par : 1) cytoplasme lourd, les mitochondries étant incluses, et cytoplasme léger (Cy + m), 2) inclusions lipidiques (L), 3) polysaccharide (G), 4) plaquettes vitellines (PV), 5) noyau (N). L'unité de volume utilisée U est égale à 10^{-5} µl.

Pour toutes ces valeurs le coefficient de variation $V\sigma$ calculé à partir de l'écart type σ est généralement compris entre 10 et 30 (moyenne pour le volume total : 17,29, pour (Cy + m) : 18,29). Mis à part les stades d'apparition ou de disparition de (L) et de (G) où les lots d'ovocytes sont particulièrement hétérogènes on trouve un $V\sigma$ moyen de 19,14 pour (L) et 30,44 pour (G) qui occupe un petit volume et est difficile à mesurer. La dispersion est surtout due au groupement de cellules de taille différente par lots. L'erreur imputable à la technique (centrifugation et mesures) est probablement d'environ 15 %.

On constate (Fig. 3) que les inclusions lipidiques apparaissent dans les cellules de volume 16 et s'accroissent ensuite à un taux constant. Le polysaccharide apparaît au volume 3–4 et montre un taux de croissance variable, il disparaît dans les gros ovocytes. Il n'a pas été possible d'obtenir des données quantitatives sur le nombre de mitochondries ou le volume qu'elles occupent aux différents stades. Il nous semble, cependant, qu'à partir du moment où elles apparaissent dans la cellule (vol. 2–3) leur nombre reste sensiblement proportionnel au volume de l'ovocyte. La figure 4 montre les résultats obtenus en calculant la respiration par unité de volume général et unité de volume de (Cy + m). Dans ce dernier cas la différence de taux respiratoire entre les ovocytes de volume 4 et 75–150 disparaît, mais on note la persistance de 2 périodes à respiration élevée. L'examen des diagrammes 2 et 3 permet de faire quelques hypothèses sur la signification de ces variations du taux respiratoire. On remarque (Fig. 3) que pendant la phase comprise entre les volumes 75 et 150 la respiration est sensiblement proportionnelle au volume de (Cy + m) et les lipides sont seuls à s'accroître notablement dans la cellule. Ceci nous permet de supposer que l'élaboration de ces inclusions lipidiques n'est pas seule en cause dans les phases à respiration élevée (vol. 8–75 et 150–230). Or c'est pendant la première de ces phases

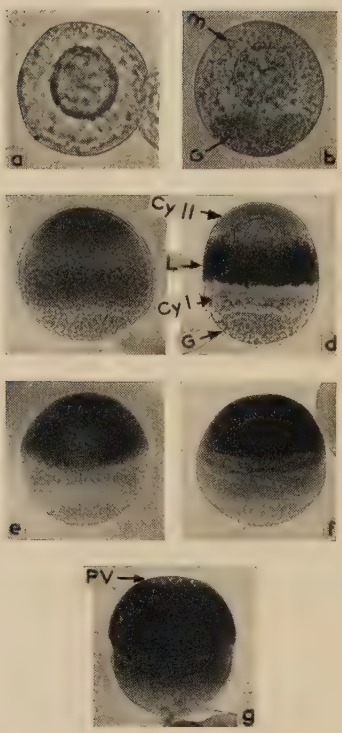

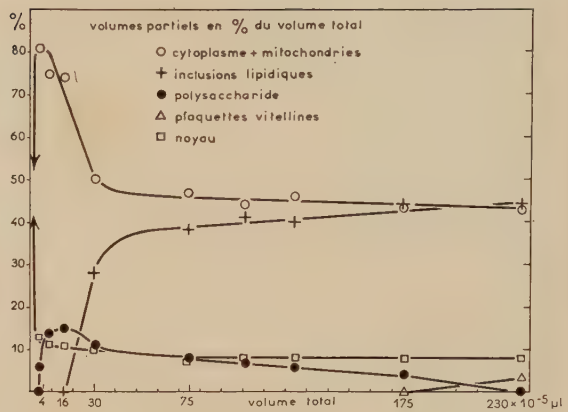

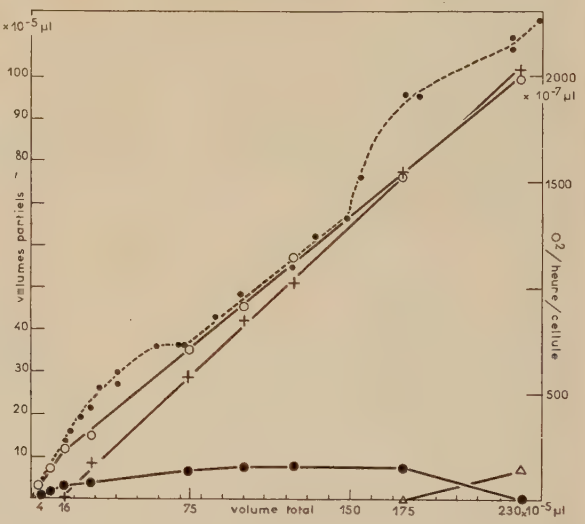

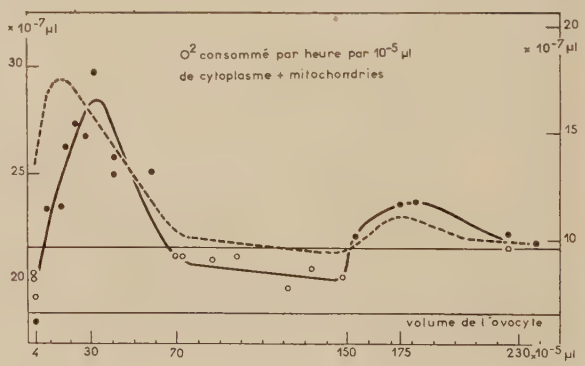

Fig. 1 (à gauche). Ovocytes centrifugés, fixés par OsO_4. Leurs volumes respectifs sont de a à g : 3,5 – 8 – 30 – 75 – 150 – 175 – 230 10^{-5} µl. Pôle centrifuge vers le bas. Détails dans le texte.

Fig. 2, 3, 4 (à droite, de haut en bas). Fig. 2: Volumes des différents constituants en % du volume total. Fig. 3: Volumes des différents constituants en valeur absolue. *En tirets :* respiration par cellule (échelle à droite). Fig. 4: *En trait plein :* respiration par unité de volume de (Cy + m). Les cercles blancs sont les valeurs ne différant pas de façon significative de $20 \cdot 10^{-7}$ µl O_2/h./U (Cy + m). *En tirets :* respiration par unité de volume général, échelle à droite, les points expérimentaux ne sont pas indiqués.

que le polysaccharide effectue tout son accroissement, à partir du volume 75 il est sensiblement stationnaire. La membrane vitelline, riche en mucosaccharide apparaît au volume 16 au moment ou le pourcentage de polysaccharide granulaire diminue (Fig. 2). Pendant la seconde de ces phases (vol. 150–230) le polysaccharide disparaît et des plaquettes vitellines se forment. Précisons que la corrélation entre ces deux phénomènes n'est pas directe, s'ils sont liés ce ne peut être que par un intermédiaire non décelable morphologiquement. On trouve en effet des cellules sans plaquettes et sans polysaccharide mais pas de cellules contenant à la fois les deux élements. Les plaquettes n'apparaissent qu'à partir du volume 175 mais à un stade variable selon les animaux entre les volumes 175 et 230.

Nous pensons pouvoir proposer deux hypothèses concernant le métabolisme respiratoire des ovocytes. Dans les deux cas nous admettrons l'existence d'un système présent dans le cytoplasme et les mitochondries qui respire à un taux à peu près constant pendant la croissance : $20 \cdot 10^{-7}$µl O_2/h./U (Cy + m). Ce système fournit ainsi l'energie nécessaire à la croissance cytoplasmique et mitochondriale et à l'élaboration des réserves lipidiques. Dans la première des hypothèses on peut supposer que pendant les deux périodes à respiration élevée un ou plusieurs autres systèmes spécialisés entrent en jeu; leur fonctionnement étant en rapport avec des synthèses particulières : polysaccharide ou vitellus des plaquettes. La respiration enregistrée pendant ces périodes est alors une résultante. Dans la seconde hypothèse le rôle essentiel serait dévolu au premier système qui se trouverait donc pendant les phases à forte respiration en quelque sorte activé, il libérerait alors une quantité d'energie plus grande qui rend possible les synthèses spécialisées. Des recherches sont en cours sur ce sujet.

Je remercie M. le Professeur P. E. Lindahl (Uppsala) qui a suggéré et suivi ce travail et le Dr. E. Zeuthen (Copenhague) qui m'a enseigné la technique du microludion.

BIBLIOGRAPHIE

1. Gonse, P. H., *Compt. Rend. Acad. Sci. Paris*, **236**, 528 (1953).
2. —— *ibid.*, **238**, 2350 (1954).

Experimental Cell Research, **8**, *554–557 (1955)*

BRIEF NOTES

THE INFLUENCE OF TEMPERATURE UPON THE NUCLEOLI OF *TRADESCANTIA*

B. SNOAD

John Innes Horticultural Institution, Bayfordbury, Hertford, Herts, England

Received February 6, 1955

Comparative studies of the behaviour of the nucleus and other organelles within the cell under different conditions of internal and external environment can often be instructive. The present note concerns differences in behaviour of nucleoli in mitotic and meiotic cells of *Tradescantia bracteata*, a diploid species, under two conditions of environment.

The chromosome complement of this species includes two pairs of chromosomes with almost terminal nucleolar organisers (Fig. 1). Therefore, the maximum number of nucleoli expected in any diploid cell will be four. But, as a result of fusion, smaller numbers of nucleoli will be found.

T. bracteata is unusual in possessing a 'cap' nucleolus at meiosis. From very early prophase this is pressed tightly up against the inside of the nuclear membrane and formed into an almost hemispherical shape (Fig. 3). In most nuclei there is only the one nucleolus during meiotic prophase. This may be due partly to chromosome pairing and partly to a form of chromosome polarisation.

Fig. 1. The chromosome complement of *Tradescantia bracteata* showing the satellited chromosomes. × 2400.

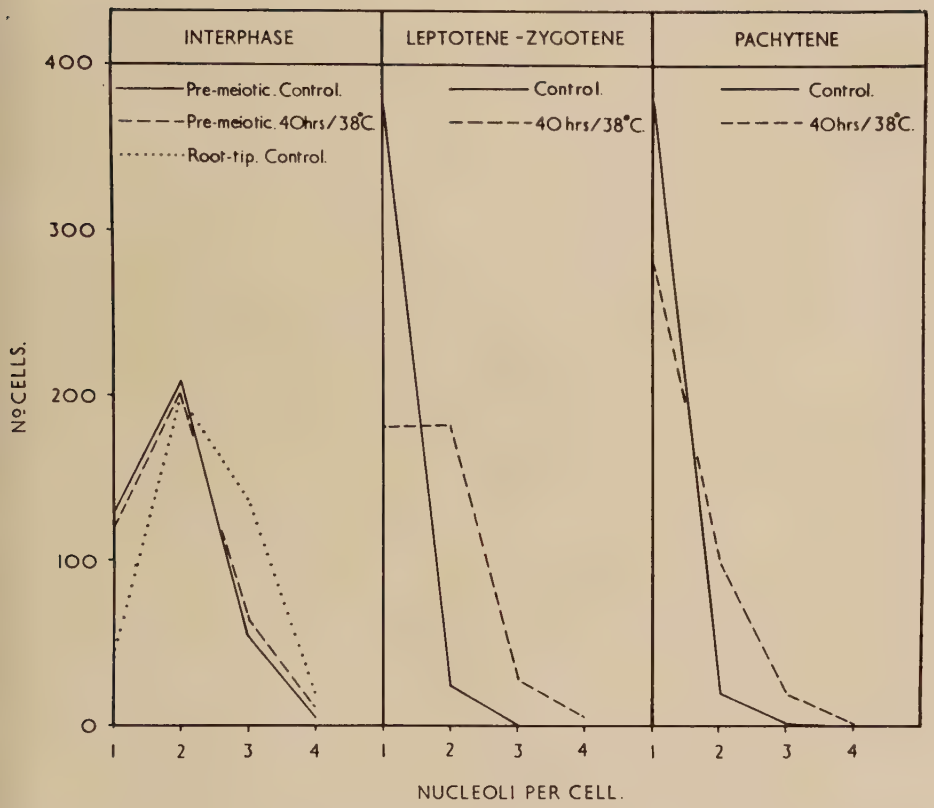

Fig. 2. Graphs illustrating the nucleolar frequencies per cell at various stages of division in plants grown under normal and high temperature conditions. 400 cells are represented in each sample.

Cap nucleoli are not common and, apart from *Tradescantia*, they seem only to have been reported in the pollen mother cells of some species of *Fritillaria* [1] and the embryo-sac mother cells of *Lilium tigrinum* [7]. No explanations, however, were offered for their unusual shape but their close similarity to those found in *Tradescantia* suggests that they also may arise through chromosome polarisation. Cap nucleoli have also been reported in the pollen mother cells of *Pisum* [2]. Here the nucleoli are organised near the centromeres so anaphase movement alone will lead to polarisation of the nucleolar organisers.

Counts were made to compare the amount of nucleolar fusion in root meristems and anthers, at different stages, of plants growing under normal glasshouse conditions (temp. 18-23° C). In root-tip cells nucleolar frequencies were determined in the interphase nuclei. In the anthers a premeiotic interphase, leptotene, zygotene and pachytene were examined (Fig. 2).

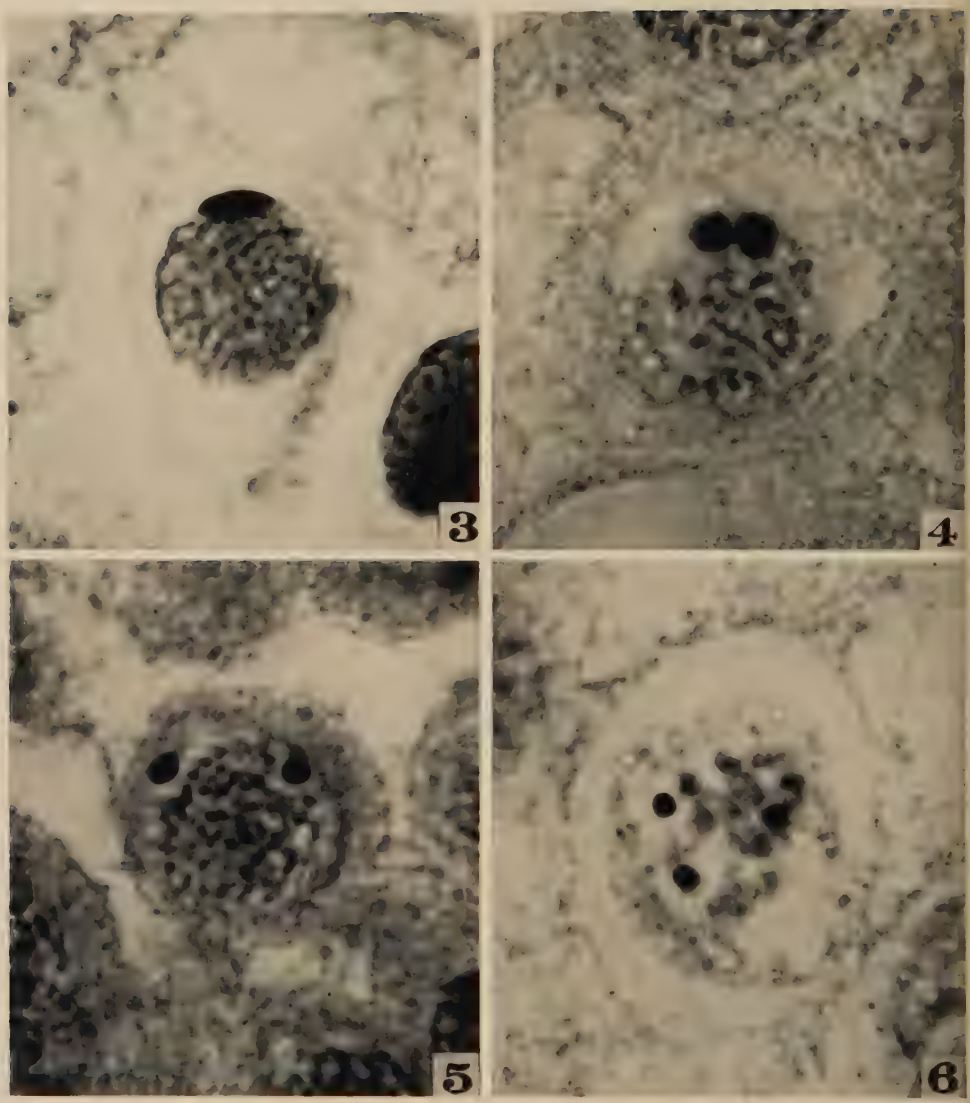

Pollen mother cells of *Tradescantia bracteata* at early prophase of meiosis. All × 2100.

Fig. 3. Material grown under normal temperature conditions. Note the cap nucleolus.
Figs. 4, 5 and 6. Material grown under high temperature conditions. Note the spherical appearance of the nucleoli and the lack of fusion.
(A modification by L. F. La Cour and J. Chayen of J. R. Baker's acid haematin reaction for phospholipids was used for these preparations.)

Nucleolar frequencies were also determined for similar stages after subjecting the plants to a temperature of 38° C for 40 hours —artificial illumination being provided. No alteration in frequency is found in the premeiotic interphase (Fig. 2). However, changes in number and form of the nucleoli occur at meiotic prophase. There are now many nuclei in which the single cap nucleolus has been replaced by two to four randomly scattered, ordinary, spherical nucleoli (Figs. 4, 5 and 6). The results of this experiment are summarised in Fig. 2.

In *Tradescantia* the heat shock has interfered with polarisation thus releasing the nucleoli from contact with the nuclear membrane and allowing them to take up their more characteristic globular shape.

Agreement has not been reached upon the mode of origin of the nucleolus although many of the observations are obviously related one to another. The most commonly accepted theory is that the nucleolus is formed at telophase by the nucleolar organisers of the chromosome complement [e.g., 3 and 4]. Rattenbury and Serra [5], on the other hand, report droplets, or even layers, of pronuclear material being formed at telophase by the "periplasm" (a mixture of nucleoplasm and cytoplasm). These droplets later coalesce and are collected together to form the nucleoli proper at specific chromosome regions or nucleolar zones.

Following their organisation fusion of the nucleoli can occur at telophase but, as shown by these observations in *Tradescantia*, fusion is not necessarily always initiated at or confined to this phase. The nucleolar frequency at premeiotic interphase in plants growing at normal temperatures is not very different from that found in leptotene-zygotene stages after the heat shock (Fig. 2). Therefore at early prophase of meiosis, before treatment began, nucleolar fusion was not complete. The increase in fusion as seen at pachytene emhpasises the strength of meiotic chromosome pairing and the effect of chromosome polarisation. The fusion of nucleoli is similar to that of blocks of heterochromatin. Both are influenced by chromosome pairing and movement and their very nature leads to coalescence after chance contact.

There is more nucleolar fusion in premeiotic interphase cells than in root-tip cells. This is probably due to somatic chromosome pairing.

Incomplete coalescence of nucleoli has been found in *Phaedranassa carmioli* [6]. Here, diverging chemical activity or state of the nucleoli inhibits normal fusion during the prophase of meiosis. A form of equilibrium results and one nucleolus becomes enclosed within the other but retains its chemical differences. Normal fusion, with no detectable chemical differences, occurs in somatic cells—indicating differences in gene activity at meiosis and mitosis.

I wish to thank Mr. L. F. La Cour for his advice and helpful criticism.

REFERENCES

1. Frankel, O. H., *Cytologia* **8**, 37 (1937).
2. Håkansson, A. and Levan, A., *Hereditas* **28**, 436 (1942).
3. Heitz, E., *Planta* **15**, 495 (1931).
4. McClintock, B., *Z. Zellforsch. u. mikroskop. Anat.* **21**, 294 (1934).
5. Rattenbury, J. A. and Serra, J. A., *Port. Acta Biol. Série A* **3**, 239 (1952).
6. Snoad, B., *Ann. Report of the J. I. H. I.* (1955).
7. Thermann, E., *Arch. Soc. "Vanamo"* **6**, 12 (1951).

THE PRIMARY AND SECONDARY CONSTRICTIONS ON THE CHROMOSOMES OF THE RAT LYMPHOBLAST

S. OHNO and R. KINOSITA

Department of Cytology, Division of Research, City of Hope Medical Center, Duarte, Calif,. U.S.A.

Received March 8, 1955

Two morphological elements, primary [7] and secondary [3] constrictions, have been noted on chromosomes of certain plants and lower animals and their location and distribution have been studied [1]. The primary constriction or kinetochore is regarded as the attachment region of the spindle fiber. The secondary constriction is a segment hardly stainable with nuclear stain, and has been called the *SAT*-zone. In mammals, however, little is known about the secondary constrictions because of technical difficulty in visualizing these morphological elements. Recently, we [4] succeeded in demonstrating "chromophobic segments" in addition to the primary constrictions on certain chromosomes of leuko- and erythroblastic cells and tumor cells from rats. Subsequent observations have indicated that the chromophobic segments are similar in structure to the *SAT*-zones (Fig. 1). These findings encouraged us to extend systematic studies on karyotypes of mammalian cells, especially referring to the primary and secondary constrictions.

Material and Methods.—Four male and two female Wayne-Pink-Eye rats, three to seven months of age, were employed. Lymphoblasts were chosen for observation because, for the most part, they have a definite diploid chromosome set, they are relatively frequent in mitosis, and the structures of the individual chromosomes at late metaphase are especially clearly demonstrable by the present method.

Fig. 1. A photomicrograph of the rat myelocyte demonstrating the chromophobic segment (*S*) with faintly stained longitudinal filaments. The microscopic preparations were prepared by the method stated in the previous paper [4]. Leitz Wetzlar Periplan 15 × eyepiece and 2 mm Apo Oel Objective were used for photomicrography.

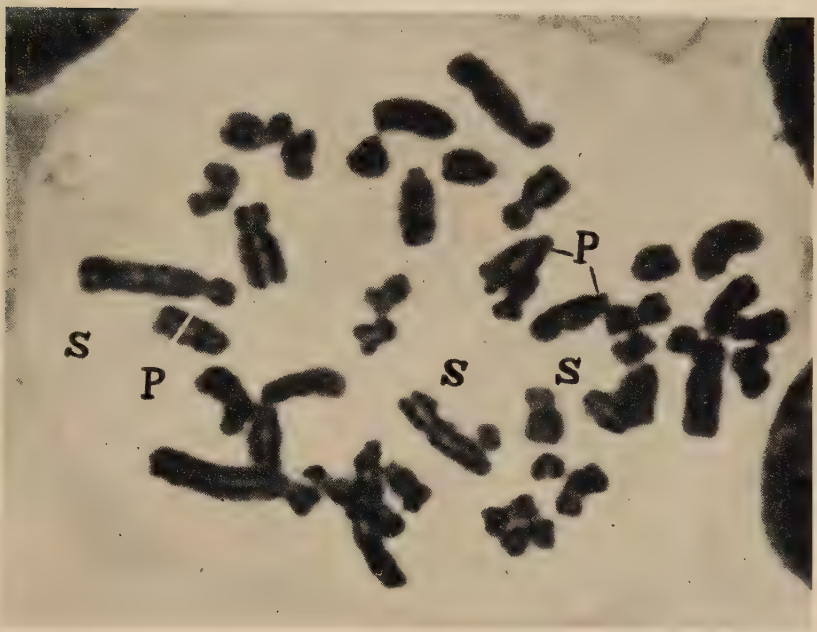

Fig. 2. A photomicrograph of the lymphoblast at late metaphase from the male rat. The method is stated in the text. Forty-two chromosomes are seen, including three with the secondary (*S*) and primary (*P*) constrictions.

Mesenteric lymph nodes were surgically removed and small pieces of the cortex were minced in about an equal volume of horse serum. An equal volume of distilled water was added for dilution. A part of the resulting fluid in which lymphoid cells were suspended was aspirated in a blood-cell-count pipette and incubated for 30 minutes at 3°C. Thin film preparations were made of the fluid by carefully spreading a drop of fluid on a clean microscopic slide. The smears were fixed with 1 per cent solution of chromic acid and methanol, then treated with 1 *N* solution of HCl for 15 minutes at 60°C, washed with distilled water, immersed in a saturated solution of picric acid for 10 minutes, and stained with Giemsa stain using McJunkins buffer solution. The azur dye sharply stained the chromosomes exclusively, leaving well-defined loci of the primary and secondary constrictions unstained. From six animals ten of such late metaphase figures were selected for minute observations. Photomicrographs were taken using Leitz Wetzlar Periplan 15× eyepieces with a 2 mm Apo Oel Objective (Fig. 2). Exact figures of the individual chromosomes were traced on a sheet of transparent paper placed on the photomicrograph, supplementarily guided by actual microscopic observations of the particular chromosomes. Pairs of homologous chromosomes were numbered in order of size. A complete set of these pairs has been placed in serial alignment as shown in Fig. 3.

Results.—The late metaphasic chromosomes at the start of longitudinal splitting demonstrated the primary and secondary constrictions most clearly, compared with

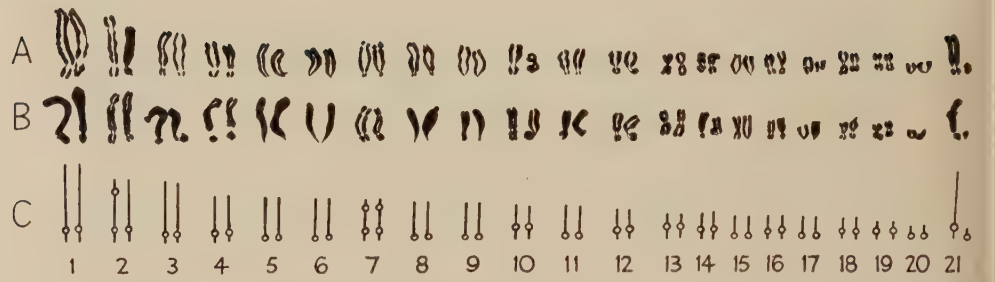

Fig. 3. Two drawings of alignment (*A* and *B*), prepared from two diploid lymphoblasts of the male rats. *A* was made from Fig. 2. *C* is a schematic drawing from *A* and *B*. The constrictions are marked by circles at their approximate positions on the individual chromosomes. Twenty pairs of the autosomes and the *X*- and *Y*-chromosomes are included.

the ana- and telophasic chromosomes. Two faintly stained filaments were distinctly observed which extended through the constrictions and into the deeply stained double-stranded parts of the chromosome on both sides of the constrictions (Figs. 1, 4). They appeared to be a single filament in the anaphase chromosome, while during telophase a double filament was observed to extend through the constriction.

The karyotype and chromosome alignment were similar in all the ten lymphoblasts. The typical chromosome alignment from two male rats is illustrated in Fig. 3. In each case, 20 pairs of autosomes and two sex chromosomes are included. The primary constrictions are situated at varied positions characteristic, however, for each individual chromosome (Figs. 2, 4). This position may be as follows: (a) at the subterminal region on the first, second and third pairs of autosomes and the *X*-chromosomes of the first large-size group, and on the fourth and seventh pairs of autosomes in the second large-size group; (b) at the submedian region on the 10th, 12th, 14th, 16th and 18th pairs of autosomes; and (c) at the median region on the 13th and 19th pairs of autosomes. The remaining chromosomes, namely the 5th, 6th, 8th, 9th, 11th, 15th, 17th, and 20th pairs of autosomes and the *Y*-chromosome, do not show typical primary constrictions which distinctly separate the chromosomes into two arms. Some of the chromosomes, however, demonstrate short, narrow portions at the ends which probably indicate small second arms, suggesting that the kinetochores are located at the regions extremely close to the ends (Fig. 4c).

The secondary constrictions were found exclusively on three of the 42 chromosomes, regardless of the sex of the animal. Their primary constrictions are subterminal and the secondary constrictions are at the opposite subterminal region. The one large chromosome bearing the secondary constriction is believed to be a member of the second pair of autosomes. The lymphoblast of the female chromosome complement presents only one large chromosome with a secondary constriction, although female rat cells are known to have two *X*-chromosomes. The other two chromosomes with the secondary constrictions are both members of the 7th pair of autosomes. These cannot be confused with the *X*-chromosomes because of wide difference in size.

Discussion.—It had been believed that each of the 42 chromosomes in the rat cell is a rod of uniform diameter with its kinetochore at one end, until recent studies

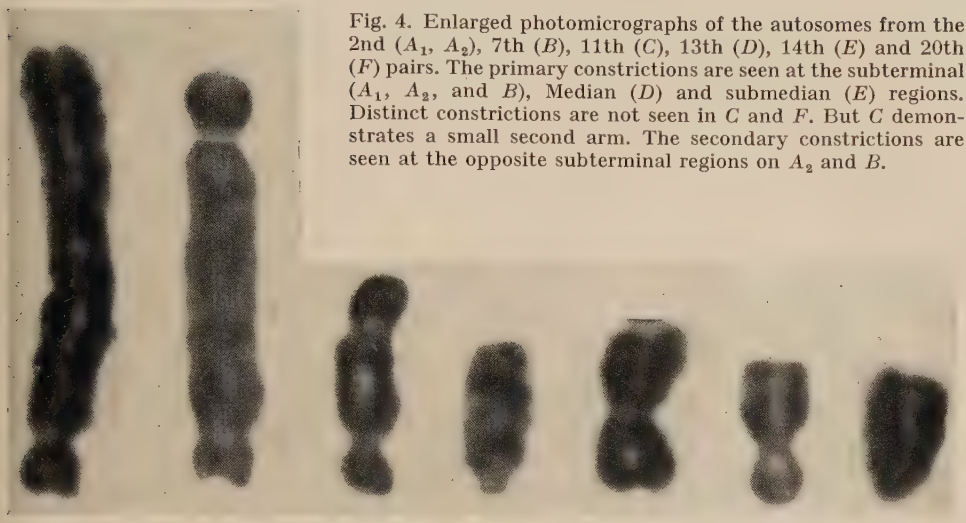

Fig. 4. Enlarged photomicrographs of the autosomes from the 2nd (A_1, A_2), 7th (B), 11th (C), 13th (D), 14th (E) and 20th (F) pairs. The primary constrictions are seen at the subterminal (A_1, A_2, and B), Median (D) and submedian (E) regions. Distinct constrictions are not seen in C and F. But C demonstrates a small second arm. The secondary constrictions are seen at the opposite subterminal regions on A_2 and B.

indicated that the primary constriction divides the chromosome into two arms in the case of 9 pairs of chromosomes [2, 5, 6]. The present study on the rat lymphoblasts further revealed that 12 pairs of autosomes and the X-chromosomes have primary constrictions at the subterminal, submedian, or median regions. The remaining 8 pairs of autosomes and the Y-chromosome appear to be rod-shaped. It is, however, still doubtful that all of them have the kinetochores literally at the terminal ends. In fact, some of them were found to have constrictions close to the ends, suggesting that the kinetochores are not terminally located but at the regions close to the ends. With further technical improvements more chromosomes may very likely be shown to have primary constrictions. In other words, chromosomes with their kinetochores literally at the terminal ends may not exist at all.

A special segment of the chromosome was first recognized on one of the large chromosomes of the rat leuko- and erythroblastic cells and of certain rat tumor cells [4]. A similar segment has been identified on three definite autosomes in the rat lymphoblast. The segment is chromophobic or faintly stained with nuclear stain. At metaphase, two filaments which are faintly staining may be seen to run through the segment and connect the deeply stained parts of the chromosome on each side of the segment. The morphological characteristics are closely similar to the secondary constriction or the SAT-zone noted in certain plants and lower animals and interpreted as a nucleolus-forming region or a nucleolus organizer [1]. It may be of considerable interest to investigate a possible relationship between the secondary constriction and the nucleoli in the rat cell.

Summary.—1. Technical improvements were employed in a reinvestigation of minute structures of chromosomes of mammalian cells.

2. The karyotype of the diploid lymphoblast from the rat was studied. The primary constrictions were found at the subterminal, submedian, and median regions on 12 pairs of autosomes and the X-chromosomes, but not on the 8 pairs of autosomes

and the *Y*-chromosome. Some chromosomes of the latter group showed small second arms at the terminal region, suggesting the location of kinetochore at positions close to the ends.

3. Three special autosomes, one of the second pair and two of the seventh pair, demonstrated primary constrictions subterminally and the secondary constrictions subterminally at the opposite end.

4. The secondary constrictions presented similar morphological characteristics as the *SAT*-zone noted in certain plants and lower animals.

REFERENCES

1. Darlington, C. D., Recent Advances in Cytology. 2nd ed., London, 1937.
2. Guenin, H. A., *J. Genetics* **49**, 23 (1948).
3. Heintz, E., *Planta* **12**, 775 (1931).
4. Kinosita, R. and Ohno, S., *Exptl. Cell Research* **7**, 581 (1954).
5. Makino, S. and Hsu, T. C., *Cytologia* **19**, 23 (1954).
6. Sachs, L., *Heredity* **6**, 357 (1952).
7. Sharp, L. W., Introduction to Cytology. New York, 1934.

Experimental Cell Research, **8**, *563–566 (1955)*

A MICROINCINERATIVE STUDY OF NORMAL AND STARVING *AMOEBA PROTEUS*

I. M. HELLER[1, 2] and M. J. KOPAC

Department of Biology, Graduate School of Arts and Science, New York University, New York, N.Y., U.S.A.

Received March 8, 1955

This work demonstrates, by microincinerative techniques, the distribution of minerals in the normal and starved *Amoeba proteus*. The possibility that the results obtained may elucidate the metabolism of protein as well as that of minerals, is discussed.

Materials and Methods.—The manner of handling, e.g., culturing, embedding of the amoebas, has been described [2]. The amoebas which had been fixed in a mixture of 9 parts of absolute ethanol and 1 part of neutral formalin were embedded in paraffin, cut at 4 μ, and mounted on cover slips. Both the mounting and incineration of the sections were carried out essentially according to the procedure described by Scott [5]. Incineration was done in a Huppert's Mighty Midget Oven. The temperature was gradually elevated 60° to 70°C every 5 minutes until 650°C was reached, at which time the heating was discontinued. After cooling, the covers slips were placed on slides and sealed with a mixture of equal parts of paraffin, beeswax, and resin. Alternate sections of the serially sectioned amoebas were used as cytologic controls and stained with either Heidenhain's hematoxylin or toluidine blue [2].

Observations of the incinerated material were made under both brightfield illumination (Köhler) and darkfield illumination. For the latter, either a darkfield condensor, Leitz D 0.8, or a condensor stop, was used in conjunction with an objective diaphragm.

Results.—The cytological detail of the incinerated sections compares favorably with that of the alternate sections stained with Heidenhain's hematoxylin or with toluidine blue (cf. Figs. 1 and 2). Under darkfield illumination, one can observe that the surface of the incinerated sectioned normal amoeba displays an alignment of coarse or fine ash, or both. The cytoplasmic matrix is seen as a reticulum-like pattern of fine ash delineating the vacuoles. Superimposed on this network are occasional small, coarse ash droplets. The prominent larger, coarse ash bodies seen, are the mineral residues of the refractive bodies (Fig. 3). Incinerated residue of the other cytoplasmic inclusions (i.e. crystals, mitochondria, and alpha granules) cannot be identified *per se* but are probably observed in the cytoplasmic ash, described above.

The nucleus can be easily identified by the conspicuous ash pattern of its numerous nucleoli which appear as discrete, refractile masses of high mineral concentration

[1] Work carried on as a Predoctoral Fellow of the National Cancer Institute, National Institutes of Health, Federal Security Agency.

[2] Present address, Division of Physics and Biophysics, Sloan-Kettering Institute for Cancer Research, 410 E. 68th St., New York, N.Y.

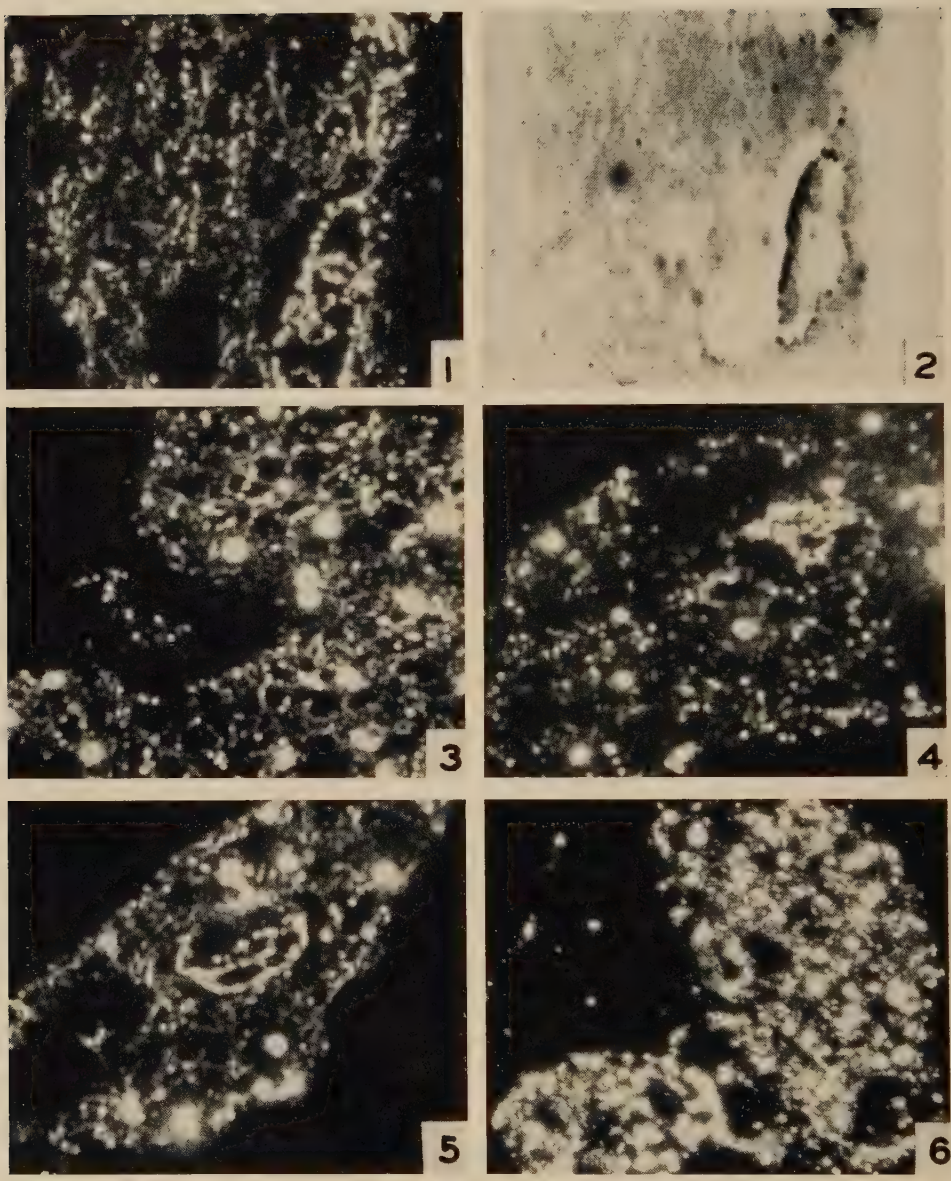

(cf. Figs. 1 and 2). The nucleolar ash, the ash of the refractive bodies, and the other coarse ash of the cytoplasm appear to be similar. One frequently finds this type of incinerated residue described as calcium or magnesium oxide, or both. The karyosomal ash is finely textured and very sparse in concentration. It resembles the fine mineral residue of the cytoplasmic matrix.

In general, the incineration of whole mounts was not successful. The incinerated residue of an entire amoeba appears as a mound of ash which has apparently collapsed and absorbed water. Such a preparation is of little value for the localization or identification of ash. In one instance, however, an incinerated preparation of a normal amoeba was seen which was not collapsed. The amoeba which had been previously centrifuged (and its components stratified) displayed a clear-cut stratification of ash. A very high concentration of white, hygroscopic ash was seen at the centrifugal end, where the food vacuoles, refractive bodies, crystals, and mitochondria are found. A lower concentration of a fine greyish ash was observed in the region which in the stratified amoeba corresponds to the cytoplasmic matrix. The centripetal end, corresponding to the lipid cap, was virtually free of ash. The ash pattern of this whole amoeba is in agreement with the observations made of sections.

No significant changes were observed in the incinerated sections of amoebas starved for 1 to 14 days. These sections are essentially like those of the unstarved controls (cf. Figs. 1, 3, 4, and 5). In sections of amoebas starved for 20 and 22 days there can be seen an appreciable increase in cytoplasmic ash as well as an alteration in the overall spatial pattern (Fig. 6). These effects are apparently due to the increased concentration of refractive bodies and crystals known to occur during starvation in *Amoeba proteus*, as well as to some change in the vacuolar nature of the cytoplasm as has been described by Andresen [1]. He observed in living starving *Amoeba proteus* that there form, by coalesence, large vacuoles containing concretions of crystals, refractive bodies and amorphous debris. The fine ash of the cytoplasmic matrix, although generally obscured by the abundant ash of the concentrated organelles and debris, can be seen in an occasional section.

The ash residues of the nucleoli persist with no reduction in size from 1 through 22 days of starvation. The tendency for fusion of the nucleolar ash observed in some of the unstarved amoebas, seems more apparent in the incinerated sections of amoebas starved for 13 days and longer. The karyosomal ash is sparse in concentration and infrequently seen in the sections of either control or starved amoebas. Consequently, it was not possible to conclude whether any alteration had occurred, during starvation in this ash pattern.

Discussion.—Scott [4] reported that portions of living cells which absorb ultra violet light of wave length 2750 Å correspond to those portions which, on incineration,

---

Fig. 1. Darkfield view of an incinerated section of a normal amoeba (cf. Fig. 2). Note the discrete concentrated ash corresponding to the peripheral nucleoli of the nucleus, as well as the reticulated appearance of the cytoplasmic ash. Approx. × 800.

Fig. 2. Section, alternate to that shown in Fig. 1, stained with toluidine blue. The nucleus is seen near the lower right margin of the sectioned amoeba.

Figs. 3-6 are darkfield views of incinerated sections of starved amoebas. Approx. × 500.

Fig. 3. One day of starvation. The relatively large, concentrated spheres of ash correspond to the refractive bodies.

Fig. 4. Seven days of starvation. This is not significantly different from the controls. Note the nucleus in the upper right.

Fig. 5. Thirteen days of starvation. This is essentially unaltered except for the slight fusion of the nucleoli of the centrally located nucleus.

Fig. 6. Twenty-one days of starvation. Note the striking increase in the ash content, presumably due, in part to the concentration of crystals and refractive bodies.

contain large residues of ash. In *Amoeba proteus*, sites which can be demonstrated by cytochemical means to contain structural sulfhydryl groups [2], reveal appreciable ash, on incineration. It would seem, therefore, that in certain parts of the cell at least, the ash residue may indicate the former site of proteins. Thus, one may look upon the ash pattern of *Amoeba proteus* (with the exception of the mineral residue associated with excretory inclusions) as indicative of minerals associated primarily with proteins.

With this point of view in mind, two possible explanations may be proposed to account for the maintenance during starvation, of the mineral residue of the cytoplasmic matrix and that of the nucleoli. One explanation is that in spite of the decrease in volume and weight during starvation, the concentrations of protein and of the salt, associated with it, do not change in these parts of the cell. This is consistent with Holter and Zeuthen's [3] report that in starving *Chaos chaos*, the decrease in cell volume parallels the decrease in reduced weight, which suggested to them that the cell volume is being regulated so as to keep the protein and salt concentrations of the cytoplasmic matrix constant.

The alternate explanation is that there may be a decrease in protein concentration with a concomitant increased salt-binding capacity of the protein. There may be a change in the binding capacity of the proteins with starvation as suggested by previous work [2]. An increased concentration of structural sulfhydryl groups was demonstrated in starved *Amoeba proteus*. Such altered protein reactivity could be due to various factors, e.g., partial unfolding of the protein molecule, unmasking of reactive groups by the breakdown of lipoprotein complexes, etc. These suggested mechanisms could account for an increase in the mineral binding capacity of the protein.

REFERENCES

1. Andresen, N., *Compt. rend. Lab. Carlsberg, Ser. chim.* **25**, 169 (1945).
2. Heller, I. M. and Kopac, M. J., *Exptl. Cell Research* **8**, 62 (1955).
3. Holter, H. and Zeuthen, E., *Compt. rend. Lab. Carlsberg, Ser. Chim.* **26**, 277 (1948).
4. Scott, G. H., *Science* **76**, 148 (1932).
5. Scott, G. H., Handbook of Microscopical Technique. 2nd ed., Edited by C. E. McClung, p. 643. New York, Paul B. Hoeber, Inc., 1937.

Experimental Cell Research, **8**, *567–571 (1955)*

A HIGH SPEED RECORDING MICRODENSITOMETER SUITABLE FOR CYTOLOGICAL RESEARCH

P. M. B. WALKER

Medical Research Council Biophysics Research Unit, King's College, London, England

Received March 21, 1955

Several methods in biological and biophysical research involve recording quantitative information photographically, and for these purposes the accurate and speedy measurement of the density of film or plate is therefore becoming increasingly important.

Most commercial microphotometers have been designed to measure spectrographic plates, recording transmissions substantially along the major axis of the plate by means either of a galvanometer and bromide paper or a commercial potentiometer recorder. Transmission measuring instruments are unsuitable for many applications such as absorption measurements of biological cells, where it is often necessary to integrate the density over an area, and inconvenient for many others. Further, the line scanned may have to be placed at any angle across the specimen and exactly related to the often complicated photographic image.

Since optical attenuators are available which obey a density law, it is possible to make a true null-point instrument which will record densities automatically by pen on paper, without the need for an external recorder, if advantage is taken of modern servo-motor and amplifier design. Direct pen recording also confers the secondary advantage that specimen and recording paper can be directly linked together, which makes it much easier to locate and compare detail on trace and film.

We have already made and described such a recording microdensitometer [2], which was designed in particular for measuring the densities of the small negatives exposed in the ultra-violet microscope. Owing to the development of other methods of investigation involving various sizes of negatives it was decided to build a more universal microdensitometer which might also act as a prototype for a commercially available instrument, which is required by many workers in the field of microspectrography [3], cell interferometry [1] and X-ray diffraction [4].

The principle of operation is based on the well-known double-beam system in which the two light beams traversing different paths are made to fall alternately on to a photo-sensitive detector. If the intensity of the two beams is different an A.C. signal is produced by the detector which, after amplification, causes a motor so to move an optical attenuator as to reduce the intensity difference. In this way a continuously self-balancing system is obtained in which the position of a suitable attenuator can be made to record the optical density of the specimen.

It is not the purpose of this communication to describe the microdensitometer in detail but to indicate its general features and performance, which may be useful to cytologists and others requiring to measure film densities from detailed photographs.

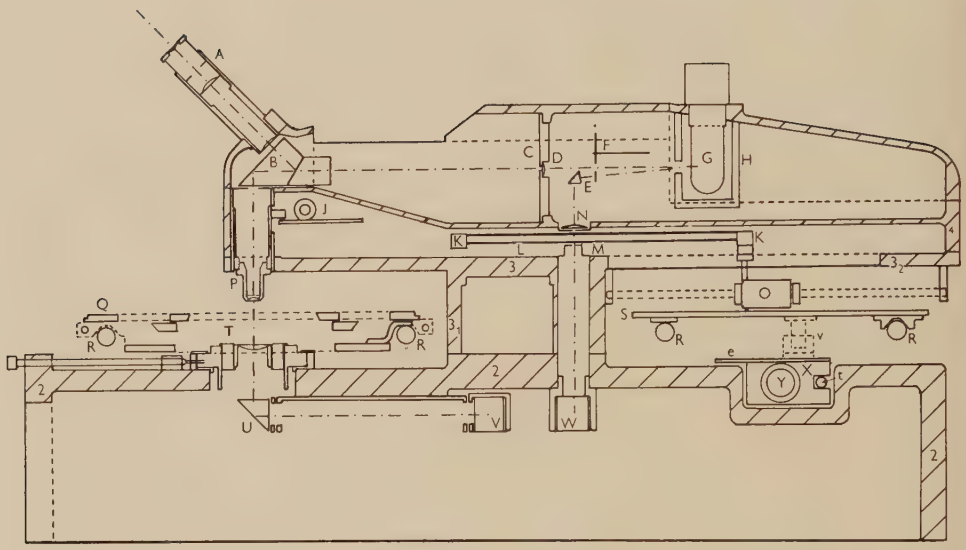

Fig. 1. Semi-diagrammatic sectional view at the centre line of the instrument. For key to lettering see below, Fig. 2.

The essential features are shown in the sectional (Fig. 1) and plan (Fig. 2) drawings and in the photograph (Fig. 3). The specimen of any size up to 10″ by 4″ is held on the table *Q*, which is coupled by a lever (*d*) to a second table (*S*), carrying the recording paper. Thus any movement of the specimen in an ordinal direction as drawn (Fig. 2) is transmitted to the recording paper table; a number of fulcrum positions are provided on the coupling lever (*d*) so that the distance moved by the paper relative to the specimen may be varied over a wide range. The specimen table can also be moved 3″ at right angles to the recording direction and is provided with a full rotary movement.

The optical attenuator (*L*), a neutral wedge, is arranged to move in a housing just above both the specimen and paper tables in an abscissal direction (Fig. 2). This arrangement allows the recording pen (*O*), which moves over the paper table, to be directly coupled to the attenuator as well as giving a very compact arrangement of the essential components.

The optical paths are shown chain dotted in Figs. 1 and 2 and are arranged so that light from a single filament of the source traverses in one beam the specimen and in the other the neutral wedge, before each beam is allowed to fall alternately onto the same part of the photomultiplier photocathode.

The electronic circuit is housed within the base of the instrument and consists, in addition to the various power supplies, of a simple A.C. amplifier and a special constant gain device, designed by Dr. E. M. Deeley of the Wheatstone Physics Laboratory, which maintains the gain of the servo-amplifier constant over a wide range of light intensities. In practice it is found possible to measure densities up to 3.0

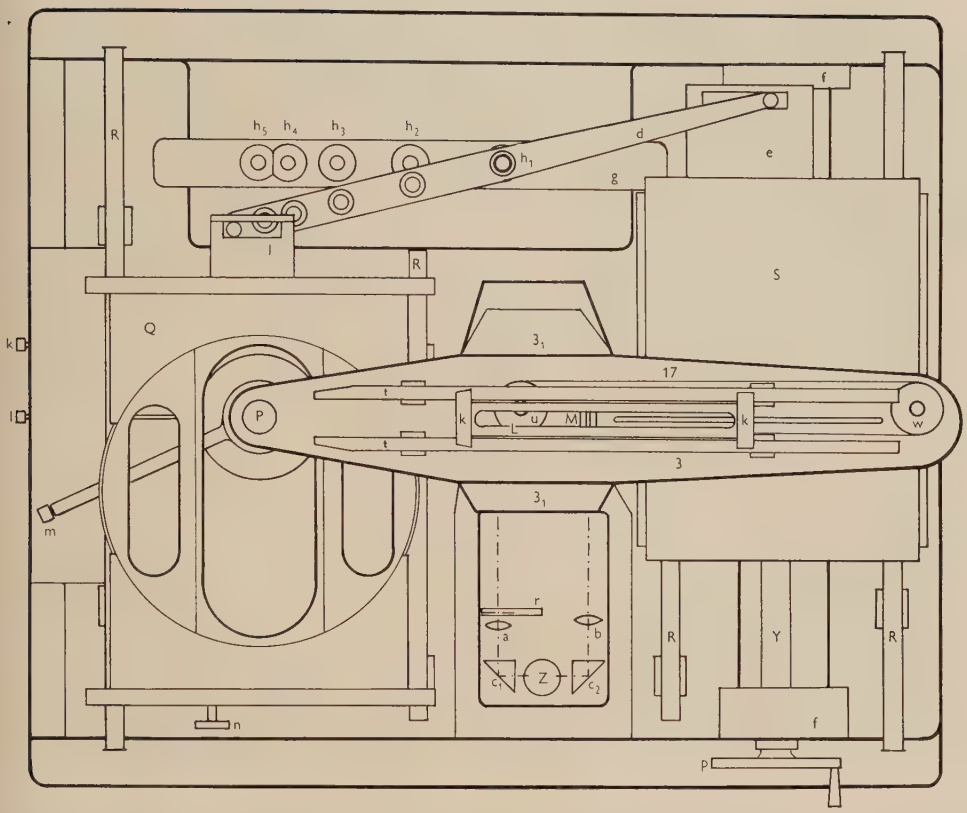

Fig. 2. Semi-diagrammatic plan view of instrument with components above the optical wedge level removed.

A = viewing ocular; *B* = prism; *C* = viewing screen; *D* = lens; *E* = prism; *F* = beam chopper; *G* = photomultiplier; *H* = photomultiplier housing; *J* = objective focusing movement; *K* = wedge holder bearings; *L* = wedge; *M* = slit; *N* = lens; *O* = recording pen; *P* = objective; *Q* = specimen table; *R* = slide bars; *S* = paper table; *T* = condenser; *U*, *V*, *W* = prisms; *X* = actuating nut; *Y* = lead screw; *Z* = lamp.

a, *b* = lenses; c_1, c_2 = prisms; *d* = lever; *e* = plate coupling nut and lever; *f* = bearing blocks of leadscrew; *g* = fulcrum plate; h_1–h_5 = alternative fulcrum positions; *j* = plate coupling object table and lever; *k*, *l* = centring adjustments for condenser; *m* = focusing adjustment for condenser; *n* = control for lateral movement of table; *p* = leadscrew handle; *r* = moveable diaphragm; *t* = wedge slide bars; *u* = driven tape drum; *v* = coupling between nut and paper table; *w* = idle tape drum.

2 = main casting; 3 = lower head casting; 3_1 = foot of lower head casting; 4 = upper head casting; 17 = steel tape driving the wedge.

from circular areas as small as 0.2 mm diameter, which corresponds to ~ 0.015 mm diameter on the specimen.

The accuracy of such a double beam instrument is independent of lamp intensity and voltage fluctuations, and provided the light from both beams falls on the same

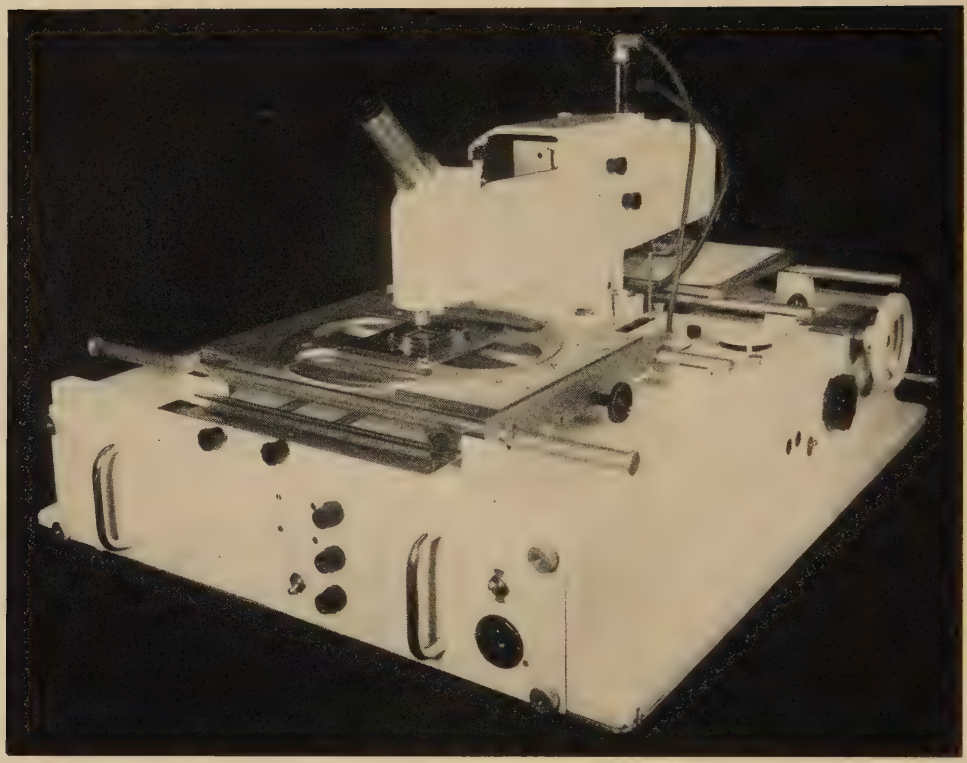

Fig. 3. General view of the complete instrument.

area of the photocathode, the accuracy depends only upon that of the attenuator. With an Ilford dyed gelatine wedge departures from the straight line density law were less than 0.5 per cent of full scale deflection. Reproducibility is very good over a large density range (0–2.5) as may be seen from a typical trace (Fig. 4), and the response time is less than 0.5 second for full-scale deflection.

Because of this rapid response and the ease of viewing and aligning the specimen, this microdensitometer has found wide use in biological research, where large numbers of measurements are often required. The only major improvement found necessary is a method for moving the specimen and paper tables independently in order that large negatives may be analysed in detail at positions other than near the centre of the specimen table. This improvement is being incorporated into the version now being commercially produced by Messrs Joyce, Loebl and Co. Ltd, Newcastle-upon-Tyne, England.

The instrument was constructed in the workshops of the Wheatstone Physics Laboratory, Kings College, and I am particularly grateful to Professor J. T. Randall for so generously supporting the project. I would also like to thank Dr. E. M. Deeley

for designing the constant gain device and for his general care of the electronic side of the instrument, and Mr. P. Hever of the workshop staff for putting so much care and skill into its construction.

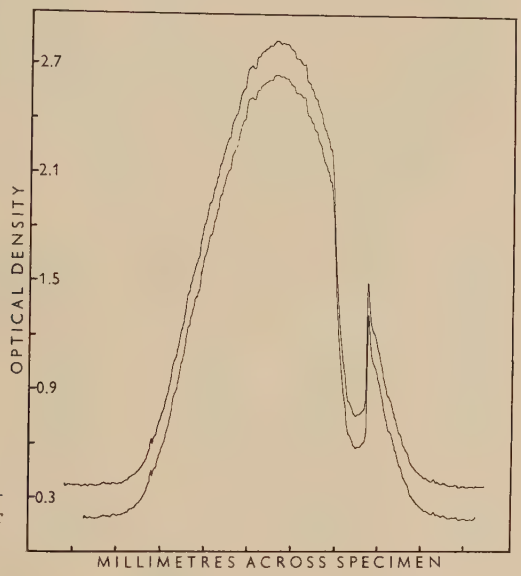

Fig. 4. A typical trace from a micro-interferogram showing the reproducibility over an intensity range of 250-1.

REFERENCES

1. Davies, H. G., Wilkins, M. H. F., Chayen, J., and La Cour, L. F., *Quart. J. Microscop. Sci.* **95**, 271 (1954).
2. Walker, P. M. B., *J. Sci. Instr.* **30**, 162 (1953).
3. Walker, P. M. B. and Yates, H. B., *Proc. Roy. Soc. B* **140**, 274 (1952).
4. Wilkins, M. H. F., Seeds, W. E., Stokes, A. R., and Wilson, H. R., *Nature* **172**, 759 (1953).

ELECTRON MICROSCOPY OF THE GLOMERULAR CAPILLARY WALL

J. RHODIN

Department of Anatomy, Karolinska Institutet, Stockholm, Sweden

Received April 1, 1955

The glomerular capillaries have been investigated with the electron microscope [1, 2, 3, 4, 5, 6, 7, 8, 10, 11, 12] though only in a few cases the measurements of the thickness of the capillary wall have been performed with any accuracy. Dalton [1] estimated the thickness of the middle dense layer to 0.1μ and Hall [2] demonstrated it to be 0.06–0.08μ.

Using improved sectioning technique [13] and after taking into consideration all the due precautions as to osmium fixation of tissues [9], the interpretation of the glomerular capillary wall in mouse may be somewhat different as compared with earlier data.

The capillary wall is built up of three layers. Only one forms a continuous sheath about the capillary loop. On either side of this continuous layer are located, on the inside the endothelium and on the outside the epithelium. However, in these two layers there are discontinuities. The cytoplasm of the epithelial cells is extended into small processes, which reach the middle layer of the capillary wall and are attached to it at varying distances from each other (0.05 0.1μ). The processes are bordered by a 100 Å thick double membrane. The cytoplasm of the endothelial cells forms an extremely thin layer, lining the luminar side of the middle layer. In this thin endothelial layer there are holes with a diameter varying from 0.05 0.1μ. In a section perpendicular to the capillary wall the holes can be seen as discontinuities of the thin layer. The cytoplasmic bulks around the holes are bordered by a membrane, 100 Å thick. The holes may be artefacts due to improper fixation but it may well be that they represent small channels into the middle layer of the capillary wall.

When using osmium tetroxide as an electron stain, there are some difficulties in the interpretation of the thickness of the middle layer. This layer is apparently built up of three components. The central one has the same density as the basement

---

Abbreviations: C.L., capillary lumen.
C.B., cavity of Bowman's capsule.

Fig. 1. Two glomerular capillaries sectioned perpendicularly to the capillary wall. In density there is a difference between C.L. and C.B. apparently due to fixation of plasma protein particles. In the left capillary the discontinuities of the epithelial and endothelial layers are easily seen. Magnification × 28,000.
Fig. 2. The capillary wall at higher magnification. Magnification × 49,000.
Fig. 3. Enlarged detail of Fig. 2. The dense middle layer has a lamellated structure and the epithelial processes are bordered by a double membrane against the less osmiophilic component of the middle layer. Magnification × 122,000.

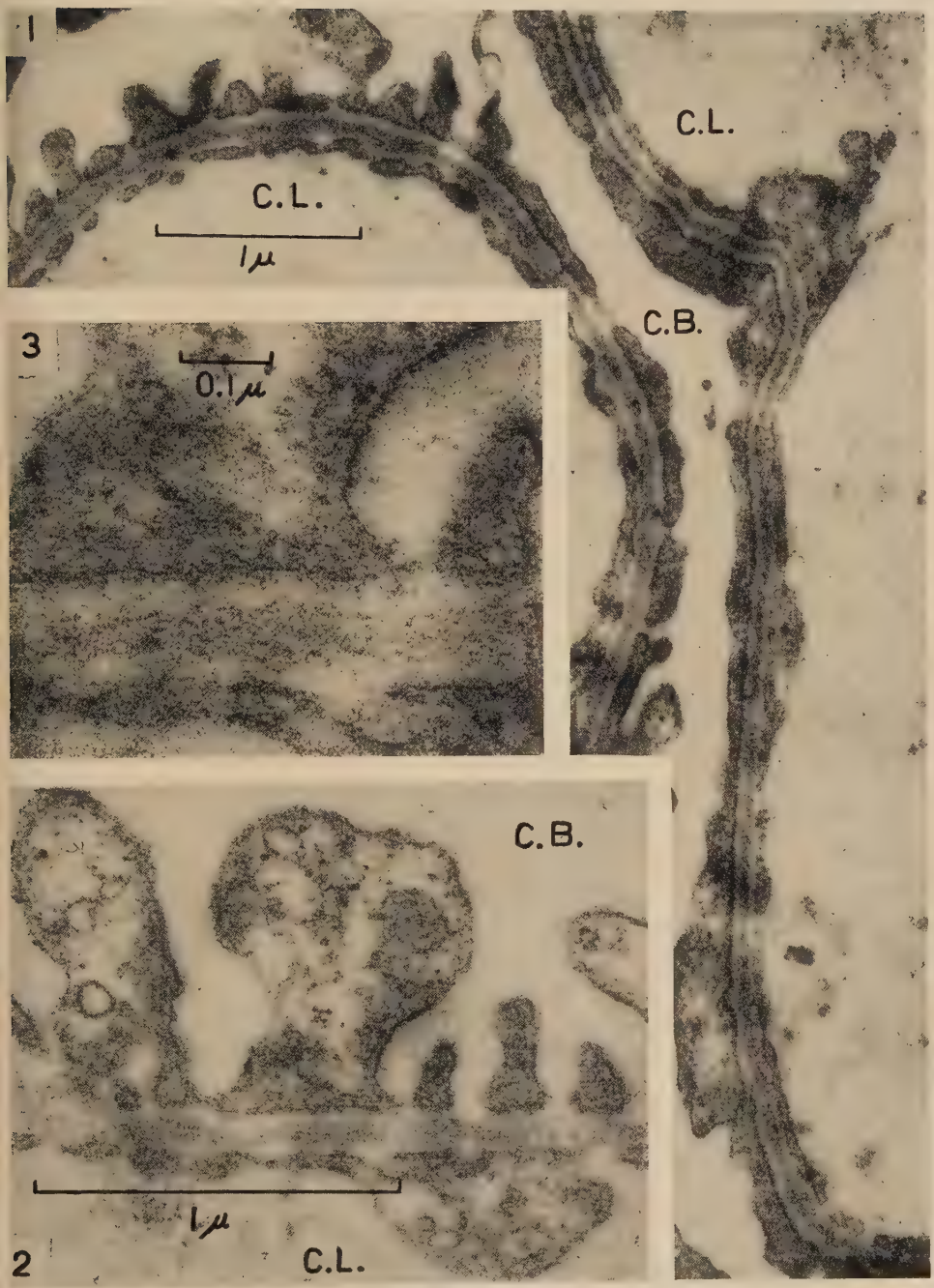
1
C.L.
1μ
C.L.
C.B.
3
0.1μ
C.B.
1μ
2
C.L.

membrane surrounding the kidney tubules and has a thickness of 650 Å ±13 ($\sigma = 96$). At higher magnification there is an indication of a lamellated structure that gives the impression of a spongy system in the layer. In addition there are always seen on either side a less osmiophilic space with a calculated thickness of 300 Å. Neither the epithelial processes nor the endothelial layer with its holes are in close contact with the dense central component. The less osmiophilic space is earlier reported in connection with the basement membrane of the kidney tubules [9, 14] and represents with the dense layer the fundamental structure of basement membranes. Thus the total thickness of the middle layer of the glomerular capillary wall is 1250 Å ± 21 ($\sigma = 159$).

REFERENCES

1. Dalton, A., *J. Natl. Cancer Inst.* **3**, 1163 (1951).
2. Hall, B. V., Proceedings of Fifth Annual Conference on the Nephrotic Syndrome, 1953.
3. —— *Anat. Rec.* **118**, 425 (1954).
4. Hall, B. V., Roth, E., and Johnson, V., *ibid.* **115**, 315 (1953).
5. Oberling, C., Gauthier, A., and Bernhard, W., *La Presse Médicale* **59**, 938 (1951).
6. Pease, D. C., *Anat. Rec.* **118**, 339 (1954).
7. Pease, D. C. and Baker, R. F., *Am. J. Anat.* **87**, 349 (1950).
8. Reid, R. T. W., *Austr. J. Exptl. Biol. Med. Sci.* **32**, 235 (1954).
9. Rhodin, J., Correlation of Ultrastructural Organization and Function in Normal and Experimentally Changed Proximal Convoluted Tubule Cells of the Mouse Kidney. Stockholm 1954.
10. Rinehart, J. F. and Farquhar, M. G., *J. Appl. Physics* **25**, 1463 (1954).
11. Rinehart, J. F., Farquhar, M. G., Jung, H. C., and Abul-Haj, S. K., *Am. J. Pathol.* **29**, 21 (1953).
12. Simer, P. H., *Anat. Rec.* **118**, 409 (1954).
13. Sjöstrand, F. S., *Experientia* **9**, 114 (1953).
14. Sjöstrand, F. S. and Rhodin, J., *Exptl. Cell Research* **4**, 426 (1953).

Experimental Cell Research, **8**, *575–577 (1955)*

TOPICAL DISTRIBUTION OF PROTEOLYTIC ACTIVITIES IN SOME TRANSPLANTED MICE TUMORS

B. SYLVÉN and H. MALMGREN

The Cancer Research Division of Radiumhemmet, Karolinska Sjukhuset, Stockholm, Sweden

Received April 5, 1955

The changes of normal mesenchymal tissues observed at the periphery of malignant tumors suggest that some proteinase(s) –possibly derived from the tumor cells— are digesting the normal structural proteins, which thus become transformed into a "gelatinous matrix" suitable for the invasion by growing tumor cells (9, 10). This is believed to constitute part of the operating chemical mechanisms involved in the infiltrative and destructive mode of growth of tumors (9). Previous analyses of proteinase activities obtained on tumor extracts express average figures at the macroscale (3, 6, 7, 11) and are thus inadequate for detailed topochemical conclusions (4). New attempts are, however, in progress to study the topical microscale distribution of cathepsin and dipeptidase activities in various transplanted mice tumors by quantitative means, under aerobic conditions, and with close regional correlation between chemical and microscopic data.

Tumor cylinders were punched out from fresh frozen tumor samples and then serially sectioned on a motor-driven microtome housed in a freezing cabinet at —10 to —15°C. On an average, each section measured 3 mm in diameter, 0.010–0.012 mm in thickness, about 0.08 mm^3 in volume; the protein content was about 8–12 μg. In sequences of 7 to 9 sections, separate ones were used for staining and microscopy, dipeptidase activity and blanks, determination of total protein (8), cathepsin activity with and/or without added activator(s), cathepsin blanks, and other purposes.

For dipeptidase measurements the micromethod of Linderström-Lang and Holter (5) was employed, generally using AlaGly as substrate. Catheptic activities were determined according to a microadaptation of Anson's hemoglobin method involving colorimetric assay of the tyrosine content of the split products. Procollagen, hemoglobin, and edestin seemed to be more suitable substrates than e.g. casein, egg albumin, and others. The tryptic activities of the tumor extracts were found negligible.

A number of serially sectioned cylinders from about 30 different non-ulcerated subcutaneous and intramuscular mice tumor transplants (C. 2146, sarcoma 37, mammary carcinomas, and solid ascites tumor transplants) have been analysed. The enzymic data were correlated with the topical location of sections, approximate tumor cell numbers, and also the regional cytology of tumor cells, roughly classified in *A* and *B* cell types (1).

The preliminary results (Figs. 1–2) have been very similar in all the investigated tumors and are essentially summarized as follows. The observed *dipeptidase* activities reached a maximum in the solid tumor regions rich in vital *B* cells. Low values were

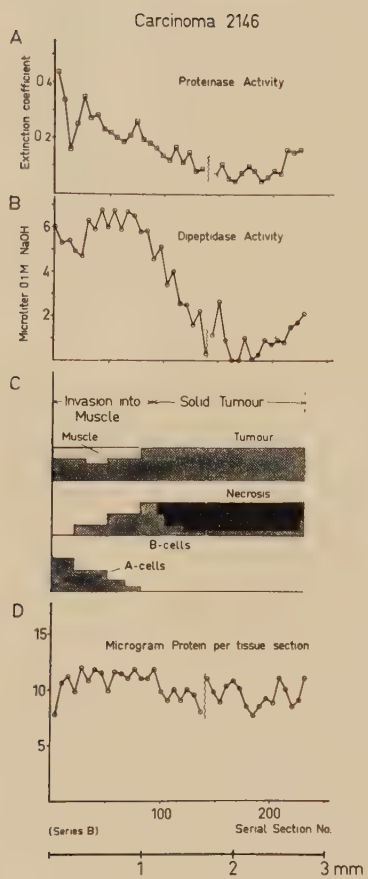

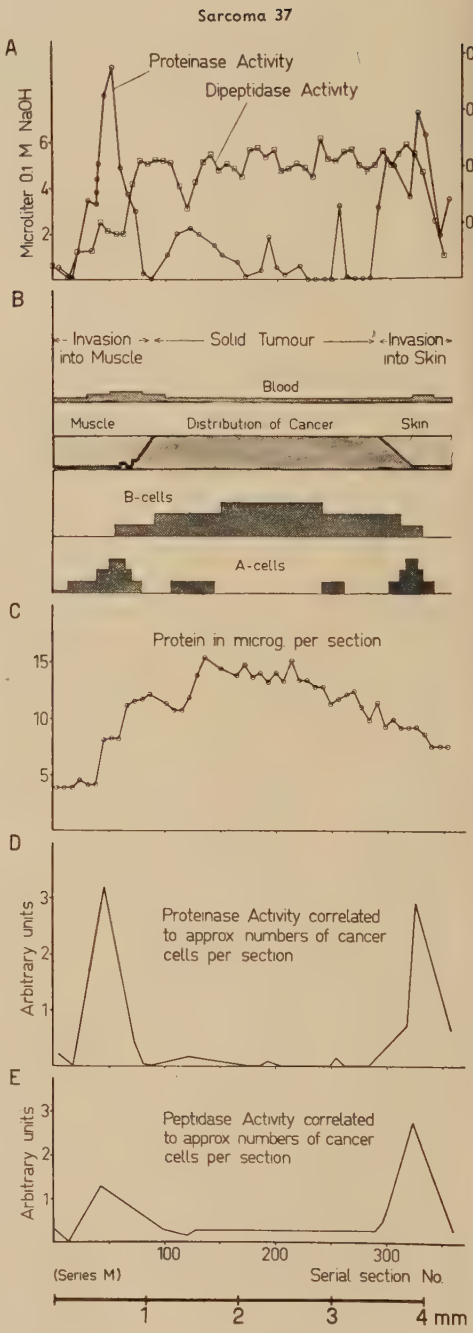

Fig. 1 (above). A 14 days old subcutaneous transplant of mouse carcinoma 2146. Sections No. 1–139 taken from the deep peripheral side of the tumor including the invasion zone. Sections No. 140–231 from the central part of the tumor. Section thickness 15 and 12 microns, respectively. The high enzyme activities in the vital tumor regions contrast sharply against the low activities in the central necrotic areas. Activators not added. Substrates AlaGly and nitrocasein. Fig. 2 (right). Analyses of 360 serial sections, 12 microns thick, of a cylinder 4.3 mm in length, traversing a 6 days old subcutaneous transplant of sarcoma 37. Both the superficial and deep zones of invasion are included. The histogram B will explain the topical distribution of tumor cells per section. Activators not added. Substrates AlaGly and edestin.

noted in necrotic areas. However, when the peptidase activities were correlated with the approximate cancer cell numbers per section (Fig. 2, E) elevated activities were obtained in the invasive peripheral zones, indicating much higher peptidase activity of the *A* cells over that of the *B* cells.

As to the observed *cathepsin* activities per section, marked peaks were observed in the original (Figs. 1, A and 2, A) as well as in the correlated figures (Fig. 2, D) *only* in the zones of tumor invasion containing *A* cells. Central tumor areas with *B* cells and necrotic regions showed insignificant cathepsin activities similar to normal skin, muscle, and red blood cells. In other experiments with added ascorbic acid, cysteine, or glutathione (final concentrations $2.5 \times 10^{-3} M/l$) activities about two to four times higher were observed throughout all vital tumor areas. The presence of at least two types of cathepsins in the tumors (2) may thus be inferred.

Present findings suggest that the peripheral invasive tumor tissues under aerobic conditions have higher dipeptidase and cathepsin activities calculated per tumor cells than the more central areas with *B* cells. The invasive tumor cells of excessive *A*-type showed a rapid concentrative uptake (12) of C^{14} labelled glycine, which was of guidance in their identification. The results further suggest that in these narrow peripheral zones, measuring about 0.25–1 mm in radial thickness, some special cellular or vascular factor(s) other than the tested –SH compounds may effectively activate the cathepsins. If the dimensions of the tumor zones with such elevated enzymic activities are considered, it seems not surprising that previous macroscale analyses failed to reveal the significant differences reported above.

Grants from Konung Gustaf V:s Jubileumsfond and the Swedish Cancer Society are gratefully acknowledged.

REFERENCES

1. Caspersson, T. and Santesson, L., Studies on Protein Metabolism in the Cells of Epithelial Tumours. *Acta Radiol., Suppl.* **46**, P. A. Norstedt & Söner, Stockholm, 1942.
2. Fruton, J. S., Irving, G. W. Jr., and Bergmann, M., *J. Biol. Chem.* **132**, 465 (1940).
3. Krebs, H. A., *Biochem. Z.* **238**, 174 (1931).
4. Linderström-Lang, K. U., Proteins and Enzymes. Lane Medical Lectures, Stanford University Press, Stanford, Calif., Vol. 6, 1952.
5. Linderström-Lang, K. U. and Holter, H., *Compt. rend. Lab. Carlsberg, Sér. chim.*, **19**, 1 (1932).
6. Maschmann, E. and Helmert, E., *Z. physiol. Chem.* **216**, 161 (1933).
7. Maver, M. E., Dunn, T. B., and Greco, A., *J. Natl. Cancer Inst.* **6**, 49 (1945/46).
8. Nayyar, S. N. and Glick, D., *J. Histochem. Cytochem.* **2**, 282 (1954).
9. Sylvén, B., Ester Sulphuric Acids of High Molecular Weight and Mast Cells in Mesenchymal Tumors. *Acta Radiol., Suppl.* **59**, P. A. Norstedt & Söner, Stockholm, 1945.
10. —— *Acta Radiol.* **32**, 11 (1949).
11. Waldschmidt-Leitz, E., McDonald, E., and collaborat., *Z. physiol. Chem.* **219**, 115 (1933).
12. Zamecnick, P. C., Frantz, I. D. Jr., Loftfield, R. B., and Stephensen, M. L., *J. Biol. Chem.* **175**, 299 (1948).

A CYTOCHEMICAL STUDY OF THE CELLULAR GRANULES IN THE STRATUM GRANULOSUM OF THE EPIDERMIS

G. MOBERGER and P. DE[1]

Institute for Cell Research and Institute of Radiopathology, Karolinska Institutet, Stockholm, Sweden

Received April 15, 1955

The granules of the cells in the stratum granulosum of the epidermis are distinguished by a high though varying stainability with basic dyes. Because of the similarity in this respect between the granules and nuclear chromatin, it has been suggested that the granules constitute disintegrated nuclear material, scattered out in the cytoplasm [7]. However, in contrast to chromatin, the granules exhibit a negative Feulgen reaction and consequently do not contain DNA [6]. Nevertheless, the cells of the stratum granulosum have a considerable absorption in ultraviolet at about 260 mμ [2] and have therefore been assumed to contain RNA in high concentration, responsible for the affinity to basic dyes of these cells. This concept has been supported by an abolished stainability of the granules with methyl-green-pyronin after digestion with ribonuclease [6]. An assumed presence of RNA in high concentration in the granules of the cells in the stratum granulosum has been interpreted to indicate an active anabolic synthesis of protein material in these cells, related to the process of keratinization [6, 12].

The following is a preliminary account on the cytochemical properties of the cells in the stratum granulosum as studied by means of roentgen and ultraviolet microspectrophotometry.

Experimental.—In human plantar epidermis (5μ paraffin-sections of frozen-dried [10] and formalin-fixed material) the dry weight (mass), as indicated by the absorption of soft continuous roentgen rays [5, 8, 9] was somewhat higher in the granular than in the spinous layer (Fig. 1 a, c). Furthermore, this increase of the dry weight

[1] Present address: Chittaranjan Cancer Hospitals, Calcutta, 26, India.

Fig. 1. *a*. Normal, human plantar epidermis. Frozen-dried. 5μ paraffin-section. Photo-micrograph of microradiogram obtained at 1.5 kV (by courtesy of Dr. B. Lindström). ×150. White areas correspond to a high roentgen absorption (high dry weight). *b*. The same section immersed in glycerin. Photo-micrograph at 257 mμ. ×150. For explanations see the text. *c*. Photo-micrograph of the same microradiogram as in *a*. ×1200. *d*. Photo-micrograph at 257 mμ of identical structures as in *c*. ×1200. Note the correspondence between the ultraviolet and the roentgen absorption in cytoplasmic areas. *e*. Normal epidermis from the foot of the rat. Frozen-dried. Photo-micrograph at 257 mμ of untreated, 5μ paraffin-section. ×220. *f*. The same section as in *e* after digestion with ribonuclease for 2 hours at 37°C. Photo-micrograph at 257 mμ. ×220. Note the persistent absorption in the stratum granulosum after digestion compared with the marked decrease of the absorption in the stratum spinosum.

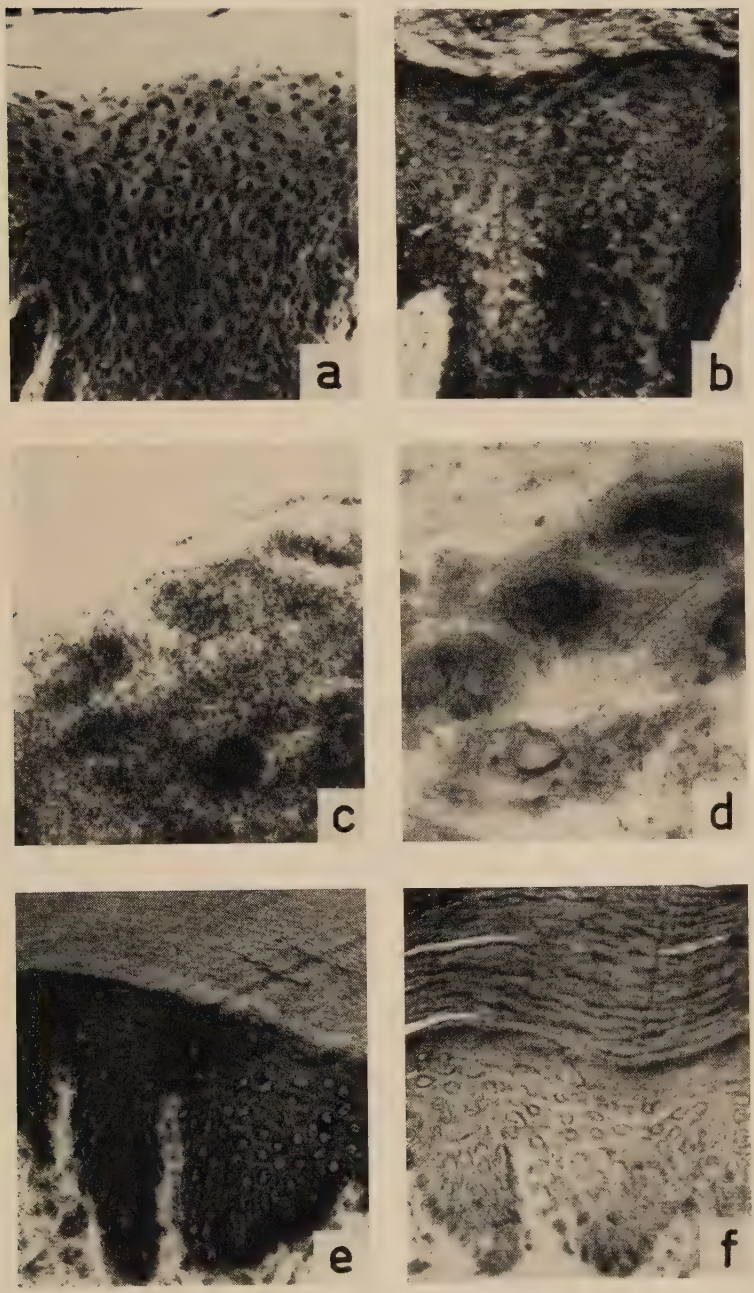
a
b
c
d
e
f

within stratum granulosum seemed to be continuous towards the superficial corneal layer which had the highest dry weight. Photometric measurements revealed a mean ratio between the dry weight of the granular and the spinous cells of about 1.2–1.5 whereas stratum corneum had a dry weight 2–4 times that of the cellular layers. Granular cells with a higher dry weight than the underlying spinous cells also had a higher affinity to basic dyes.

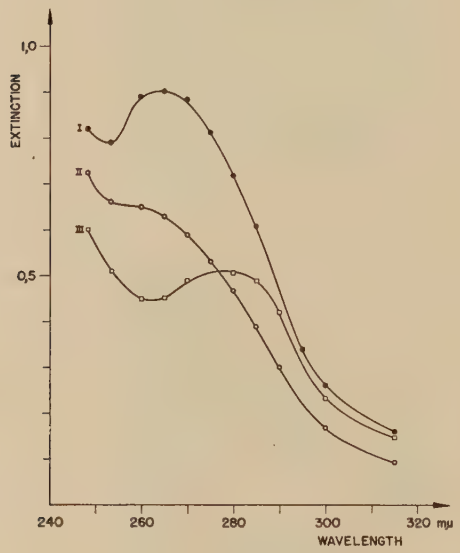

Fig. 2. Ultraviolet absorption spectra from cytoplasmic areas in the spinous layer (I) and the granular layer (II) and from stratum corneum (III) in normal epidermis from the foot of the rat.

Ultraviolet absorption measurements were performed on identical structures in the same sections which were used for the roentgen absorption analyses. A fairly high absorption at 257 mμ was generally found in the granular layer, equal to or somewhat exceeding that found in the spinous layer (Fig. 1 b). However, granular cells with a rather high cytoplasmic absorption at 257 mμ (Fig. 1 d) also had a considerable roentgen absorption (Fig. 1 c) and, hence, a high dry weight. Despite the rather high dry weight of stratum corneum, as indicated by a high roentgen absorption, this layer had a remarkably low absorption in ultraviolet at 257 mμ (Fig. 1 b, d).

Quantitative ultraviolet absorption measurements were performed in different layers of frozen-dried epidermis from the foot of the rat by means of the scanning, photo-electric microspectrophotometric device developed by Caspersson [3]. Complete ultraviolet absorption spectra from cytoplasmic areas in the spinous and granular layers as well as from stratum corneum are shown in Fig. 2. The rather high absorption of the spinous cells with a maximum at about 260 mμ indicates the presence of nucleic acids in these cells. In comparison the absorption spectrum from the granular cells had no characteristic absorption maximum despite of the rather high absorption capacity of these cells in this wave length range. The low absorption of stratum corneum at about 260 mμ corresponds to a minimum in the absorption

spectrum at this wave length. A maximum at about 280 mμ indicates the protein nature of the keratinized material in this layer.

Ultraviolet absorption measurements were also performed in cytoplasmic areas in the granular and spinous layers respectively (5μ paraffin-sections of frozen-dried epidermis from the foot of the rat) before and after incubation with ribonuclease (0.2 mg/ml) as well as hydrolysis with 1*N* HCl for 2 hours at 37°C. A marked decrease of the ultraviolet absorption at 257 mμ occurred in the spinous layer after digestion and after acid hydrolysis whereas in the granular layer the absorption was considerably less affected (Fig. 1 e and f). The results from the absorption measurements are summarized in Table I.

TABLE I

Ratios between mean extinctions at 265 and 280 mμ in cytoplasmic areas in stratum granulosum and stratum spinosum.

	λ	Untreated	After dig. with rnase	After acid hydrol.	Contr.
Ratio s.gran./s.spin	265 mμ	0.83	1.42	1.12	1.09
,,	280 mμ	0.96	1.52	1.12	0.99

The selective action by digestion with ribonuclease and by acid hydrolysis upon the absorption capacity of the spinous cells as compared with the granular cells is evident from the absorption measurements.

Discussion.—In normal and untreated plantar epidermis the ultraviolet absorption at about 260 mμ is thus often somewhat higher in stratum granulosum than in stratum spinosum. The absorption of the cells in the granular layer is, however, considerably less affected by digestion with ribonuclease or by acid hydrolysis than the corresponding absorption of the spinous cells. Conclusively the concentration of RNA, mostly responsible for the fairly high absorption of the spinous cells, is considerably lower in the granular than in the spinous cells. The comparative roentgen and ultraviolet absorption analyses have shown that the rather high ultraviolet absorption nevertheless found in the cytoplasm of the granular cells in untreated sections is caused, to a great extent, by an increased concentration of organic material (increased dry weight). Inhomogeneities exhibited by the granular structure of the cytoplasm of the cells in the stratum granulosum may also, due to light scattering and reflection, facilitate "unspecific" light losses in the image of these cells by ultraviolet microscopy and spectrophotometry and, hence, contribute to the rather high absorption of these cells.

The concept that an active synthesis of keratin proteins occurs in stratum granulosum in the presence of nucleic acids (RNA) in high concentration [6, 12] seems to be contradicted by the results from this investigation. These further support the view that the marked basophilia exhibited by the cells in the stratum granulosum is caused by acid groups other than nucleic acids. A metabolic process involving sulfur-containing amino acids [4] or carbohydrates [11] and a concomitant abrupt change in the pH [1] probably accounts for the histochemical appearance of the cells in the stratum granulosum.

REFERENCES

1. Bejdl, W., *Mikroskopie* **5**, 83 (1950).
2. Caspersson, T., *Naturwissenschaften* **29**, 33 (1941).
3. —— *Exptl. Cell Research* **1**, 595 (1950).
4. Dempsey, E. W., Singer, M., and Wislocke, B., *Stain Technol.* **25**, 73 (1950).
5. Engström, A. and Lindström, B., *Biochim. et Biophys. Acta* **4**, 351 (1950).
6. Leuchtenberger, C. and Lund, H. Z., *Exptl. Cell Research* **2**, 150 (1951).
7. Ludford, R. J., *Quart. J. Microscop. Sci.* **69**, 27 (1924).
8. Lindström, B., *Exptl. Cell Research* **6**, 537 (1954).
9. —— *Acta Radiol., Suppl. 125* (1955).
10. Moberger, G., Lindström, B., and Andersson, L., *Exptl. Cell Research* **6**, 228 (1954).
11. Patzelt, V., *Acta Anat.* **21**, 349 (1954).
12. Sandritter, W., *Frankfurt. Z. Pathol.* **64**, 520 (1953).

Experimental Cell Research, **8**, *583–585 (1955)*

ÉTUDE AU MICROSCOPE ÉLECTRONIQUE DE LA CENTROSPHÈRE DES LEUCOCYTES DES MAMMIFÈRES

A. POLICARD et M. BESSIS

Centre National de Transfusion Sanguine, Paris, France

Reçu le 22 Avril 1955

Dans les leucocytes sanguins ou conjonctifs des mammifères (rat, souris) la centrosphère apparaît comme une masse cytoplasmique sphérique de 2 à 4 μ, relativement chromophobe, aux contours flous, ne renfermant pas de mitochondries ou de granulations spécifiques. Aucune membrane ne la limite (un « noyau sans membrane » disait R. Hertwig en 1895).

Sur la cellule vivante, par microdissection (Chambers), cette centrosphère apparaît très visqueuse, presque rigide. La microcinématographie en contraste de phase (2) révèle plusieurs de ses propriétés : capacité de déformer le noyau, plus mou; absence, dans son intérieur, de tout mouvement protoplasmique; arrêt à sa périphérie des déplacements de granules ou de mitochondries; mouvements pendulaires réguliers d'une durée d'oscillation de 1 minute environ.

La centrosphère semble plus riche en substances protéiques et plus pauvre en eau que le reste du cytoplasme. Sur des cellules étalées sur lame, désséchées et ombrées la centrosphère fait une saillie souvent accentuée (2)

Sur des coupes ultrafines après fixation osmique, le microscope électronique permet les constatations suivantes (figures).

La centrosphère apparaît comme une région cytoplasmique sans mitochondries, lamelles doubles ni granulations. Ces structures l'entourent mais n'y pénètrent pas. En dedans du cercle plus ou moins complet formé par ces structures s'observent souvent des vacuoles ou canalicules (1000 à 4000 Å de large). A leur niveau, dans certains cas, se voient des travées de substance dense, épaisses de 500 à 1000 Å d'épaisseur longues de 0,2 à 0,6 microns environ et ressemblant aux formations décrites par Dalton et Felix [1] et rapportées à l'appareil de Golgi.

La substance même de la centrosphère est floue mais jamais homogène. Sur son fond assez dense s'observent de très fines vacuoles aux limites imprécises, lui donnant un aspect spumeux et de très fins granules plus denses de 100 à 200 Å, très mal limités.

Au centre de la centrosphère se voit quelquefois une granulation plus grosse et plus dense, aux contours assez dégradés, d'environ 0,5 micron. Peut-être s'agit-il du centriole révélé par les techniques de l'hématoxyline ferrique.

Cette morphologie inframicroscopique s'accorde avec ce que montre la microcinématographie en contraste de phase et les examens cytologiques habituels. Autour

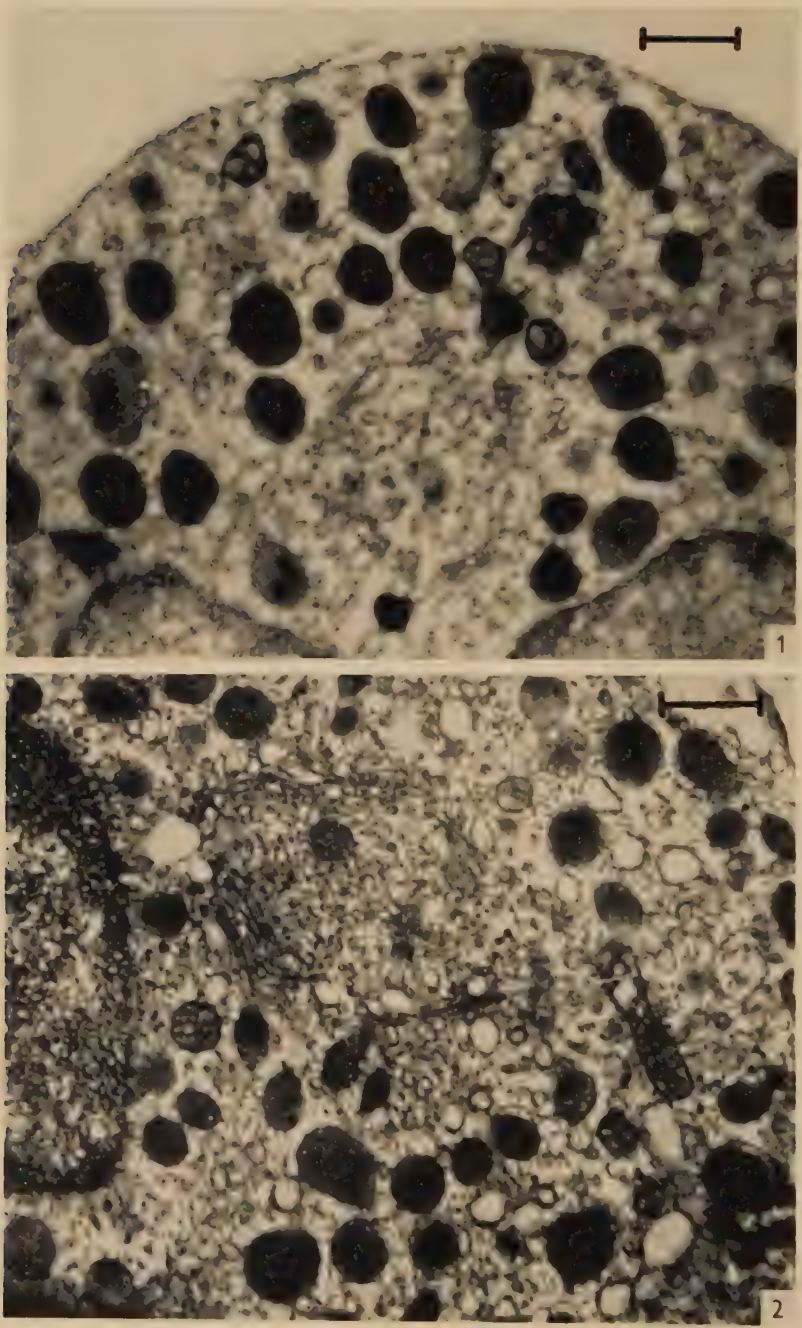
1
2

de la centrosphère, à son contact immédiat, peuvent se trouver les vacuoles et canalicules caractéristiques de l'appareil de Golgi. Ce système vacuolaire ne paraît pas pouvoir pénétrer dans la centrosphère.

BIBLIOGRAPHIE

1. Dalton, A. J. et Felix, M. D., *Am. J. Anat.* **92**, 277 (1953).
2. Policard, A. et Bessis, M., *Exptl. Cell Research*, **4**, 202 (1953).

Fig. 1. *Leucocyte éosinophile.* Noter l'arrêt des granulations et des mitochondries aux limites de la centrosphère. Autour de celle-ci série de petites vacuoles et de canalicules. Au centre masse dense (centriole ?). En bas, les bords du noyau.
Fig. 2. *Leucocyte éosinophile.* Noter ici l'abondance des vacuoles périphériques et des formations lamellaires de Dalton-Felix. Au sein de la centrosphère se trouve une granulation de nature indéterminée (coupe tergentielle d'une granulation marginale ?).

CORRELATION OF OPTICAL DENSITY AND OXIDATIVE PHOSPHORYLATION IN RECONSTRUCTED MITOCHONDRIAL SYSTEMS

R. E. BEYER[1], L. ERNSTER, H. LÖW and TINA BEYER

Department of Biophysics, Wenner-Grens Institut, University of Stockholm, Sweden

Received May 9, 1955

The ATP-Mn^{++} induced reconstruction of phosphorylation accompanying the aerobic oxidation of succinate in mitochondrial systems aged in Mg^{++} free incubation medium has been the object of recent study in this laboratory (2). It was observed that during the aging process, coincident with the loss of the phosphorylative ability, the mitochondrial suspensions turned translucent. This note deals with some optical density studies of the reconstructed systems.

Experimental. Mitochondria were prepared and aged in the suspending medium as described by Ernster and Löw (2). Initially, incubations were carried out in 1 cm Beckman cuvettes at room temperature; later studies have been performed in 25 ml Erlenmeyer flasks at 30°C. Optical density was determined in 1 cm cuvettes in a Beckman DU spectrophotometer at 510 mμ after placing silica plungers of 9 mm path length into the cuvettes. The plungers reduced the light path through the mitochondrial suspension to 1 mm and also served as aeration devices. Phosphorylation was determined according to a modification (3, 4) of the Martin and Doty method (5).

Results. Fig. 1 illustrates the fall in optical density which occurs when mitochondria, suspended in a Mg^{++} free incubation medium containing hexokinase, are aged at room temperature in a Beckman cuvette (broken line). It may be seen that the presence of Mn^{++} in the incubation medium delays the fall (upper solid line), while the addition of Mn^{++} after the fall has occurred has no effect (lower solid line). It may also be seen that the addition of 0.8 mM ATP has no effect after the fall has occurred.

In the experiment represented in Fig. 2 a mitochondrial suspension has been exposed to aging for 60 minutes under the same conditions as above, but in an Erlenmeyer flask (see experimental section). At the end of this aging period, succinate, together with 0.8 mM ATP and 0.5 mM Mn^{++}, was added. Aliquots were removed at 5 minute intervals, and optical density and phosphate uptake determined. These values are plotted against time of incubation in Fig. 2. The reconstruction of phosphorylation is accompanied by a recovery of optical density, both processes being increased in rate as a function of incubation time.

These data furthermore indicate a close correlation between the integral of the optical density and the net uptake of phosphate over a given period of incubation. In the experiment in Fig. 3 this correlation has been investigated as a function of

[1] United States Public Health Service Postdoctoral Fellow.

time of aging. From a mitochondrial suspension, exposed to aging as above, aliquots were removed at different time intervals, divided in two, and one was incubated with succinate while the other was incubated with succinate, Mn^{++} and ATP. Optical density was determined before and after 20 minutes of incubation, and

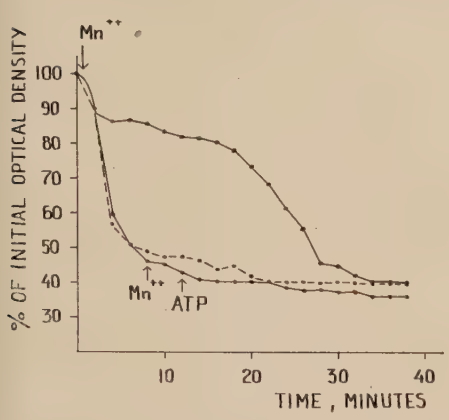

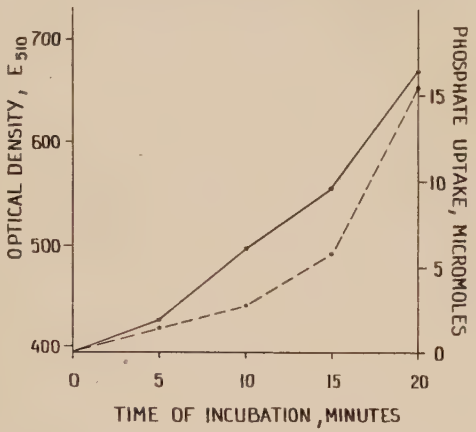

Fig. 1 (left). The effect of Mn^{++} and ATP on the optical density of mitochondrial suspensions.
Fig. 2 (right). The effect of succinate, ATP and Mn^{++} on the reconstitution of optical density and phosphorylation in an aged (60 min.) mitochondrial suspension.
O. D. ————; Phos. – – – –.

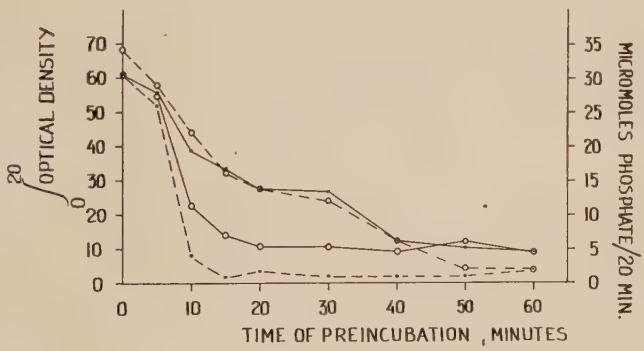

Fig. 3. The effect of Mg^{++} free aging time on the optical density and phosphorylation response to incubation with succinate (O. D. –o–o–; Phos. –·–·–·–) and succinate, ATP and Mn^{++} (O. D. —·—·—; Phos. – – o – – o –).

phosphate uptake was recorded for the same period. The integrals of the optical density values for the period 0–20 minutes were computed by assuming, for the sake of simplicity, that the changes were linear.

In Fig. 3 the values of net phosphate uptake are compared with the integrals of the optical density (expressed in arbitrary units) in both series of samples. A close correlation may be seen to exist between the two sets of curves. The correlation prevails in the native as well as in the reconstructed system.

Discussion. As has been previously concluded (2), the intramitochondrial level of ATP is of a primary significance in determining the phosphorylative ability of a

mitochondrial system. Brenner-Holzach and Raaflaub (1) have demonstrated a close relationship between mitochondrial ATP level and the structural state of the particles by showing that the depletion of the former was accompanied by a decrease of the optical density of mitochondrial suspensions. As pointed out by Raaflaub (6), and also found in the present study (Fig. 1), the mere addition of ATP to such a swollen system is not able to induce a reversal of the structural alterations. The fact that the establishment of an active oxidative phosphorylation in connection with the addition of ATP does result in a recovery of the optical density may be understood in terms of a preservation, or even an elevation, by the active phosphorylative process, of the ATP level initially established by the ATP addition. This may also explain the autocatalytic character of the reconstruction process (cf. Fig. 2) and the fact, discussed previously (2) that the recovery of phosphorylation, as measured during the initial period of reconstruction, may appear to be partial as compared to the level that prevailed in the intact system.

REFERENCES

1. Brenner-Holzach, O., and Raaflaub, J., *Helv. Physiol. Acta*, **12**, 242 (1954).
2. Ernster, L., and Löw, H., *Exptl. Cell Research*, Suppl. 3, in press (1955).
3. Ernster, L., Zetterström, R., and Lindberg, O., *Acta Chem. Scand.*, **4**, 942 (1950).
4. Lindberg, O., Ljunggren, M., Ernster, L., and Révész, L., *Exptl. Cell Research*, **4**, 243 (1953).
5. Martin, J. M., and Doty, D. M., *Anal. Chem.*, **21**, 965 (1949).
6. Raaflaub, J., *Helv. Physiol. Acta* **11**, 142 (1953).

AUTHOR INDEX

A

Abood, L. G. and Romanchek, L. Some chemical and physical properties of microsomes, 459
Afzelius, B. A. The ultrastructure of the nuclear membrane of the sea urchin oocyte as studied with the electron microscope, 147
Agrell, I. A mitotic rhythm in the appearance of mitochondria during the early cleavages of the sea urchin embryo, 232
Albert, E. and Felix, K. Über die Kerne der Ganglien- und Gliazellen und ihre Veränderungen in Rohrzuckerlösungen, 523
Allen, R. D. The fertilization reaction in isolated cortical material from sea urchin eggs, 397
Anderson, N. G. Studies on isolated cell components. VII. A reexamination of the preparation and properties of rat liver homogenates, 91
Austin, C. R. and Braden, A. W. H. Observations on nuclear size and form in living rat and mouse eggs, 163

B

Bessis, M. See Policard, 583
Beyer, R. E. *et al.* Correlation of optical density and oxidative phosphorylation in reconstructed mitochondrial systems, 586
Bernhard, W. Appareil de deshydratation continue, 248
Bors, J. P. See Giese, 369
Boss, J. Mitosis in cultures of newt tissues. IV. The cell surface in late anaphase and the movements of ribonucleoprotein, 181
Braden, A. W. H. See Austin, 163

C

Carlsen, F. and Knappeis, G. G. The anisotropic and isotropic bands of skeletal muscle in light- and electron microscopy, 329
Cheney, R. H. and Lansing, A. I. Caffeine inhibition of fertilization in *Arbacia*, 173
Clermont, Y. *et al.* Presence of carbohydrates in the acrosome of the guinea pig spermatozoon, 453
Couceiro, A. See Torres de Castro, 245

D

Danes, B. S. Metabolism of the embryonic chick heart fibroblast grown in tissue culture, 543
De, P. See Moberger, 578

E

Ernster, L. See Beyer, 586

F

Felix, K. See Albert, 523
Finamore, F. J. A study of ribonuclease and desoxyribonuclease during the early developmental stages of *Rana pipiens*, 533
Fox, H. The effect of sodium sulphadiazine on the nuclear population of the pronephros in *Triturus cristatus karelinii* (Strauch), 250

G

Giardina, G. and Monroy, A. Changes in the proteins of the sea urchin egg at fertilization, 466
Giese, A. C. *et al.* Peroxide and ultraviolet radiation effects, 369
Glegg, R. E. See Clermont, 453
Glücksmann, A. See Pelc, 336
Godman, G. C. The effect of colchicine on striated muscle in tissue culture, 488
Gonse, P. H. Recherches sur la physiologie de l'ovogenèse chez *Phascolosoma vulgare*, 550
— et Yotsuyanagi, Y. Note sur la réduction intracellulaire du triphényl-tétrazolium dans les œufs d'oursin, 500
Gordon, M. W. and Nurnberger, J. I. Acute cold-induced changes in cellular protein and nucleic acids in rat liver and brain, 279
Gray, L. H. See Holmes *et al.*, 101
Gustafson, T. Observations on differentiation with inhibited cleavage in the sea urchin egg, 118
— and Lenicque, P. Studies on mitochondria in early cleavage stages of the sea urchin egg, 114
— See Hjelte *et al.*, 76

H

Hagström, B. See Runnström, 1; Runnström *et al.*, 235
Hall, D. A. *et al.* Electron microscope studies of elastic tissue, 35
Harman, J. W. and Kitiyakara, A. Studies on mitochondria. VI. The relationship between the structure, osmotic reactivity and ATPase activity of mitochondria from pigeon skeletal muscle, 411
— See Kaltenbach, J. C., 435
Heller, I. M. and Kopac, M. J. Cytochemical reactions of normal and starving *Amoeba proteus*. I. Localization of thiols, DNA, RNA and other organic phosphates, 62
— A microincinerative study of normal and starving *Amoeba proteus*, 563
Hjelte, M.-B. *et al.* Studies on growth factors from the sea urchin egg, 76
Holmes, B. E. *et al.* The nucleic acid content of cells in the meristematic elongating and fully elongated segments of roots of *Vicia faba*, 101
Hornsey, S. See Holmes *et al.*, 101

I

Iverson, R. M. See Giese *et al.*, 369

J

Jensen, W. A. A morphological and biochemical analysis of the early phases of cellular growth in the root tip of *Vicia faba*, 506

K

Kaltenbach, J. C. and Harman, J. W. Studies on mitochondria VII. The relationship between the control of structure and the dinitrophenol stimulation of adenosinetriphosphatase in liver mitochondria, 435
Kaplan, J. G., The alteration of intracellular enzymes. I. Yeast catalase and the Euler effect, 305
Kautz, J. and De Marsh, Q. B. Fine structure of the nuclear membrane in cells from the chick embryo: on the nature of the so-called "pores" in the nuclear membrane, 394
Kihlman, B. Chromosome breakage in *Allium* by 8-ethoxycaffeine and X-rays, 345; Studies on the effect of oxygen on chromosome breakage induced by 8-ethoxycaffeine, 404
— and Overgaard-Hansen, K. Inhibition of muscle phosphorylase by methylated oxypurines, 252
Kinosita, R. See Ohno, 558
Kitiyakara, A. See Harman, 411
Klein, E. Gradual transformation of solid into ascites tumors. Evidence favoring the mutation-selection theory, 188
— Immediate transformation of solid into ascites tumors. Studies on a mammary carcinoma of an inbred strain, 213
Knappeis, G. G. See Carlsen, 329
Kopac, M. J. See Heller, 62, 563

L

Lallier, R. Animalisation de l'œuf d'oursin par les sels de zinc et de cadmium, 230
Lansing, A. I. See Cheney, 173
Lasnitzki, I. The effect of excess vitamin A on mitosis in chick heart fibroblasts *in vitro*, 121
Leblond, C. P. See Clermont, 453
Lenicque, P. See Gustafson, 114
Löw, H. See Bayer *et al.*, 586; Runnström *et al.*, 235

M

Maggio, R. and Monroy, A. Some experiments pertaining to the chemical mechanisms of the cortical reaction in fertilization of sea urchin eggs, 240
Malmgren, H. See Sylvén, 575
De Marsh, Q. B. See Kautz, 394
Marshak, A. and Marshak, C. Quantitative determination of desoxyribonucleic acid in echinoderm germ cells, 126
Marshak, C. See Marshak, 126
Mee, L. K. See Holmes, 101
Meyer-Arendt, E. und Meyer-Arendt, J. Grundlagen der Photometrie mit Wechsellicht, 387
Meyer-Arendt, J. See Meyer-Arendt, 387
Mikaelsen, K. The protective property of thiourea against radiation induced chromosome aberrations, 400
Moberger, G. and De, P. A cytochemical study of the cellular granules in the stratum granulosum of the epidermis, 578
Monroy, A. See Giardina, 466; Maggio, 240

N

Naora, H. Microspectrophotometry of cell nucleus stained by Feulgen reaction, 259
Nurnberger, J. I. See Gordon, 279

O

Ohno, S. and Kinosita, R. The primary and secondary constrictions on the chromosomes of the rat lymphoblasts, 558
Overgaard-Hansen, K. See Kihlman, 252

P

Pelc, S. R. and Glücksmann, A. Sulphate metabolism in the cartilage of the trachea, pinna and xiphoid process of the adult mouse as indicated by autoradiographs, 336
Policard, A. et Bessis, M., Etude au microscope électronique de la centrosphère des leucocytes des mammifères, 583
Prescott, D. M. Culturing of *Amoeba proteus* on *Tetrahymena*, 256

R

Reed, R. See Hall, 35
Rhodin, J. Electron microscopy of the glomerular capillary wall, 572
Ribi, E. and Shepard, C. Morphology of *Bacterium tularense* during its growth cycle in liquid medium as revealed by the electron microscope, 474
Robertson, J. D. Recent electron microscope observations on the ultrastructure of the crayfish median-to-motor giant synapse, 226
Romanchek, L. See Abood, 459
Runnström, J. Changes in the submicroscopic structure of the cytoplasm attending maturation and activation of the sea urchin egg, 49
— and Hagström, B. Studies on the action of the "fucus fertilization inhibitor" on sea urchin egg and sperm, 1
— *et al.* On the effect of ribonuclease on a jelly precipitating factor from the egg of the sea urchin, *Psammechinus miliaris*, 235

S

Sanders, R. T. See Giese, 369
Schneider, R. M. The effect of anion on the optical properties of rat liver nuclei isolated in glycerol solutions, 24
Shepard, C. See Ribi, 474
Sjöstrand, F. See Steinmann, 15
Snoad, B. The influence of temperature upon the nucleoli of *Tradescantia*, 554
Steinmann, E. and Sjöstrand, F. The ultrastructure of chloroplasts, 15
Sylvén, B. and Malmgren, H. Topical distribution of proteolytic activities in some transplanted mice tumors, 575

T

Thorén, I. See Hjelte, 76
Torres de Castro, F. and Couceiro, A. Studies on vital staining of protozoa, 245
Tunbridge, R. E. See Hall, 35

W

Walker, P. M. B. A high speed recording microdensitometer suitable for cytological research, 567
Weinreb, E. L. Histochemical demonstration of sites of acid phosphatase activity in mitochondria, 159
Wigand, R. Cytochemischer Nachweis der Nucleoproteide durch enzymatischen Abbau, 408

Y

Yotsuyanagi, Y. See Gonse, 500

SUBJECT INDEX

A

Acid phosphatase, sites of, in mitochondria, WEINREB, 159
Allium, chromosome breakage in, by 8-ethoxycaffeine and X-ray, KIHLMAN, 345
Amoeba proteus — culturing on *Tetrahymena*, PRESCOTT, 256; cytochemical reactions of normal and starving, HELLER and KOPAC, 62; microincinerative study of, HELLER and KOPAC, 563
Animalisation of sea urchin egg by zinc and cadmium, LALLIER, 230
Anion, effect of, on optical properties of rat liver nuclei, SCHNEIDER, 24
Apparatus for continuous dehydration, BERNHARD, 248
Ascites tumors — gradual transformation of solid into, KLEIN, 188; immediate transformation of solid into, KLEIN, 213
ATPase — of skeletal muscle, HARMAN and KITIYAKARA, 411; stimulation of, by dinitrophenol in mitochondria, KALTENBACH and HARMAN.
Autoradiography of sulphate metabolism in cartilage, PELC and GLÜCKSMANN, 336

B

Bacterium tularense, morphology of, during growth, RIBI and SHEPARD, 474
Brain, rat, acute cold-induced changes in protein and nucleic acids, GORDON and NURNBERGER, 279

C

Cadmium, animalisation of sea urchin egg by, LALLIER, 230
Caffeine, inhibition of fertilization in *Arbacia* by, CHENEY and LANSING, 173
Carbohydrates in the acrosome of guinea pig spermatozoon, CLERMONT *et al.*, 453
Carcinoma, studies of, on transformation of solid into ascites tumors, KLEIN, 213
Cartilage, sulphate metabolism in, PELC and GLÜCKSMANN, 336
Catalase, yeast and Euler effect, KAPLAN, 305
Cell — components, isolated, ANDERSON, 91; surface in late anaphase in mitosis, BOSS, 181
Chick — embryo, fine structure of nuclear membrane in, KAUTZ and DE MARSH, 394; heart fibroblasts, effect of excess vitamin A on mitosis, LASNITZKI, 121; heart fibroblast, metabolism of, DANES, 543
Chloroplasts, ultrastructure of, STEINMANN and SJÖSTRAND, 15
Chromosome — aberrations, protective property of thiourea against radiation, MIKAELSEN, 400; breakage in *Allium* by 8-ethoxycaffeine and X-ray, KIHLMAN, 345; breakage, effect of, induced by 8-ethoxycaffeine, KIHLMAN, 404; of rat lymphoblasts, primary and secondary constrictions on, OHNO and KINOSITA, 558
Cleavage — differentiation with, inhibited, in sea urchin egg, GUSTAFSON, 118; stages and mitochondria in sea urchin egg, GUSTAFSON and LENICQUE, 114
Colchicine, effect of striated muscle in tissue culture, GODMAN, 488
Cortical — material, isolated, fertilization reaction in, ALLEN, 397; reaction in fertilization of sea urchin egg, MAGGIO and MONROY, 240
Cytochemical reactions, localization of thiols, DNA, RNA by, HELLER and KOPAC, 62
Cytochemistry — demonstration of, by enzymic degradation, WIGAND, 408; of the cellular granules in stratum granulosum of the epidermis, MOBERGER and DE, 578
Cytoplasm, submicroscopic structure of, in sea urchin egg, RUNNSTRÖM, 49

D

Dehydration, continuous, apparatus for, BERNHARD, 248
Desoxyribonuclease — during developmental stages of *Rana pipiens*, FINAMORE, 533; localization of, in *Amoeba proteus*, HELLER and KOPAC, 62
Desoxyribonucleic acid, quantitative determination of, in echinoderm germ cells, MARSHAK and MARSHAK, 126

Differentiation with inhibited cleavage in sea urchin egg, GUSTAFSON, 118
Dinitrophenol stimulation of ATPase activity in mitochondria, relation to control of structure, KALTENBACH and HARMAN, 435

E

Echinoderm germ cells, desoxyribonucleic acid in, MARSHAK and MARSHAK, 126
Elastic tissue, electron microscopy of, HALL *et al.*, 35
Electron microscopy — of anisotropic and isotropic bands of skeletal muscle, CARLSEN and KNAPPEIS, 329; glomerular capillary walls, RHODIN, 572; of *Bacterium tularense* during growth, RIBI and SHEPARD, 474; of caffeine inhibition of fertilization in *Arbacia*, CHENEY and LANSING, 173; of elastic tissue, HALL *et al.*, 35; of nuclear membrane of sea urchin oocyte, AFZELIUS, 147; on the ultrastructure of crayfish giant synapse, ROBERTSON, 226
Enzymes, intracellular, alteration of, KAPLAN, 305
Epidermis, cytochemical study of cellular granules, in, MOBERGER and DE, 578
8-ethoxycaffeine — chromosome breakage in *Allium* by, KIHLMAN, 345; effect of oxygen on chromosome breakage induced by, KIHLMAN, 404
Euler effect and yeast catalase, KAPLAN, 305

F

Fertilization — chemical mechanisms of the cortical reaction in, MAGGIO and MONROY, 240; inhibition of, by caffeine in *Arbacia*, CHENEY and LANSING, 173; inhibitor, action of, on sea urchin egg and sperm, RUNNSTRÖM and HAGSTRÖM, 1; of the sea urchin egg, changes in proteins, GIARDINA and MONROY, 466; reaction of, in isolated cortical material, ALLEN, 397
Feulgen reaction, microspectrophotometry of cell nucleus stained by, NAORA, 259
Fibroblasts — effect of excess vitamin A on mitosis in, LASNITZKI, 121; metabolism of chick heart in tissue culture, DANES, 543
Fucus fertilization inhibitor, action of, on sea urchin egg and sperm, RUNNSTRÖM and HAGSTRÖM, 1

G

Ganglion cells — nuclei of, in sucrose solution, ALBERT and FELIX, 523
Glia cells, nuclei of, in sucrose solution, ALBERT and FELIX, 523
Glomerular capillary wall, electron microscopy of, RHODIN, 572
Granules, cellular, cytochemical study of, in the stratum granulosum of, MOBERGER and DE, 578
Growth — cycle of *Bacterium tularense* in liquid medium, RIBI and SHEPARD, 474; factors in sea urchin egg, HJELTE *et al.*, 76; morphological and biochemical analysis of, in *Vicia faba*, JENSEN, 506
Guinea pig spermatozoon, presence of carbohydrates in the acrosome of, CLERMONT *et al.*, 453

H

Histochemistry, determination of acid phosphatase in mitochondria, WEINREB, 159

J

Jelly precipitating factor of sea urchin egg, effect of ribonuclease on, RUNNSTRÖM *et al.*, 235

L

Lymphoblasts, rat, primary and secondary constrictions on chromosomes of, OHNO and KINOSITA, 558

M

Microdensitometer, high speed recording, for cytological research, WALKER, 567
Mitochondria — correlation of optical density and oxidative phosphorylation in reconstructed systems, BEYER *et al.*, 586

N

Nuclear — membrane, fine structure of, KAUTZ and DE MARSH, 394; size and form in living rat and mouse egg, AUSTIN and BRADEN, 163
Nuclei — the effect of anion on the optical properties of rat liver, SCHNEIDER, 24; of ganglion and glia cells, changes of, in sucrose solutions, ALBERT and FELIX, 523
Nucleic acid content in roots of *Vicia faba*, HOLMES *et al.*, 101
Nucleoli, of *Tradescantia*, influence of temperature upon, SNOAD, 554
Nucleoprotein, demonstration of, by enzymic degradation, WIGAND, 408

O

Oögenesis, physiology of, in *Phascolosoma vulgare*, GONSE, 550

Optical — density, correlation with oxidative phosphorylation in mitochondria, BEYER *et al.*, 586; properties, the effect of anions on, in rat liver nuclei, SCHNEIDER, 24
Organic phosphates, cytochemical localization of, HELLER and KOPAC, 62
Oxidative phosphorylation — correlation with optical density in reconstructed mitochondrial systems, BEYER *et al.*, 586
Oxygen, effect of, on induced chromosome breakage, KIHLMAN, 404

P

Peroxide, radiation effect, GIESE *et al.*, 369
Phascolosoma vulgare, physiology of oögenesis in, GONSE, 550
Photometry with intermittent light, fundaments of, MEYER-ARENDT *et al.*, 387
Pronephros, effect of sodium sulphadiazine on nuclear population of, FOX, 250
Proteins, changes in, at fertilization, GIARDINA and MONROY, 466
Proteolytic activity, topical distribution of, in transplanted mice tumors, SYLVÉN and MALMGREN, 575
Protozoa, vital staining of, TORRES DE CASTRO and COUCEIRO, 245
Psammechinus miliaris, effect of ribonuclease on a jelly precipitating factor from, RUNNSTRÖM *et al.*, 235

R

Radiation, effect, peroxide and ultraviolet, GIESE *et al.*, 369
Rana pipiens, ribonuclease and desoxyribonuclease during early developmental stages of, FINAMORE, 533
Ribonuclease — cytochemical localization of, HELLER and KOPAC, 62; effect of, on a jelly precipitating factor from, RUNNSTRÖM *et al.*, 235; in developmental stages of *Rana pipiens*, FINAMORE, 533

S

Sea urchin — oocyte of, ultrastructure of nuclear membrane in, AFZELIUS, 147
Sea urchin egg — action of, on the fucus fertilization inhibitor, RUNNSTRÖM and HAGSTRÖM, 1; animalization of, by zinc and cadmium, LALLIER, 230; changes in proteins of, at fertilization, GIARDINA and MONROY, 466; cortical reaction in fertilization of, MAGGIO and MONROY, 240; differentiation with inhibited cleavage, GUSTAFSON, 118; effect of ribonuclease on a jelly precipitating factor from, RUNNSTRÖM *et al.*, 235; fertilization reaction in isolated cortical material from, ALLEN, 397; growth factors in, HJELTE *et al.*, 76; intracellular reduction of triphenyltetrazolium, GONSE and YOTSUYANAGI, 500; submicroscopic structure of cytoplasm in, RUNNSTRÖM, 49
Sea urchin sperm, action of, on the fucus fertilization inhibitor, RUNNSTRÖM and HAGSTRÖM, 1
Sodium sulphadiazine, effect of on nuclear population, FOX, 250
Spermatozoon, acrosome, presence of carbohydrates in, CLERMONT *et al.*, 453
Synapse, median-to-motor, giant, ultrastructure of, ROBERTSON, 226

T

Tetrahymena, culturing on, of *Amoeba proteus*, PRESCOTT, 256
Thiols, cytochemical localization of, HELLER and KOPAC, 62
Thiourea, protective property of, against radiation induced chromosome aberration, MIKAELSEN, 400
Tradescantia, influence of temperature on the nucleoli of, SNOAD, 554
Triphenyltetrazolium, intracellular reduction of, in sea urchin egg, GONSE and YOTSUYANAGI, 500
Triturus cristatus karelinii (Strauch), nuclear population of pronephros in, FOX, 250
Tumors, transplanted, topical distribution of proteolytic activity in, SYLVÉN and MALMGREN, 575

U

Ultrastructure — of chloroplasts, STEINMANN and SJÖSTRAND, 15; of crayfish median-to-motor giant synapse, ROBERTSON, 226; of nuclear membrane of sea urchin oocyte, AFZELIUS, 147

V

Vicia faba — morphological and biochemical analysis of, JENSEN, 506; nucleic acid content in roots of, HOLMES *et al.*, 101
Vital staining of protozoa, TORRES DE CASTRO and COUCEIRO, 245

X

X-ray, chromosome breakage in *Allium* by, KIHLMAN, 345

Z

Zinc, animalization of sea urchin by, LALLIER, 230